The background of the cover is a light blue color. At the top and bottom, there are dark blue, irregular, wavy shapes that resemble amoebae. Within these dark blue areas, there are several white circles of varying sizes, some containing green rod-shaped bacteria. In the bottom dark blue area, there are also several white circles, some containing orange, wavy, rod-shaped structures. The central text is positioned in the light blue area.

# Free-living amoebae and infections

Perpetrators and facilitators

Maarten Sarink

# **Free-living amoebae and infections**

**Perpetrators and facilitators**

**Maarten Sarink**

Cover design: Maarten Sarink  
Layout: Douwe Oppewal  
Print: Ipskamp Printing, Enschede

Copyright © 2025 Maarten Sarink

All rights reserved. No part of this thesis may be reproduced, stored, or transmitted in any way or by any means without the prior permission of the author, or when applicable, of the publishers of the scientific papers.

# **Free-living amoebae and infections** **Perpetrators and facilitators**

Vrij-levende amoeben en infecties  
Daders en ondersteuners

Proefschrift

ter verkrijging van de graad van doctor aan de  
Erasmus Universiteit Rotterdam  
op gezag van de  
rector magnificus  
Prof.dr.ir. A.J. Schuit

en volgens besluit van het College voor Promoties.  
De openbare verdediging zal plaatsvinden op

woensdag 23 april 2025 om 15.30 uur  
door

**Maarten Just Sarink**  
geboren te Gouda.

The logo of Erasmus University Rotterdam, featuring the word 'Erasmus' in a stylized, cursive script.

**Erasmus University Rotterdam**

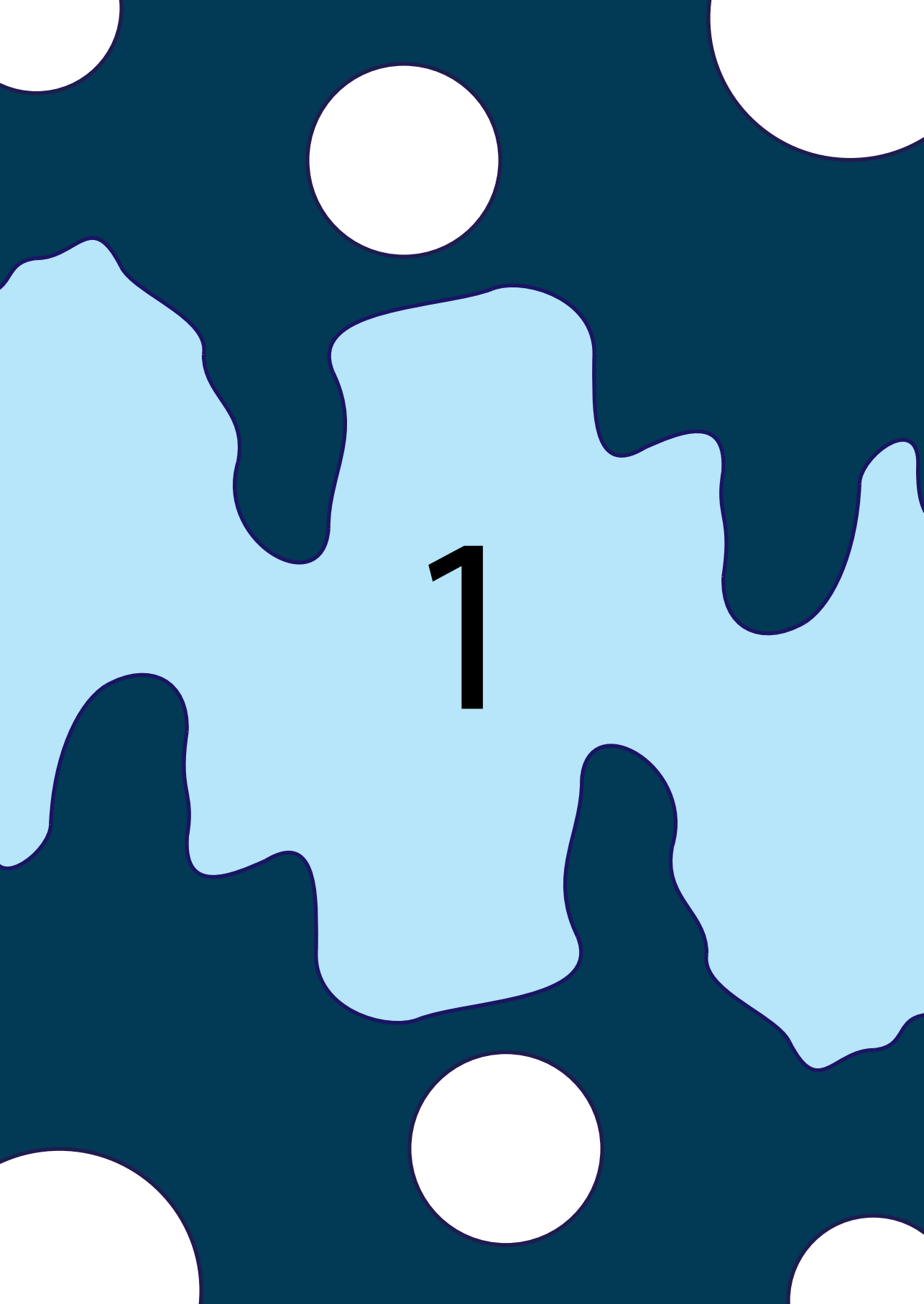
**Promotiecommissie:**

**Promotoren:** Prof.dr. A.G.M. Tielens  
Prof.dr. A. Verbon  
Prof.dr. J.J. van Hellemond

**Overige leden:** Prof.dr. E.C.M. van Gorp  
Prof.dr. M. Yazdanbakhsh  
Prof.dr. J. Tachezy

## Table of contents

<b>Chapter 1</b>	Introduction	7
<b>Chapter 2</b>	Three encephalitis-causing amoebae and their distinct interactions with the host	29
<b>Chapter 3</b>	Inhibition of fatty acid oxidation as a new target to treat Primary Amoebic Meningoencephalitis	59
<b>Chapter 4</b>	<i>Acanthamoeba castellanii</i> trophozoites need oxygen for normal functioning and lipids are their preferred substrate, offering new possibilities for treatment	79
<b>Chapter 5</b>	An international External Quality Assessment Scheme to assess the diagnostic performance of polymerase chain reaction detection of <i>Acanthamoeba keratitis</i>	107
<b>Chapter 6</b>	<i>Vermamoeba vermiformis</i> resides in water-based heater-cooler units and can enhance <i>Mycobacterium chimaera</i> survival after chlorine exposure	127
<b>Chapter 7</b>	<i>Acanthamoeba castellanii</i> interferes with adequate chlorine disinfection of multidrug-resistant <i>Pseudomonas aeruginosa</i>	141
<b>Chapter 8</b>	<i>Acanthamoeba castellanii</i> can facilitate plasmid transfer between environmental <i>Pseudomonas</i> spp.	153
<b>Chapter 9</b>	Summarising discussion and perspectives	167
<b>Appendices</b>	Nederlandstalige samenvatting	184
	Dank(kruis)woord	188
	Curriculum vitae	190
	PhD portfolio	191
	List of publications	194



1

# CHAPTER 1

---

Introduction

## Introduction to free-living amoeba

In 1674, Antoni van Leeuwenhoek described microscopic life-forms for the first time in his home town of Delft, naming them “animalcules” <sup>1</sup>. The creatures he saw were bacteria and protists, microorganisms that have been on earth for billions of years <sup>2</sup>. Bacteria are characterized by their small size and prokaryotic entity, indicating that these organisms lack an enveloped enclosed nucleus. Protists are eukaryotes, meaning that cells of these organisms do contain a cell nucleus. One type of organism that belongs to the protist group is the amoeba. Although Antoni van Leeuwenhoek described a lot of microorganisms, he never wrote of something resembling an amoeba. The first description of an amoeba was published by AJ Roesel von Rosenhof in *Insecten-Belustigung* in 1755, who named the creature he saw “der kleine Proteus”, after the shape-shifting Greek god <sup>3</sup>. The term “Proteus animalcule” remained in use throughout the 18th and 19th centuries, as an informal name for any large, free-living amoeboid organism <sup>4</sup>. The genus ‘amoeba’ (from the Greek ἀμείβω, meaning “change”) was erected in 1826, describing membranous, diffluent microorganisms whose shape is constantly changed to their liking <sup>5</sup>.

Long before this time, some 1.6 billion years ago, the first eukaryotes were present on earth <sup>6</sup>. These first eukaryotes are thought to originate from either a symbiotic event between two prokaryotic cells or from a primitive amitochondriate eukaryote which obtained mitochondria by phagocytosing an  $\alpha$ -proteobacterium <sup>7</sup>. The latter theory has been challenged in recent years, as no amitochondriate eukaryotes have been found and the rationale behind the selective pressures for a eukaryote to obtain a mitochondrion are not convincing <sup>8</sup>. Since this first event, a wide variety of mitochondria appeared and a versatility of organisms emerged, among which the amoeba <sup>3</sup>. Amoebae can be organised based on many different characteristics, but for the purposes of this thesis we prepared a classification based on their way of living and pathogenic capacities (shown in Table 1).

Free-living amoebae (FLA) are those amoebae that live freely in the environment without any need for a host, as opposed to parasitic amoebae that require a host during their life cycle <sup>3,9</sup>. However, some FLA are also capable of parasitising on a host, indicating that they are facultative parasites. FLA are spread out across four clades of the eukaryotic tree, with most FLA gathered in the Amoebozoa and Excavata supergroups and some in the Rhizaria and Opisthokonta supergroups <sup>10,11</sup>. The Amoebozoa are assumed to contain approximately 20,000 species <sup>12</sup>. Most other amoebae, approximately 200 species, are present in the Heterolobosea group, within the Excavata supergroup <sup>12</sup>. Using molecular techniques, some high-quality phylogenetic studies have been performed <sup>13,14</sup>. However, outside of the Amoebozoa supergroup detailed studies are still lacking. The widespread phylogenetic presence of amoeba has therefore not been fully enlightened.

**Table 1.** Classification of amoebae based on life style and pathogenicity with examples of relevant species.

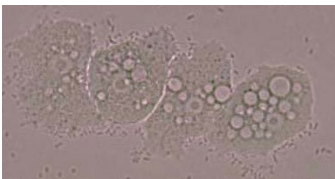
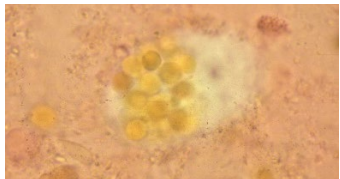
		<b>Free-living</b>	<b>Dependent on host</b>
	Name	Free-living organism	Commensal
	Example(s)	<i>Naegleria gruberi</i> <i>Vermamoeba vermiformis</i>	<i>Entamoeba dispar</i>
<b>Non-pathogenic</b>	Image	 A	 B
	Name	Facultative parasite	Obligate parasite
	Example(s)	<i>Naegleria fowleri</i> <i>Acanthamoeba</i> spp. <i>Balamuthia mandrillaris</i>	<i>Entamoeba histolytica</i>
<b>Pathogenic</b>	Image	 C	 D

Image A shows a phase contrast image of a trophozoite stage of *Naegleria gruberi*. Image B shows an iodine stained cyst of *Entamoeba dispar*, which is morphologically indistinguishable from *Entamoeba histolytica* cysts. Image C shows a phase contrast image of trophozoites of *Acanthamoeba* spp. Image D shows an eosin stained trophozoite of *E. histolytica* that has phagocytosed multiple erythrocytes. Image courtesy: A: microENVISION, B and D: Rob Koelewijn, C: Maarten Sarink.

Besides being present in various clades of the phylogenetic tree, amoebae are also physically present in various environments all over the earth. Amoebae have been isolated from both fresh and salt water as well as from soil. In aquatic environments amoebae have been detected in lakes and rivers<sup>15</sup>, geothermal springs<sup>16</sup>, seawater<sup>17</sup> and man-made water systems such as drinking water systems<sup>18</sup> and hospital water systems<sup>19,20</sup>. The abundance in soil differs depending on soil type and location, as amoebae are widely present in forest and grassland soil, but not so much in peatland soils<sup>21</sup>. Amoebae have also been detected in more extreme environments such as sediments from deep-sea mud volcanoes<sup>22</sup>. This might be a result of the ability of amoebae to transform into stress-

resistant and dormant cysts to survive harsh environmental conditions<sup>23</sup>. Some amoebae, mainly those within the Heterolobosea group, have another life stage, the flagellate, which can travel longer distances by the use of flagella<sup>24</sup>.

Most FLA are professional phagocytes, which means that they use pseudopods to encircle and engulf live prey or particles of scavenged material. As such, they can live without the need for a host, contrary to parasitic amoebae such as *Entamoeba histolytica*<sup>3</sup>. However, some FLA have the potential to infect other organisms and as such, cause illness. The three FLA that can infect humans are *Naegleria fowleri*, *Acanthamoeba* spp. and *Balamuthia mandrillaris*<sup>9</sup>. These three pathogenic FLA will be discussed in more detail in the next paragraphs.

## **Naegleria spp.**

Over 40 *Naegleria* species have been identified, with the most studied *Naegleria* species being *Naegleria fowleri*, *N. gruberi* and *N. lovaniensis*. Both *N. gruberi* and *N. lovaniensis* are non-pathogenic and are often used as model organisms for their pathogenic family member, *N. fowleri*<sup>25</sup>. All *Naegleria* spp. belong to the Heterolobosea group within the Excavata supergroup. *Naegleria* trophozoites measure 10-25 µm and have an irregular, curvy shape and move with large and broad hemispherical bulges<sup>26</sup>. All *Naegleria* spp. can transform into a cyst stage when conditions are harsh and most can transform into a pear-shaped flagellate stage to travel longer distances<sup>25</sup>. As *N. fowleri* is the pathogenic member of the *Naegleria* spp., we will focus mostly on this organism.

### **Naegleria fowleri**

*N. fowleri* is ubiquitously present, as it has been reported on all continents except Antarctica<sup>25</sup>. It resides in freshwater and is thermophilic, meaning that it can thrive at relatively high temperatures, in contrast with its non-pathogenic counterparts<sup>27</sup>. The best growth temperature for *N. fowleri* is 37-43 °C, but *N. fowleri* can also grow at 25 °C, albeit slower<sup>28</sup>. Trophozoites degenerate within hours below 10 °C, but cysts survive at 4 °C for 12 months<sup>29</sup>. *N. fowleri* has therefore been observed in high concentrations in hot springs, cooling ponds of nuclear power plants and warm freshwater<sup>30-33</sup>, although *N. fowleri* has also been isolated from drinking water systems with a lower temperature<sup>34,35</sup>. Groundwater has been postulated to be the largest natural niche and most important reservoir of *N. fowleri*<sup>27,33</sup>.

## Metabolism

In a previous study, it was unexpectedly discovered that *N. gruberi* shuns carbohydrates and prefers lipids for its energy metabolism<sup>36</sup>. This remarkable result could be explained retrospectively by reviewing the food sources of *Naegleria* spp. *Naegleria* spp. feed mainly on bacteria, both Gram-positive as well as Gram-negative, but can also feed on algae and yeast<sup>37</sup>. All these organisms are low in carbohydrates and relatively high in lipids, explaining the observed lipid preference of *N. gruberi*<sup>38</sup>. This unique metabolic characteristic of *N. gruberi* could also hold true for *N. fowleri*, as metabolic pathways are usually conserved and as their diet is similar. Furthermore, this lipid preference could then be exploited to generate a new treatment for infections caused by *N. fowleri*.

## Pathogenic potential

*N. fowleri* can cause Primary Amoebic Meningoencephalitis (PAM), a rapidly fatal disease with a mortality rate of over 95%<sup>27,37,39</sup>. PAM is contracted when water containing *N. fowleri* contacts the nasal epithelium, after which the trophozoite stage of the amoeba can migrate along the olfactory nerve, through the cribriform plate to the olfactory bulb within the CNS<sup>37,40</sup>. Further details of the infectious route will be discussed in chapter 2. In the United States, *N. fowleri* infections occur mostly in healthy children and young adults during recreational water activities, such as swimming, diving, and rafting<sup>31,41,42</sup>. In the Indian subcontinent, the correlation with age is less clear, probably because ablution rituals, washing, and a lack of chlorination play a large role in the epidemiology<sup>27,43</sup>. As *N. fowleri* is a thermophilic organism, there is concern that global warming and changes in the ecosystems that *N. fowleri* inhabits may lead to more cases worldwide<sup>27,44</sup>.

## Signs and symptoms, diagnosis and treatment

The first symptoms of PAM are headaches, fever, nausea, vomiting and irritability or restlessness. Subsequently, other symptoms such as photophobia, lethargy, seizures and confusion appear, ultimately leading to coma and death<sup>33,45</sup>. The first symptoms usually arise within 2-7 days after exposure to *N. fowleri*, death occurs generally within 7-10 days following symptom onset<sup>41,45</sup>. As symptoms of PAM are not distinct from a bacterial or viral meningitis, diagnosis is often difficult and delayed<sup>27,45</sup>. Direct microscopic examination of cerebrospinal fluid (CSF) is the diagnostic method of choice early on in disease, although high powered microscopes and a skilled technician are necessary. Examination of CSF with molecular techniques such as polymerase chain reaction (PCR) are far more sensitive, but usually only available in expert centres<sup>27,46</sup>. CSF abnormalities such as an increase in red blood cell count, white blood cell count, CSF pressure or protein concentration are not distinctive for PAM. Furthermore, neuroimaging can also not distinguish PAM from meningitis due to another cause<sup>37</sup>. Once the diagnosis is confirmed, treatment usually consists of amphotericin B and miltefosine, although only sporadic evidence exists to

support any treatment regimen. Other drugs that have been used to successfully treat patients are rifampin, miconazole, fluconazole, dexamethasone and azithromycin <sup>37</sup>. Because of the high mortality rate, new treatment options are urgently needed <sup>47</sup>. At present, it is not known whether the brain damage in patients suffering from PAM is mostly due to the amoeba or due to the immune response of the patient itself <sup>48,49</sup>. Further details about the pathogenicity mechanisms of *N. fowleri* and the immune responses of PAM patients will be discussed in chapter 2.

## ***Acanthamoeba* spp.**

*Acanthamoeba* trophozoites measure 15-50 µm and have an angular shape, with a granular cytoplasm containing vacuoles. Fully formed *Acanthamoeba* cysts have a diameter of 10-20 µm and possess a double wall <sup>26</sup>. *Acanthamoeba* trophozoites use spiky projections named acanthopodia to move around and to feed, their menu consists of bacteria, algae and yeast <sup>26,50</sup>. *Acanthamoeba* has been isolated from a plethora of places, usually as the sole or most abundant free-living amoeba present. Examples include bottled water <sup>51</sup>, contact lens cases <sup>52</sup>, dental units <sup>53</sup>, drinking water <sup>54</sup> and hospital water systems <sup>20</sup>. *Acanthamoeba* can survive in harsh conditions and can exhibit resistance towards biocides, chlorination and antibiotics, but they do not grow well at higher temperatures <sup>55,56</sup>.

## **Metabolism**

The energy metabolism of *Acanthamoeba* has not been examined in-depth. Most studies have focused on the respiratory chain, and demonstrated the presence of a complete mammalian-type electron-transport chain, in combination with an alternative oxidase and an uncoupling protein <sup>57</sup>. Regarding substrate use, research has mostly focused on glucose consumption. However, this does not fit with the diet of *Acanthamoeba* spp., which consists mostly of bacteria that are rich in lipids and proteins <sup>50,58</sup>. Furthermore, it has been postulated that *Acanthamoeba* spp. have a hydrogenosomal capacity for anaerobic ATP production, although the functionality of this putative pathway was not examined <sup>59</sup>. If a specific aerobic or anaerobic capacity can be revealed or certain nutrient preferences can be determined, this could provide a target that can be blocked to halt *Acanthamoeba* spp. growth and constitute a new treatment strategy. ATP generation is central in energy metabolism, and ATP cannot be taken from the direct environment of the parasite, contrary to other molecules for metabolic purposes. This essential part of energy metabolism is therefore a desirable target for drug development.

## Phylogeny and genotypes

All *Acanthamoeba* spp. are centramoebids and are included in the Amoebozoa supergroup<sup>14</sup>. The phylogeny within *Acanthamoeba* spp. is complicated, as differences within the *Acanthamoeba* species were first assessed by comparing sequences of the nuclear 18S rRNA gene, resulting in 22 sequence types designated T1 to T22<sup>60</sup>. However, substantial differences were found within some sequence types, requiring a higher resolution of typing. This resulted in subtypes, which generated for instance seven subtypes within sequence type T4<sup>60</sup>. In the environment, the majority of sequence types found are T3 and T4<sup>61-63</sup>. Distinct sequence types differ in their pathogenic properties, as both *Acanthamoeba* keratitis and *Acanthamoeba* granulomatous amoebic encephalitis (GAE) are often caused by species of sequence type T4<sup>64-68</sup>.

## *Acanthamoeba* keratitis

One type of infection *Acanthamoeba* spp. can cause in humans, is an eye infection. Acanthamoebae then infect the cornea, causing a keratitis which can lead to blindness in some cases<sup>69</sup>. Major risk factors of acquiring *Acanthamoeba* keratitis (AK) are the inappropriate handling and wearing of contact lenses, and corneal trauma<sup>70</sup>. AK incidence is rising in the Netherlands, affecting 1 in 21,000 soft contact lens wearers<sup>71</sup>. An increase in cases was also observed in Denmark<sup>72</sup> and the United Kingdom<sup>73</sup>. Symptoms include pain, redness of the eye, photophobia and reduced vision<sup>74</sup>. These clinical features are often mistaken for a fungal or herpes simplex infection, which can lead to a delay in diagnosis and appropriate treatment<sup>70</sup>. AK can be diagnosed via culture of corneal scraping on non-nutrient agar plates seeded with *Escherichia coli*, confocal microscopy of the cornea, or molecular techniques such as PCR and loop-mediated isothermal amplification (LAMP) of corneal scraping or other materials<sup>74</sup>. Treatment consists of chlorhexidine, polyhexamethylene biguanide and/or diamidines, but this treatment is lengthy and intensive, and therefore, new treatment options are more than welcome<sup>70</sup>. Furthermore, recurrences after treatment are not unusual, which are attributed to the dormant cyst stage being resistant to therapy.

## *Acanthamoeba* granulomatous amoebic encephalitis

Besides the eye, *Acanthamoeba* spp. can also infect the skin, the lungs and other cavities in the body, from which they can then spread to the brain<sup>26,75</sup>. The exact infectious routes that *Acanthamoeba* spp. can take, will be discussed in chapter 2. Once *Acanthamoeba* has infected the brain, the mortality rate is around 97-98%<sup>76</sup>. *Acanthamoeba* GAE is a very rare disease, with only 83 cases reported in the literature between 1990 and 2018<sup>55</sup>. It should be realised however, that many cases are not reported and diagnosis of *Acanthamoeba* GAE is often missed<sup>55</sup>. Most cases of *Acanthamoeba* GAE occur among immunocompromised patients, which will be discussed in detail in chapter 2. *Acanthamoeba* GAE starts with

headache, nausea, irritability and fever, which progresses to seizures, lethargy, coma and eventually death<sup>55</sup>. No clearly defined treatment regimen exists, but the usual treatments include amphotericin B, trimethoprim-sulfamethoxazole, rifampin and ketoconazole<sup>55</sup>. New treatment options are much needed, because of the very high mortality rate.

## Other free-living amoebae

### ***Balamuthia mandrillaris***

First discovered in the brain of a mandrill baboon that died of meningoencephalitis<sup>77</sup>, *Balamuthia mandrillaris* is an amoeba classified to the Amoebozoa supergroup. *B. mandrillaris*, like *Acanthamoeba*, is a centramoebid, which situates it far from *Naegleria* spp. on a phylogenetic level. *B. mandrillaris* trophozoites measure 12-60 µm, whereas *B. mandrillaris* cysts are 12-30 µm in diameter. The trophozoite shape is characterized as slender, with finger-like projections which they use to feed and move<sup>26</sup>. *B. mandrillaris* has been isolated from hot springs<sup>78</sup> and soil in tropical regions<sup>79</sup> and can cause skin and brain infections. Skin lesions are characterized as indurated plaques with rubbery to stone hardness measuring a few millimetres thick and one to several centimetres wide<sup>80</sup>. A *Balamuthia* skin infection can develop into a brain infection named *Balamuthia* GAE, although this can also develop without a preceding skin infection<sup>80-82</sup>. Manifestation of a brain infection by *B. mandrillaris* usually starts with symptoms such as headache, nausea and fever, which over the course of weeks or months progress to seizures, coma and death in approximately 90% of cases<sup>26,81</sup>. Further details and characteristics of *Balamuthia* GAE will be discussed in chapter 2.

### ***Vermamoeba vermiformis***

Originally named *Hartmanella vermiformis*, *Vermamoeba vermiformis* belongs to the Amoebozoa supergroup, within the family *Hartmannellidae*. The trophozoites of *V. vermiformis* are elongated and slug-like and are usually monopodial, but can become multipodial when changing direction<sup>83,84</sup>. *V. vermiformis* has only been associated with human infection a few times and is therefore not regarded as a pathogenic amoeba<sup>85,86</sup>. *V. vermiformis* is commonly found in fresh surface water, tap water and hospital water systems, where it has been isolated more frequently than *Acanthamoeba* spp.<sup>15,87,88</sup>. Therefore, the interest in *V. vermiformis* has mostly involved the interaction between *V. vermiformis* and other microorganisms. Several examples of bacteria that can survive inside this amoeba are *Legionella pneumophila*, *Pseudomonas aeruginosa* and nontuberculous mycobacteria<sup>89-91</sup>. In this way, *V. vermiformis* has been implicated in the spread and persistence of these microorganisms. Details of these interactions between amoeba and bacteria will be discussed in the next paragraph.

## Interactions with bacteria

The interaction between eukaryotes and prokaryotes is ancient, as eukaryotes are assumed to have evolved from an endosymbiotic event between prokaryotes or from an amitochondriate eukaryote phagocytosing a prokaryote<sup>8</sup>. Either theory encompasses a very close relationship between eukaryotes and prokaryotes, starting about 1.6 billion years ago. Since then, evolution has resulted in different types of relationships between the two types of organisms, ranging from mutualism to commensalism and predation in both directions<sup>3,92,93</sup>. FLA might be one of the most important drivers in this evolutionary race as most FLA feed on bacteria, resulting in a close relationship with prokaryotes. For instance, in soil FLA function as the main predators controlling bacterial populations<sup>94,95</sup>. An important part of the human innate immune system consists of macrophages, which phagocytose bacterial pathogens to prevent disease. However, some bacteria can withstand this process and survive intracellularly. It has been suggested that the strategies that these bacteria employ were developed in response to amoeboid predation<sup>93</sup>. Therefore, FLA are often termed a “training ground” for bacteria to secure intracellular survival in human macrophages<sup>96</sup>. This indicates the important role that FLA play in evolution and in human infections by bacterial pathogens.

Most research on the interaction between FLA and bacteria has focused on *Acanthamoeba* spp., and *Vermamoeba* spp., as these FLA are more permissive for intracellular bacteria than other FLA species. For instance, only a small percentage of *N. lovaniensis* has been shown to ingest *L. pneumophila*, compared to 100% of *Acanthamoeba* spp.<sup>97</sup>. On the bacterial side, most studies have focused on *L. pneumophila*, as this was the first organism with which such a relationship was described<sup>98</sup>. However, more recently a variety of bacteria have been described to interact in many ways<sup>99</sup>. Even more, viruses have also been described to interact with FLA<sup>100</sup>. An overview of interactions between *Acanthamoeba* spp, *Vermamoeba* spp. and bacteria is presented in Table 2.

**Table 2.** Types of interaction between *Acanthamoeba* spp., *Vermamoeba* spp. and different bacterial species.

FLA	Bacterium	Interaction	Reference
<i>Acanthamoeba</i> spp. <i>Vermamoeba</i> spp.	<i>Legionella</i> spp.	Bacterial survival inside trophozoites and cysts Bacterial resuscitation	89,98,101-103
<i>Acanthamoeba</i> spp. <i>Vermamoeba</i> spp.	Mycobacteria	Bacterial survival inside trophozoites and cysts Enhancement of bacterial virulence	104-107
<i>Acanthamoeba</i> spp.	<i>Campylobacter jejuni</i>	Bacterial survival inside trophozoites Bacterial resuscitation	108,109
<i>Acanthamoeba</i> spp.	<i>Staphylococcus aureus</i>	Bacterial survival inside trophozoites and cysts	110
<i>Acanthamoeba</i> spp.	<i>Francisella tularensis</i>	Bacterial survival inside cysts	111
<i>Acanthamoeba</i> spp.	<i>Helicobacter pylori</i>	Enhanced bacterial survival when attached to FLA Bacterial survival inside trophozoites	112,113
<i>Acanthamoeba</i> spp.	<i>Escherichia coli</i>	Bacterial survival inside trophozoites and cysts	114
<i>Acanthamoeba</i> spp.	<i>Salmonella typhimurium</i>	Bacterial survival inside trophozoites	115
<i>Acanthamoeba</i> spp.	<i>Yersinia pestis</i>	Bacterial survival inside trophozoites and cysts	116
<i>Acanthamoeba</i> spp.	<i>Stenotrophomonas maltophilia</i>	Bacterial survival inside trophozoites	117
<i>Acanthamoeba</i> spp.	<i>Vibrio cholera</i>	Bacterial survival inside trophozoites	118
<i>Acanthamoeba</i> spp.	<i>Streptococcus</i> spp.	Bacterial survival inside trophozoites and cysts	119
<i>Acanthamoeba</i> spp.	<i>Shigella</i> spp.	Bacterial survival inside trophozoites	120

### Interaction with *Pseudomonas* spp.

The interaction between *Acanthamoeba* spp. and *Pseudomonas* spp. has been studied in some detail, an overview can be seen in Table 3. It is clear that there is some disagreement as to what happens when *Acanthamoeba* spp. meet *Pseudomonas* spp., as some studies describe harmful effects of *P. aeruginosa* against *Acanthamoeba*, whereas other studies report the other way around. This can partly be explained by different bacterial characteristics (e.g. possession of distinct secretion systems) and co-culture conditions (e.g. multiplicity of infection and growth medium), as this can have a major impact on the interaction. However, many factors that affect this relationship, both bacterial as well as amoebal, are still unknown in this research field.

Table 3. Types of interaction between *Acanthamoeba* spp. and *Pseudomonas* spp.

FLA	Bacterium	Interaction	Reference
<i>Acanthamoeba castellanii</i>	<i>Pseudomonas aeruginosa</i>	Harmful effects of <i>P. aeruginosa</i> against <i>Acanthamoeba</i>	121-124
<i>Acanthamoeba castellanii</i>	<i>Pseudomonas aeruginosa</i>	Increased <i>Acanthamoeba</i> growth in presence of <i>P. aeruginosa</i>	125
<i>Acanthamoeba castellanii</i>	<i>Pseudomonas aeruginosa</i>	Bacterial survival inside trophozoites and cysts	126
<i>Acanthamoeba castellanii</i>	<i>Pseudomonas aeruginosa</i>	Killing of <i>Pseudomonas</i> by <i>Acanthamoeba</i>	127
<i>Acanthamoeba polyphaga</i>	<i>Pseudomonas aeruginosa</i>	Killing of <i>Pseudomonas</i> by <i>Acanthamoeba</i>	128

Within the *Pseudomonas* spp., research has mostly focused on *P. aeruginosa*, as this organism has pathogenic capacities. *P. aeruginosa* can cause a range of infections, both acute and chronic, affecting mostly immunocompromised patients<sup>129</sup>. It is seen as a nosocomial pathogen, as transmission occurs within hospitals through unidentified and presumably persistent sources, most likely in the water distribution system or wastewater drains<sup>130,131</sup>. *Acanthamoeba* spp. can also be present in these environments and the co-occurrence of the two organisms has been documented multiple times<sup>132-134</sup>.

## Antimicrobial resistance

Bacteria, viruses, fungi and parasites can adapt to antimicrobial drugs, resulting in antimicrobial resistance (AMR), which renders treatment ineffective. Although AMR occurs naturally, this process is accelerated by the overuse and misuse of antibiotics<sup>135,136</sup>. The burden of bacterial AMR has been estimated to be 700,000 deaths per year<sup>137</sup>, but more reliable data are needed to accurately measure the magnitude of this problem<sup>138,139</sup>. On a biological level, bacteria acquire resistance to antimicrobials through spontaneous mutations in chromosomal genes, or by horizontal gene transfer (HGT) of antimicrobial resistance genes (ARGs). ARGs can be present on a mobile genetic element (MGE), a segment of DNA that can move within the genome of one bacterium, or from one bacterium to another. An example of an MGE is a plasmid, a small circular piece of DNA that is distinct from the primary bacterial chromosome and can replicate independently. Plasmids have a vital role in the accumulation and transfer of ARGs, mainly in Gram-negative bacteria<sup>140</sup>. However, factors that affect the rate and occurrence of plasmid transfer in the environment are largely unknown.

## Aim and outline of this thesis

Free-living amoebae (FLA) are an understudied subject in microbiology. Many aspects of FLA biology, pathogenesis and interaction with other microorganisms are unknown at this time. The aim of this thesis is to shed light on multiple aspects of this field of research.

In **Chapter 2**, the three different amoebae that can infect the human brain, *N. fowleri*, *Acanthamoeba* spp. and *B. mandrillaris*, are discussed. Many aspects of the diseases that these three amoebae cause are similar, although there are also some intriguing differences between the three. An overview of the clinical aspects, infectious route(s), attachment, invasion and brain infection of each amoeba is reviewed, after which similarities and differences between these three amoebae are discussed.

**Chapter 3** is focused on *Naegleria* spp., as we further exploit the lipid preference of *N. gruberi* that was identified in a previous study<sup>36</sup>. Several currently used drugs inhibit the oxidation of lipids, and the effects of these drugs on the growth of *Naegleria* spp. were determined. A first drug screen was set up with *N. gruberi*, after which successful drugs were also tested on *N. fowleri*. Furthermore, synergy between different drugs was also evaluated. This research aimed to generate new possible treatment options for PAM caused by *N. fowleri*.

Metabolic and drug screening research is extended to *Acanthamoeba castellanii* in **Chapter 4**. We determined that *A. castellanii* trophozoites need oxygen for normal functioning and that they possess a branched electron transport chain. Using radioactively labelled substrates we observed that *A. castellanii* preferred lipids over glucose and amino acids. This lipid preference was also observed in our earlier research on *N. gruberi*. Furthermore, the same drugs that inhibited growth of *N. gruberi* and *N. fowleri* were also active against *A. castellanii*. This work connects fundamental biochemical research to preclinical *in vitro* research and aimed to provide new possible treatment options for GAE caused by *Acanthamoeba* spp.

An international external quality assessment scheme (EQAS) for the detection of *Acanthamoeba* trophozoites and cysts is introduced in **Chapter 5**. We prepared homogenous and stable samples containing different amounts of *Acanthamoeba* trophozoites, cysts and DNA. These samples were distributed to 16 clinical diagnostic laboratories, which reported qualitative as well as quantitative results, together with a description of their methodologies. We found a large variety in reported methodologies and diagnostic performance, which indicated that pre-treatment can influence the

molecular detection of *Acanthamoeba*. Overall, the EQAS is informative for laboratories to identify diagnostic difficulties and improve laboratory procedures.

Another amoeba, *Vermamoeba vermiformis*, is studied in **Chapter 6**, as we identified that it is present in heater-cooler units which are designed to stabilize the blood temperature of patients during heart surgery. These machines are regularly cleaned with potent disinfectants, however *V. vermiformis* could be cultured consistently. Another microorganism, the bacterium *Mycobacterium chimaera*, is also repeatedly present in these machines, despite extensive cleaning. We found that the *V. vermiformis* strain present in the heater cooler can harbour *M. chimaera*, which also originated from this heater cooler.

In **Chapter 7**, research on amoeba-bacterial interactions was extended to a different bacterial-amoebal combination: *A. castellanii* amoebae and *Pseudomonas aeruginosa* bacteria. Both *P. aeruginosa* and *Acanthamoeba* spp. can persist in hospital water systems, and *P. aeruginosa* has been shown to survive inside of *Acanthamoeba* spp. As *Acanthamoeba* spp. are known to be resistant to chlorine, we hypothesised that *Acanthamoeba* can interfere with chlorine disinfection of *P. aeruginosa*. This hypothesis was confirmed, as co-culture and subsequent disinfection of environmental multidrug resistant *P. aeruginosa* and *A. castellanii* revealed that *A. castellanii* can protect *P. aeruginosa* from exposure to chlorine. This research indicates that *Acanthamoeba* spp. can contribute to the persistent colonization of *P. aeruginosa* of water systems after chlorine treatment.

The interaction between *A. castellanii* and *P. aeruginosa* was further studied in **Chapter 8**, with the focus on transfer of antimicrobial resistance genes. We mimicked an environmental biofilm containing *P. aeruginosa*, *P. oleovorans* and *A. castellanii* *in vitro* and observed increased transfer of a carbapenem-resistance gene from one *Pseudomonas* species to the other in the presence of *A. castellanii*. Furthermore, both *Pseudomonads* were found inside of *A. castellanii*, indicating that horizontal gene transfer of the antimicrobial resistance gene could have taken place in this way.

The conclusions and implications of these studies are discussed in **Chapter 9**.

## References

- 1 Lane, N. The unseen world: reflections on Leeuwenhoek (1677) 'Concerning little animals'. *Philos Trans R Soc B* **370** (2015).
- 2 Parfrey, L. W., Lahr, D. J., Knoll, A. H. & Katz, L. A. Estimating the timing of early eukaryotic diversification with multigene molecular clocks. *Proc Natl Acad Sci U S A* **108**, 13624-13629 (2011).
- 3 Samba-Louaka, A., Delafont, V., Rodier, M. H., Cateau, E. & Héchard, Y. Free-living amoebae and squatters in the wild: ecological and molecular features. *FEMS Microbiol Rev* **43**, 415-434 (2019).
- 4 McAlpine, D. & McAlpine, A. N. *Biological atlas: a guide to the practical study of plants and animals*. (Johnston, 1881).
- 5 Bory de Saint-Vincent, J-B. *Essai d'une classification des animaux microscopiques*. (L'imprimerie de Mme Veuve Agasse, Paris, La France, 1826).
- 6 Javaux, E. J., Knoll, A. H. & Walter, M. R. Morphological and ecological complexity in early eukaryotic ecosystems. *Nature* **412**, 66-69, (2001).
- 7 Martin, W. F., Tielens, A. G. M., Mentel, M., Garg, S. G. & Gould, S. B. The physiology of phagocytosis in the context of mitochondrial origin. *Microbiol Mol Biol Rev* **81** e00008-17 (2017).
- 8 Martin, W. F., Tielens, A. G. M. & Mentel, M. *Mitochondria and anaerobic energy metabolism in eukaryotes*. (De Gruyter, 2020).
- 9 Schuster, F. L. & Visvesvara, G. S. Free-living amoebae as opportunistic and non-opportunistic pathogens of humans and animals. *Int J Parasitol* **34**, 1001-1027 (2004).
- 10 Bass, D. *et al.* Phylogeny of novel naked Filose and Reticulose Cercozoa: Granofilosea cl. n. and Proteomyxidea revised. *Protist* **160**, 75-109 (2009).
- 11 Brown, M. W., Spiegel, F. W. & Silberman, J. D. Phylogeny of the "forgotten" cellular slime mold, *Fonticula alba*, reveals a key evolutionary branch within Opisthokonta. *Mol Biol Evol* **26**, 2699-2709 (2009).
- 12 Adl, S. M. *et al.* Diversity, nomenclature, and taxonomy of protists. *Syst Biol* **56**, 684-689 (2007).
- 13 Kang, S. *et al.* Between a pod and a hard test: the deep evolution of amoebae. *Mol Biol Evol* **34**, 2258-2270 (2017).
- 14 Cavalier-Smith, T. *et al.* Multigene phylogeny resolves deep branching of Amoebozoa. *Mol Phylogenet Evol* **83**, 293-304 (2015).
- 15 Kuiper, M. W. *et al.* Quantitative detection of the free-living amoeba *Hartmannella vermiformis* in surface water by using real-time PCR. *Appl Environ Microbiol* **72**, 5750-5756, (2006).
- 16 Oliverio, A. M. *et al.* The ecology and diversity of microbial eukaryotes in geothermal springs. *The ISME Journal* **12**, 1918-1928, (2018).
- 17 Massana, R. *et al.* Marine protist diversity in European coastal waters and sediments as revealed by high-throughput sequencing. *Environ Microbiol* **17**, 4035-4049 (2015).
- 18 Garner, E. *et al.* Microbial Ecology and Water Chemistry Impact Regrowth of Opportunistic Pathogens in Full-Scale Reclaimed Water Distribution Systems. *Environ Sci Technol* **52**, 9056-9068 (2018).
- 19 Thomas, V., Herrera-Rimann, K., Blanc, D. S. & Greub, G. Biodiversity of amoebae and amoeba-resisting bacteria in a hospital water network. *Appl Environ Microbiol* **72**, 2428-2438 (2006).
- 20 Muchesa, P. *et al.* Coexistence of free-living amoebae and bacteria in selected South African hospital water distribution systems. *Parasitol Res* **116**, 155-165 (2017).
- 21 Geisen, S. *et al.* Metatranscriptomic census of active protists in soils. *The ISME Journal* **9**, 2178-2190, (2015).
- 22 Coelho, F. J. R. C. *et al.* Integrated analysis of bacterial and microeukaryotic communities from differentially active mud volcanoes in the Gulf of Cadiz. *Sci Rep* **6**, 35272, (2016).

- 23 Fouque, E. *et al.* Cellular, biochemical, and molecular changes during encystment of free-living amoebae. *Eukaryot Cell* **11**, 382-387 (2012).
- 24 Brugerolle, G. & Simpson, A. G. The flagellar apparatus of heteroloboseans. *J Eukaryot Microbiol* **51**, 96-107 (2004).
- 25 De Jonckheere, J. F. Origin and evolution of the worldwide distributed pathogenic amoeboflagellate *Naegleria fowleri*. *Infect Genet Evol* **11**, 1520-1528 (2011).
- 26 Visvesvara, G. S., Moura, H. & Schuster, F. L. Pathogenic and opportunistic free-living amoebae: *Acanthamoeba* spp., *Balamuthia mandrillaris*, *Naegleria fowleri*, and *Sappinia diploidea*. *FEMS Immunol Med Microbiol* **50**, 1-26 (2007).
- 27 Maciver, S. K., Piñero, J. E. & Lorenzo-Morales, J. Is *Naegleria fowleri* an emerging parasite? *Trends Parasitol* **36**, 19-28, (2020).
- 28 Zaongo, S. D., Shaio, M. F. & Ji, D. D. Effects of culture media on *Naegleria fowleri* growth at different temperatures. *J Parasitol* **104**, 451-456 (2018).
- 29 Gupta, S. & Das, S. R. Stock cultures of free-living amebas: effect of temperature on viability and pathogenicity. *J Parasitol* **85**, 137-139 (1999).
- 30 Huizinga, H. W. & McLaughlin, G. L. Thermal ecology of *Naegleria fowleri* from a power plant cooling reservoir. *Appl Environ Microbiol* **56**, 2200-2205 (1990).
- 31 Cope, J. R. *et al.* Primary amebic meningoencephalitis associated with rafting on an artificial whitewater river: case report and environmental investigation. *Clin Infect Dis* **66**, 548-553 (2018).
- 32 Vugia, D. J. *et al.* Notes from the field: fatal *Naegleria fowleri* meningoencephalitis after swimming in hot spring water - California, 2018. *MMWR Morb Mortal Wkly Rep* **68**, 793-794 (2019).
- 33 Retana Moreira, L., Zamora Rojas, L., Grijalba Murillo, M., Molina Castro, S. E. & Abrahams Sandí, E. Primary amebic meningoencephalitis related to groundwater in Costa Rica: diagnostic confirmation of three cases and environmental investigation. *Pathogens* **9** (2020).
- 34 Cope, J. R. *et al.* The first association of a primary amebic meningoencephalitis death with culturable *Naegleria fowleri* in tap water from a US treated public drinking water system. *Clin Infect Dis* **60**, e36-42 (2015).
- 35 Miller, H. C. *et al.* Preferential feeding in *Naegleria fowleri*; intracellular bacteria isolated from amoebae in operational drinking water distribution systems. *Water Res* **141**, 126-134, (2018).
- 36 Bexkens, M. L. *et al.* Lipids are the preferred substrate of the protist *Naegleria gruberi*, relative of a human brain pathogen. *Cell Rep* **25**, 537-543 e533, (2018).
- 37 Siddiqui, R., Ali, I. K. M., Cope, J. R. & Khan, N. A. Biology and pathogenesis of *Naegleria fowleri*. *Acta Trop* **164**, 375-394 (2016).
- 38 Alberts, B. *et al.* *Molecular Biology of the Cell (5th ed.)*. (W.W. Norton & Company, 2008).
- 39 Cope, J. R. & Ali, I. K. Primary amebic meningoencephalitis: what have we learned in the last 5 years? *Curr Infect Dis Rep* **18**, 31 (2016).
- 40 Jarolim, K. L., McCosh, J. K., Howard, M. J. & John, D. T. A light microscopy study of the migration of *Naegleria fowleri* from the nasal submucosa to the central nervous system during the early stage of primary amebic meningoencephalitis in mice. *J Parasitol* **86**, 50-55 (2000).
- 41 Yoder, J. S., Eddy, B. A., Visvesvara, G. S., Capewell, L. & Beach, M. J. The epidemiology of primary amoebic meningoencephalitis in the USA, 1962-2008. *Epidemiol Infect* **138**, 968-975 (2010).
- 42 Stowe, R. C. *et al.* Primary amebic meningoencephalitis in children: a report of two fatal cases and review of the literature. *Pediatr Neurol* **70**, 75-79 (2017).
- 43 Shakoor, S. *et al.* Primary amebic meningoencephalitis caused by *Naegleria fowleri*, Karachi, Pakistan. *Emerg Infect Dis* **17**, 258-261 (2011).
- 44 Kemple, S. K. *et al.* Fatal *Naegleria fowleri* infection acquired in Minnesota: possible expanded range of a deadly thermophilic organism. *Clin Infect Dis* **54**, 805-809 (2012).
- 45 Król-Turmińska, K. & Olender, A. Human infections caused by free-living amoebae. *Ann Agric Environ Med* **24**, 254-260 (2017).

- 46 Zhang, L. L. *et al.* Identification and molecular typing of *Naegleria fowleri* from a patient with primary amebic meningoencephalitis in China. *Int J Infect Dis* **72**, 28-33 (2018).
- 47 Martínez-Castillo, M. *et al.* *Naegleria fowleri* after 50 years: is it a neglected pathogen? *J Med Microbiol* **65**, 885-896 (2016).
- 48 Baig, A. M. Pathogenesis of amoebic encephalitis: Are the amoebae being credited to an 'inside job' done by the host immune response? *Acta Trop* **148**, 72-76 (2015).
- 49 Moseman, E. A. Battling brain-eating amoeba: Enigmas surrounding immunity to *Naegleria fowleri*. *PLoS Pathog* **16**, e1008406 (2020).
- 50 Khan, N. A. *Acanthamoeba*: biology and increasing importance in human health. *FEMS Microbiol Rev* **30**, 564-595 (2006).
- 51 Maschio, V. J. *et al.* *Acanthamoeba* T4, T5 and T11 isolated from mineral water bottles in southern Brazil. *Curr Microbiol* **70**, 6-9 (2015).
- 52 Gray, T. B., Cursons, R. T., Sherwan, J. F. & Rose, P. R. *Acanthamoeba*, bacterial, and fungal contamination of contact lens storage cases. *Br J Ophthalmol* **79**, 601-605 (1995).
- 53 Castro-Artavia, E., Retana-Moreira, L., Lorenzo-Morales, J. & Abrahams-Sandí, E. Potentially pathogenic *Acanthamoeba* genotype T4 isolated from dental units and emergency combination showers. *Mem Inst Oswaldo Cruz* **112**, 817-821 (2017).
- 54 Kilvington, S. *et al.* *Acanthamoeba* keratitis: the role of domestic tap water contamination in the United Kingdom. *Invest Ophthalmol Vis Sci* **45**, 165-169 (2004).
- 55 Kalra, S. K., Sharma, P., Shyam, K., Tejan, N. & Ghoshal, U. *Acanthamoeba* and its pathogenic role in granulomatous amebic encephalitis. *Exp Parasitol* **208**, 107788 (2020).
- 56 Nielsen, M. K., Nielsen, K., Hjortdal, J. & Sørensen, U. B. Temperature limitation may explain the containment of the trophozoites in the cornea during *Acanthamoeba castellanii* keratitis. *Parasitol Res* **113**, 4349-4353 (2014).
- 57 Czarna, M. & Jarmuszkiewicz, W. Activation of alternative oxidase and uncoupling protein lowers hydrogen peroxide formation in amoeba *Acanthamoeba castellanii* mitochondria. *FEBS Lett* **579**, 3136-3140 (2005).
- 58 Anupama & Ravindra, P. Value-added food: single cell protein. *Biotechnol Adv* **18**, 459-479 (2000).
- 59 Leger, M. M., Gawryluk, R. M., Gray, M. W. & Roger, A. J. Evidence for a hydrogenosomal-type anaerobic ATP generation pathway in *Acanthamoeba castellanii*. *PLoS One* **8**, e69532 (2013).
- 60 Fuerst, P. A. & Booton, G. C. Species, sequence types and alleles: dissecting genetic variation in *Acanthamoeba*. *Pathogens* **9** (2020).
- 61 Leal, D. A. G. *et al.* Genotypic characterization and assessment of infectivity of human waterborne pathogens recovered from oysters and estuarine waters in Brazil. *Water Res* **137**, 273-280 (2018).
- 62 Geisen, S., Fiore-Donno, A. M., Walochnik, J. & Bonkowski, M. *Acanthamoeba* everywhere: high diversity of *Acanthamoeba* in soils. *Parasitol Res* **113**, 3151-3158 (2014).
- 63 Niyiyati, M. *et al.* Genotyping of *Acanthamoeba* isolates from clinical and environmental specimens in Iran. *Exp Parasitol* **121**, 242-245 (2009).
- 64 Yera, H. *et al.* The genotypic characterisation of *Acanthamoeba* isolates from human ocular samples. *Br J Ophthalmol* **92**, 1139-1141 (2008).
- 65 De Jonckheere, J. F. Epidemiological typing of *Acanthamoeba* strains isolated from keratitis cases in Belgium. *Bull Soc Belge Ophtalmol*, 27-33 (2003).
- 66 Taher, E. E., Méabed, E. M. H., Abdallah, I. & Abdel Wahed, W. Y. *Acanthamoeba* keratitis in noncompliant soft contact lenses users: Genotyping and risk factors, a study from Cairo, Egypt. *J Infect Public Health* **11**, 377-383 (2018).
- 67 Behera, H. S., Satpathy, G. & Tripathi, M. Isolation and genotyping of *Acanthamoeba* spp. from *Acanthamoeba* meningitis/ meningoencephalitis (AME) patients in India. *Parasit Vectors* **9**, 442 (2016).

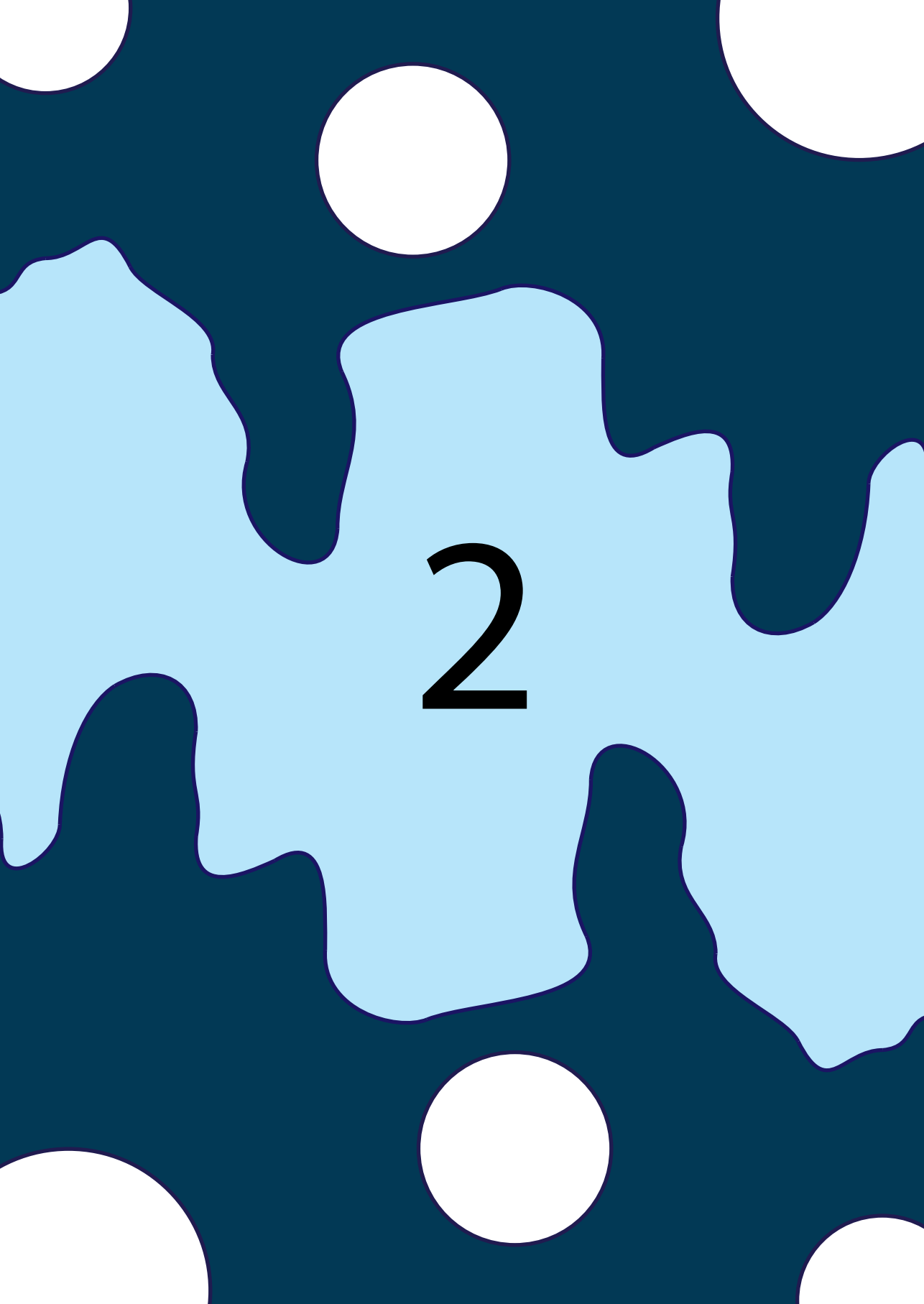
- 68 Booton, G. C., Visvesvara, G. S., Byers, T. J., Kelly, D. J. & Fuerst, P. A. Identification and distribution of *Acanthamoeba* species genotypes associated with nonkeratitis infections. *J Clin Microbiol* **43**, 1689-1693 (2005).
- 69 Bataillie, S., Van Ginderdeuren, R., Van Calster, J., Foets, B. & Delbeke, H. How a devastating case of *Acanthamoeba* sclerokeratitis ended up with serious systemic sequelae. *Case Rep Ophthalmol* **11**, 348-355 (2020).
- 70 Maycock, N. J. & Jayaswal, R. Update on *Acanthamoeba* keratitis: diagnosis, treatment, and outcomes. *Cornea* **35**, 713-720 (2016).
- 71 Randag, A. C. *et al.* The rising incidence of *Acanthamoeba* keratitis: A 7-year nationwide survey and clinical assessment of risk factors and functional outcomes. *PLoS One* **14**, e0222092 (2019).
- 72 Nielsen, S. E., Ivarsen, A. & Hjortdal, J. Increasing incidence of *Acanthamoeba* keratitis in a large tertiary ophthalmology department from year 1994 to 2018. *Acta Ophthalmol* (2019).
- 73 Carnt, N. *et al.* *Acanthamoeba* keratitis: confirmation of the UK outbreak and a prospective case-control study identifying contributing risk factors. *British Journal of Ophthalmology* **102**, 1621, (2018).
- 74 de Lacerda, A. G. & Lira, M. *Acanthamoeba* keratitis: a review of biology, pathophysiology and epidemiology. *Ophthalmic Physiol Opt* (2020).
- 75 Guirguis, D., Kashat, L., Moradi, S. & Bonaiuto, G. S. An unusual source of sinonasal disease in an immunocompromised patient: a case report of the clinical presentation, diagnosis, and treatment of *Acanthamoeba* rhinosinusitis. *Ear Nose Throat J*, 145561320968936 (2020).
- 76 Kot, K., Lanocha-Arendarczyk, N. A. & Kosik-Bogacka, D. I. Amoebas from the genus *Acanthamoeba* and their pathogenic properties. *Ann Parasitol* **64**, 299-308 (2018).
- 77 Visvesvara, G. S., Schuster, F. L. & Martinez, A. J. *Balamuthia mandrillaris*, N. G., N. Sp., agent of amebic meningoencephalitis in humans and other animals. *J Eukaryot Microbiol* **40**, 504-514 (1993).
- 78 Latifi, A. R. *et al.* Presence of *Balamuthia mandrillaris* in hot springs from Mazandaran province, northern Iran. *Epidemiol Infect* **144**, 2456-2461 (2016).
- 79 Cabello-Vílchez, A. M. *et al.* The isolation of *Balamuthia mandrillaris* from environmental sources from Peru. *Parasitol Res* **113**, 2509-2513 (2014).
- 80 Wang, L. *et al.* *Balamuthia mandrillaris* infection in China: A retrospective report of 28 cases. *Emerg Microbes Infect* **9**, 2348-2357 (2020).
- 81 Cope, J. R. *et al.* The epidemiology and clinical features of *Balamuthia mandrillaris* disease in the United States, 1974-2016. *Clin Infect Dis* **68**, 1815-1822 (2019).
- 82 van der Beek, N. A. *et al.* Fatal *Balamuthia mandrillaris* Meningoencephalitis in the Netherlands after Travel to The Gambia. *Emerg Infect Dis* **21**, 896-898 (2015).
- 83 Fouque, E. *et al.* Morphological study of the encystment and excystment of *Vermamoeba vermiformis* revealed original traits. *J Eukaryot Microbiol* **62**, 327-337 (2015).
- 84 Delafont, V., Rodier, M. H., Maisonneuve, E. & Cateau, E. *Vermamoeba vermiformis*: a free-living amoeba of interest. *Microb Ecol* **76**, 991-1001 (2018).
- 85 Abedkhozasteh, H. *et al.* First report of *Hartmannella* keratitis in a cosmetic soft contact lens wearer in Iran. *Iran J Parasitol* **8**, 481-485 (2013).
- 86 Centeno, M. *et al.* *Hartmannella vermiformis* isolated from the cerebrospinal fluid of a young male patient with meningoencephalitis and bronchopneumonia. *Arch Med Res* **27**, 579-586 (1996).
- 87 Armand, B., Motazedian, M. H. & Asgari, Q. Isolation and identification of pathogenic free-living amoeba from surface and tap water of Shiraz City using morphological and molecular methods. *Parasitol Res* **115**, 63-68 (2016).
- 88 Pagnier, I., Valles, C., Raoult, D. & La Scola, B. Isolation of *Vermamoeba vermiformis* and associated bacteria in hospital water. *Microb Pathog* **80**, 14-20 (2015).

- 89 Murga, R. *et al.* Role of biofilms in the survival of *Legionella pneumophila* in a model potable-water system. *Microbiology (Reading)* **147**, 3121-3126 (2001).
- 90 Cateau, E., Imbert, C. & Rodier, M. H. *Hartmanella vermiformis* can be permissive for *Pseudomonas aeruginosa*. *Lett Appl Microbiol* **47**, 475-477 (2008).
- 91 Delafont, V. *et al.* First evidence of amoebae-mycobacteria association in drinking water network. *Environ Sci Technol* **48**, 11872-11882 (2014).
- 92 Wang, Z. & Wu, M. Comparative genomic analysis of *Acanthamoeba* endosymbionts highlights the role of amoebae as a “melting pot” shaping the *Rickettsiales* evolution. *Genome Biol Evol* **9**, 3214-3224 (2017).
- 93 Casadevall, A. Evolution of intracellular pathogens. *Annu Rev Microbiol* **62**, 19-33 (2008).
- 94 Rodríguez-Zaragoza, S. Ecology of free-living amoebae. *Crit Rev Microbiol* **20**, 225-241 (1994).
- 95 Adl, M. S. & Gupta, V. S. Protists in soil ecology and forest nutrient cycling. *Can. J. For. Res.* **36**, 1805-1817, (2006).
- 96 Molmeret, M., Horn, M., Wagner, M., Santic, M. & Abu Kwaik, Y. Amoebae as training grounds for intracellular bacterial pathogens. *Appl Environ Microbiol* **71**, 20-28 (2005).
- 97 Declerck, P. *et al.* Impact of non-*Legionella* bacteria on the uptake and intracellular replication of *Legionella pneumophila* in *Acanthamoeba castellanii* and *Naegleria lovaniensis*. *Microb Ecol* **50**, 536-549 (2005).
- 98 Rowbotham, T. J. Preliminary report on the pathogenicity of *Legionella pneumophila* for freshwater and soil amoebae. *J Clin Pathol* **33**, 1179-1183, (1980).
- 99 Goñi, P., Fernández, M. T. & Rubio, E. Identifying endosymbiont bacteria associated with free-living amoebae. *Environ Microbiol* **16**, 339-349 (2014).
- 100 Balczun, C. & Scheid, P. L. Free-living amoebae as hosts for and vectors of intracellular microorganisms with public health significance. *Viruses* **9**, 65 (2017).
- 101 Epalle, T. *et al.* Viable but not culturable forms of *Legionella pneumophila* generated after heat shock treatment are infectious for macrophage-like and alveolar epithelial cells after resuscitation on *Acanthamoeba polyphaga*. *Microb Ecol* **69**, 215-224 (2015).
- 102 Kilvington, S. & Price, J. Survival of *Legionella pneumophila* within cysts of *Acanthamoeba polyphaga* following chlorine exposure. *J Appl Bacteriol* **68**, 519-525 (1990).
- 103 Steinert, M., Emödy, L., Amann, R. & Hacker, J. Resuscitation of viable but nonculturable *Legionella pneumophila* Philadelphia JR32 by *Acanthamoeba castellanii*. *Appl Environ Microbiol* **63**, 2047-2053 (1997).
- 104 Adékambi, T., Ben Salah, S., Khlif, M., Raoult, D. & Drancourt, M. Survival of environmental mycobacteria in *Acanthamoeba polyphaga*. *Appl Environ Microbiol* **72**, 5974-5981 (2006).
- 105 Cirillo, J. D., Falkow, S., Tompkins, L. S. & Bermudez, L. E. Interaction of *Mycobacterium avium* with environmental amoebae enhances virulence. *Infect Immun* **65**, 3759-3767 (1997).
- 106 Drancourt, M. Looking in amoebae as a source of mycobacteria. *Microb Pathog* **77**, 119-124 (2014).
- 107 Sanchez-Hidalgo, A., Obregón-Henao, A., Wheat, W. H., Jackson, M. & Gonzalez-Juarrero, M. *Mycobacterium bovis* hosted by free-living-amoebae permits their long-term persistence survival outside of host mammalian cells and remain capable of transmitting disease to mice. *Environ Microbiol* **19**, 4010-4021 (2017).
- 108 Axelsson-Olsson, D., Waldenström, J., Broman, T., Olsen, B. & Holmberg, M. Protozoan *Acanthamoeba polyphaga* as a potential reservoir for *Campylobacter jejuni*. *Appl Environ Microbiol* **71**, 987-992 (2005).
- 109 Maal-Bared, R., Dixon, B. & Axelsson-Olsson, D. Fate of internalized *Campylobacter jejuni* and *Mycobacterium avium* from encysted and excysted *Acanthamoeba polyphaga*. *Exp Parasitol* **199**, 104-110 (2019).
- 110 Cardas, M., Khan, N. A. & Alsam, S. *Staphylococcus aureus* exhibit similarities in their interactions with *Acanthamoeba* and ThP1 macrophage-like cells. *Exp Parasitol* **132**, 513-518, (2012).

- 111 El-Etr, S. H. *et al.* *Francisella tularensis* type A strains cause the rapid encystment of *Acanthamoeba castellanii* and survive in amoebal cysts for three weeks postinfection. *Appl Environ Microbiol* **75**, 7488-7500 (2009).
- 112 Hojo, F. *et al.* *Acanthamoeba castellanii* supports extracellular survival of *Helicobacter pylori* in co-culture. *J Infect Chemother* **26**, 946-954 (2020).
- 113 Moreno-Mesonero, L., Moreno, Y., Alonso, J. L. & Ferrús, M. A. DVC-FISH and PMA-qPCR techniques to assess the survival of *Helicobacter pylori* inside *Acanthamoeba castellanii*. *Res Microbiol* **167**, 29-34 (2016).
- 114 Siddiqui, R., Malik, H., Sagheer, M., Jung, S. Y. & Khan, N. A. The type III secretion system is involved in *Escherichia coli* K1 interactions with *Acanthamoeba*. *Exp Parasitol* **128**, 409-413 (2011).
- 115 Gaze, W. H., Burroughs, N., Gallagher, M. P. & Wellington, E. M. Interactions between *Salmonella typhimurium* and *Acanthamoeba polyphaga*, and observation of a new mode of intracellular growth within contractile vacuoles. *Microb Ecol* **46**, 358-369 (2003).
- 116 Benavides-Montaño, J. A. & Vadyvaloo, V. *Yersinia pestis* resists predation by *Acanthamoeba castellanii* and exhibits prolonged intracellular survival. *Appl Environ Microbiol* **83**, e00593-17 (2017).
- 117 Denet, E., Vasselon, V., Burdin, B., Nazaret, S. & Favre-Bonté, S. Survival and growth of *Stenotrophomonas maltophilia* in free-living amoebae (FLA) and bacterial virulence properties. *PLoS One* **13**, e0192308 (2018).
- 118 Van der Henst, C. *et al.* Molecular insights into *Vibrio cholerae*'s intra-amoebal host-pathogen interactions. *Nat Commun* **9**, 3460 (2018).
- 119 Siddiqui, R., Yee Ong, T. Y., Jung, S. Y. & Khan, N. A. *Acanthamoeba castellanii* interactions with *Streptococcus pneumoniae* and *Streptococcus pyogenes*. *Exp Parasitol* **183**, 128-132 (2017).
- 120 Saeed, A., Abd, H., Edvinsson, B. & Sandström, G. *Acanthamoeba castellanii* an environmental host for *Shigella dysenteriae* and *Shigella sonnei*. *Arch Microbiol* **191**, 83-88 (2009).
- 121 Abd, H. *et al.* *Pseudomonas aeruginosa* utilises its type III secretion system to kill the free-living amoeba *Acanthamoeba castellanii*. *J Eukaryot Microbiol* **55**, 235-243 (2008).
- 122 Cengiz, A. M., Harmis, N. & Stapleton, F. Co-incubation of *Acanthamoeba castellanii* with strains of *Pseudomonas aeruginosa* alters the survival of amoeba. *Clin Exp Ophthalmol* **28**, 191-193 (2000).
- 123 Lee, X., Reimann, C., Greub, G., Sufrin, J. & Croxatto, A. The *Pseudomonas aeruginosa* toxin L-2-amino-4-methoxy-trans-3-butenic acid inhibits growth and induces encystment in *Acanthamoeba castellanii*. *Microbes Infect* **14**, 268-272 (2012).
- 124 Matz, C. *et al.* *Pseudomonas aeruginosa* uses type III secretion system to kill biofilm-associated amoebae. *Isme J* **2**, 843-852 (2008).
- 125 de Moraes, J. & Alfieri, S. C. Growth, encystment and survival of *Acanthamoeba castellanii* grazing on different bacteria. *FEMS Microbiol Ecol* **66**, 221-229 (2008).
- 126 Siddiqui, R., Lakhundi, S. & Khan, N. A. Interactions of *Pseudomonas aeruginosa* and *Corynebacterium* spp. with non-phagocytic brain microvascular endothelial cells and phagocytic *Acanthamoeba castellanii*. *Parasitol Res* **114**, 2349-2356 (2015).
- 127 Willcox, M. D., Low, R., Hon, J. & Harmis, N. Does *Acanthamoeba* protect *Pseudomonas aeruginosa* from the bactericidal effects of contact lens disinfecting systems? *Aust N Z J Ophthalmol* **26**, S32-35 (1998).
- 128 Weitere, M., Bergfeld, T., Rice, S. A., Matz, C. & Kjelleberg, S. Grazing resistance of *Pseudomonas aeruginosa* biofilms depends on type of protective mechanism, developmental stage and protozoan feeding mode. *Environ Microbiol* **7**, 1593-1601 (2005).
- 129 Moradali, M. F., Ghods, S. & Rehm, B. H. *Pseudomonas aeruginosa* lifestyle: A paradigm for adaptation, survival, and persistence. *Front Cell Infect Microbiol* **7**, 39 (2017).
- 130 Voor In 't Holt, A. F. *et al.* VIM-positive *Pseudomonas aeruginosa* in a large tertiary care hospital: matched case-control studies and a network analysis. *Antimicrob Resist Infect Control* **7**, 32 (2018).

- 131 Walker, J. & Moore, G. *Pseudomonas aeruginosa* in hospital water systems: biofilms, guidelines, and practicalities. *J. Hosp. Infect.* **89**, 324-327, (2015).
- 132 Gomes, T. S. *et al.* Presence and interaction of free-living amoebae and amoeba-resisting bacteria in water from drinking water treatment plants. *Sci Total Environ* **719**, 137080 (2020).
- 133 Garcia, A. *et al.* Identification of free-living amoebae and amoeba-associated bacteria from reservoirs and water treatment plants by molecular techniques. *Environ Sci Technol* **47**, 3132-3140 (2013).
- 134 Michel, R., Burghardt, H. & Bergmann, H. *Acanthamoebae* isolated from a highly contaminated drinking-water system of a hospital exhibited natural infections with *Pseudomonas aeruginosa*. *Zentralbl Hyg Umweltmed* **196**, 532-544 (1995).
- 135 Van Boeckel, T. P. *et al.* Reducing antimicrobial use in food animals. *Science* **357**, 1350 (2017).
- 136 Mladenovic-Antic, S. *et al.* Correlation between antimicrobial consumption and antimicrobial resistance of *Pseudomonas aeruginosa* in a hospital setting: a 10-year study. *J Clin Pharm Ther* **41**, 532-537 (2016).
- 137 O'Neill, J. Tackling Drug-Resistant Infections Globally: final report and recommendations - The review on antimicrobial resistance. <https://wellcomecollection.org/works/thvwsuba> (2016).
- 138 Hay, S. I. *et al.* Measuring and mapping the global burden of antimicrobial resistance. *BMC Medicine* **16**, 78, (2018).
- 139 World Health Organization. Antimicrobial Resistance: Global Report on Surveillance 2014. (2014).
- 140 Vrancianu, C. O., Popa, L. I., Bleotu, C. & Chifiriuc, M. C. Targeting Plasmids to Limit Acquisition and Transmission of Antimicrobial Resistance. *Front Microbiol* **11**, 761 (2020).





2

# CHAPTER 2

---

## Three encephalitis-causing amoebae and their distinct interactions with the host

Maarten J. Sarink<sup>1</sup>, Nadia L. van der Meijs<sup>1</sup>, Kristin Denzer<sup>2</sup>, Leo Koenderman<sup>2,3</sup>,  
Aloysius G.M. Tielens<sup>1</sup>, Jaap J. van Hellemond<sup>1</sup>

<sup>1</sup> Erasmus MC, University Medical Center Rotterdam, Department of Medical Microbiology and Infectious Diseases, Rotterdam, the Netherlands

<sup>2</sup> Center for Translational Immunology (CTI), University Medical Center Utrecht, Utrecht, the Netherlands

<sup>3</sup> Department of Respiratory Medicine, University Medical Center Utrecht, Utrecht, the Netherlands.

Trends in Parasitology. Volume 38, March 2022



**On the cover:** The cover shows three free-living amoebae that can cause human brain infections: *Naegleria fowleri* (top), *Balamuthia mandrillaris* (middle) and *Acanthamoeba castellanii* (bottom). Although infections by these “brain-eating” amoebae cause similar clinical symptoms, the brain inflammation and disease course are quite distinct. So far, little is known about the factors that determine the pathogenicity of amoebae and why these three amoebae cause different types of encephalitis. In this issue of *Trends in Parasitology*, Sarink *et al.* discuss possible host and parasite factors that could contribute to the differences among the distinct types of amoebic encephalitis. Cover credit: Getty Images/Kateryna Kon/Science Photo Library, Elsevier.

## Abstract

*Naegleria fowleri*, *Balamuthia mandrillaris*, and *Acanthamoeba* spp. can cause devastating brain infections in humans which almost always result in death. The symptoms of the three infections overlap, but brain inflammation and the course of the disease differ, depending on the amoeba that is responsible. Understanding the differences between these amoebae can result in the development of strategies to prevent and treat these infections. Recently, numerous scientific advancements have been made in the understanding of pathogenicity mechanisms in general, and the basic biology, epidemiology, and the human immune response towards these amoebae in particular. In this review, we combine this knowledge and aim to identify which factors can explain the differences between the lethal brain infections caused by *N. fowleri*, *B. mandrillaris*, and *Acanthamoeba* spp.

### Highlights

- *Acanthamoeba* spp. are most abundant in nature, but they cause fewer brain infections in humans than do *Naegleria fowleri* and *Balamuthia mandrillaris*.
- *N. fowleri* is a pathogen that can infect immunocompetent individuals, while *Acanthamoeba* and *B. mandrillaris* are opportunistic amoebae that predominantly infect immunocompromised patients.
- The neuro-olfactory route provides *N. fowleri* quick access to the brain and results in an impaired adaptive immune response, causing a very rapid disease course.
- *Acanthamoeba* evokes a mixed-type immune response with limited inflammation, whereas *N. fowleri* evokes a proinflammatory immune response with extensive brain-tissue damage.

## Free-living amoebae that go for the brain

**Free-living amoebae** (FLA) (see **Glossary**) are unicellular eukaryotes ubiquitously present in nature. Human brain infections by these amoebae have devastating effects and almost always result in death. Three different FLA are responsible for the human brain: *Naegleria fowleri*, *Acanthamoeba* spp. and *Balamuthia mandrillaris* <sup>1</sup>. *N. fowleri* causes **primary amoebic meningoencephalitis** (PAM), a rapid and acute infection characterized by necrotic and haemorrhagic patches in the brain <sup>2-4</sup>. In contrast, *B. mandrillaris* and *Acanthamoeba* spp. cause chronic but fatal **granulomatous amoebic encephalitis** (GAE), which has a slower onset and disease progression <sup>3-6</sup>. Although the brain infections by these three free-living amoebae cause similar clinical symptoms, the brain inflammation and disease course are quite distinct (summarized in Table 1). A few brain infections by FLA in other animals are reported, but not well documented.

It is currently incompletely understood why these different free-living amoebae cause a different type of encephalitis. The host-parasite interaction is probably an important factor, as recent advancements have shown that the immune response to the three amoeba genera is different. *N. fowleri* induces an acute inflammatory response, mainly involving neutrophils and macrophages, the production of proinflammatory **cytokines** and substantial tissue damage <sup>7</sup>. In contrast, the immune response to *Acanthamoeba* spp. and *B. mandrillaris* involves mainly macrophages and T cells, and induces the formation of **granulomas** <sup>3,5</sup>. So far, little is known about the factors that determine the pathogenicity of the amoebae and the host factors that influence the pathogenicity <sup>5-7</sup>. Comparison of the epidemiology, pathogenicity and clinical features of the three FLA can help to dissect the differences in disease between the three amoebic infections. This review aims to discuss which possible host and parasite factors can contribute to the differences between amoebic encephalitis caused by *N. fowleri*, *Acanthamoeba* spp. and *B. mandrillaris*.

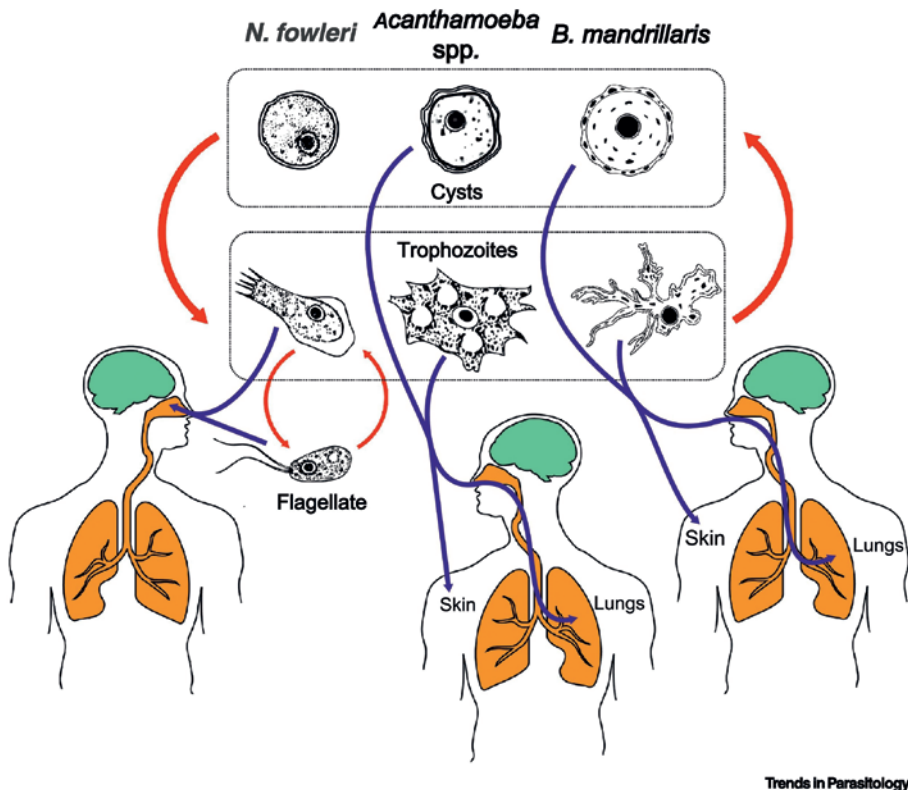
**Table 1.** Characteristics of *N. fowleri*, *Acanthamoeba* spp. and *B. mandrillaris*.

	<i>Naegleria fowleri</i>	<i>Acanthamoeba</i> spp.	<i>Balamuthia mandrillaris</i>
<b>General features</b>			
Presence in nature	Freshwater > 25°C	Freshwater, brackish water, soil, dust, air	Mainly soil, also freshwater and dust
Tropism	Brain	Skin, eye, brain	Skin, brain
Food	Bacteria, algae and yeast		Smaller amoebae, fungi
Initial entry point	Nasal mucosa	Ulcerated or broken skin, and nasal passage to lungs	
Route(s) of infection	Through olfactory neuroepithelium	Haematogenous spread from skin or lungs	
Trophozoite appearance	Irregular curvy shape. Moves with broad pseudopods. Size: 10-25 µm	Angular shape. Moves with spiky pseudopods. Size: 15-50 µm	Slender shape. Moves with finger-like pseudopods. Size: 12-60 µm
<b>Infection of the brain</b>			
Type of encephalitis	Primary amoebic meningoencephalitis (PAM)	Granulomatous amoebic encephalitis (GAE)	
Time from symptoms to death	< 1-2 weeks	1-2 months	
Risk factor(s)	Recreational activities in warm freshwater and nasal cleaning rituals	Compromised immune system (~ 100% of patients)	- Compromised immune system (~ 40% of patients) - Soil exposure and (recreational) water activities
Symptoms	Fever, headache, nausea, seizures, lethargy, coma		
Histopathology	Necrosis, haemorrhage, angiitis, inflammation		
Type of inflammation	Neutrophilic	Granulomatous	
Mortality of brain infection	> 95%	90-94%	
Cases described in the literature	431 (ref <sup>2</sup> )	83 (ref <sup>5</sup> )	> 200 (ref <sup>6,8</sup> )

## The biology of amoebae

The three species of encephalitis-causing free-living amoebae are found in different branches of the eukaryotic evolutionary tree. *Acanthamoeba* spp. and *B. mandrillaris* are evolutionary closely related as both are centramoebids that are included in the Amoebozoa group, which was earlier considered to be a supergroup, but is now

often regarded as a member of the supergroup Amorphea<sup>9</sup>. In contrast, *N. fowleri* is a Heterolobosea, part of the supergroup Discoba<sup>9</sup>. All three species can exist in trophozoite and cyst stages, but only *N. fowleri* can also transform into a flagellate stage (Figure 1). In all species, the trophozoite is the feeding stage that actively moves and replicates. All three species can transform into a cyst-form when the environment is not suitable for continued feeding and growth (such as cold temperatures, or shortage of nutrients). Cysts are environmentally resistant and increase the chances of survival until better environmental conditions occur. Regarding the metabolism of the three FLA, *Acanthamoeba* spp. as well as *N. fowleri* possess aerobically functioning mitochondria with Krebs-cycle activity, an electron-transport chain and oxidative phosphorylation, and they need oxygen for normal functioning and growth<sup>10-12</sup>. The metabolism of *B. mandrillaris* has not yet been investigated, indicating the need for future studies.



Trends in Parasitology

**Figure 1.** Life cycles of *N. fowleri*, *Acanthamoeba* spp. and *B. mandrillaris*.

Red lines indicate transformation between amoebic stages. Blue lines indicate routes of infection of the brain. The flagellate form of *N. fowleri* is not fully known to migrate from nose to brain as this form is almost never found in brain tissue. Adapted from the Centers for Disease Control and Prevention (<https://www.cdc.gov/dpdx/freelivingamebic/index.html>).

## ***Naegleria fowleri***

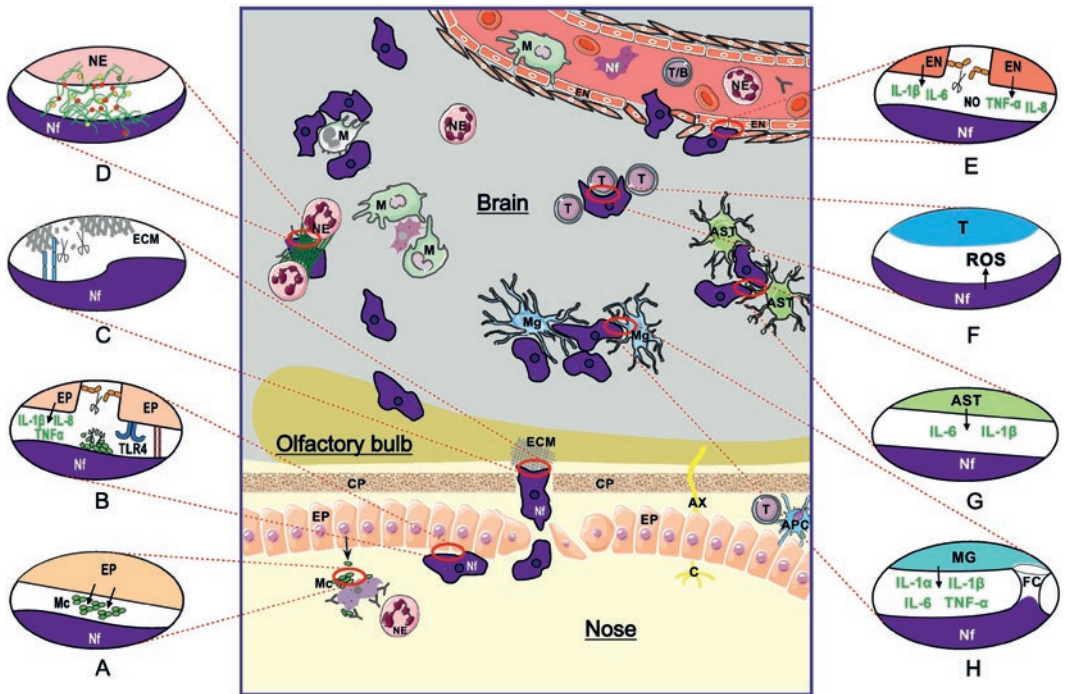
### ***Invasion of the brain occurs directly via the nose***

The route of infection used by *N. fowleri*, and the clinical aspects, are briefly presented in Box 1. *N. fowleri* enters the human body via the nose and penetrates the olfactory mucosa, after which it moves to the brain and causes PAM (Figure 2). For successful infection, *N. fowleri* needs to adhere to the olfactory mucosa. In this process,  $\alpha$ -D-mannose and  $\alpha$ -L-fucose residues on the amoebae are involved. Secretory immunoglobulin (Ig) A and mucus prevent adhesion of *N. fowleri* to apical membrane epithelial cells and, after invasion also inhibit basolaterally the adhesion to collagen (Figure 2A) <sup>13-15</sup>. However, *N. fowleri* counters this by secreting mucin-degrading proteins such as glycosidases <sup>16</sup>. Epithelial cells recognize *N. fowleri* through Toll-like receptor 4 (TLR4) and react with a proinflammatory response by producing interleukin-1-beta (IL-1 $\beta$ ), IL-8 and tumor-necrosis factor-alpha (TNF- $\alpha$ ) (Figure 2B) <sup>17,18</sup>. In mice, this immune response will recruit leukocytes to the area, and neutrophils will bind to amoebae opsonized with IgA <sup>13</sup>. Mucus production, IgA secretion, and neutrophil influx are mechanisms that slow down or even clear the *N. fowleri* infection in the nose. However, if these mechanisms are absent, or if *N. fowleri* can evade these attacks, binding to the epithelial lining will occur and tissue invasion starts. *N. fowleri* will then disrupt the tight junctions connecting the epithelial cells to make its way through the epithelial lining without causing destruction (Figure 2B) <sup>19</sup>. By using this strategy, there will be no products originating from apoptotic or necrotic cells that attract and activate immune cells, which probably enables *N. fowleri* to invade without eliciting a strong immune response. Once past the epithelial lining, *N. fowleri* adheres to the **extracellular matrix** (ECM) by an integrin-like protein <sup>20</sup> and secretes a range of proteases <sup>21-24</sup> to break down the ECM (Figure 2C). In this way, *N. fowleri* penetrates the epithelium and swiftly migrates towards the **central nervous system** (CNS).

### ***Infection of the brain occurs very rapidly and attracts neutrophils***

Although replication of *N. fowleri* starts already after arrival in the olfactory bulb, this does not immediately result in brain inflammation or damage <sup>25</sup>. The first influx of immune cells is seen approximately 4 days postinfection, and consists of eosinophils and neutrophils. A decline in eosinophils and recruitment of additional neutrophils follows, together with the influx of macrophages <sup>25</sup>. At a later stage, tissue damage occurs, consisting of extensive necrotic areas, hemorrhage and formation of cellular debris <sup>25</sup>.

Neutrophilic inflammation and concurrent damage are abundant in PAM and the neutrophils then produce extracellular traps (NETs) and secrete myeloperoxidase (MPO) (Figure 2D) <sup>26-29</sup>. NETs consist of DNA fibers that immobilize *N. fowleri*, whereas MPO damages *N. fowleri* as well as the surrounding cells. *N. fowleri* reacts to MPO by



Trends in Parasitology

**Figure 2.** Host-pathogen interactions during *N. fowleri* infection.

*N. fowleri* (Nf) enters the human body via the nasal mucosa. Epithelial cells in the nose (EP) produce mucus (Mc) that can harm Nf (oval A). Neutrophils (NE) can also affect Nf, especially when it is bound with antibody. Antibodies are produced by T cells (T) after recognition of Nf by antigen-presenting cells (APC). Nf can break down intercellular junctions and mucus, after which it moves in between EP, which produce several proinflammatory cytokines in reaction to Nf presence (oval B). Following penetration of the olfactory neuro-epithelium, ECM is degraded using a wide range of secreted proteolytic enzymes (oval C), after which Nf traverses the cribriform plate (CP) and arrives in the olfactory bulb, where it replicates. Neutrophils are the first to react, employing neutrophil extracellular traps (oval D). Endothelial cells react by producing a range of proinflammatory cytokines. Intercellular junctions of endothelial cells are disrupted by proteases produced by Nf (oval E). T cells produce reactive oxygen species (ROS) in reaction to Nf (oval F). Astrocytes produce IL-6 and IL-1 $\beta$  after exposure to Nf (oval G). Microglia produce a range of cytokines in reaction to Nf, but are attacked by Nf with food cups (FC) (oval H). Macrophages (M) can either kill Nf or be killed by Nf. Killed cells are indicated with grey colour, proinflammatory cytokines are indicated in green, anti-inflammatory cytokines are indicated in red. In *N. fowleri* infections of the brain, only trophozoites are found but no cysts or flagellates. An axon (AX) and cilia (C) of an olfactory neuron, which passes through tiny holes in the cribriform plate, are shown in yellow. The icons in this figure are adaptations from icons in the Servier Medical Art collection, <https://smart.servier.com>.

overexpressing antioxidants such as glutathione peroxidase, superoxide dismutase, catalase, thioredoxin reductase and peroxiredoxin, which neutralize the effects of MPO and thus improve survival of *N. fowleri* <sup>29</sup>. However, neutrophils can kill *N. fowleri* if they are opsonized with IgG and/or IgA, indicating that previous contact with *N. fowleri*

promotes protection<sup>28</sup>. Furthermore, *in vitro* experiments indicate that *N. fowleri* induces a proinflammatory cytokine response, in microglia and brain microvascular endothelial cells. This response leads to an increased expression of IL-6, IL-1 $\beta$  and TNF- $\alpha$  in microglia (Figure 2E, 2H)<sup>30-32</sup>, and of IL-6 and IL-1 $\beta$  in astrocytes (Figure 2G)<sup>33</sup>. This proinflammatory cytokine response boosts the recruitment of immune cells and subsequent inflammation. Macrophages are recruited, although the battle between *N. fowleri* and macrophages can go either way<sup>25,26,34</sup>. *N. fowleri* can damage macrophages, but *N. fowleri* can also be the victim, as direct cytolytic mechanisms of activated macrophages can lyse *N. fowleri*<sup>35,36</sup>. These direct cytolytic mechanisms include the production of nitric oxide and have been described as nonphagocytic events<sup>35</sup>. Conversely, *N. fowleri* can also produce nitric oxide and reactive oxygen species, which participate in damaging brain cells and T cells (Figure 2F)<sup>37,38</sup>.

*N. fowleri* causes damage to brain cells by several cytopathic strategies, one of which involves specialized structures, called food cups, that are used to damage cells, in a similar way to trophocytosis (Figure 2H)<sup>36,39</sup>. Furthermore, the aforementioned proteolytic secretions described to degrade ECM in the nose (Figure 2C) can degrade the brain ECM, which is essential for several vital functions<sup>40</sup>. However, brain damage during PAM is probably caused mainly by the over-reacting host immune response, as less damage is present in areas of the brain with trophozoites, but without immune cells<sup>25</sup>. Inflammation is regulated by the **adaptive immune system**, and indeed an *in vivo* study demonstrated that protection of mice immunized against *N. fowleri* occurred via an anti-inflammatory Th2-biased immune response<sup>41</sup>. In addition, in CD38 knockout mice, lacking natural killer cells, T and B cells, inflammation and mortality were delayed after infection with *N. fowleri*<sup>25</sup>.

**Box 1.** *Naegleria fowleri*, route of infection and clinical aspects

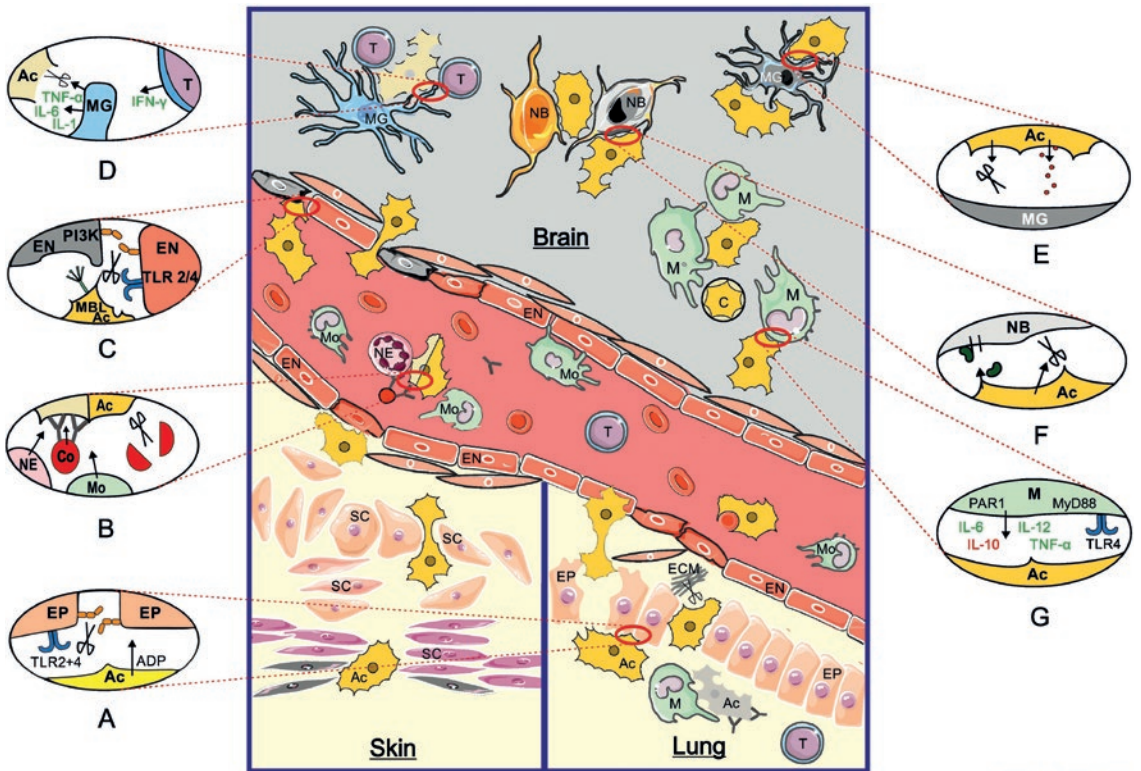
*Naegleria fowleri* is a world-wide-distributed free-living amoeba that lives in warm water and occasionally infects humans. Most infections with *N. fowleri* occur during swimming in water heated by the sun, or thermally polluted by industries<sup>42</sup>. Among the many identified species of *Naegleria*, *N. fowleri* is the only one that is a human pathogen, causing an acute encephalitis. Despite extensive studies, it is still unknown what makes *N. fowleri* pathogenic – in contrast to *N. gruberi* and other *Naegleria* species which are nonpathogenic<sup>43</sup>. The route by which *N. fowleri* enters the brain is via the olfactory neuroepithelium. Infection by *N. fowleri* is most commonly associated with activities that result in water entering the nose, such as water recreation or ablution rituals<sup>2-4</sup>. Deep inhalation of infected water brings the trophozoites to the upper regions of the nose, where they attach and invade the olfactory epithelium (see **Figure 2** in main text). Subsequently, the trophozoites migrate through the lamina propria and the cribriform plate towards the olfactory bulb<sup>2-4</sup>. This neuro-olfactory route circumvents the normal barriers that protect the CNS and provides access to the brain without much resistance<sup>25</sup>. However, once *N. fowleri* arrives in the brain, inflammation and tissue damage are extensive, leading to primary amoebic meningoencephalitis (PAM). *N. fowleri* trophozoites have only sporadically been observed outside the CNS.

PAM is a severe and fast-developing disease, as symptoms develop 5-7 days after contact and can rapidly progress, with patients usually dying 7-10 days after the appearance of the first symptoms<sup>2-4</sup>. Diagnosis is difficult, as PAM symptoms (fever, headache, nausea, lethargy, coma) overlap with symptoms from a bacterial or viral meningitis. PAM is a rare disease, as only 431 case descriptions have been published according to a recent review, although many more cases are probably not reported<sup>2</sup>. Furthermore, it is assumed that even more cases remain undiagnosed, as *N. fowleri* is not often suspected or diagnostic tools are not available<sup>44</sup>. Antibodies against *N. fowleri* (IgA, IgM, and IgG) are present in a high number of children and adolescents<sup>45</sup>, hospitalized patients<sup>46</sup> and healthy adults<sup>47</sup>. However, this high prevalence could also reflect exposure to *Naegleria lovaniensis*, a widely present non-pathogenic relative of *N. fowleri*, leading to cross-reactive antibodies recognizing *N. fowleri* antigens<sup>46</sup>.

## *Acanthamoeba* spp.

### *Invasion of the brain occurs via lungs and skin.*

The route of infection used by *Acanthamoeba* spp., and the clinical aspects, are briefly presented in Box 2. *Acanthamoeba* spp. can access the brain through two different



Trends in Parasitology

**Figure 3.** Host-pathogen interactions during *Acanthamoeba* spp. infection.

*Acanthamoeba* (Ac) enters the human body via the skin or the lower respiratory tract, attaching to skin cells (SC) or epithelial cells (EP). Ac can be phagocytosed by Macrophages (M), especially when Ac is bound with antibody, produced by T cells (T). When infecting via the lung, Ac degrades intercellular junctions and uses ADP to attack epithelial cells, that recognise Ac by TLR 2 and 4 (oval A). When infecting via skin or lung, Ac degrades ECM using proteases and moves in between endothelial cells (EN) to enter the bloodstream. Once in the bloodstream, Ac is bound by antibodies and attacked by monocytes (Mo), neutrophils (NE) and the complement system (Co) (oval B). Ac breaches the blood-brain barrier by binding to EN and moving in between them, using mannose-binding lectin (MBL) and PI-3kinase (PI3K) to induce cell death (oval C). Microglia (MG) can kill Ac with proteases and the release of proinflammatory cytokine with the help of T cells (oval D). Ac can kill MG by secreting proteases and extracellular vesicles (oval E). Ac can produce a pore-forming protein and proteases which kill neuroblastoma cells (NB) (oval F). In response to Ac, M produce a range of cytokines, both pro- and anti-inflammatory (oval G). Cyst-forms are indicated with (C), killed cells are indicated with grey colour, proinflammatory cytokines are indicated in green, anti-inflammatory cytokines are indicated in red. The icons in this figure are adaptations from icons in the Servier Medical Art collection, <https://smart.servier.com>.

**routes of infection** (Figure 3), via the lungs and via the skin. Therefore it has to be able to attach to multiple cell types. *Acanthamoeba* spp. can also invade the corneal surface of the eye and destroy monolayers of skin keratinocytes, which can result in severe keratitis in otherwise healthy persons<sup>3,48</sup>. Adhesion studies focused mostly on attachment to corneal epithelial cells to mimic *Acanthamoeba* keratitis, revealing the involvement of a mannose-binding protein<sup>49</sup>, but it is unknown whether this transmembrane protein on the surface of the amoebae is also important in *Acanthamoeba* adhesion to skin or lung or epithelial cells. In mice, adherence and invasion of the epithelium occur without apparent damage to epithelial cells<sup>50,51</sup>. Whereas earlier *in vitro* studies described cytopathic effects of *Acanthamoeba* spp. to epithelial cells, more recent studies showed that *Acanthamoeba* trophozoites can degrade claudin 2 *in vitro*, impairing tight junction function and allowing invasion without damaging the cells (Figure 3A)<sup>50,52</sup>. During the invasion, *Acanthamoeba* trophozoites produce a range of proteases that break down collagen and elastin (major components of the ECM) and hemoglobin<sup>53,54</sup>.

The hematological route requires *Acanthamoeba* to survive in blood, which is challenging, and different outcomes have been reported when the amoebae were exposed to human serum (Figure 3B). *Acanthamoeba* trophozoites can be lysed by complement activation via the alternative pathway<sup>55</sup> and they can be killed by neutrophils and macrophages in the presence of serum<sup>56</sup>. However, in other studies, a small *Acanthamoeba* subpopulation survived in undiluted serum<sup>57</sup> or a substantial population in diluted serum<sup>58</sup>. Furthermore, *Acanthamoeba* spp. degrade components of the complement system, which will support survival in blood<sup>59</sup>. *Acanthamoeba* spp. can also phagocytose and degrade erythrocytes<sup>60</sup>. Altogether, *Acanthamoeba* spp. may survive in blood if conditions are favorable, for instance, when the host is immunocompromised. Once *Acanthamoeba* trophozoites have spread in the blood, the next barrier to breach is the blood-brain barrier (BBB). Several factors are important in this process, contact-dependent as well as contact-independent factors (Figure 3C). *Acanthamoeba* spp. produce proteases that degrade tight-junction proteins of **human brain microvascular endothelial cells** (HBMECs), providing access to the brain through movement between the cells<sup>54</sup>. *Acanthamoeba* can also induce programmed cell death in HBMEC *in vitro*<sup>61</sup>. The extent to which *Acanthamoeba* trophozoites use either their BBB-damaging capacities or their strategy for stealthy brain invasion by moving in between cells is unknown.

### ***Infection of the brain is chronic and includes granuloma formation***

*Acanthamoeba* infection is associated with the recruitment to the brain of a variety of immune cells; T cells, macrophages, dendritic cells, neutrophils, B cells and natural killer cells<sup>62</sup>. Granulomas are formed in reaction to *Acanthamoeba* spp. in the brain<sup>26</sup>.

Several *in vitro* studies characterized the interactions of *Acanthamoeba* spp. with macrophages, microglia, T cells, Schwann cells and neuroblastoma cells. The interactions of microglia and *Acanthamoeba* spp. have been studied extensively and this showed that the outcome of the combination of T cells, microglia and *Acanthamoeba* is dependent on interferon-gamma (IFN- $\gamma$ ) release by T cells, which induces IL-6 and TNF- $\alpha$  release by microglia and the destruction of *A. castellanii* (Figure 3D) <sup>63</sup>. The proinflammatory response by microglia results in the production of IL-1 $\alpha$ , IL-1 $\beta$  and TNF- $\alpha$  <sup>64,65</sup>. Interestingly, the outcome can be different for distinct *Acanthamoeba* species, as *A. castellanii* is killed by microglia whereas *A. culbertsoni* kills the microglia <sup>64-66</sup>. Extracellular vesicles and peptidases are postulated as mechanisms by which *Acanthamoeba* trophozoites kill glioma cells (Figure 3E) <sup>66,67</sup>. *Acanthamoeba culbertsoni* produces a specific cytotoxic pore-forming protein that lyses neuroblastoma cells (Figure 3F) <sup>68</sup>. Furthermore, *Acanthamoeba* can induce apoptosis in neuroblastoma cells via caspases and Bax-proteins <sup>69</sup>. *In vitro* attachment of *A. culbertsoni* to Schwann cells results in necrosis and autophagy <sup>70</sup>.

*In vitro* interactions between macrophages and various *Acanthamoeba* spp. are different. *A. culbertsoni* destroys macrophages, whereas *A. polyphaga* and *A. castellanii* show limited destruction, although this balance depends on activation of the macrophages, as activated macrophages damage or even phagocytose these amoebae <sup>71</sup>. Toll-like receptors (TLRs) are involved in the activation of macrophages and it was shown that TLR4 is important in the recognition of and response to *Acanthamoeba* spp. <sup>72</sup>. Macrophages release a mixture of cytokines in response to *Acanthamoeba*, which consists of TNF- $\alpha$ , IL-6, IL-10 and IL-12, mediated through MyD88 and PAR1 (Figure 3G) <sup>72-74</sup>. TNF- $\alpha$ , IL-6 and IL-12 are regarded as proinflammatory cytokines, but the significant production of the anti-inflammatory cytokine IL-10 suggests a mixed-type immune response, which might allow immune evasion of *Acanthamoeba* and limit the inflammatory response <sup>73</sup>. Furthermore, pathogenic *Acanthamoeba* strains induce a mixed-type immune response, whereas nonpathogenic *Acanthamoeba* strains induce mainly a proinflammatory response <sup>74,75</sup>, which could result in rapid elimination of nonpathogenic *Acanthamoeba* spp.

*Acanthamoeba* spp. can partially evade the inflammatory response by transforming into a cyst form, as intact *Acanthamoeba* cysts do not attract macrophages or neutrophils *in vitro* <sup>76</sup>. However in mice challenged with formalin-fixed cysts, the anti-*Acanthamoeba* IgG production and T cell proliferation occur, showing that cysts are immunogenic and antigenic <sup>77</sup>. Furthermore, cysts can be phagocytosed by macrophages and are killed by neutrophils through the secretion of myeloperoxidase <sup>76</sup>.

The T cell response might be important in *Acanthamoeba* infections, as there are differences in T cell response between immunocompetent mice and methylprednisolone-

induced immunocompromised mice after nasal *Acanthamoeba* infection. In immunocompetent mice, selective Th1, Th2 and Th17 responses are induced, whereas in immunocompromised mice, *Acanthamoeba* induces a robust Th1-mediated immunity without the participation of Th17<sup>78</sup>. In humans, the type of T cell response also seems to be important, as proinflammatory T cell clones directed against *Acanthamoeba* spp. are found in healthy individuals<sup>79</sup>.

**Box 2.** *Acanthamoeba* spp., route of infection and clinical aspects

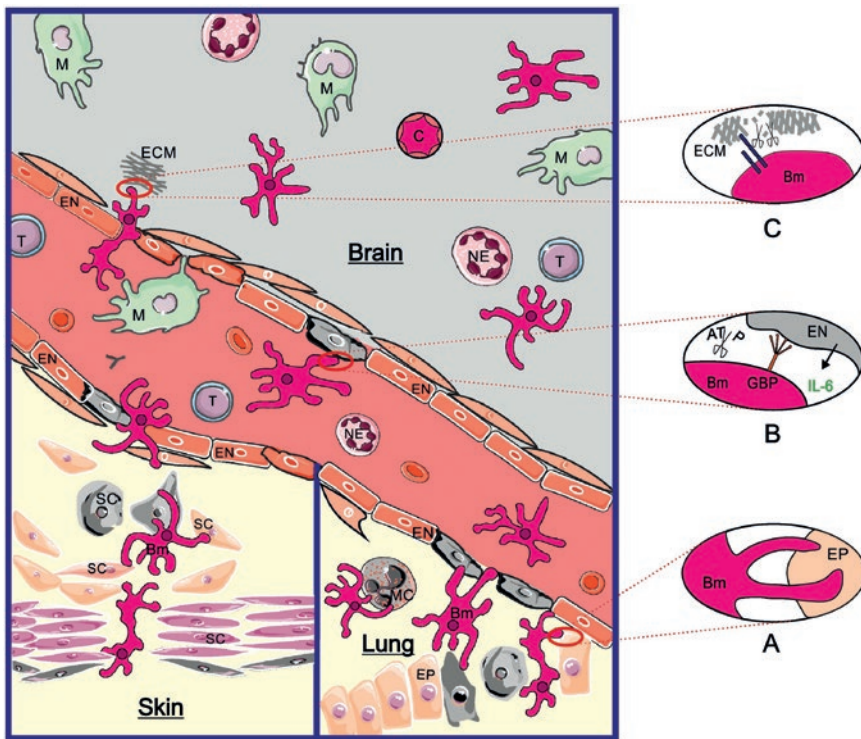
*Acanthamoeba* spp. are opportunistic parasites of humans. The exposures leading to acanthamoebiasis are generally unknown but are thought to be soil or water exposures<sup>8</sup>. *Acanthamoeba* spp. can enter via the lower respiratory tract or via lesions in the skin, and, in immunocompromised persons, can then invade the CNS via the bloodstream - or infection can result in skin lesions with or without CNS involvement. Apart from infections via lungs or broken skin, *Acanthamoeba* spp. can also infect the eye; this can result in severe keratitis in otherwise healthy persons. Because of the slow development of granulomatous amoebic encephalitis (GAE), the exact route of *Acanthamoeba* spp. in humans to the brain is not always clear, but lungs and skin are thought to be the most important points of entry<sup>8</sup>. The amoebae will then reach the brain via hematogenous spreading<sup>8</sup>. A recent murine model, evaluating an *Acanthamoeba* skin infection, identified amoebal presence in the brain only after the infected skin was chronically irradiated by UV-B light<sup>80</sup>. This corresponds to the idea that a breach in the skin is required for *Acanthamoeba* to access the bloodstream from the skin.

*Acanthamoeba* GAE symptoms consist of fever, headache, nausea, seizures, lethargy, and coma. *Acanthamoeba* GAE is often a slow and chronic disease, although quick progression sometimes occurs<sup>5,81</sup>. The time from *Acanthamoeba* contact to the start of symptoms is often unclear as it is difficult to trace back the initial contact due to its ubiquitous presence and multiple possible routes of infection. Furthermore, a thorough study of the epidemiological features and clinical characteristics of *Acanthamoeba* spp. GAE is still lacking. Once symptoms have started, it can take one to two months until death occurs<sup>5</sup>. At least 83 human cases have been reported, although many more cases probably occurred, as *Acanthamoeba* GAE is seldom suspected and diagnostic tools might not be available<sup>5</sup>. Antibodies against *Acanthamoeba* (IgA, IgM, and IgG) are universally present in the healthy population, which is in line with the ubiquitous environmental presence of *Acanthamoeba*<sup>45</sup>. Although *Acanthamoeba* GAE usually develops in immunocompromised patients, it can occur in immunocompetent individuals as well<sup>5</sup>.

## *Balamuthia mandrillaris*

### *Invasion of the brain occurs via lungs and skin*

The route of infection used by *B. mandrillaris*, and the clinical aspects, are briefly presented in Box 3. A schematic overview of the host-pathogen interactions used by *B. mandrillaris* can be seen in Figure 4. *B. mandrillaris* can destroy and feed on mammalian cells *in vitro* by invading the cells with its pseudopods first, before fully entering and consuming its cytoplasm (Figure 4A) <sup>48,82,83</sup>. The nucleus is consumed later, whereafter the amoeba invades another cell. It is hypothesized that the intracellular location of *B. mandrillaris*



Trends in Parasitology

**Figure 4.** Host-pathogen interactions during *Balamuthia mandrillaris* infection.

*B. mandrillaris* (Bm) can enter the human body via the skin [SC (skin cells)] or the lower respiratory tract. Bm can induce cytopathic effects on epithelial cells (EP) by penetration of finger-like projections (oval A). After the epithelial layer, Bm can efficiently kill mastocytoma cells (MC). After infection via the skin and lung, Bm reaches endothelial cells (EN) and enters the bloodstream. The blood-brain barrier is breached using cytopathic effects such as a galactose-binding protein (GBP) and ATPase (oval B). EN react by the production of the proinflammatory cytokine IL-6 (oval B). Bm can bind to and break down the extracellular matrix (ECM) (oval C). In the brain, cyst forms are sometimes found (C), alongside neutrophils (NE), T cells (T) and macrophages (M). Killed cells are indicated with gray color, proinflammatory cytokines are indicated in green. The icons in this figure are adaptations from icons in the Servier Medical Art collection (<http://smart.servier.com>).

facilitates evasion of the immune system<sup>82</sup>. *B. mandrillaris* kills human skin fibroblasts, but not keratinocyte cells, indicating that *B. mandrillaris* cannot breach the intact epidermis, and it has to invade via broken or ulcerated skin<sup>48</sup>. Once past the epidermis, *in vitro* studies showed that *B. mandrillaris* can kill mastocytoma cells efficiently, mainly in a contact-dependent manner<sup>83</sup>. *Balamuthia* is known to ingest bits and pieces of host tissue and to produce enzymes that degrade the tissue<sup>4</sup>.

*B. mandrillaris* is thought to enter the brain via the bloodstream. The next barrier is the BBB, to which *B. mandrillaris* binds via a galactose-binding protein (Figure 4B)<sup>84</sup>. *B. mandrillaris* secretes proteases and an ecto-ATPase, but most of the cellular damage is caused via contact-dependent mechanisms<sup>83,85</sup>. The secreted proteases are hypothesized to facilitate *B. mandrillaris* infection by degrading ECM proteins (Figure 4C)<sup>86</sup>.

### ***Infection of the brain is chronic and includes granuloma formation***

Once in the brain, trophozoites aggregate around blood vessels and induce a broad immune response in mice and humans<sup>26,87</sup>. Numerous lymphocytes and macrophages, as well as some eosinophils and multinucleated giant cells, are seen in the brains of mice infected with *B. mandrillaris*<sup>88</sup>. The immune response is important to survive a *B. mandrillaris* infection. The immune response is absent in brains of severe combined immunodeficiency (SCID) mice, which are deficient in B and T lymphocytes and thus lack immunoglobulins and cell-mediated immunity. Of SCID mice, 70% died after intranasal inoculation, compared to 10% of normal mice<sup>88</sup>. This difference is also observed in human cases, as histopathological examination of brains with a *B. mandrillaris* encephalitis revealed a broad spectrum, ranging from acute neutrophilic inflammation to granulomatous inflammation, possibly reflecting the **immune status** of the affected patient<sup>26</sup>.

The T cell response is thought to be essential, as SCID mice survived infection if they received spleen cells from wild type mice, but died if the CD4+ T cells were removed from these spleen cells<sup>89</sup>. Furthermore, wild type mice that were depleted of CD4+ T cells were susceptible to infection<sup>89</sup>. These T cells are thus thought to play an essential role in curbing a *B. mandrillaris* encephalitis by the recruitment and activation of macrophages and granulocytes.

**Box 3.** *Balamuthia mandrillaris*, route of infection and clinical aspects

*B. mandrillaris* is an opportunistic parasite of humans, and infection results in cutaneous lesions with or without infection of the brain. Soil exposure is commonly reported as the origin of an infection with *B. mandrillaris*, and over one-third of the cases had an immunocompromised condition<sup>8</sup>. Infection of the brain results in granulomatous amoebic encephalitis (GAE). After entry via the respiratory tract or through the skin, hematogenous spreading can result in GAE. Following oral infection of mice, amoebae were found in various organs, indicating that there is extensive haematogenous spreading<sup>90</sup>. For humans, the skin is a favored route of infection, as skin abnormalities were often described in patients in Peru and China<sup>91,92</sup>. So far no animal studies describing this route of infection have been performed.

Regarding clinical presentation, two patterns have been described in *Balamuthia* GAE: some patients develop an initial skin lesion followed by the development of neurologic manifestations within weeks or months, whereas others present with primary CNS involvement<sup>1</sup>. The skin lesions appear as indurated plaques with rubbery to stone hardness measuring a few millimeters thick and one to several centimeters wide<sup>92</sup>. The time between the appearance of skin lesions and the onset of neurological symptoms can range from 1 month to 9 years, or progression to a brain infection may not even occur<sup>92</sup>. *Balamuthia* GAE symptoms initially manifest as headache and photophobia and later include nausea and vomiting, fever, myalgia, weight loss and seizures, resulting in death in approximately 90% of the cases. At least 200 cases have been reported, although the actual number of cases is probably much higher, as cases are not reported or not diagnosed<sup>6</sup>. The presence of serum antibodies against *B. mandrillaris* depends on the characteristics of the population tested. Seropositivity increases with age and seropositivity prevalence is reported to be high in non-western rural areas and can be very high among people in these areas who regularly go outdoors. In high-income countries, *B. mandrillaris* antibodies are rarely present<sup>45,93</sup>. A link to the immune status of the patient is evident, as 40% of the *Balamuthia* GAE patients are immunocompromised<sup>94</sup>.

### Comparison of the three amoeba species

There are evident differences and similarities between the brain infections caused by *N. fowleri*, *Acanthamoeba* spp. and *B. mandrillaris*. Differences include the environmental presence of the amoebae, the route of infection, the pathogenicity mechanisms, the immune response that is induced and the immune status of the host. Could these factors explain the differences between the three diseases caused by these amoebae? Conversely, it should also be realized that *Naegleria*, a member of the Heterolobosea, is evolutionarily

very distant from *Acanthamoeba* and *Balamuthia*, which are both Amoebozoa. It is unknown to what extent these evolutionary aspects might explain the differences and similarities between the three brain infections. In this respect it is tempting to speculate that an evolutionary background exists which could explain why both of these two Amoebozoa induce a chronic granulomatous brain infection while *N. fowleri* induces a rapid neutrophilic infection.

### Environmental presence

Differences exist in the environmental presence of the three FLA, as *Acanthamoeba* spp. are found more often in natural bodies of water<sup>95,96</sup>, swimming pools<sup>97</sup>, water treatment plants<sup>96</sup> and drinking water<sup>98</sup> compared to *N. fowleri* and *B. mandrillaris*. It is intriguing that *Acanthamoeba* spp. are the most abundant pathogenic FLA, but cause fewer brain infections than *N. fowleri* and *B. mandrillaris*. This ubiquitous presence of *Acanthamoeba* spp. correlates with the high seropositivity rate among the general population<sup>45,99</sup>. The seropositivity rate for *B. mandrillaris*, which is far less widespread, is low in high-income countries in moderate climates and higher in rural Africa<sup>93,100</sup>. The seropositivity rate of *N. fowleri* was in the 1980s reported to be very high, but more recent data are not available<sup>46,101,102</sup>.

The efficiency of brain infection by FLA seems very low, considering the rather limited incidence of such infections, despite the widespread presence of them in the environment<sup>103-105</sup>. Using serological methods, attempts have been performed to estimate the human exposure to FLA. These studies showed that specific antibodies can be demonstrated in PAM and GAE patients and that cross reactivity between FLA infections is limited<sup>93,104,106</sup>. In addition, these studies showed that sera of healthy volunteers demonstrate some reactivity and if the reactivity in sera of healthy volunteers against the three FLA are compared, it seems that most reactivity is found against *Balamuthia* and *Acanthamoeba*, which could suggest that contact with those FLA occurs more frequently than with *N. fowleri*<sup>101,104,106</sup>. However, it is questionable whether an observed low reactivity is specific and really reflects previous exposure or a past infection. Reliable determination of the exposure rate in healthy humans cannot be determined reliably by serological methods, and therefore, the exposure:infection ratio is still unknown.

The concentration of the different amoebae in the environment also varies and this results in exposure to different amounts of amoebae. *N. fowleri* is thermophilic and can be present in up to hundreds of amoebae per liter water when conditions are favorable, such as in geothermal baths and in the cooling water of power plants<sup>107</sup>. *Acanthamoeba* spp. and *B. mandrillaris* are found not only in watery environments but also in soil and dust. Their presence in the environment was mostly determined using qualitative molecular

tools, allowing no direct comparison with the presence of *N. fowleri*<sup>96,108</sup>. A comprehensive study on the amounts of FLA present in their respective environments would be valuable.

### **Routes of infection**

The route of infection taken by the FLA is likely to impact the disease progression. For infections of *Acanthamoeba* spp. and *B. mandrillaris*, the route is often unknown, but these amoebae rarely, if ever, use the neuro-olfactory route, the one and only route of *N. fowleri*. As the neuro-olfactory route results in fast access to the brain, the adaptive immune response is probably insufficient, which might promote rapid disease progression. The hematogenous routes of infection used by *Acanthamoeba* spp. and *B. mandrillaris* are lengthier and, obviously, involve the bloodstream, which normally results in a strong immune response that combats the amoebae. The amoebae counter the actions of the immune system, and the result is a more chronic disease course that is similar to other immune-evading infectious diseases. Many animal studies of *Acanthamoeba* spp. and *B. mandrillaris* used intranasal infection, with a recent exception describing successful *Acanthamoeba* brain infection originating from irradiated skin<sup>80</sup>. Studies on the lung or skin infection routes in mice are most likely more applicable to the human situation. Furthermore, proper determination of the relative importance of the different infective routes in humans by *Acanthamoeba* spp. and *B. mandrillaris* could be valuable, as this could lead to more targeted preventative measures.

### **Biology and pathogenicity mechanisms**

The difference in course of the disease could be due to inherent biological characteristics of the amoebae, such as speed of movement, reproduction rate and pathogenicity mechanisms. Most studies investigating these factors are *in vitro* studies, limiting the clinical translation of the results. An important factor within these *in vitro* studies is the temperature at which the experiments are performed. Generally, *Acanthamoeba* spp. grow best at 25°C, with the ability to grow at higher temperatures, where thermotolerance correlates with pathogenicity of the amoebae<sup>109</sup>. In numerous *in vitro* studies, *Acanthamoeba* cultures are maintained at 25°C or 30°C and experiments are not performed at 37°C. Despite these differences in cultivation, multiplication time and speed of movement are not distinctly different between the three amoebae in a nutrient-rich medium, although this condition is hardly comparable to the human body. Furthermore, all three free-living amoebae possess several pathogenicity mechanisms, of which the mechanisms of *N. fowleri* and *Acanthamoeba* spp. have been studied in most detail, but mainly *in vitro*. All three amoebae use contact-independent and contact-dependent mechanisms to damage human cells or ECM, comprising protease secretion and phagocytic strategies. For instance, *N. fowleri* and *Acanthamoeba* spp. both invade tissues

by migrating in between cells, as they break down the intercellular junctions and secrete a wide range of proteases, which facilitate migration through the extracellular matrix. However, the extent to which these pathogenicity mechanisms are active and critical *in vivo* will decide the course of infection. Therefore, the pathogenicity mechanisms of the amoebae have to be studied in more detail, especially in studies describing the different amoebic species side by side in similar, preferably *in vivo*, conditions.

### Immune response

A balanced immune response is paramount to prevent infection, but also to prevent the immune system from damaging host tissue (Box 4). The human immune response is quite different in case of the different forms of encephalitis caused by the three amoeba species. *N. fowleri* PAM patients show an acute neutrophilic inflammation whereas *Acanthamoeba* GAE results in granulomatous inflammation of the brain. Brain tissue of patients with *B. mandrillaris* GAE showed either acute neutrophilic inflammation or granulomatous inflammation. Differences in immune response were also observed in mice, as intranasal infection of immunocompetent mice with *N. fowleri* or *Acanthamoeba* spp. resulted in extensive brain tissue damage and inflammation 96 h after infection with *N. fowleri*, whereas brains of the same breed of mice infected with *Acanthamoeba* spp. showed very limited inflammation at that same time after infection<sup>25,51</sup>. A possible explanation can be the cytokine response after infection by the different amoebae, as several cytokines are produced in response to pathogenic *Acanthamoeba* spp. but not in reaction to *N. fowleri*. One of these cytokines is IL-10, which is considered to be a key regulator of the **innate immune response** and suppresses inflammation and macrophage activity. IL-12, IL-4 and IL-17 were also produced in reaction to *Acanthamoeba* spp., but not in response to *N. fowleri*. These cytokines are involved in T cell regulation, promoting the differentiation of CD4+ T cells into Th1, Th2 and Th17, respectively. This differentiation is impaired in immunocompromised mice infected with *Acanthamoeba* spp., indicating the importance of the T cell lineages. Furthermore, CD4+ T cells are essential for mice to survive a *B. mandrillaris* infection<sup>89</sup>. However, the immune response could also be contra-productive for the host, as brain damage in an *N. fowleri* infection corresponded to the intensity of the host immune response *in vivo*<sup>25</sup>. The extent to which the immune response is responsible for the clinical course in *Acanthamoeba* spp. or *B. mandrillaris* GAE is unknown. Further research should focus on the identification of key features in the immune response to the three different amoebae, to build a comprehensive map of the disease pathophysiology.

**Box 4.** The YIN and YANG of the innate immune response

The powerful innate immune response has to tune its potential to the danger of the threat to prevent collateral damage.

YANG, the sunny side: Fast and robust cytotoxic responses are essential to combat and neutralize invading microorganisms<sup>110</sup>. The effector cells of the innate immune response are phagocytes that can engage with the pathogens either intracellularly after phagocytosis or extracellularly by releasing toxic compounds in the close vicinity of the invaders. These killing mechanisms mainly rely on the production of reactive oxygen species produced by a membrane-bound NADPH-oxidase and degranulation of cytotoxic proteins by fusing of granules containing these proteins with the membranes of the phagolysosome (intracellular killing) or the plasma membrane (extracellular killing)<sup>111</sup>. Intracellular killing is important for targets that are smaller than immune cells and can be phagocytosed. Neutrophils and to a lesser extent monocytes, mainly utilize this route. Larger targets such as multicellular parasites are killed extracellularly as they are too big to be phagocytosed. Eosinophils are specialized for attacking large targets<sup>112</sup> although neutrophils can contribute through the release of first granules and then their DNA that in turn forms neutrophil extracellular traps (NETs)<sup>113</sup>.

YIN, the shady side: robust innate immune responses run the risk of hyperactivation, that is, more activation than necessary for the killing of the target. Under these conditions, the surrounding tissues are damaged as well<sup>114</sup>. This can even lead to a situation in which the damage caused by the innate immune response outweighs the importance of the killing of the invading microorganism(s). This situation can lead to acute inflammatory responses with massive tissue damage such as seen during sepsis caused by meningococci<sup>115</sup>. In addition, chronic activation can lead to continuous damage to the host tissue which is seen in a multitude of chronic inflammatory diseases such as asthma, inflammatory bowel disease, and auto-immune diseases. This tissue damage can even aid microorganisms to enter tissues normally protected by adequate barriers.

A healthy immune response is balanced, such that sufficient activity leads to the containment of the invading micro-organism without causing tissue damage. Therefore, in infectious diseases, as well as in inflammatory diseases, treatment should be focused on restoring this balance - preventing that collateral damage can facilitate a porte-d'entrée of more or different pathogens. In conclusion, the innate immune response is necessary to engage with free-living amoebae, but this response should be contained to prevent tissue damage that potentially facilitates the infection.

## Host immune status

Another major difference between the three different amoebic brain infections is the immune status of the affected patients. *N. fowleri* affects healthy and relatively young individuals, whereas *Acanthamoeba* spp. specifically target immunocompromised patients. *B. mandrillaris* can infect immunocompetent individuals, but immunocompromised individuals are affected at a far higher rate. This could be a result of several factors, one of which is the route of infection. *N. fowleri* solely uses the olfactory route and does not survive well in the bloodstream. *Acanthamoeba* spp. and *B. mandrillaris* usually reach the brain through the bloodstream, which is a hostile environment for pathogens. In immunocompetent people, the immune system is better able to kill *Acanthamoeba* spp. and *B. mandrillaris* that are present in the blood, eradicating the infection before the brain is reached. In immunocompromised patients, this barrier is easier to breach, possibly leading to higher rates of infection in this group.

## Concluding remarks

Brain infections by free-living amoebae pose a small, but intimidating, threat to society. Understanding how these amoebae operate is the basis of the development of strategies to prevent and treat these infections. Several different subjects still require attention (see **Outstanding questions**). As these infections are under-reported, it is imperative to estimate the current burden of amoebic encephalitis and to know whether the infections are indeed increasing or just better registered. The striking difference in clinical course between PAM and GAE can only be explained by multiple factors. The route of infection, as well as the immune response, probably play a key role. *N. fowleri* circumvents the immune system by travelling via the olfactory nerve to the CNS. Upon arrival, the immune response is fierce, resulting in the influx of neutrophils with subsequent damage to brain tissue. This is in contrast with the route taken by *Acanthamoeba* spp. and *B. mandrillaris*, which first have to deal with the immune system in the blood. Therefore, in this case, a strategy evolved to remain relatively undetected, resulting in a more chronic disease course and a slowly building immune response. In the end, however, each of the three amoebic brain infections leads to death in almost all cases.

In recent years, good progress was made in understanding host-parasite interactions but there remains a lot to be discovered. Future studies using different strains of mice could solve questions on the genetic factors of the host that influence the susceptibility for a brain infection. Preferably, these experiments should be performed with distinct amoeba strains to identify genetic factors that influence their pathogenicity. This will also shed some light on the limited incidence of FLA brain infections despite the wide spread of these amoebae in the environment.

## Outstanding questions

- What is the actual burden of amoebic encephalitis currently?
- Is exposure of humans to an infectious dose of *N. fowleri*, *Acanthamoeba* spp. and *B. mandrillaris* increasing?
- What factors of these amoebae are crucial in the type and extent of the immune response?
- Do genetic factors of the host influence the susceptibility to a brain infection?
- Do genetic factors of the amoebae influence their pathogenicity?

## Acknowledgements

We thank the Netherlands Centre for One Health (NCOH), the Graduate School of Life Sciences Utrecht University, and the Erasmus Medical Center for their support.

## Declaration of Interests

The authors declare no competing interests.

## Glossary

**Adaptive immune system:** Part of the immune system that targets a specific pathogen as it mounts an immune response against unique antigens. It is slow to develop, but protection can be very long-lasting.

**Central nervous system (CNS):** The combination of the brain and the spinal cord, which is described as an area with immune privilege, as it shows an attenuated response to antigens. Access to the CNS is restricted and possible only through certain barriers.

**Cytokines:** A group of small proteins used in cell signaling, most important in the communication between immune cells. Examples of proinflammatory cytokines are tumor necrosis factor alpha (TNF- $\alpha$ ), interferon gamma (IFN- $\gamma$ ), interleukin 1 beta (IL-1 $\beta$ ), IL-6, IL-8, and IL-12. An example of an anti-inflammatory cytokine is IL-10.

**Extracellular matrix (ECM):** A three-dimensional network made of fibrous proteins and proteoglycans that provides structural and biochemical support to surrounding cells.

**Free-living amoeba (FLA):** Eukaryotic unicellular organism that can live freely in the environment but can also enter a host as an opportunistic pathogen. Three free-living amoebae are well known human pathogens: *Naegleria fowleri*, *Balamuthia mandrillaris*, and *Acanthamoeba* spp.

**Granuloma:** An area, with a high density of immune cells, which is formed in response to chronic inflammation. Granulomas predominantly consist of mature macrophages which try to encapsulate the pathogen from the body and facilitate its eradication.

**Granulomatous Amoebic Encephalitis (GAE):** An infection of the brain by either *Acanthamoeba* spp. or *B. mandrillaris*. It is characterized by slow disease progression and granuloma formation.

**Human brain microvascular endothelial cells (HBMECs):** Cells that are the major component of the blood-brain barrier, often used in *in vitro* studies.

**Immune status:** The ability of the immune system to fight off microorganisms. Immunocompetent people can clear most microorganisms whereas immunocompromised people are less capable due to a reduction of the activation or the efficacy of the immune system. This can be the result of a disease or of immunosuppressive medication.

**Innate immune response:** Part of the immune system that forms the first line of defense against pathogens. It consists of physical, chemical, and cellular defenses and is nonspecific but very quick to respond.

**Primary Amoebic Meningoencephalitis (PAM):** An infection of the brain by the free-living amoeba *Naegleria fowleri*. It is characterized by a very rapid disease progression.

**Route of infection:** The physical path a pathogenic microorganism takes inside the human body during infection.

## References

- 1 Król-Turmińska, K. & Olender, A. Human infections caused by free-living amoebae. *Ann Agric Environ Med* **24**, 254-260 (2017).
- 2 Maciver, S. K., Piñero, J. E. & Lorenzo-Morales, J. Is *Naegleria fowleri* an emerging parasite? *Trends Parasitol* **36**, 19-28 (2020).
- 3 Cope, J., Ali, I. & Visvesvara, G. Pathogenic and Opportunistic Free-Living Ameba Infections. In *Hunter's Tropical Medicine and Emerging Diseases* (10th edn) (Ryan, E.T. et al., eds), pp. 814–820, Elsevier (2020)
- 4 Visvesvara, G. S. Infections with free-living amoebae. *Handb Clin Neurol* **114**, 153-168 (2013).
- 5 Kalra, S. K., Sharma, P., Shyam, K., Tejan, N. & Ghoshal, U. *Acanthamoeba* and its pathogenic role in granulomatous amoebic encephalitis. *Exp Parasitol* **208**, 107788 (2020).
- 6 Lorenzo-Morales, J. et al. Is *Balamuthia mandrillaris* a public health concern worldwide? *Trends Parasitol* **29**, 483-488 (2013).
- 7 Moseman, E. A. Battling brain-eating amoeba: Enigmas surrounding immunity to *Naegleria fowleri*. *PLoS Pathog* **16**, e1008406 (2020).
- 8 Cope, J.R. et al. Free-living amoeba. In *Neurological Complications of Infectious Diseases* (Hasbun, R. et al., eds), pp. 255–270, Springer Nature (2021)
- 9 Burki, F., Roger, A. J., Brown, M. W. & Simpson, A. G. B. The New Tree of Eukaryotes. *Trends Ecol Evol* **35**, 43-55 (2020).
- 10 Zíková, A., Hampl, V., Paris, Z., Týč, J. & Lukeš, J. Aerobic mitochondria of parasitic protists: Diverse genomes and complex functions. *Mol Biochem Parasitol* **209**, 46-57 (2016).
- 11 Bexkens, M. L. et al. Lipids are the preferred substrate of the protist *Naegleria gruberi*, relative of a human brain pathogen. *Cell Rep* **25**, 537-543 e533 (2018).
- 12 Sarink, M. J., Tielens, A. G. M., Verbon, A., Sutak, R. & van Hellemond, J. J. Inhibition of Fatty Acid Oxidation as a New Target To Treat Primary Amoebic Meningoencephalitis. *Antimicrob Agents Chemother* **64**, e00344-00320 (2020).
- 13 Jarillo-Luna, A. et al. Intranasal immunization with *Naegleria fowleri* lysates and Cry1Ac induces metaplasia in the olfactory epithelium and increases IgA secretion. *Parasite Immunol* **30**, 31-38 (2008).
- 14 Cervantes-Sandoval, I. et al. *Naegleria fowleri* induces MUC5AC and pro-inflammatory cytokines in human epithelial cells via ROS production and EGFR activation. *Microbiology* **155**, 3739-3747 (2009).
- 15 Cervantes-Sandoval, I., Serrano-Luna, J. J., Garcia-Latorre, E., Tsutsumi, V. & Shibayama, M. Mucins in the host defence against *Naegleria fowleri* and mucinolytic activity as a possible means of evasion. *Microbiology* **154**, 3895-3904 (2008).
- 16 Martinez-Castillo, M. et al. Nf-GH, a glycosidase secreted by *Naegleria fowleri*, causes mucin degradation: an in vitro and in vivo study. *Future Microbiol* **12**, 781-799 (2017).
- 17 Martinez-Castillo, M., Santos-Argumedo, L., Galvan-Moroyoqui, J. M., Serrano-Luna, J. & Shibayama, M. Toll-like receptors participate in *Naegleria fowleri* recognition. *Parasitol Res* **117**, 75-87 (2018).
- 18 Carrasco-Yepepe, M. et al. Intranasal coadministration of Cholera toxin with amoeba lysates modulates the secretion of IgA and IgG antibodies, production of cytokines and expression of plgR in the nasal cavity of mice in the model of *Naegleria fowleri* meningoencephalitis. *Exp Parasitol* **145** Suppl, S84-92 (2014).
- 19 Shibayama, M. et al. Disruption of MDCK cell tight junctions by the free-living amoeba *Naegleria fowleri*. *Microbiology* **159**, 392-401 (2013).

- 20 Jamerson, M., da Rocha-Azevedo, B., Cabral, G. A. & Marciano-Cabral, F. Pathogenic *Naegleria fowleri* and non-pathogenic *Naegleria lovaniensis* exhibit differential adhesion to, and invasion of, extracellular matrix proteins. *Microbiology* **158**, 791-803 (2012).
- 21 Lam, C., Jamerson, M., Cabral, G., Carlesso, A. M. & Marciano-Cabral, F. Expression of matrix metalloproteinases in *Naegleria fowleri* and their role in invasion of the central nervous system. *Microbiology* **163**, 1436-1444 (2017).
- 22 Vyas, I. K., Jamerson, M., Cabral, G. A. & Marciano-Cabral, F. Identification of peptidases in highly pathogenic vs. weakly pathogenic *Naegleria fowleri* amoebae. *J Eukaryot Microbiol* **62**, 51-59 (2015).
- 23 Chavez-Munguia, B. et al. *Naegleria fowleri*: contact-dependent secretion of electron-dense granules (EDG). *Exp Parasitol* **142**, 1-6 (2014).
- 24 Martinez-Castillo, M., Ramirez-Rico, G., Serrano-Luna, J. & Shibayama, M. Iron-Binding Protein Degradation by Cysteine Proteases of *Naegleria fowleri*. *Biomed Res Int* **2015**, 416712 (2015).
- 25 Cervantes-Sandoval, I., Serrano-Luna, J. d. J., García-Latorre, E., Tsutsumi, V. & Shibayama, M. Characterization of brain inflammation during primary amoebic meningoencephalitis. *Parasitol Int* **57**, 307-313 (2008).
- 26 Guarner, J. et al. Histopathologic spectrum and immunohistochemical diagnosis of amoebic meningoencephalitis. *Mod Pathol* **20**, 1230-1237 (2007).
- 27 Carrasco-Yeppez, M. M. et al. Mouse neutrophils release extracellular traps in response to *Naegleria fowleri*. *Parasite Immunol* **41**, e12610 (2019).
- 28 Contis-Montes de Oca, A. et al. Neutrophils extracellular traps damage *Naegleria fowleri* trophozoites opsonized with human IgG. *Parasite Immunol* **38**, 481-495 (2016).
- 29 Flores-Huerta, N. et al. The MPO system participates actively in the formation of an oxidative environment produced by neutrophils and activates the antioxidant mechanism of *Naegleria fowleri*. *J Leukoc Biol* **108**, 895-908 (2020).
- 30 Lee, J. et al. Excretory and Secretory Proteins of *Naegleria fowleri* Induce Inflammatory Responses in BV-2 Microglial Cells. *J Eukaryot Microbiol* **64**, 183-192 (2017).
- 31 Coronado-Velazquez, D., Betanzos, A., Serrano-Luna, J. & Shibayama, M. An In Vitro Model of the Blood-Brain Barrier: *Naegleria fowleri* Affects the Tight Junction Proteins and Activates the Microvascular Endothelial Cells. *J Eukaryot Microbiol* **65**, 804-819 (2018).
- 32 Lee, Y. J. et al. *Naegleria fowleri* lysate induces strong cytopathic effects and pro-inflammatory cytokine release in rat microglial cells. *Korean J Parasitol* **49**, 285-290 (2011).
- 33 Kim, J. H. et al. IL-1beta and IL-6 activate inflammatory responses of astrocytes against *Naegleria fowleri* infection via the modulation of MAPKs and AP-1. *Parasite Immunol* **35**, 120-128 (2013).
- 34 Carrasco-Yeppez, M. M. et al. *Naegleria fowleri* immunization modifies lymphocytes and APC of nasal mucosa. *Parasite Immunol* **40** (2018).
- 35 Fischer-Stenger, K. & Marciano-Cabral, F. The arginine-dependent cytolytic mechanism plays a role in destruction of *Naegleria fowleri* amoebae by activated macrophages. *Infect Immun* **60**, 5126-5131 (1992).
- 36 Jung, S. Y. et al. Gene silencing of *nfa1* affects the in vitro cytotoxicity of *Naegleria fowleri* in murine macrophages. *Mol Biochem Parasitol* **165**, 87-93 (2009).
- 37 Rojas-Hernandez, S. et al. Nitric oxide production and nitric oxide synthase immunoreactivity in *Naegleria fowleri*. *Parasitol Res* **101**, 269-274 (2007).
- 38 Song, K. J. et al. Reactive oxygen species-dependent necroptosis in Jurkat T cells induced by pathogenic free-living *Naegleria fowleri*. *Parasite Immunol* **33**, 390-400 (2011).
- 39 Sohn, H. J., Kim, J. H., Shin, M. H., Song, K. J. & Shin, H. J. The Nf-actin gene is an important factor for food-cup formation and cytotoxicity of pathogenic *Naegleria fowleri*. *Parasitol Res* **106**, 917-924 (2010).

- 40 Krishnaswamy, V. R., Benbenishty, A., Blinder, P. & Sagi, I. Demystifying the extracellular matrix and its proteolytic remodeling in the brain: structural and functional insights. *Cell Mol Life Sci* **76**, 3229-3248 (2019).
- 41 Carrasco-Yopez, M., Rojas-Hernandez, S., Rodriguez-Monroy, M. A., Terrazas, L. I. & Moreno-Fierros, L. Protection against *Naegleria fowleri* infection in mice immunized with Cry1Ac plus amoebic lysates is dependent on the STAT6 Th2 response. *Parasite Immunol* **32**, 664-670 (2010).
- 42 De Jonckheere, J. F. Origin and evolution of the worldwide distributed pathogenic amoeboflagellate *Naegleria fowleri*. *Infect Genet Evol* **11**, 1520-1528 (2011).
- 43 Herman, E. K. *et al.* Genomics and transcriptomics yields a system-level view of the biology of the pathogen *Naegleria fowleri*. *BMC Biol* **19**, 142 (2021).
- 44 Matanock, A., Mehal, J. M., Liu, L., Blau, D. M. & Cope, J. R. Estimation of Undiagnosed *Naegleria fowleri* Primary Amebic Meningoencephalitis, United States. *Emerg Infect Dis* **24**, 162-164 (2018).
- 45 Lares-Jimenez, L. F. *et al.* Detection of serum antibodies in children and adolescents against *Balamuthia mandrillaris*, *Naegleria fowleri* and *Acanthamoeba* T4. *Exp Parasitol* **189**, 28-33 (2018).
- 46 Dubray, B. L., Wilhelm, W. E. & Jennings, B. R. Serology of *Naegleria fowleri* and *Naegleria lovaniensis* in a hospital survey. *J Protozool* **34**, 322-327 (1987).
- 47 Rivera, V. *et al.* IgA and IgM anti-*Naegleria fowleri* antibodies in human serum and saliva. *Can J Microbiol* **47**, 464-466 (2001).
- 48 Yera, H. *et al.* In vitro growth, cytopathic effects and clearance of monolayers by clinical isolates of *Balamuthia mandrillaris* in human skin cell cultures. *Exp Parasitol* **156**, 61-67 (2015).
- 49 Soto-Arredondo, K. J., Flores-Villavicencio, L. L., Serrano-Luna, J. J., Shibayama, M. & Sabanero-Lopez, M. Biochemical and cellular mechanisms regulating *Acanthamoeba castellanii* adherence to host cells. *Parasitology* **141**, 531-541 (2014).
- 50 Flores-Maldonado, C. *et al.* *Acanthamoeba* (T4) trophozoites cross the MDCK epithelium without cell damage but increase paracellular permeability and transepithelial resistance by modifying tight junction composition. *Exp Parasitol* **183**, 69-75 (2017).
- 51 Omana-Molina, M. *et al.* In vivo CNS infection model of *Acanthamoeba* genotype T4: the early stages of infection lack presence of host inflammatory response and are a slow and contact-dependent process. *Parasitol Res* **116**, 725-733 (2017).
- 52 Omana-Molina, M. *et al.* Reevaluating the role of *Acanthamoeba* proteases in tissue invasion: observation of cytopathogenic mechanisms on MDCK cell monolayers and hamster corneal cells. *Biomed Res Int* **2013**, 461329 (2013).
- 53 Ramirez-Rico, G., Martinez-Castillo, M., de la Garza, M., Shibayama, M. & Serrano-Luna, J. *Acanthamoeba castellanii* Proteases are Capable of Degrading Iron-Binding Proteins as a Possible Mechanism of Pathogenicity. *J Eukaryot Microbiol* **62**, 614-622 (2015).
- 54 Sissons, J. *et al.* Identification and properties of proteases from an *Acanthamoeba* isolate capable of producing granulomatous encephalitis. *BMC Microbiol* **6**, 42 (2006).
- 55 Pumidonming, W., Walochnik, J., Dauber, E. & Petry, F. Binding to complement factors and activation of the alternative pathway by *Acanthamoeba*. *Immunobiology* **216**, 225-233 (2011).
- 56 Stewart, G. L. *et al.* Antibody-dependent neutrophil-mediated killing of *Acanthamoeba castellanii*. *Int J Parasitol* **24**, 739-742 (1994).
- 57 Sissons, J. *et al.* Use of in vitro assays to determine effects of human serum on biological characteristics of *Acanthamoeba castellanii*. *J Clin Microbiol* **44**, 2595-2600 (2006).
- 58 Toney, D. M. & Marciano-Cabral, F. Resistance of *Acanthamoeba* species to complement lysis. *J Parasitol* **84**, 338-344 (1998).
- 59 Huang, J. M., Chang, Y. T., Shih, M. H., Lin, W. C. & Huang, F. C. Identification and characterization of a secreted M28 aminopeptidase protein in *Acanthamoeba*. *Parasitol Res* **118**, 1865-1874 (2019).
- 60 Alvarado-Ocampo, J., Retana-Moreira, L. & Abrahams-Sandi, E. In vitro effects of environmental isolates of *Acanthamoeba* T4 and T5 over human erythrocytes and platelets. *Exp Parasitol* **210**, 107842 (2020).

- 61 Sissons, J. *et al.* *Acanthamoeba castellanii* induces host cell death via a phosphatidylinositol 3-kinase-dependent mechanism. *Infect Immun* **73**, 2704-2708 (2005).
- 62 Massilamany, C. *et al.* SJL mice infected with *Acanthamoeba castellanii* develop central nervous system autoimmunity through the generation of cross-reactive T cells for myelin antigens. *PLoS One* **9**, e98506 (2014).
- 63 Benedetto, N. *et al.* Defense mechanisms of IFN-gamma and LPS-primed murine microglia against *Acanthamoeba castellanii* infection. *Int Immunopharmacol* **3**, 825-834 (2003).
- 64 Marciano-Cabral, F., Ludwick, C., Puffenbarger, R. A. & Cabral, G. A. Differential stimulation of microglial pro-inflammatory cytokines by *Acanthamoeba culbertsoni* versus *Acanthamoeba castellanii*. *J Eukaryot Microbiol* **51**, 472-479 (2004).
- 65 Shin, H. J. *et al.* Cytopathic changes in rat microglial cells induced by pathogenic *Acanthamoeba culbertsoni*: morphology and cytokine release. *Clin Diagn Lab Immunol* **8**, 837-840 (2001).
- 66 Harrison, J. L. *et al.* *Acanthamoeba culbertsoni* elicits soluble factors that exert anti-microglial cell activity. *Infect Immun* **78**, 4001-4011 (2010).
- 67 Huang, J. M. *et al.* Pathogenic *Acanthamoeba castellanii* Secretes the Extracellular Aminopeptidase M20/M25/M40 Family Protein to Target Cells for Phagocytosis by Disruption. *Molecules* **22** (2017).
- 68 Michalek, M. *et al.* Structure and function of a unique pore-forming protein from a pathogenic acanthamoeba. *Nat Chem Biol* **9**, 37-42 (2013).
- 69 Chusattayanond, A. D., Boonsilp, S., Kasisit, J., Boonmee, A. & Warit, S. Thai *Acanthamoeba* isolate (T4) induced apoptotic death in neuroblastoma cells via the Bax-mediated pathway. *Parasitol Int* **59**, 512-516 (2010).
- 70 Castelan-Ramírez, I. *et al.* Schwann Cell Autophagy and Necrosis as Mechanisms of Cell Death by *Acanthamoeba*. *Pathogens* **9** (2020).
- 71 Marciano-Cabral, F. & Toney, D. M. The interaction of *Acanthamoeba* spp. with activated macrophages and with macrophage cell lines. *J Eukaryot Microbiol* **45**, 452-458 (1998).
- 72 Cano, A., Mattana, A., Henriquez, F. L., Alexander, J. & Roberts, C. W. *Acanthamoeba* proteases contribute to macrophage activation through PAR1, but not PAR2. *Parasite Immunol* **41**, e12612 (2019).
- 73 Mattana, A. *et al.* *Acanthamoeba castellanii* Genotype T4 Stimulates the Production of Interleukin-10 as Well as Proinflammatory Cytokines in THP-1 Cells, Human Peripheral Blood Mononuclear Cells, and Human Monocyte-Derived Macrophages. *Infect Immun* **84**, 2953-2962 (2016).
- 74 Cano, A. *et al.* *Acanthamoeba* Activates Macrophages Predominantly through Toll-Like Receptor 4- and MyD88-Dependent Mechanisms To Induce Interleukin-12 (IL-12) and IL-6. *Infect Immun* **85**, e01054-01016 (2017).
- 75 Costa, A. O. *et al.* Distinct immunomodulatory properties of extracellular vesicles released by different strains of *Acanthamoeba*. *Cell Biol Int* **45**, 1060-1071 (2021).
- 76 Hurt, M., Proy, V., Niederkorn, J. Y. & Alizadeh, H. The interaction of *Acanthamoeba castellanii* cysts with macrophages and neutrophils. *J Parasitol* **89**, 565-572 (2003).
- 77 McClellan, K., Howard, K., Mayhew, E., Niederkorn, J. & Alizadeh, H. Adaptive immune responses to *Acanthamoeba* cysts. *Exp Eye Res* **75**, 285-293 (2002).
- 78 Lanocha-Arendarczyk, N. *et al.* Changes in the immune system in experimental acanthamoebiasis in immunocompetent and immunosuppressed hosts. *Parasit Vectors* **11**, 517 (2018).
- 79 Tanaka, Y. *et al.* *Acanthamoeba*-specific human T-cell clones isolated from healthy individuals. *Parasitol Res* **80**, 549-553 (1994).
- 80 Hernández-Jasso, M. *et al.* Morphological Description of the Early Events during the Invasion of *Acanthamoeba castellanii* Trophozoites in a Murine Model of Skin Irradiated under UV-B Light. *Pathogens* **9** (2020).
- 81 Schimmel, M. & Mehta, I. Granulomatous Amebic Encephalitis. *N Engl J Med* **383**, 1262-1262 (2020).

- 82 Dunnebacke, T. H. The amoeba *Balamuthia mandrillaris* feeds by entering into mammalian cells in culture. *J Eukaryot Microbiol* **54**, 452-464 (2007).
- 83 Kiderlen, A. F. *et al.* Cytopathogenicity of *Balamuthia mandrillaris*, an opportunistic causative agent of granulomatous amebic encephalitis. *J Eukaryot Microbiol* **53**, 456-463 (2006).
- 84 Matin, A. *et al.* *Balamuthia mandrillaris* interactions with human brain microvascular endothelial cells in vitro. *J Med Microbiol* **56**, 1110-1115 (2007).
- 85 Matin, A. & Khan, N. A. Demonstration and partial characterization of ecto-ATPase in *Balamuthia mandrillaris* and its possible role in the host-cell interactions. *Lett Appl Microbiol* **47**, 348-354 (2008).
- 86 Rocha-Azevedo, B., Jamerson, M., Cabral, G. A., Silva-Filho, F. C. & Marciano-Cabral, F. The interaction between the amoeba *Balamuthia mandrillaris* and extracellular matrix glycoproteins in vitro. *Parasitology* **134**, 51-58 (2007).
- 87 Kiderlen, A. F. & Laube, U. *Balamuthia mandrillaris*, an opportunistic agent of granulomatous amebic encephalitis, infects the brain via the olfactory nerve pathway. *Parasitol Res* **94**, 49-52 (2004).
- 88 Janitschke, K., Martínez, A. J., Visvesvara, G. S. & Schuster, F. Animal model *Balamuthia mandrillaris* CNS infection: contrast and comparison in immunodeficient and immunocompetent mice: a murine model of "granulomatous" amebic encephalitis. *J Neuropathol Exp Neurol* **55**, 815-821 (1996).
- 89 Kiderlen, A. F., Radam, E., Laube, U. & Martinez, A. J. Resistance to intranasal infection with *Balamuthia mandrillaris* amoebae is T-cell dependent. *J Eukaryot Microbiol* **62**, 26-33 (2015).
- 90 Kiderlen, A. F., Laube, U., Radam, E. & Tata, P. S. Oral infection of immunocompetent and immunodeficient mice with *Balamuthia mandrillaris* amoebae. *Parasitol Res* **100**, 775-782 (2007).
- 91 Bravo, F. G. & Seas, C. *Balamuthia mandrillaris* amoebic encephalitis: an emerging parasitic infection. *Curr Infect Dis Rep* **14**, 391-396 (2012).
- 92 Wang, L. *et al.* *Balamuthia mandrillaris* infection in China: A retrospective report of 28 cases. *Emerg Microbes Infect* **9**, 2348-2357 (2020).
- 93 Kiderlen, A. F. *et al.* *Balamuthia* and *Acanthamoeba*-binding antibodies in West African human sera. *Exp Parasitol* **126**, 28-32 (2010).
- 94 Cope, J. R. *et al.* The epidemiology and clinical features of *Balamuthia mandrillaris* disease in the United States, 1974-2016. *Clin Infect Dis* **68**, 1815-1822 (2019).
- 95 Hsu, B. M., Lin, C. L. & Shih, F. C. Survey of pathogenic free-living amoebae and *Legionella* spp. in mud spring recreation area. *Water Res* **43**, 2817-2828 (2009).
- 96 Magnet, A. *et al.* A year long study of the presence of free living amoeba in Spain. *Water Res* **47**, 6966-6972 (2013).
- 97 De Jonckheere, J. F. Pathogenic free-living amoebae in swimming pools: survey in Belgium. *Ann Microbiol (Paris)* **130B**, 205-212 (1979).
- 98 Yousuf, F. A., Siddiqui, R., Subhani, F. & Khan, N. A. Status of free-living amoebae (*Acanthamoeba* spp., *Naegleria fowleri*, *Balamuthia mandrillaris*) in drinking water supplies in Karachi, Pakistan. *J Water Health* **11**, 371-375 (2013).
- 99 Borecka, A. *et al.* *Acanthamoeba* - pathogen and vector of highly pathogenic bacteria strains to healthy and immunocompromised individuals. *Cent Eur J Immunol* **45**, 228-232 (2020).
- 100 Kiderlen, A. F., Radam, E. & Tata, P. S. Assessment of *Balamuthia mandrillaris*-specific serum antibody concentrations by flow cytometry. *Parasitol Res* **104**, 663-670 (2009).
- 101 Cursons, R. T., Brown, T. J., Keys, E. A., Moriarty, K. M. & Till, D. Immunity to pathogenic free-living amoebae: role of humoral antibody. *Infect Immun* **29**, 401-407 (1980).
- 102 Marciano-Cabral, F., Cline, M. L. & Bradley, S. G. Specificity of antibodies from human sera for *Naegleria* species. *J Clin Microbiol* **25**, 692-697 (1987).

- 103 Jackson, B. R. *et al.* Serologic survey for exposure following fatal *Balamuthia mandrillaris* infection. *Parasitol Res* **113**, 1305-1311 (2014).
- 104 Schuster, F. L., Honarmand, S., Visvesvara, G. S. & Glaser, C. A. Detection of antibodies against free-living amoebae *Balamuthia mandrillaris* and *Acanthamoeba* species in a population of patients with encephalitis. *Clin Infect Dis* **42**, 1260-1265 (2006).
- 105 De Jonckheere, J. F. What do we know by now about the genus *Naegleria*? *Exp Parasitol* **145 Suppl**, S2-9 (2014).
- 106 Huang, Z. H., Ferrante, A. & Carter, R. F. Serum antibodies to *Balamuthia mandrillaris*, a free-living amoeba recently demonstrated to cause granulomatous amoebic encephalitis. *J Infect Dis* **179**, 1305-1308 (1999).
- 107 De Jonckheere, J. F. The impact of man on the occurrence of the pathogenic free-living amoeboflagellate *Naegleria fowleri*. *Future Microbiol* **7**, 5-7 (2012).
- 108 Kao, P. M. *et al.* Real-time PCR method for the detection and quantification of *Acanthamoeba* species in various types of water samples. *Parasitol Res* **112**, 1131-1136 (2013).
- 109 Baltaza, W. *et al.* Comparative examination on selected amphizoic amoebae in terms of their in vitro temperature tolerance - a possible indirect marker of potential pathogenicity of *Acanthamoeba* strains. *Ann Parasitol* **64**, 317-322 (2018).
- 110 Brubaker, S. W., Bonham, K. S., Zanoni, I. & Kagan, J. C. Innate immune pattern recognition: a cell biological perspective. *Annu Rev Immunol* **33**, 257-290 (2015).
- 111 Koenderman, L., Buurman, W. & Daha, M. R. The innate immune response. *Immunol Lett* **162**, 95-102 (2014).
- 112 Klion, A. D. & Nutman, T. B. The role of eosinophils in host defense against helminth parasites. *J Allergy Clin Immunol* **113**, 30-37 (2004).
- 113 Sollberger, G., Tilley, D. O. & Zychlinsky, A. Neutrophil Extracellular Traps: The Biology of Chromatin Externalization. *Dev Cell* **44**, 542-553 (2018).
- 114 Mortaz, E., Alipoor, S. D., Adcock, I. M., Mumby, S. & Koenderman, L. Update on Neutrophil Function in Severe Inflammation. *Front Immunol* **9**, 2171 (2018).
- 115 Rosenstein, N. E., Perkins, B. A., Stephens, D. S., Popovic, T. & Hughes, J. M. Meningococcal disease. *N Engl J Med* **344**, 1378-1388 (2001).



3

# CHAPTER 3

---

## Inhibition of fatty acid oxidation as a new target to treat Primary Amoebic Meningoencephalitis

Maarten J. Sarink<sup>1</sup>, Aloysius G.M. Tielens<sup>1,2</sup>, Annelies Verbon<sup>1</sup>, Robert Sutak<sup>3</sup>,  
Jaap J. van Hellemond<sup>1</sup>

<sup>1</sup> Department of Medical Microbiology and Infectious Diseases, Erasmus MC University Medical Center Rotterdam, The Netherlands

<sup>2</sup> Department of Biochemistry and Cell Biology, Faculty of Veterinary Medicine, Utrecht University, Utrecht, The Netherlands

<sup>3</sup> Department of Parasitology, Faculty of Science, Charles University, BIOCEV, Vestec, Czech Republic

## Abstract

Primary Amoebic Meningoencephalitis (PAM) is a rapidly fatal infection caused by the free-living amoeba *Naegleria fowleri*. The amoeba migrates along the olfactory nerve to the brain, resulting in seizures, coma, and, eventually, death. Previous research has shown that *Naegleria gruberi*, a close relative of *N. fowleri*, prefers lipids over glucose as an energy source. Therefore, we tested several already approved inhibitors of fatty acid oxidation alongside the currently used drugs amphotericin B and miltefosine. Our data demonstrate that etomoxir, orlistat, perhexiline, thioridazine, and valproic acid inhibited growth of *N. gruberi*. We then tested these compounds on *N. fowleri* and found etomoxir, perhexiline, and thioridazine to be effective growth inhibitors. Hence, not only are lipids the preferred food source for *N. gruberi*, but oxidation of fatty acids also seems to be essential for growth of *N. fowleri*. Inhibition of fatty acid oxidation could result in new treatment options, as thioridazine inhibits *N. fowleri* growth in concentrations that can be reached at the site of infection. It could also potentiate currently used therapy, as checkerboard assays revealed synergy between miltefosine and etomoxir. Animal testing should be performed to confirm the added value of these inhibitors. Although the development of new drugs and randomized controlled trials for this rare disease are nearly impossible, inhibition of fatty acid oxidation seems a promising strategy as we showed effectivity of several drugs that are or have been in use and that thus could be repurposed to treat PAM in the future.

## Introduction

The amoeba *Naegleria fowleri* causes primary amoebic meningoencephalitis (PAM), a rapidly fatal disease of the central nervous system (CNS) <sup>1-3</sup>. *N. fowleri* is one of the three most common free-living amoebae that can infect humans, the others being *Acanthamoeba* spp. and *Balamuthia mandrillaris*. These amoebae are ubiquitously present, with *N. fowleri* reported on all continents, except Antarctica <sup>4</sup>. In the United States, *N. fowleri* infections occur mostly in healthy children and young adults during recreational water activities, such as swimming, diving, and rafting <sup>5-7</sup>. In the Indian subcontinent, the correlation with age is less clear, probably because ablution rituals, washing and a lack of chlorination play a large role in the epidemiology <sup>7,8</sup>. When water containing *N. fowleri* makes contact with the nasal epithelium, the trophozoite stage of the amoeba can migrate along the olfactory nerve, through the cribriform plate to the olfactory bulb within the CNS <sup>2,3,9</sup>. Once inside the brain, the trophozoites cause necrosis and acute inflammation, ultimately leading to death in over 95% of the cases <sup>1,3</sup>. There is concern that global warming and changes in the ecosystems that *N. fowleri* inhabits may lead to more cases worldwide <sup>7,8,10</sup>. A wide range of antifungals and antibiotics have been used to treat PAM with various degrees of effectivity. Most evidence is available for amphotericin B and miltefosine, but CNS penetration of these drugs is poor <sup>11-14</sup>. Because of the high mortality rate, more-effective drugs are urgently needed <sup>15</sup>.

Inhibition of metabolic processes essential to microorganisms is a fruitful strategy for the development of effective drugs <sup>16</sup>. Several widely used drugs target the metabolism of the pathogen to exert their killing effect, such as the antimalarials atovaquone and proguanil, and the broad-spectrum antiprotozoal, antihelminthic, and antiviral drug nitazoxanide <sup>17,18</sup>.

Previous research by our group showed that *N. gruberi*, a close relative to *N. fowleri*, prefers fatty acids as a food source <sup>19</sup>. This led us to the hypothesis that inhibiting fatty acid oxidation (FAO) could inhibit growth of or even kill the amoeba. We identified several drugs that are currently used or have been used that inhibit fatty acid metabolism in different parts of this pathway. All of those drugs target enzymes that are present in the *N. gruberi* and *N. fowleri* genome <sup>19</sup> (see also Fig. 1 and Discussion). As the fatty acid preference was shown in *N. gruberi*, we first determined the effects of these compounds on *N. gruberi*. We then tested promising compounds on the actual pathogen, *N. fowleri*, and finally determined whether there was synergy present when compounds were combined in a checkerboard assay.

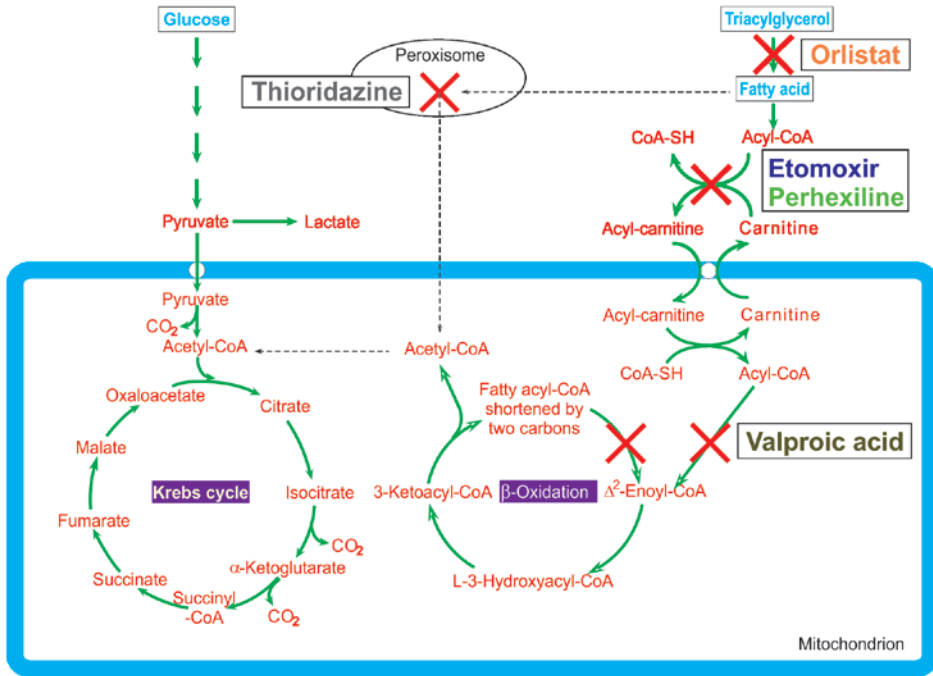


**Figure 1.** Main pathways of energy metabolism of *N. gruberi* with targets of different fatty acid oxidation inhibitors depicted as crosses.

Dashed lines indicate uncertainties of the actual processes.

## Results

The inhibitory effects of all compounds on *N. gruberi* determined through area under the curve (AUC) calculation are represented in Fig. 2. Thioridazine (TDZ) inhibited growth of *N. gruberi* in a concentration-dependent manner, inhibiting 50 % of growth at approximately 10  $\mu$ M (Fig. 2A). Addition of perhexiline (PHX) resulted in an inhibition level of about 50% in concentrations above 50  $\mu$ M (Fig. 2B). Etomoxir (ETO) addition resulted in clear inhibition at concentrations above 600  $\mu$ M (Fig. 2C), addition of valproic acid (VPA) resulted in inhibition of growth in a concentration dependent manner, with inhibition of 50 % of growth around 700  $\mu$ M (Fig. 2D). Orlistat (ORL) inhibited circa 50% of growth in concentrations of 50  $\mu$ M and higher (Fig. 2E), amphotericin B (AMB) was very effective at inhibiting growth, inhibiting circa 75 % at concentrations of 0.2  $\mu$ M and higher (Fig. 2F). Addition of miltefosine (MIL) resulted in inhibition in a concentration dependent manner with efficient inhibition of growth at 80  $\mu$ M (Fig. 2G). The capacities for regrowth of the amoebae after 5 days of exposure differed for the examined compounds, as can be seen in the bars above the individual graphs in Fig. 2. Amoebae incubated with VPA and ORL

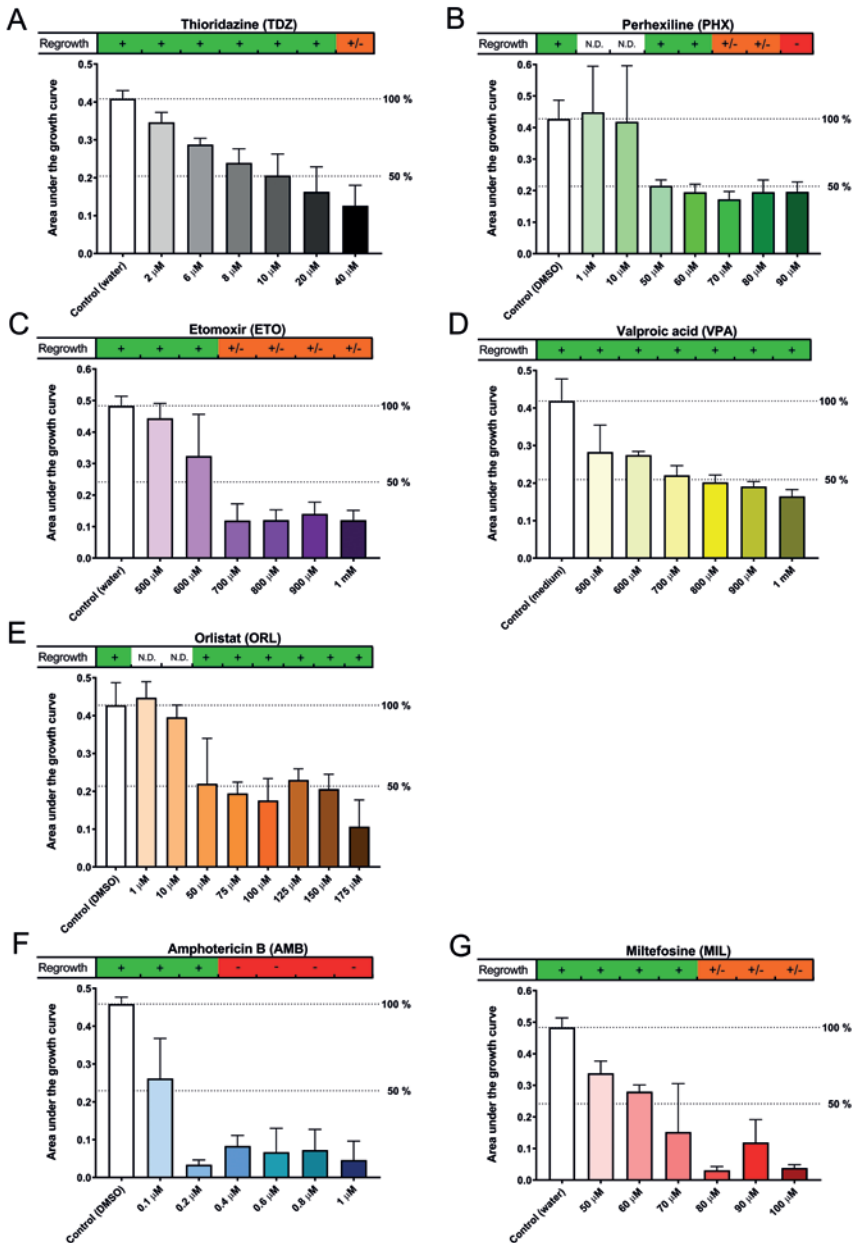


**Figure 2.** Growth curves of *Naegleria gruberi* were obtained in the presence or absence of inhibitors of fatty acid oxidation or drugs currently used to treat primary amoebic meningoencephalitis.

Optical density was measured daily over a 5-day period. Shown is the Area Under the growth Curve (AUC) of compounds and respective controls. Indicated are lines of 100 % and 50 % of the control AUC. On top of the graph the capacity for regrowth is shown. + : clear regrowth; +/- : inconsistent or little regrowth; - : never any regrowth; N.D. : Not done. Experiments were performed twice in triplicate wells, error bars are SD.

showed regrowth for all concentrations used, while PHX consistently prevented regrowth at 90  $\mu\text{M}$ . The amoebae showed regrowth after TDZ exposure at up to a concentration of 20  $\mu\text{M}$ , while the amoebae showed regrowth after ETO exposure at up to a concentration of 600  $\mu\text{M}$ . Amoebae incubated with MIL showed regrowth after exposure to concentrations below 80  $\mu\text{M}$  and inconsistent regrowth at the examined concentrations over 80  $\mu\text{M}$ . AMB was most effective in preventing regrowth, always blocking regrowth at a concentration of 0.4  $\mu\text{M}$  or higher (Fig. 2).

Next, the compounds were also assessed for their effect on *N. fowleri*. This was done in two ways: via viability staining with CellTiter-GLO and with direct cell counting using a flow cytometer. The 50% inhibitory ( $\text{IC}_{50}$ ) concentrations of all drugs on both organisms can be seen in Table 1. The  $\text{IC}_{50}$  results of compounds tested on *N. gruberi* represent an approximation, as the range of concentrations tested is narrow. Results of the CellTiter-GLO viability stain assay can be seen in Fig. 3, results of cell counting can be seen in Figure S1. These figures show that absence of viability and absence of cell growth were observed after exposure to TDZ, PHX and ETO, revealing that these compounds are effective against *N. fowleri* as well as against *N. gruberi*. The efficacy of ETO and PHX was higher against *N. fowleri* than against *N. gruberi*, the  $\text{IC}_{50}$  levels of both drugs against *N. fowleri* was about 5-fold lower than against *N. gruberi*. VPA and ORL showed some inhibition of *N. fowleri* growth at high concentrations, but their efficacy was much lower against *N. fowleri* than against *N. gruberi*. The effects of AMB and MIL were roughly similar against *N. gruberi* and *N. fowleri*. The  $\text{IC}_{50}$  calculations show concordance between both methods, confirming the efficacy of the compounds against *N. fowleri* in two ways (Table 1). Next, compounds were combined in these  $\text{IC}_{50}$  concentrations to screen for a possible synergistic effect of combinations of compounds on *N. fowleri* (see Table S1 in the supplemental material). Checkerboard assays were performed for the best six combinations of the drugs, after which  $F_{\text{min}}$  was calculated. The combinations MIL + PHX, MIL + TDZ, MIL + VPA, PHX + TDZ and TDZ + VPA showed additivity. The combination of ETO and MIL resulted in an  $F$  of 0.5, indicating that synergy when these drugs are combined (Table S1). Further analysis of the synergistic effect of the combination ETO and MIL with the program Combobenefit resulted in a mapped surface analysis whose results can be seen in Fig. 4. This map shows that synergy is most pronounced when 12.5 and 25  $\mu\text{M}$  concentrations of MIL are combined with 25 – 200  $\mu\text{M}$  concentrations of ETO.

**Table 1.** IC<sub>50</sub> concentrations in  $\mu\text{M}$  with 95% confidence interval (CI) of compounds tested on *Naegleria gruberi* and *N. fowleri*.

	Target	<i>Naegleria gruberi</i>			<i>Naegleria fowleri</i>		
		IC <sub>50</sub> ( $\mu\text{M}$ ) (Area under the growth curve)	95% CI	IC <sub>50</sub> ( $\mu\text{M}$ ) (CellTiter-GLO)	95% CI	IC <sub>50</sub> ( $\mu\text{M}$ ) (Cell counting)	95% CI
Thioridazine	Peroxisomal lipid oxidation <sup>20</sup>	13	(10.6 – 16.0)	6.5	(5.0 – 8.4)	9.8	(7.3 – 12.9)
Perhexiline	CPT-1 <sup>21</sup>	56	(46.6 – 65.3)	7.5	(6.0 – 9.4)	17.4	(14.9 – 20.4)
Etomoxir	CPT-1 <sup>22</sup>	666	(625 – 708)	146.0	(114.9 – 185.5)	108.7	(78.2 – 148)
Valproic acid	Acyl-CoA dehydrogenase <sup>23</sup>	788	(741 – 845)	*		*	
Orlistat	Lipase <sup>24</sup>	75	(56.1 – 98.2)	*		*	
Amphotericin B	Sterols <sup>15</sup>	0.09	(0.04 – 0.13)	0.011	(0.007 – 0.016)	0.027	(0.016 – 0.044)
Miltefosine	Unknown <sup>25</sup>	61	(56.5 – 64.7)	28.2	(23.8 – 33.4)	33.4	(25.6 – 43.0)

Growth curves of *N. gruberi* were obtained by measuring optical density daily over a 5-day period, after which area under the growth curve was calculated. The IC<sub>50</sub> results of compounds tested on *N. gruberi* are an approximation, as the range of concentrations tested is narrow. *N. fowleri* was tested in two ways, with CellTiter-GLO ATP stain and through cell counting with guava EasyCyte flow cytometer. CellTiter-GLO luminescence was determined after 24 hours of incubation, cell counts were determined after 72 hours of incubation. Raw data were normalised as a percentage of the respective control. Nonlinear regression was performed by GraphPad Prism 8 as [Inhibitor] vs. normalized response with a variable slope, after which IC<sub>50</sub> was calculated. \* : calculation not possible.

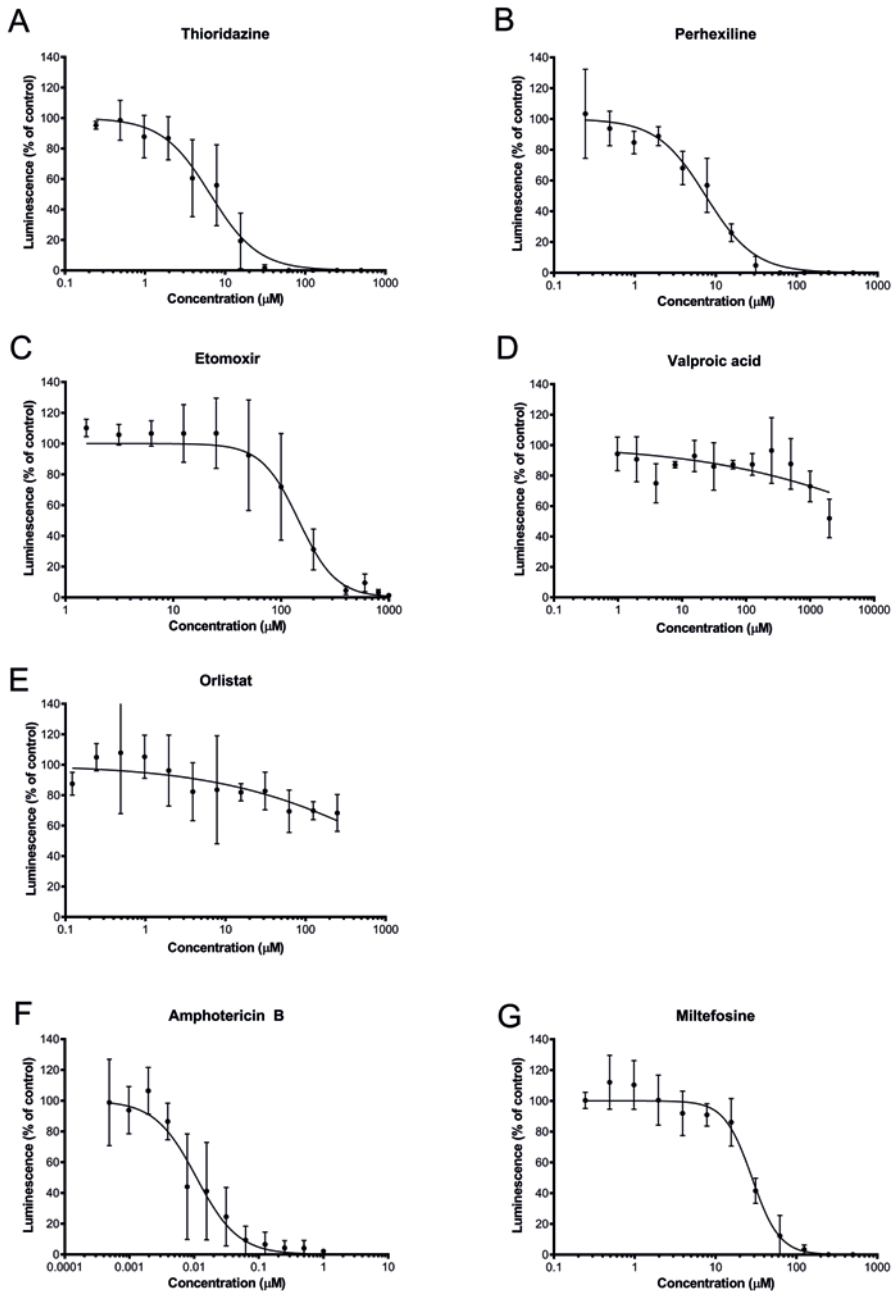


**Figure 3.** Luminescence as a percentage of control after compound exposure to *Naegleria fowleri* for 24 hours in twofold serial dilutions.

Luminescence was measured after addition of CellTiter-GLO ATP stain, in the presence or absence of inhibitors of fatty acid oxidation or drugs currently used to treat primary amoebic meningoencephalitis. Experiments were performed in triplicate, error bars are SD.

## Discussion

Our study showed that fatty acid oxidation (FAO) inhibitors clearly inhibited growth of both *N. gruberi* and *N. fowleri* *in vitro*. Hence, not only are lipids the preferred food source for *N. gruberi*, but oxidation of fatty acids seems to be essential also for growth of *N. fowleri*. The current treatment of miltefosine (MIL) and amphotericin B (AMB) was confirmed to be effective at inhibiting growth *in vitro*, which is in agreement with previous reports<sup>(26-29)</sup> and validates our assays performed to detect compounds that inhibit growth of *Naegleria*. The importance of fatty acid oxidation for *N. fowleri* was demonstrated in a recent *in vivo* study, as Herman et al. observed upregulation of genes of *N. fowleri* involved in FAO after mouse passage<sup>30</sup>. Our results now show that FAO inhibition is a valid target for new PAM therapy options, as etomoxir (ETO), perhexiline (PHX) and thioridazine (TDZ) showed total growth inhibition of *N. fowleri*. Furthermore, our results show that there is additivity of MIL combined with PHX, TDZ, and valproic acid (VPA) and synergy between ETO and MIL, providing evidence that inhibition of fatty acid oxidation can be a valuable addition to the current treatment regimen.

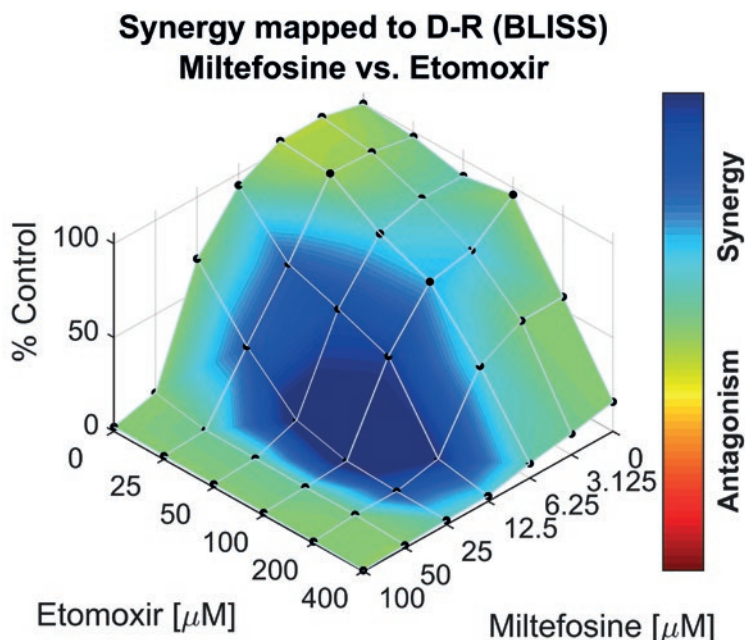


**Figure 4.** Concentrations surface response plot of checkerboards assay with etomoxir and miltefosine against *Naegleria fowleri* using the BLISS model.

Etomoxir and miltefosine were separately tested and combined in 5 and 6 concentrations, respectively. Luminescence was measured after 24 hours of exposure, after addition of CellTiter-GLO ATP stain. Raw luminescence data was normalised as a percentage of the control, results were analysed and plot was generated with the combenefit program. Colours indicate presence or absence of synergy.

We observed some differences between *N. gruberi* and *N. fowleri* in the levels of efficacy of the FAO inhibitors. All FAO inhibitors affected *N. gruberi* growth, but the effects of VPA and orlistat (ORL) were much less profound on *N. fowleri* than on *N. gruberi*. In contrast, ETO and PHX were more effective at inhibiting growth of *N. fowleri* than *N. gruberi*. When the targets of the FAO inhibitors are taken into account, we can hypothesize on the reasons for these differences. The investigated FAO inhibitors affect different enzymes involved in lipid metabolism (depicted in Fig. 1). TDZ inhibits peroxisomal oxidation of lipids<sup>20,31</sup>. ORL inhibits lipases, enzymes that hydrolyze triacylglycerol, thereby obstructing the first step in the breakdown of lipids<sup>24</sup>. ETO and PHX inhibit the carnitine palmitoyltransferase-1 (CPT-1), blocking transport of fatty acids into mitochondria<sup>21,22</sup>. Among other activities, VPA interferes mainly with mitochondrial  $\beta$ -oxidation<sup>23</sup>. The targets of the FAO inhibitors are present in the *N. gruberi* as well as in the *N. fowleri* genome, showing that regarding the metabolic properties, both organisms are very much alike<sup>19,32,33</sup>. However, this does not imply that the enzymes are exactly identical in amino acid sequence. Minor amino acid differences could result in small structural differences and hence in differences in the effects of the various drugs. Furthermore, unavoidable differences between *N. fowleri* and *N. gruberi* under *in vitro* growth conditions could play a role, as optimal culture medium (PYNFH vs Bacto Casitone) and culture temperature (25 °C vs 37 °C) are different between the two, resulting in different metabolic rates.

We observed that several FAO inhibitors show additivity (PHX, TDZ, and VPA) or synergy (ETO) when combined with MIL. Unfortunately, synergy between AMB and the FAO inhibitors was not observed. This would be of importance, as AMB has serious side-effects<sup>14</sup>. There is also a risk for serious adverse events when using MIL<sup>34</sup>. We did observe synergy between ETO and MIL, which is a promising result as this could potentially lead to lowering of MIL dosages and subsequent reduction in the risk of serious adverse events. ETO has been in use for some time, but was retired due to its adverse side effects in the liver. Currently, it is being repurposed as an anticancer agent<sup>35</sup>. Unfortunately, there are no data on the pharmacokinetics of ETO, so we do not know the clinical applicability of ETO. We found a relatively high  $IC_{50}$  against *N. fowleri* of approximately 100 to 150  $\mu$ M, but the synergy shown with MIL deserves further investigation in an animal model.

Of all FAO inhibitors tested, TDZ showed the lowest  $IC_{50}$  (approximately 6 to 10  $\mu$ M) against *N. fowleri* in our study. TDZ has been in use as an antipsychotic drug since the early 1950s and was originally identified as a dopamine receptor 2 antagonist. Later, TDZ was also shown to be a selective inhibitor of peroxisomal  $\beta$ -oxidation<sup>20,31</sup>. It is now being repurposed as an anticancer, anti-inflammatory and antimicrobial agent<sup>36-39</sup>. The pharmacokinetics of TDZ are well studied. In a recent clinical study, the sum of TDZ and its metabolites in

serum approached 10  $\mu\text{M}$  <sup>38</sup>. Furthermore, TDZ has been shown to accumulate in brain tissue of chronically treated patients, resulting in concentrations 10-fold higher than that in serum <sup>40</sup>. Although AMB is effective at nanomolar concentrations, AMB and MIL are known to have poor CNS penetration <sup>11-14</sup>. This could possibly explain the poor prospects for treatment of patients with PAM and emphasizes the possible benefit of TDZ.

Development and testing of new drugs for PAM are difficult, as randomized controlled trials for the treatment of PAM are impossible due to the rapidly fatal nature of the disease and its relatively rare occurrence. Repurposing existing drugs is therefore the most promising way to obtain additional drugs to combat PAM. There are numerous examples of drugs that have been successfully repurposed to treat rare diseases <sup>41</sup>. All tested FAO inhibitors (including TDZ and ETO) have been or are still in clinical use. TDZ inhibits *N. fowleri* growth in concentrations that can be reached at the site of infection, and checkerboard assays revealed synergy between MIL and ETO. Further animal testing should be performed to confirm the added value of these inhibitors.

## Materials and Methods

### Chemicals and amoeba culture.

*N. gruberi* strain NEG-M (ATCC® 30224) was grown axenically at 25 °C in modified PYNFH medium (peptone, yeast extract, yeast nucleic acid, folic acid, 10% heat-inactivated fetal bovine serum, 100 units/ml penicillin, 100  $\mu\text{g}/\text{ml}$  streptomycin, and 40  $\mu\text{g}/\text{ml}$  gentamicin) (ATCC medium 1034), as described before <sup>19</sup>. *N. fowleri* strain HB-1, kindly provided by Hana Pecková (Institute of Parasitology, Biology Center CAS, Czech Republic), was grown axenically at 37 °C in Bacto Casitone medium. Experiments with *N. fowleri* were conducted at biosafety level 2 BSL 2 safety level according to the ATCC guidelines and as specified by the Charles University. Modified PYNFH is composed of peptone, yeast extract, yeast nucleic acid, folic acid, 10% heat-inactivated fetal bovine serum, 100 units/ml penicillin, 100  $\mu\text{g}/\text{ml}$  streptomycin, and 40  $\mu\text{g}/\text{ml}$  gentamicin. Bacto Casitone medium is composed of 2% Bacto Casitone, 10% heat-inactivated fetal bovine serum, penicillin (100 U/ml), and streptomycin (100  $\mu\text{g}/\text{ml}$ ). All experiments were performed using trophozoites harvested during logarithmic-phase growth by repeatedly tapping cell culture flasks with amoebae to detach trophozoites. Amphotericin B (AMB), etomoxir (ETO), miltefosine (MIL), thioridazine (TDZ), orlistat (ORL), perhexiline (PHX), and valproic acid (VPA) were purchased from Sigma. CellTiter-Glo 2.0 Cell Viability Assay was purchased from Promega. Translucent flat-bottom 96 wells plates were purchased from Greiner Bio-One. Black flat bottom 96-wells plates were purchased from Thermo Fisher Scientific.

### **Inhibition assays for *N. gruberi***

To screen the effects of fatty acid oxidation inhibitors and current therapies for PAM on *N. gruberi*, we determined compound efficacy with optical density (OD) measurements. Drugs were prepared as stock solutions as follows: TDZ: 10 mM in water, PHX: 50 mM in dimethyl sulfoxide (DMSO), ETO: 10 mM in water, VPA: 20 mM in water, ORL: 35 mM in DMSO, AMB: 10 mM in DMSO, MIL: 10 mM in water. Stock solutions were diluted in water or PYNFH medium and added as a volume of 10  $\mu$ L to  $1 \times 10^4$  *N. gruberi* trophozoites in 90  $\mu$ L of PYNFH. Compounds were tested per plate in triplicate in at least two independent experiments; controls contained equivalent concentrations of compound solvents (water, PYNFH or DMSO). Plates were incubated at 25°C, and OD measurements of the contents of the 96 wells were performed every 24 h using a FLUOstar OPTIMA microplate reader. Regrowth capacity was assessed by collecting the whole contents of the wells at day 5 by vigorous pipetting after which the content (100  $\mu$ L) was added to Eppendorf tubes containing 1 mL PYNFH medium. Samples were washed by centrifugation at 1,000 relative centrifugal force (rcf) and subsequent careful replacement of the supernatant with fresh PYNFH medium. After repeating this washing cycle three times, 1 ml supernatant was discarded and the remaining contents were added to a new plate. Controls were diluted 10x after the washing step to allow proper detection of regrowth in these samples. OD was measured for a further period of 9 days of incubation at 25 °C.

### **Inhibition assays for *N. fowleri***

For *N. fowleri*, two independent methods were used to determine compound efficacy: a CellTiter-GLO luminescence-based ATP stain (less sensitive to number of amoeba, but more sensitive to viability) and cell counting by flow cytometry (sensitive to the number of amoeba but with count determined irrespective of viability). Similar stock solutions were prepared for *N. fowleri* experiments as those used for *N. gruberi* experiments. For CellTiter-GLO experiments, stock solutions were diluted and added to a black 96-well plate as 10  $\mu$ L compound + 80  $\mu$ L Bacto Casitone after which 300 *N. fowleri* cells in 10  $\mu$ L Bacto Casitone were added to each well for a total volume of 100  $\mu$ L. After 24 hours of incubation at 37 °C CellTiter-GLO reagent was added and luminescence was determined by the use of a CLARIOstar microplate reader. For flow cytometry experiments, stock solutions were diluted and added to translucent 96-well plate wells as 20  $\mu$ L compound + 178  $\mu$ L Bacto Casitone after which 60 *N. fowleri* cells in 2  $\mu$ L Bacto Casitone were added to each well for a total volume of 200  $\mu$ L. After 72 hours of incubation at 37 °C, paraformaldehyde was added to obtain a 1.5% concentration, after which cell counting was performed by the use of a Guava EasyCyte flow cytometer. Appropriate gating was applied to all samples. Experiments were all performed in triplicate, all plates contained positive controls in triplicate wells with equivalent concentrations of compound solvents (water, Bacto Casitone, or DMSO) and negative controls without amoebae.

## Checkerboards assay

Twofold dilutions were prepared of MIL (100 to 3.13  $\mu\text{M}$ ), ETO (400 to 25  $\mu\text{M}$ ), PHX (25 to 1.61  $\mu\text{M}$ ), TDZ (25 to 0.8  $\mu\text{M}$ ) and VPA (2000 to 62.5  $\mu\text{M}$ ). Drugs were added to black 96-well plates in a 5-by-6 checkerboard design as described before<sup>42</sup>. 96-well plates were inoculated with 300 *N. fowleri* cells in Bacto Casitone per well. After 24 hours of incubation at 37 °C CellTiter-GLO reagent was added and luminescence was determined by a CLARIOstar microplate reader. Experiments were all performed in triplicate, all plates contained positive controls in triplicate wells with equivalent concentrations of compound solvents (water, Bacto Casitone or DMSO) and negative controls without amoebae.

## Data analysis

GraphPad Prism 8 was used to process data. For *N. gruberi*, graphs of separate wells were constructed with OD values on the y axis, time (days) on the x axis. Area under the curve (AUC) was then calculated by the use of GraphPad Prism 8, where after these were combined into a bar chart. To determine  $\text{IC}_{50}$  values, results were normalized and nonlinear regression with variable slope was performed. For *N. fowleri*, luminescence data and cell counts were normalised as a percentage of the respective control, after which nonlinear regression with variable slope was performed to determine  $\text{IC}_{50}$ . To determine synergy, analysis was performed using the Fractional Inhibitory Concentration index ( $\text{FIC}_i$ ), as described before<sup>42</sup>. Briefly, the  $\text{FIC}_i$  was determined for the wells with the lowest concentration of drugs that resulted in <10% luminescence of the growth control without drugs.  $\text{FIC}_i$  was calculated as  $\Sigma\text{FIC} = \frac{C_a}{\text{MIC}_a} + \frac{C_b}{\text{MIC}_b}$  with  $C_a$  and  $C_b$  being the concentrations of the drugs in the well and  $\text{MIC}_a$  and  $\text{MIC}_b$  the lowest concentration of separate drugs that resulted in <10% of luminescence.  $F_{\text{min}}$  was defined as the lowest  $\Sigma\text{FIC}$ -value. Additivity was determined as  $0.5 < \Sigma\text{FIC} < 2$ , synergy as  $\Sigma\text{FIC} \leq 0.5$  and antagonism as  $\Sigma\text{FIC} > 2$ . Surface response analysis was performed with the Combenefit program.<sup>43</sup>

## Acknowledgements

MS acknowledges the European Molecular Biology Organisation (EMBO) for Short-Term Fellowship #8453 and the Netherlands Centre for One Health & the Erasmus MC for support. RS acknowledges Czech Science Foundation (20-28072S) and CZ.02.1.01/0.0/0.0/16\_019/0000759 CePaViP provided by ERDF and MEYS.

## References

- 1 Cope, J. R. & Ali, I. K. Primary amebic meningoencephalitis: what have we learned in the last 5 years? *Curr Infect Dis Rep* **18**, 31 (2016).
- 2 Grace, E., Asbill, S. & Virga, K. *Naegleria fowleri*: pathogenesis, diagnosis, and treatment options. *Antimicrob Agents Chemother* **59**, 6677-6681 (2015).
- 3 Siddiqui, R., Ali, I. K. M., Cope, J. R. & Khan, N. A. Biology and pathogenesis of *Naegleria fowleri*. *Acta Trop* **164**, 375-394 (2016).
- 4 De Jonckheere, J. F. Origin and evolution of the worldwide distributed pathogenic amoeboflagellate *Naegleria fowleri*. *Infect Genet Evol* **11**, 1520-1528 (2011).
- 5 Cope, J. R. *et al.* Primary Amebic Meningoencephalitis Associated With Rafting on an Artificial Whitewater River: Case Report and Environmental Investigation. *Clin Infect Dis* **66**, 548-553 (2018).
- 6 Stowe, R. C. *et al.* Primary amebic meningoencephalitis in children: a report of two fatal cases and review of the literature. *Pediatr Neurol* **70**, 75-79 (2017).
- 7 Maciver, S. K., Piñero, J. E. & Lorenzo-Morales, J. Is *Naegleria fowleri* an emerging parasite? *Trends Parasitol* **36**, 19-28 (2020).
- 8 Shakoor, S. *et al.* Primary amebic meningoencephalitis caused by *Naegleria fowleri*, Karachi, Pakistan. *Emerg Infect Dis* **17**, 258-261 (2011).
- 9 Jarolim, K. L., McCosh, J. K., Howard, M. J. & John, D. T. A light microscopy study of the migration of *Naegleria fowleri* from the nasal submucosa to the central nervous system during the early stage of primary amebic meningoencephalitis in mice. *J Parasitol* **86**, 50-55 (2000).
- 10 Kemble, S. K. *et al.* Fatal *Naegleria fowleri* infection acquired in Minnesota: possible expanded range of a deadly thermophilic organism. *Clin Infect Dis* **54**, 805-809 (2012).
- 11 Nau, R., Sorgel, F. & Eiffert, H. Penetration of drugs through the blood-cerebrospinal fluid/blood-brain barrier for treatment of central nervous system infections. *Clin Microbiol Rev* **23**, 858-883 (2010).
- 12 Roy, S. L. *et al.* Assessment of blood-brain barrier penetration of miltefosine used to treat a fatal case of granulomatous amebic encephalitis possibly caused by an unusual *Balamuthia mandrillaris* strain. *Parasitol Res* **114**, 4431-4439 (2015).
- 13 Monogue, M. L. *et al.* Minimal Cerebrospinal Concentration of Miltefosine Despite Therapeutic Plasma Levels During the Treatment of Amebic Encephalitis. *Antimicrob Agents Chemother* (2019).
- 14 Vogelsinger, H. *et al.* Amphotericin B tissue distribution in autopsy material after treatment with liposomal amphotericin B and amphotericin B colloidal dispersion. *J Antimicrob Chemother* **57**, 1153-1160 (2006).
- 15 Martinez-Castillo, M. *et al.* *Naegleria fowleri* after 50 Years: Is it a neglected pathogen? *J Med Microbiol* (2016).
- 16 Fidock, D. A., Rosenthal, P. J., Croft, S. L., Brun, R. & Nwaka, S. Antimalarial drug discovery: efficacy models for compound screening. *Nat Rev Drug Discov* **3**, 509 (2004).
- 17 Horn, D. & Duraisingh, M. T. Antiparasitic chemotherapy: from genomes to mechanisms. *Annu Rev Pharmacol Toxicol* **54**, 71-94 (2014).
- 18 Shakya, A., Bhat, H. R. & Ghosh, S. K. Update on Nitazoxanide: A Multifunctional Chemotherapeutic Agent. *Curr Drug Discov Technol* **15**, 201-213 (2018).
- 19 Bexkens, M. L. *et al.* Lipids are the preferred substrate of the protist *Naegleria gruberi*, relative of a human brain pathogen. *Cell Rep* **25**, 537-543 e533 (2018).
- 20 Van den Branden, C. & Roels, F. Thioridazine: a selective inhibitor of peroxisomal beta-oxidation in vivo. *FEBS Lett* **187**, 331-333 (1985).

- 21 Kennedy, J. A., Unger, S. A. & Horowitz, J. D. Inhibition of carnitine palmitoyltransferase-1 in rat heart and liver by perhexiline and amiodarone. *Biochem Pharmacol* **52**, 273-280 (1996).
- 22 Weis, B. C., Cowan, A. T., Brown, N., Foster, D. W. & McGarry, J. D. Use of a selective inhibitor of liver carnitine palmitoyltransferase I (CPT I) allows quantification of its contribution to total CPT I activity in rat heart. Evidence that the dominant cardiac CPT I isoform is identical to the skeletal muscle enzyme. *J Biol Chem* **269**, 26443-26448 (1994).
- 23 Silva, M. F. *et al.* Valproic acid metabolism and its effects on mitochondrial fatty acid oxidation: a review. *J Inherit Metab Dis* **31**, 205-216 (2008).
- 24 Hadvary, P., Lengsfeld, H. & Wolfer, H. Inhibition of pancreatic lipase in vitro by the covalent inhibitor tetrahydrolipstatin. *Biochem J* **256**, 357-361 (1988).
- 25 Dorlo, T. P., Balasegaram, M., Beijnen, J. H. & de Vries, P. J. Miltefosine: a review of its pharmacology and therapeutic efficacy in the treatment of leishmaniasis. *J Antimicrob Chemother* **67**, 2576-2597 (2012).
- 26 Debnath, A. *et al.* Corifungin, a new drug lead against Naegleria, identified from a high-throughput screen. *Antimicrob Agents Chemother* **56**, 5450-5457 (2012).
- 27 Kim, J. H. *et al.* Effect of therapeutic chemical agents in vitro and on experimental meningoencephalitis due to Naegleria fowleri. *Antimicrob Agents Chemother* **52**, 4010-4016 (2008).
- 28 Colon, B. L., Rice, C. A., Guy, R. K. & Kyle, D. E. Phenotypic Screens Reveal Posaconazole as a Rapidly Acting Amebicidal Combination Partner for Treatment of Primary Amoebic Meningoencephalitis. *J Infect Dis* **219**, 1095-1103 (2018).
- 29 Kangussu-Marcolino, M. M., Ehrenkauf, G. M., Chen, E., Debnath, A. & Singh, U. Identification of plicamycin, TG02, panobinostat, lestaurtinib, and GDC-0084 as promising compounds for the treatment of central nervous system infections caused by the free-living amoebae Naegleria, Acanthamoeba and Balamuthia. *Int J Parasitol Drugs Drug Resist* **11**, 80-94 (2019).
- 30 Herman, E. K. *et al.* A comparative 'omics approach to candidate pathogenicity factor discovery in the brain-eating amoeba Naegleria fowleri. *bioRxiv*, 2020.01.16.908186 (2020).
- 31 Shi, R., Zhang, Y., Shi, Y., Shi, S. & Jiang, L. Inhibition of peroxisomal beta-oxidation by thioridazine increases the amount of VLCFAs and Abeta generation in the rat brain. *Neurosci Lett* **528**, 6-10 (2012).
- 32 Fritz-Laylin, L. K. *et al.* The genome of Naegleria gruberi illuminates early eukaryotic versatility. *Cell* **140**, 631-642 (2010).
- 33 Zysset-Burri, D. C. *et al.* Genome-wide identification of pathogenicity factors of the free-living amoeba Naegleria fowleri. *BMC genomics* **15**, 496-496 (2014).
- 34 Pijpers, J., den Boer, M. L., Essink, D. R. & Ritmeijer, K. The safety and efficacy of miltefosine in the long-term treatment of post-kala-azar dermal leishmaniasis in South Asia - A review and meta-analysis. *PLoS Negl Trop Dis* **13**, e0007173-e0007173 (2019).
- 35 Cheng, S. *et al.* Fatty acid oxidation inhibitor etomoxir suppresses tumor progression and induces cell cycle arrest via PPAR $\gamma$ -mediated pathway in bladder cancer. *Clin Sci (Lond)* **133**, 1745-1758 (2019).
- 36 Baig, M. S. *et al.* Repurposing Thioridazine (TDZ) as an anti-inflammatory agent. *Sci Rep* **8**, 12471 (2018).
- 37 Wassmann, C. S. *et al.* Molecular mechanisms of thioridazine resistance in Staphylococcus aureus. *PLoS One* **13**, e0201767 (2018).
- 38 Aslostovar, L. *et al.* A phase 1 trial evaluating thioridazine in combination with cytarabine in patients with acute myeloid leukemia. *Blood Adv* **2**, 1935-1945 (2018).
- 39 Varga, B. *et al.* Possible Biological and Clinical Applications of Phenothiazines. *Anticancer Res* **37**, 5983-5993 (2017).

- 40 Svendsen, C. N., Hrbek, C. C., Casendino, M., Nichols, R. D. & Bird, E. D. Concentration and distribution of thioridazine and metabolites in schizophrenic post-mortem brain tissue. *Psychiatry Res* **23**, 1-10 (1988).
- 41 Pushpakom, S. *et al.* Drug repurposing: progress, challenges and recommendations. *Nat Rev Drug Discov* **18**, 41-58 (2019).
- 42 Meletiadis, J., Pournaras, S., Roilides, E. & Walsh, T. J. Defining fractional inhibitory concentration index cutoffs for additive interactions based on self-drug additive combinations, Monte Carlo simulation analysis, and in vitro-in vivo correlation data for antifungal drug combinations against *Aspergillus fumigatus*. *Antimicrob Agents Chemother* **54**, 602-609 (2010).
- 43 Di Veroli, G. Y. *et al.* Combenefit: an interactive platform for the analysis and visualization of drug combinations. *Bioinformatics* **32**, 2866-2868 (2016).

## Supplementary data

**Supplementary Table S1:** Synergy between fatty acid oxidation inhibitors and currently used drugs.

Combination	Percentage of separate drug #1	Percentage of separate drug #2	Average	Further checker-boards?	F <sub>min</sub> of checker-board	Interpretation
ETO + MIL	2.8	3.8	3.3	YES	0.5	Synergy
ETO + PHX	66.7	84.1	75.4	NO		
ETO + AMB	93.8	77.5	85.7	NO		
ETO + ORL	113.2	131.4	122.3	NO		
ETO + TDZ	63.0	107.1	85.1	NO		
ETO + VPA	74.6	82.0	78.3	NO		
MIL + PHX	56.8	52.7	54.7	YES	1.0625	Additivity
MIL + AMB	118.1	70.3	94.2	NO		
MIL + ORL	74.8	62.6	68.7	NO		
MIL + TDZ	42.7	53.2	48.0	YES	1.0312	Additivity
MIL + VPA	74.6	60.1	67.4	YES	1.0156	Additivity
PHX + AMB	96.0	62.3	79.2	NO		
PHX + ORL	77.4	71.1	74.2	NO		
PHX + TDZ	46.7	63.1	54.9	YES	1.0	Additivity
PHX + VPA	79.7	69.3	74.5	NO		
AMB + ORL	81.1	115.2	98.2	NO		
AMB + TDZ	48.7	101.6	75.1	NO		
AMB + VPA	77.5	105.0	91.3	NO		
ORL + TDZ	62.8	92.9	77.9	NO		
ORL+ VPA	97.7	93.6	95.6	NO		
TDZ + VPA	80.2	51.7	65.9	YES	1.0	Additivity

Fatty acid oxidation inhibitors and drugs currently used to treat primary amoebic meningoencephalitis were added separately and combined in IC50 concentrations to *Naegleria fowleri*. Luminescence was measured at 24 hours after addition of CellTiter-GLO. Luminescence data of wells with combined drugs was normalised as a percentage of the luminescence of respective drugs tested separately. Experiments were performed in triplicate.

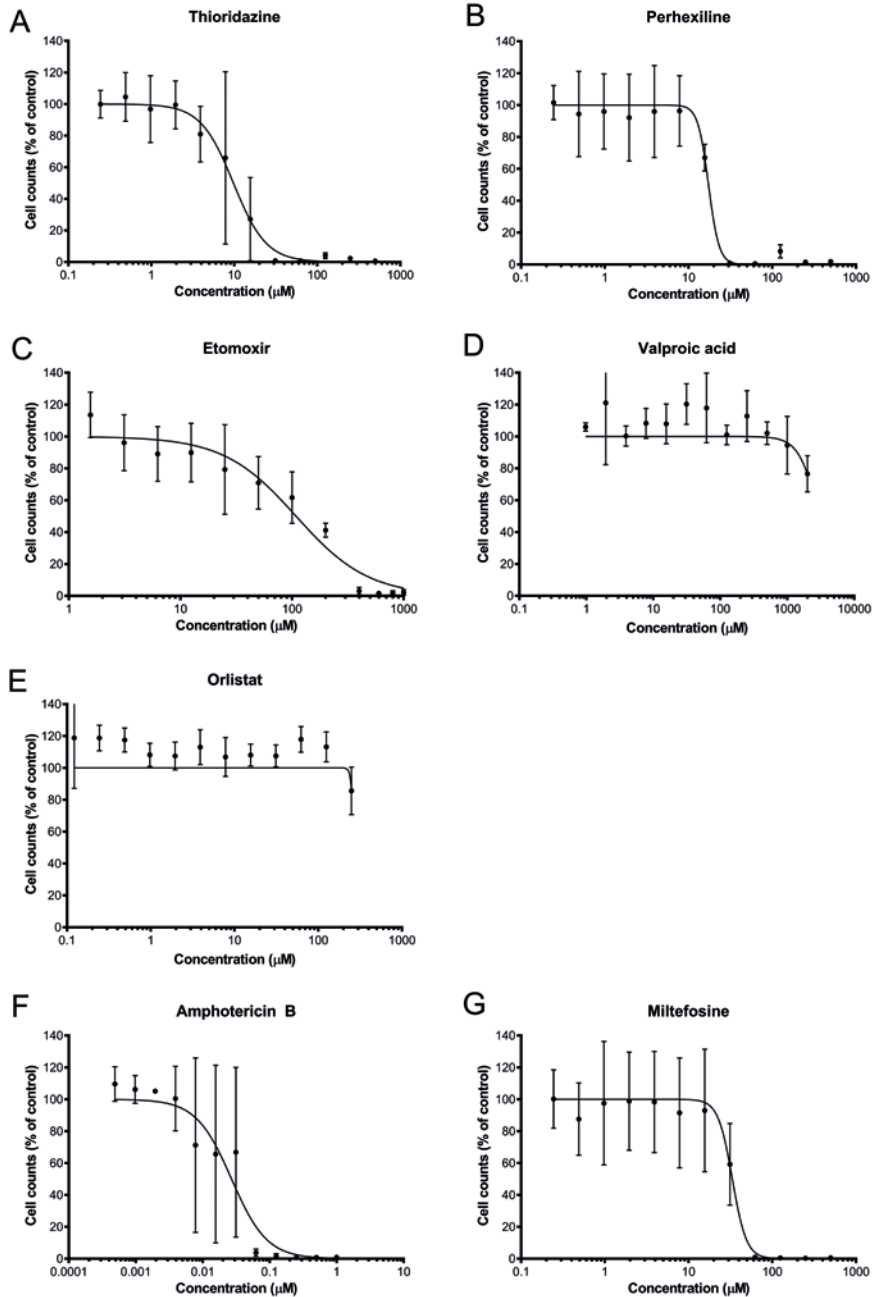


**Figure S1.** Cell counts as a percentage of control after compound exposure to *Naegleria fowleri* for 72 hours in twofold serial dilutions.

Cells were counted by guava EasyCyte flow cytometer in the presence or absence of inhibitors of fatty acid oxidation or drugs currently used to treat primary amoebic meningoencephalitis. Experiments were performed in triplicate, error bars are SD.





4

# CHAPTER 4

---

*Acanthamoeba castellanii* trophozoites need oxygen for normal functioning and lipids are their preferred substrate, offering new possibilities for treatment

Maarten J. Sarink<sup>1</sup>, Anna Z. Mykytyn<sup>1</sup>, Aïsha Jedidi<sup>1</sup>, Martin Houweling<sup>2</sup>,  
Jos F. Brouwers<sup>3</sup>, George Ruijter<sup>4</sup>, Annelies Verbon<sup>1</sup>, Jaap. J. van Hellemond<sup>1</sup>,  
Aloysius G. M. Tielens<sup>1</sup>

<sup>1</sup> Department of Medical Microbiology and Infectious Diseases, Erasmus MC University Medical Center, Rotterdam, The Netherlands

<sup>2</sup> Department Biomolecular Health Sciences, Faculty of Veterinary Medicine, Utrecht University, Utrecht, The Netherlands

<sup>3</sup> Avans University of Applied Sciences, School of Life Sciences and Technology, Research Group for Analysis Techniques in the Life Sciences, Breda, The Netherlands.

<sup>4</sup> Department of Clinical Genetics, Erasmus MC, University Medical Center, Rotterdam, The Netherlands.

## Abstract

*Acanthamoebae*, pathogenic free-living amoebae, can cause Granulomatous Amoebic Encephalitis (GAE) and keratitis, and for both types of infection no adequate treatment options are available. As the metabolism of pathogens is an attractive treatment target, we set out to examine the energy metabolism of *Acanthamoeba castellanii* and studied the aerobic and anaerobic capacities of the trophozoites. Under anaerobic conditions, or in the presence of inhibitors of the electron-transport chain, *A. castellanii* trophozoites became rounded, moved sluggishly and stopped multiplying. This demonstrates that oxygen and the respiratory chain are essential for movement and replication. Furthermore, the simultaneous activities of both terminal oxidases, cytochrome *c* oxidase and the plant-like alternative oxidase, are essential for normal functioning and replication. The inhibition of normal functioning caused by the inactivity of the respiratory chain was reversible. Once respiration was made possible again, the rounded, rather inactive amoebae formed acanthopodia within four hours and resumed moving, feeding and multiplying. Experiments with radiolabelled nutrients revealed a preference for lipids over glucose and amino acids as food. Subsequent experiments showed that adding lipids to a standard culture medium of trophozoites strongly increased the growth rate. *A. castellanii* trophozoites have a strictly aerobic energy metabolism and  $\beta$ -oxidation of fatty acids, the Krebs cycle, and an aerobic electron-transport chain coupled to the ATP synthase, produce most of the used ATP. The preference for lipids can be exploited, as we show that three known inhibitors of lipid oxidation strongly inhibited the growth of *A. castellanii*. In particular, thioridazine and perhexiline showed potent effects in low micromolar concentrations. Therefore, this study revealed a new drug target with possibly new options to treat *Acanthamoeba* infections.

## Highlights

- *Acanthamoeba castellanii* needs oxygen for normal functioning and growth
- *A. castellanii* trophozoites prefer lipids over glucose as an energy source
- Lipid breakdown uses a branched electron-transport chain, both ends using oxygen
- Use of both these terminal oxidases is essential for normal functioning and growth
- The preference for lipids seems an attractive new drug target

## 1. Introduction

Acanthamoebae are pathogenic free-living protists that can infect humans in multiple ways. Acanthamoebae can infect the brain, resulting in Granulomatous Amoebic Encephalitis (GAE) <sup>1,2</sup>. GAE usually affects immunocompromised patients and results in mortality in over 90% of the cases <sup>3</sup>. Although awareness and the reported number of cases are increasing worldwide, GAE is still underreported as a cause of infectious mortality <sup>3,4</sup>. The high mortality rate is attributed to late diagnosis and a lack of effective therapeutics, indicating the importance of new treatment possibilities. Acanthamoebae can also infect the cornea, causing a hard-to-treat keratitis which leads to blindness if left untreated <sup>5-7</sup>. *Acanthamoeba* keratitis is often seen in contact lens wearers.

New drugs to treat *Acanthamoeba* keratitis that could shorten treatment time or cause fewer side effects would be very useful, because a lengthy treatment with diamidines and/or biguanides is now required to treat *Acanthamoeba* keratitis <sup>8</sup>. In the past, metabolic studies have resulted in the identification of new targets and drugs for the treatment of infectious diseases <sup>9</sup>. However, studies on the metabolic properties of Acanthamoebae are scarce.

*A. castellanii* possesses mitochondria that are equipped for a classical aerobic metabolism. Oxygen can be used by *A. castellanii* as a terminal electron acceptor in a branched electron-transport chain <sup>10-14</sup>. A schematic overview of the branched electron-transport chain of *A. castellanii* is shown in Figure 1. *A. castellanii* has a canonical eukaryotic electron-transport chain consisting of the complexes I-IV, where complex IV (cytochrome c oxidase) donates the electrons to oxygen <sup>10,11</sup>. However, *A. castellanii* also has a plant-like, cyanide-insensitive, alternative oxidase, which donates electrons directly from ubiquinol to oxygen without the further concomitant proton translocation across the mitochondrial inner membrane <sup>12</sup>. The energy of the proton gradient generated by the electron-transport chain can be used by *A. castellanii* to produce ATP via a classical F<sub>1</sub>F<sub>o</sub> ATP synthase. However, in *A. castellanii* the protons can also be transported back into the mitochondrial matrix via an uncoupling protein without the concomitant production of ATP <sup>14</sup>. The electron-transport chain is not only branched at the exit but also at the entrance side, because the mitochondria of *A. castellanii* possess apart from NADH-dehydrogenase (complex I) also alternative dehydrogenases (Ndh2), which transfer electrons from NAD(P)H to ubiquinone without proton translocation (Fig. 1) <sup>10,13</sup>.

Investigations on the oxygen dependence of *A. castellanii* led to controversial results. It has been reported that the use of oxygen is essential for normal functioning and growth of *A. castellanii* <sup>15-17</sup>. On the other hand, the use of an anaerobic metabolism has also

been reported <sup>16,18,19</sup>. However, in contrast to the many bioenergetic studies that have been performed over the years on the *A. castellanii* mitochondrial flow of electrons, relatively little attention has been paid to the identification of the catabolic pathways that are used to degrade substrates. In compositional and functional complexity, the mitochondrial proteome of *A. castellanii* rivals that of classical mitochondria <sup>20</sup>. However, genomic and proteome analyses indicated that *A. castellanii* possesses next to the mitochondrial machinery for a classical aerobic metabolism, a set of enzymes that could enable a hydrogenosomal type of anaerobic ATP generation <sup>21-24</sup>. This would suggest that *A. castellanii* has mitochondria that can toggle between an aerobic and an anaerobic type of metabolism. However, the assumed functionality of these anaerobic pathways has not been shown yet.

In fact, even the characteristics of its aerobic metabolism are still unknown. Genomic analyses indicate that *A. castellanii* possesses enzymes for the classical complete oxidation to carbon dioxide of carbohydrates, lipids and proteins <sup>25</sup>. The presence of an active mitochondrial electron-transport chain and ATP synthase also suggests that at least part of the used substrates is oxidized with oxygen as the terminal electron acceptor. However, whether the substrates are mainly degraded to carbon dioxide or are also degraded to other end products is yet unknown. The relative importance for the metabolism of *A. castellanii* of the three types of substrates, carbohydrates, lipids and amino acids, is also still unknown. In its predatory behaviour and feeding on bacteria, *A. castellanii* resembles

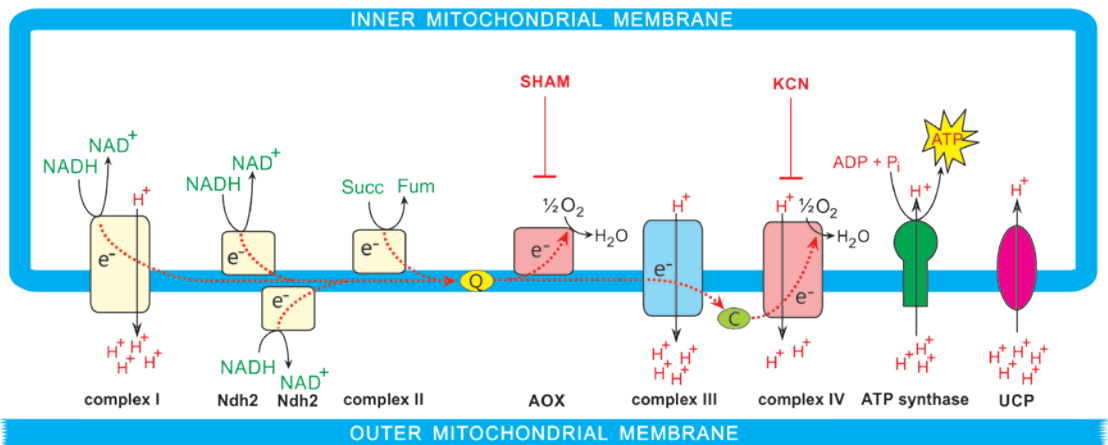


**Figure 1:** The branched electron-transport chain of *Acanthamoeba castellanii*.

Schematic overview of the entrance of electrons, which occurs via the two yellow boxes, and of the exit of the electrons, which occurs via the two pink terminal oxidases. AOX, alternative oxidase; c, cytochrome c; KCN, potassium cyanide; Ndh2, alternative NADH dehydrogenase; SHAM, salicylhydroxamic acid; UCP, uncoupling protein; Q, ubiquinone pool.

the pathogenic free-living amoeba *Naegleria gruberi*, which prefers lipids for food <sup>26</sup>. Therefore, it is conceivable that *Acanthamoeba* also uses lipids as an important food source. We now studied the aerobic and anaerobic capacities of *A. castellanii* trophozoites and their possible preference for the type of food, to identify possible essential processes which could be new targets for treatment.

## 2. Materials and Methods

### 2.1. *Acanthamoeba* strain and culture media

*Acanthamoeba castellanii* strain "Neff" (ATCC 30010) was grown in cell culture flasks at 25°C with PYG medium, which contains proteose peptone, yeast extract and glucose with salt additives (ATCC medium 712). This medium was supplemented with 40 µg/ml gentamicin, 100 units/ml penicillin and 100 µg/ml streptomycin. For radiolabelled nutrient experiments, cultures were maintained in PY with 1 mM glucose (PY1G) instead of regular PYG, which contains 100 mM glucose. All experiments with trophozoites were conducted with trophozoites growing in logarithmic phase, collected by placing a cell culture flask on ice for 20 minutes and subsequent repeated tapping to detach trophozoites. Cysts were obtained by replacing the PYG medium of a culture of *Acanthamoeba* trophozoites with encystation medium (NEM) as described by Neff et al. <sup>27</sup>.

### 2.2. Respiration

To determine the oxygen consumption, a Clark-type electrode was used at 25°C in 2 ml air-saturated fresh medium containing *A. castellanii* trophozoites. Potassium cyanide was purchased from Sigma (St. Louis, MO, USA) diluted in water and used at a final concentration of 1 mM. Salicylhydroxamic acid (SHAM) was purchased from Sigma, diluted in 96% ethanol, and used at a final concentration of 1.5 mM. Experiments were performed in triplicate.

### 2.3. Culturing of *A. castellanii* in the absence of oxygen, in the presence of inhibitors of the terminal oxidases, and in the presence of lipids

To investigate the anaerobic capacity of *A. castellanii* trophozoites, 5 x 10<sup>3</sup> trophozoites in 5 µl of PYG were added to the edge of 15mm x 55mm strips of non-nutrient agar seeded with 4.0 McFarland *E. coli* (strain ATCC 25922) in tissue culture dishes. The edge of the amoebae inoculate was marked after which the plates were stored in Oxoid Jars and incubated at 25°C. Anaerobic conditions were achieved by replacing the air in a jar with a mixture of 85% N<sub>2</sub>, 10% CO<sub>2</sub>, and 5% H<sub>2</sub>, using an Anoxomat and the addition of palladium as catalyst to ensure anaerobic conditions (Mart Microbiology, Drachten, The Netherlands).

Aerobic conditions were achieved by incubating in an identical jar under atmospheric air conditions. Distance of the furthest visible edge of multiple trophozoites was measured in millimetres daily for aerobic conditions and after 4 days for anaerobic conditions (after the jars were opened). After 4 days of anaerobic incubation, the distance was recorded for a further 4 days in aerobic conditions. Experiments were performed at least twice with triplicate plates. Images were recorded with a Leica ICC50W microscope using LAS X software. Fluorescent images were recorded using an Olympus IX51 microscope with cellSens software after incubation for 30 minutes with a cellulose-binding fluorophore (Uvitex 2B, 8 mg/l), which was washed off with PBS. As a positive control for the Uvitex staining of cysts, 5  $\mu$ l of encysted *Acanthamoeba* were added to identical plates and incubated in the same conditions.

To determine the effects of respiratory chain inhibitors on the cell growth of *A. castellanii*, trophozoites were seeded in PYG medium on day 1 at a density of 30,000 trophozoites per ml. Upon reaching log growth (day 2) respiratory chain inhibitors were added, KCN was added to the culture in a final concentration of 1 mM to block the activity of complex IV, SHAM was added to the culture at a final concentration of 1.5 mM to block the AOX. The ethanol vehicle was maintained at 0.5% (v/v) and control incubations included ethanol at that concentration. Throughout cell growth experiments, the medium was changed daily, and KCN and SHAM were added fresh daily. Amoebae were counted using Differential Interference Contrast (DIC) microscopy and images taken were analysed using Cell<sup>^</sup>F Software (Olympus).

To investigate the effect of lipids on the growth, trophozoites of *A. castellanii* were cultured in PY1G supplemented with i) 200  $\mu$ M oleic acid bound to delipidated bovine serum albumin (BSA) plus 200  $\mu$ M octanoic acid, or ii) micelles prepared by sonication of 0.2 mg/ml phosphatidylglycerol (16:0/18:1) and 0.2 mg/ml phosphatidylethanolamine (16:0/18:1). Phosphatidylglycerol and phosphatidylethanolamine were from Avanti Polar Lipids (Alabaster, AL, USA), delipidated BSA and oleic acid were purchased from Sigma (St. Louis, MO, USA).

## 2.4. Nutrient consumption

Substrate-degradation experiments were performed as earlier described <sup>26</sup>. Briefly, *A. castellanii* trophozoites (1.4 – 3.4 million) grown in PY1G were harvested during logarithmic growth and transferred to a sealed 25 ml Erlenmeyer with 5 ml PY1G. The incubation was started by the addition of one of the labelled substrates (all supplied by PerkinElmer, Boston, MA, USA): D-[6-<sup>14</sup>C] glucose (1.0 mM, 5  $\mu$ Ci), [1-<sup>14</sup>C] octanoic acid (200  $\mu$ M, 5  $\mu$ Ci), [1-<sup>14</sup>C] oleic acid (200  $\mu$ M, 5  $\mu$ Ci), [U-<sup>14</sup>C] isoleucine (1.0 mM, 3  $\mu$ Ci), [U-<sup>14</sup>C] valine (1.6 mM, 3  $\mu$ Ci) and [U-<sup>14</sup>C] lysine (1.0 mM, 3  $\mu$ Ci). The concentration shown in brackets

is the concentration of the unlabeled substrate, present in all incubations. The very high specific activity ( $\mu\text{Ci}/\mu\text{mol}$ ) of the added radioactive substrates implies that the addition of these  $^{14}\text{C}$ -labeled substrates to an incubation does not change the concentration of that substrate, because the tracer amount of that labeled substrate is negligible compared to the amount of that substrate already present in the standard medium. This means that the substrate composition of all six types of incubations was the same, but in each incubation only one of the substrates was labeled. Blank incubations without trophozoites were started simultaneously. All samples were incubated at  $25^\circ\text{C}$ . After 18-24 hours the incubations were terminated and the production of radioactive  $\text{CO}_2$  was determined as described before <sup>28</sup>. In short, the medium was acidified to pH2 by the addition of HCl through the septum of the sealed Erlenmeyer flask. Carbon dioxide was trapped for 2.5 hours in 200  $\mu\text{L}$  4M KOH in a centre well suspended above the incubation medium. Afterwards, the trapping solution was transferred to a vial containing water and Luma-gel (Lumac\*LCS, Groningen, The Netherlands), after which radioactivity was measured in a scintillation counter. The incorporation of labelled nutrients in proteins, phospholipids and triacylglycerols was analysed after separate parallel incubations in 25  $\text{cm}^2$  cell culture flasks (Greiner Bio-One, The Netherlands) in 5 ml PY1G. Labelled substrates were added in an identical way as done in the substrate-degradation experiments. After 24 hours of incubation at  $25^\circ\text{C}$ , the supernatant was carefully discarded after which the trophozoites were gently washed three times with PY1G. Cell culture flasks were subsequently placed on ice for 20 minutes after which the trophozoites were collected after repeated tapping. After the addition of rat-liver lipids as carrier, the lipid fraction of this sample was isolated according to a chloroform/methanol extraction procedure <sup>29</sup>. The pellet of the first phase of this extraction procedure contained the amoebal proteins. The phospholipids and triacylglycerols in the lipid fraction were isolated via a thin-layer chromatography step and the radioactivity in these subfractions was determined. Radioactivity of all samples was counted in a scintillation counter after the addition of LUMA-gel (Lumac\*LCS, Groningen, the Netherlands). Experiments were performed at least in triplicate. The concentrations of isoleucine, valine and lysine in PY1G were determined by LC-Orbitrap MS (QExactive plus, Thermo Fisher Scientific, Breda, The Netherlands). Non-esterified fatty acids and acidic phospholipids were analysed by LC-MS in the negative mode as reported earlier (Retra et al., 2008). SPLASH-II Lipidomix (Merck, Darmstadt, Germany) supplemented with [U- $^{13}\text{C}$ ] stearic acid was used as an internal standard. Triacylglycerols, sterol(-esters) and other complex lipids were analysed by LC-MS in the positive ionization mode on a Q-ToF type instrument (X500R, Sciex, Framingham, MA, USA).

## 2.5. Growth inhibition

Etomoxir (ETO), perhexiline maleate salt (PHX) and thioridazine (TDZ) were purchased from Sigma (St. Louis, MO, USA). Growth inhibitory activity was assessed as described earlier <sup>30</sup>.

Briefly, stock solutions were prepared as follows: ETO and TDZ 10 mM in water, PHX: 50 mM in DMSO. Stock solutions were diluted in water and added as 10  $\mu$ L to  $1 \times 10^4$  *A. castellanii* trophozoites in 90  $\mu$ L of PYG. Compounds were tested per plate in triplicate in at least two independent experiments; controls contained equivalent concentrations of compound solvents (water or DMSO). Plates were incubated at 25°C and OD measurements of the 96 wells were performed every 24 hours using a FLUOstar OPTIMA microplate reader. Data were plotted using GraphPad Prism 7.0 with OD-values on the Y-axis and time (days) on the X-axis, after which the Area Under the Curve (AUC) was determined and plotted into a bar chart.

## 3. Results

### 3.1. *A. castellanii* trophozoites need oxygen and respiratory-chain activity for normal functioning

To gain an overview of the respiratory capabilities of *A. castellanii* trophozoites, the consumption of oxygen was measured before and after the addition of cyanide and salicylhydroxamic acid (SHAM), an inhibitor of cytochrome *c* oxidase (Complex IV) and the plant-like alternative oxidase (AOX), respectively. The addition of cyanide did not change the rate of the consumption of oxygen (Fig. 2A, trace A). However, after the subsequent addition of SHAM, oxygen consumption stopped. Likewise, if SHAM was added first, oxygen consumption did not change, whereas after the subsequent addition of cyanide, the consumption of oxygen again stopped (Fig. 2A, trace B). These results confirm that *A. castellanii* trophozoites have a branched electron-transport chain with two terminal oxidases: Complex IV and AOX (Fig. 1). Furthermore, our experiments now reveal that *A. castellanii* trophozoites can instantaneously change the ratio of the flow of electrons through the two terminal branches of the electron-transfer chain. When one of the two terminal oxidases is inhibited, electrons take the other route to reduce oxygen. Furthermore, our experiments showed that both branches of the electron-transport chain possess a substantial overcapacity, as oxygen consumption did not decrease when one of the two pathways was blocked.

To test their viability and capacity to grow (multiply) under long-term inhibition of one or both of the two terminal oxidases, we cultured *A. castellanii* trophozoites in the presence of SHAM, or cyanide, or cyanide plus SHAM. The presence of cyanide and/or SHAM resulted within 24 hr in changes in morphology, a decrease of the gliding movements and a complete growth arrest under all three conditions, (Fig. 2B, Supplementary Fig. S1 and Supplementary Movies 1-5). In the presence of both cyanide and SHAM, the change in motility and morphology was more pronounced than in the presence of only one of the two inhibitors.

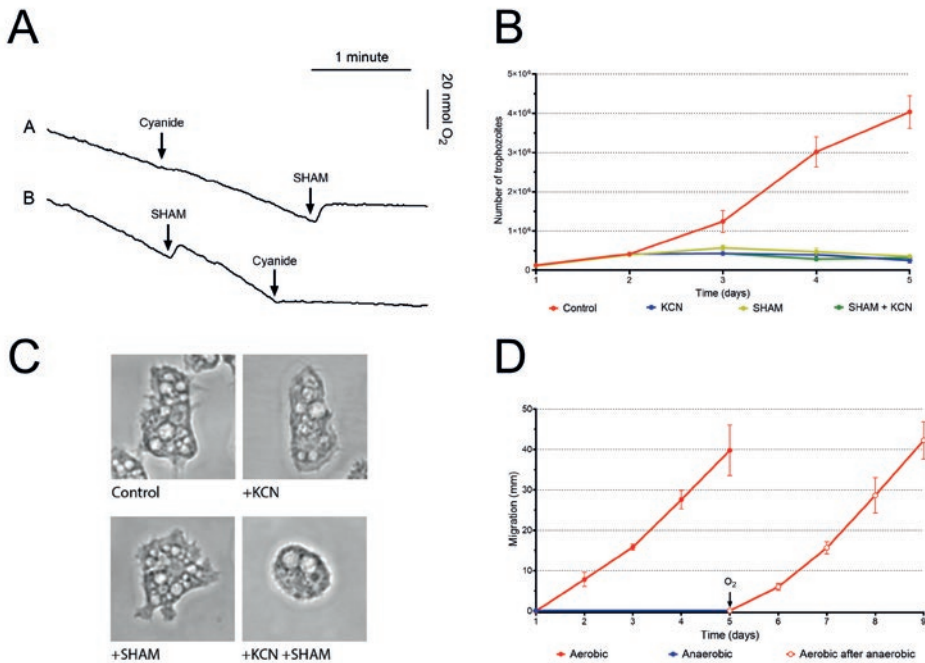


**Figure 2:** Oxygen consumption by *Acanthamoeba castellanii* trophozoites and their growth and shape under aerobic and anaerobic conditions.

(A) Oxygen consumption of *A. castellanii* was measured with a Clark-type electrode. Salicylhydroxamic acid (SHAM), at a final concentration of 1.5 mM, and cyanide, at a final concentration of 1 mM, was added at the indicated time points. Experiments were performed in duplicate, and representative examples are shown.

(B) Growth curves of *A. castellanii* trophozoites were measured in the presence or absence of respiratory chain inhibitors. Amoebae were cultured in PYG for 4 days. KCN (blue line), SHAM (yellow line) or SHAM plus KCN (green line) were added on day 2. Controls (red line) were cultured in identical conditions. Shown is a representative example of three independent experiments. Results of triplicate incubations are shown and error bars are standard deviations. Representative images of the trophozoites on days 3, 4 and 5 under the various culture conditions and videos made on day 3 (after one-day presence of inhibitors) are shown in the Supplemental Information (Supplementary Fig. S1; Supplementary Videos 1-5).

(C) Photographs of the trophozoites from Figure 2B, taken on day 3 (one day after the addition of the inhibitors). Shown are representative trophozoites of the Supplementary Fig. S1 (see legend part B).

(D) The migration of *A. castellanii* trophozoites was measured on non-nutrient agar strips on a lawn of *E. coli* in the presence and absence of oxygen. After four days the amoebae of the anaerobic incubation were reintroduced to an aerobic environment and growth was measured for a further four days. Experiments were performed at least twice with triplicate agar strips, error bars are standard deviation.

An obvious difference was the disappearance of the acanthopodia in the simultaneous presence of cyanide and SHAM (Fig. 2C). The observed decrease in mobility and arrest of growth of the trophozoites in the presence of cyanide, which blocks the branch via complex III and IV of their electron-transport chain, indicates that oxidative phosphorylation is an important source of ATP production in *A. castellanii* trophozoites. Furthermore, the observed effects of SHAM in these experiments show that also a functioning alternative oxidase is essential for the vitality and growth of *A. castellanii* trophozoites, although the efficiency of ATP formation is lower when this oxidase is used instead of complex IV (cytochrome *c* oxidase). The inhibitory effects of the presence of these inhibitors are reversible; when after 3 days in the presence of inhibitors, the incubations were continued in the absence of inhibitors, in all three conditions the acanthamoebae started multiplying again (Supplementary Fig. S1).

Furthermore, we also tested the capacity to function anaerobically by an analysis of the growth (spreading out) of *A. castellanii* trophozoites on strips of non-nutrient-agar seeded with *E. coli*. These agar strips were incubated in jars under anaerobic conditions, or in jars containing oxygen at atmospheric levels. The distance covered under aerobic conditions by the trophozoites was measured daily and averaged 10 mm per day, with a total of 40 mm after four days (Fig. 2D). Migration of trophozoites is used as a function of cell division, as an advancing front of amoebae is created by both migrating and reproducing amoebae<sup>17</sup>. In contrast to aerobic conditions, during the incubations under anaerobic conditions, trophozoites did not cover any distance in four days. These trophozoites that were incubated in the absence of oxygen were rounded and had no acanthopodia. They were not mature cysts after these four days and contained no inner cyst wall (Fig. 3). This was confirmed by the absence of visible staining with Uvitex 2B, a fluorescent dye that binds to cellulose, an important component of the inner cyst wall<sup>31</sup>. Directly after ending the anaerobic incubations, the agar slips could be inspected under the microscope. The trophozoites had not moved nor multiplied for four days. They were still in the position on the agar slips where they were put at the beginning of the experiment, but the activity of moving vacuoles and organelles inside the trophozoites was clearly visible (Supplementary Movie S6). Four hours later, the amoebae again possessed acanthopodia and they were actively moving and started multiplying, as if nothing had happened (Fig. 3 and Supplementary Movie S7). After this reintroduction of oxygen, their migration was similar to cells in aerobic conditions that were not previously cultured in anaerobic conditions (i.e.  $\approx$  10 mm per day, Fig. 2D).

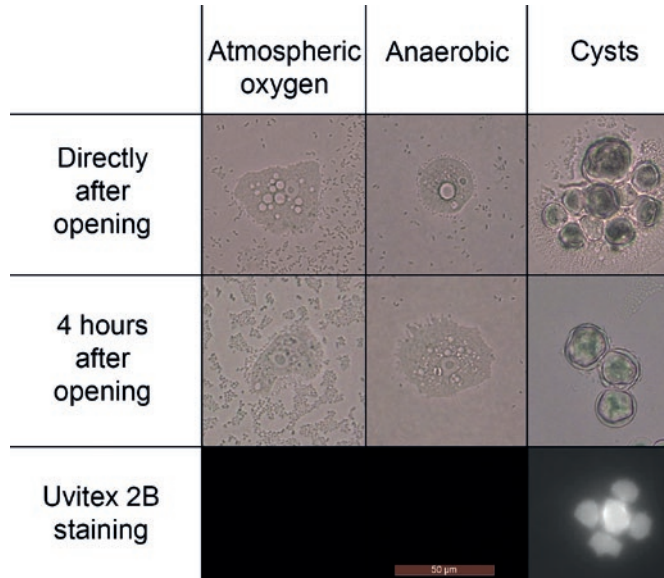


**Figure 3:** Morphology of *Acanthamoeba castellanii* after incubation for 4 days with or without oxygen.

Images of the amoebae of the experiment shown in Figure 2C were taken directly after the reintroduction of atmospheric oxygen, as well as four hours later. Uvitex 2B staining was performed directly after opening. The aerobic trophozoites showed no staining, nor did the rounded amoebae of the anaerobic incubations (bottom row). As a positive control, we produced cysts by a 72h-preincubation in NEM, then incubated them in jars under similar anaerobic conditions and showed that they were stained indeed by Uvitex 2B (bottom in column "Cysts"). Experiments were performed in duplicate and representative examples are shown.

### 3.2. *A. castellanii* trophozoites prefer fatty acids as food over glucose and amino acids

To determine the use of different nutrient substrates by *A. castellanii*, trophozoites were incubated with the  $^{14}\text{C}$ -labelled substrates glucose, octanoic acid, oleic acid, isoleucine, lysine and valine. After 24 hours of incubation, carbon dioxide was trapped and radioactivity in this fraction was measured to determine to what extent complete oxidation of these labelled substrates had occurred (Table 1).

The oxidation of [6-<sup>14</sup>C]-glucose to labelled carbon dioxide demonstrates that trophozoites of *A. castellanii* use Krebs cycle activity for the degradation of glucose, because the liberation of carbon number 6 from glucose happens only in the second and further rounds of the Krebs cycle, after the reaction of acetyl-CoA and oxaloacetate, catalysed by citrate synthase. Furthermore, <sup>14</sup>C-labelled carbon dioxide from [6-<sup>14</sup>C]-glucose cannot be the result of for instance acetate or ethanol production. Radioactively labelled fatty acids were completely oxidized to labelled carbon dioxide, which reveals an important role for the  $\beta$ -oxidation in the metabolism of *A. castellanii* trophozoites and proves the central role of acetyl-CoA and the Krebs cycle, the only way to oxidize fatty acids to carbon dioxide.

These lipids were catabolized at high rates, as octanoic acid and oleic acid were converted into carbon dioxide at a rate of 151 and 21 nmol per 10<sup>6</sup> trophozoites per 24 hours, respectively. These rates are substantially higher than the oxidation of glucose at 7 nmol per 10<sup>6</sup> trophozoites per 24 hours. Furthermore, the oxidation of one molecule of octanoic or oleic acid to carbon dioxide yields 50 and 118 molecules of ATP, respectively, which compares favourably to the 30 molecules of ATP that are formed by the oxidation of one molecule of glucose. Together, the oxidation of these two fatty acids was estimated to have produced 45 times as much ATP (10,000 nmol in 24 hours per million amoebae) as the oxidation of glucose did (222 nmol) (Table 1). The labelled amino acids isoleucine, valine and lysine were also oxidized to carbon dioxide, at rates of 10, 47 and 3 nmol per 10<sup>6</sup> trophozoites per 24 hours, respectively, which in total yielded an estimated 1700 nmol ATP in 24 hours per million amoebae <sup>32</sup>.

As all of these substrates can also be used for anabolic processes, we determined the incorporation of the five radioactively labelled substrates into three classes of biomolecules: phospholipids, triacylglycerols and proteins. These experiments demonstrated that all investigated substrates, sugars, lipids and amino acids, were used by *A. castellanii* trophozoites for biosynthetic purposes. Fatty acids were predominantly incorporated into phospholipids and triacylglycerols, oleic acid to a far greater extent than octanoic acid. Glucose and amino acids were predominantly incorporated into proteins (Table 1).

**Table 1:** Analysis of the degradation of  $^{14}\text{C}$ -labelled substrates to carbon dioxide and the incorporation of these substrates into phospholipids, triacylglycerols and proteins by *Acanthamoeba castellanii* trophozoites during 24 hours of incubation in PY1G at 25 °C

Labeled substrate	Substrate degraded to carbon dioxide ( $\text{nmol} \cdot 24 \text{ h}^{-1} \cdot 10^6 \text{ amoebae}^{-1}$ )	Estimated production of ATP ( $\text{nmol} \cdot 24 \text{ h}^{-1} \cdot 10^6 \text{ amoebae}^{-1}$ )	Incorporation of substrate ( $\text{nmol} \cdot 24 \text{ h}^{-1} \cdot 10^6 \text{ amoebae}^{-1}$ )		
			Phospholipids	Triacylglycerols	Proteins
D-[6- $^{14}\text{C}$ ] glucose	7.4 ( $\pm$ 1.6)	222	4.0 ( $\pm$ 0.3)	0.1 ( $\pm$ 0.0)	25.9 ( $\pm$ 2.9)
[1- $^{14}\text{C}$ ] octanoic acid	150.8 ( $\pm$ 42.4)	7550	8.3 ( $\pm$ 4.2)	0.2 ( $\pm$ 0.2)	7.5 ( $\pm$ 3.3)
[1- $^{14}\text{C}$ ] oleic acid	21.3 ( $\pm$ 10.1)	2488	54.3 ( $\pm$ 36.5)	22.7 ( $\pm$ 4.7)	3.9 ( $\pm$ 2.5)
[U- $^{14}\text{C}$ ] isoleucine	10.1 ( $\pm$ 1.5)	340	1.9 ( $\pm$ 0.8)	1.2 ( $\pm$ 0.8)	26.6 ( $\pm$ 3.5)
[U- $^{14}\text{C}$ ] valine	46.9 ( $\pm$ 3.2)	1293	1.4 ( $\pm$ 0.3)	1.4 ( $\pm$ 0.3)	39.9 ( $\pm$ 9.6)
[U- $^{14}\text{C}$ ] lysine	3.4 ( $\pm$ 0.1)	58	0.2 ( $\pm$ 0.1)	0.2 ( $\pm$ 0.1)	2.7 ( $\pm$ 0.3)

The substrate composition of the medium was the same in the six types of incubations, but in each incubation only one of the substrates was labeled (see Section 2.4). The values shown for “Substrate degraded to carbon dioxide” and “Incorporation of substrate” reflect the degradation and incorporation of the compound of which a  $^{14}\text{C}$ -labeled tracer was added (left column). The rough estimation of the amount of ATP produced by the oxidation of the various substrates is based on the premise that the *A. castellanii* trophozoites used only the classical electron-transport chain (complexes I-IV) and the  $\text{F}_1\text{F}_0$  ATP synthase. All values are corrected for blank incubations and are shown as mean ( $\pm$  S.D.).

### 3.3. Lipids stimulate the growth of *A. castellanii* trophozoites

The standard culture medium (PYG) for *A. castellanii* contains as substrates for growth, the water-soluble portions of an animal-protein hydrolysate and autolysed yeast cells, supplemented with a large amount of glucose (100 mM). In contrast to the immense quantities of protein and carbohydrate, only traces of lipids are present in PYG. Our analysis of the lipid content showed that PYG contains approximately 8  $\mu\text{M}$  free fatty acids and an additional 3  $\mu\text{M}$  fatty acids are esterified as triacylglycerols, phospholipids or cholesterol esters (Supplementary data Table T1). Having noticed that *A. castellanii* trophozoites prefer lipids over glucose as substrate, we investigated whether the addition of lipids influenced their growth. We incubated them in PY1G supplemented with either a mixture of octanoate and oleate, or with micelles prepared from phosphatidylglycerol and phosphatidylethanolamine. These additions of lipids strongly increased the growth rate (Fig. 4).

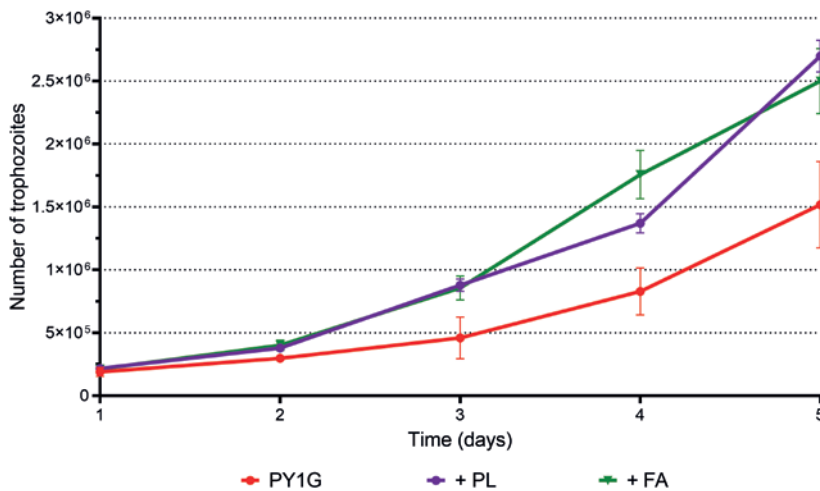


**Figure 4:** Influence of lipids on the proliferation of trophozoites.

Growth curves of *A. castellanii* trophozoites were measured in PY1G in the absence (red line) or presence of added vesicles of phospholipids (+ PL, purple line), or the fatty acids oleate and octanoate (+ FA, green line). Shown is the average of three incubations, error bars are standard deviation.

### 3.4. Growth of *A. castellanii* trophozoites can be inhibited by inhibitors of fatty acid degradation

To determine whether this observed preference for lipids as food, could be exploited to inhibit the growth of trophozoites, we tested three known inhibitors of fatty acid degradation for their growth-inhibiting effects, thioridazine, an inhibitor of peroxisomal lipid oxidation, and etomoxir and perhexiline, inhibitors of carnitine palmitoyltransferase, a component of the system for the transport of fatty acids into mitochondria for the subsequent breakdown via  $\beta$ -oxidation. We observed concentration-dependent inhibition of growth in the presence of these inhibitors. Thioridazine and perhexiline showed potent effects in low micromolar concentrations (Fig. 5). It cannot be ruled out that these compounds were inhibiting cell proliferation through off-target effects, but anyway, they were active at low concentrations.

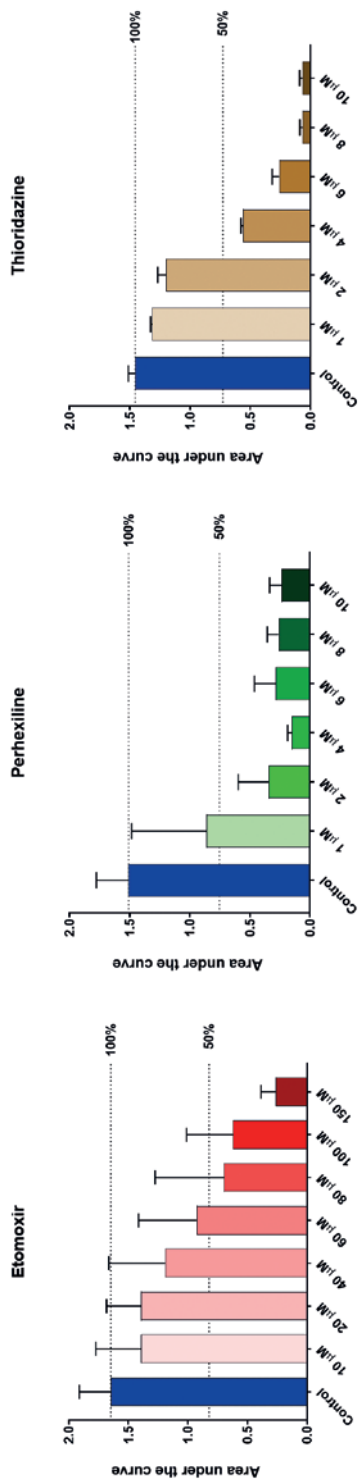


**Figure 5:** Effects of fatty acid oxidation inhibitors on the growth of *Acanthamoeba castellanii*. Growth curves of *A. castellanii* were obtained in the presence or absence of inhibitors of fatty acid oxidation. Optical density was measured daily over 5 days. Shown is the Area Under the Growth Curve (AUC) of compounds and respective controls. Indicated are lines of 100 % and 50 % of the control AUC. Experiments were performed at least twice in triplicate wells, error bars show the standard deviation.

## 4. Discussion

We provide an overview of the functional metabolism of *A. castellanii* with some compelling results. Our studies on oxygen consumption by trophozoites confirmed earlier studies which showed that *A. castellanii* possesses a branched electron-transport chain, which contains two terminal oxidases, apart from cytochrome *c* oxidase (Complex IV) also a cyanide-insensitive alternative oxidase (AOX) (Fig. 1)<sup>10,11</sup>. Our experiments showed that trophozoites still consume oxygen in the presence of either cyanide or SHAM, but not in the presence of both inhibitors. We now also discovered that *A. castellanii* trophozoites can instantaneously alter the use of the two separate branches and can redirect the flow of electrons from one branch to the other. Furthermore, our experiments showed that each of these two branches has sufficient capacity to transfer to oxygen all the electrons that enter the electron-transport chain.

Our experiments revealed that functioning of the AOX is essential for normal functioning and growth of *A. castellanii* trophozoites. Plant-like AOXs do not pump protons and they bypass the proton-pumping complexes III and IV (Fig. 1). Therefore, the flow of electrons through the AOX to oxygen markedly reduces the ATP yield of respiration because the oxidation of ubiquinol is then directly coupled with the reduction of oxygen. Normally, the oxidation of substrates, electron transport to oxygen and the formation of ATP are tightly coupled processes, but the presence of an active AOX offers a way to relax this coupling. In fact, the presence in *A. castellanii* of alternative dehydrogenases (Ndh2), which transfer electrons from NADH to ubiquinone without proton translocation, offers the possibility to completely uncouple the oxidation of substrates from the formation of ATP (Fig. 1). It is known that in plants the co-expression of AOX and the canonical electron-transport chain provides the metabolic flexibility to respond to a range of environmental conditions<sup>33</sup>. This role of the AOX is especially important when oxidative stress and the production of Reactive Oxygen Species (ROS) are high. Uncoupling of the oxidation of substrates and the formation of ATP can also be achieved by an uncoupling protein (UCP), which allows the flow of protons back to the matrix of the mitochondria without the concomitant formation of ATP by ATP synthase. It has been shown in isolated mitochondria of *A. castellanii* that activation of AOX and UCP lowers the production of hydrogen peroxide<sup>34</sup>. Therefore, it is most likely that also in *A. castellanii*, the AOX and UCP have a crucial role in protection against oxidative stress.

When cytochrome *c* oxidase or the AOX was inhibited by cyanide or SHAM, respectively, the growth of the amoebae stopped (Fig. 2B) but they still had the characteristic trophozoite appearance with acanthopodia (Supplementary Fig. S1). However, when both terminal oxidases were inhibited by the presence of cyanide plus SHAM, the shape

of the amoebae changed, they no longer possessed acanthopodia and became rounded (Supplementary Fig. S1). Apparently, although inhibition of only one of the two terminal oxidases is enough to result in growth arrest, a complete loss of the possibility to use oxygen is more severe. This pronounced effect of the inability to use oxygen was also observed in our anaerobic experiments with trophozoites on agar strips covered with *E. coli*. When these trophozoites were incubated anaerobically, they did not grow, were rounded and also had no acanthopodia (Fig. 3). This confirmation of the severe effect of the inability to use the respiratory chain, this time not by inhibitors but by the absence of oxygen, implies that the same effects in the incubations in the presence of inhibitors of the terminal oxidases are not off-target effects of these inhibitors.

To survive when conditions get harsh, *A. castellanii* forms cysts, to re-immerge as trophozoites only when conditions improve. Encystation starts with the rounding up of the trophozoites, followed by the formation of an outer and an inner cyst wall<sup>27,35</sup>. During this encystation, the trophozoite encloses itself within a resistant casing and becomes metabolically inactive after an initial burst of metabolic activity<sup>36</sup>. In our anaerobic incubations, or when the use of oxygen was blocked by cyanide plus SHAM, the trophozoites also rounded up, but mature cysts with two cyst walls were not formed and the amoebae were not stained by Uvitex B (Fig. 3 and Supplementary Fig. S1). Encystment and the formation of the cyst walls is an energy-consuming process and also involves the production of many enzymes, including the ones necessary to produce cellulose from the endogenous glycogen reserves (reviewed by<sup>37</sup>). In our experiments, blocking their aerobic metabolism resulted in trophozoites that lacked the energy to move and multiply. Apparently, these trophozoites also did not have enough energy to form cysts and they ended up rounded without acanthopodia. When thereafter an aerobic metabolism became possible, the round amoebae formed again acanthopodia and resumed multiplying (Supplementary Fig. S1).

Genomic and proteomic studies have suggested that *A. castellanii* possesses the capacity for the anaerobic generation of ATP<sup>21-24</sup>. However, whether such a putative system is active, and to what extent, is still an open question. We found that, if present at all, the anaerobic capacity does not support motility or growth and is therefore not comparable with the anaerobic metabolism known to occur in eukaryotes that possess hydrogenosomes or so-called anaerobic mitochondria<sup>38</sup>. Taken together, our oxygen consumption measurements and culture experiments show that *A. castellanii* trophozoites generate the bulk of their ATP via oxidative phosphorylation and that they require oxygen for homeostasis and growth, while our results provide no indication of an anaerobic energy metabolism that enables normal functioning.

The observed revival after four days of anaerobic conditions or in the presence of inhibitors of the electron-transfer chain is in line with studies on the survival of *A. castellanii* cysts, which showed that they can survive desiccation or a stay in water of 4 degrees for more than 20 years without losing their viability and maintaining their pathogenicity<sup>39,40</sup>. This implies that these acanthamoebae can enter a metabolic arrest stage and can revive when external conditions improve.

The nutrient preferences of *A. castellanii* trophozoites reveal remarkable characteristics. In contrast to most parasites, these trophozoites prefer lipids over glucose as their favourite food source for the formation of ATP (Table 1). Amino acids were also more favoured food than glucose. For the comparison of the preference for fatty acids or amino acids, it should be realized that in our experiments not all lipids and proteins were <sup>14</sup>C-labelled. PY1G contains all 20 amino acids but we added only three <sup>14</sup>C-labelled amino acids and the detection of the amount of <sup>14</sup>C-CO<sub>2</sub> enabled us to determine how much of these three amino acids was completely oxidised to carbon dioxide. Taking into account that we only determined the degradation of those three amino acids, and presupposing that the average rate of degradation of the other 17 amino acids sort of equals the average rate of degradation of the three amino acids that were labelled in our experiment, a rough estimation would result in a total of 11,300 nmol ATP produced by amino acid oxidation in 24 hours by one million amoebae. This is comparable to the amount produced by the oxidation of the two labelled lipids. The standard culture medium for *A. castellanii* PY contains Proteose peptone and Yeast extract, which are the water-soluble products of meat and yeast hydrolysates, respectively. Our analysis of the lipid content showed that PY medium contains indeed only traces of lipids (Supplementary Tabel T1)

Obviously, *A. castellanii* trophozoites are very selective and picky. The cells more readily catabolise fatty acids and amino acids compared to glucose. If available, as is the case in PYG and PY1G, they consume the flimsy amount of lipids that is present in an abundance of amino acids, while at the same time, glucose is hardly consumed. The preferential consumption of lipids and amino acids is in accordance with the food that free-living trophozoites of *A. castellanii* encounter while they are feeding on bacteria, which contain little or no free glucose but contain a large amount of proteins and lipids that can be used as substrates<sup>41</sup>. The preference for fatty acids is also in line with the pathogenic characteristics of *A. castellanii* trophozoites when they infect the brain, an organ rich in lipids due to the myelin sheaths covering the axons of nerve cells<sup>42</sup>. Genomic analysis has shown that *A. castellanii* possesses a sphingomyelin phosphodiesterase that can break down these brain lipids, explaining its pathogenic potential<sup>24</sup>. Besides the brain,

*Acanthamoeba* can also infect the eye, which is covered in a lipid-rich secretion called meibum<sup>43</sup>. Meibum contains complex lipids of extreme length, which could serve as a rich source of nutrients if *Acanthamoeba* is located on or in the cornea of the eye.

Lastly, we investigated whether the preference for lipids can result in a new treatment strategy. We tested three known inhibitors of the breakdown of lipids, etomoxir, perhexiline and thioridazine. Etomoxir and perhexiline inhibit carnitine palmitoyltransferases CPT1 and CPT2, thereby blocking the transport of fatty acids into mitochondria<sup>44,45</sup>. Thioridazine inhibits the peroxisomal oxidation of lipids<sup>46,47</sup>, and peroxisomes are known to be present in *Acanthamoeba* spp.<sup>48</sup>.

Thioridazine and perhexiline strongly inhibited the growth of *A. castellanii* trophozoites. The use of thioridazine, a phenothiazine and first-generation antipsychotic agent that is no longer in common use, could be a promising new option to treat GAE, as concentrations of 10  $\mu\text{M}$  strongly inhibited growth and the concentration of thioridazine and its metabolites in serum already approaches 10  $\mu\text{M}$  when 50 mg is administered every 6 hours<sup>49</sup>. Furthermore, thioridazine and its major metabolites have been shown to accumulate in the brain, resulting in concentrations up to 10-fold higher than in serum<sup>50</sup>. Therefore, this drug could impact *Acanthamoeba* at the location where it is needed to treat GAE. Thioridazine could also be effective against *Acanthamoeba* keratitis, as peroxisomes are involved in the degradation of very long-chain fatty acids, which are present in meibum<sup>43</sup>. Perhexiline was originally developed for the treatment of angina pectoris and is currently used in several countries as a last-line treatment in patients with therapy-refractory angina. Recently, promising results of perhexiline as an anti-cancer drug have been shown, and as the safety profile is relatively well understood, repurposing of this drug is feasible<sup>51</sup>. We have shown strong inhibition of the growth of *A. castellanii* at a concentration of 2  $\mu\text{M}$ , which can be achieved in plasma<sup>52</sup>. Therefore, perhexiline might also be a possible future treatment option for the treatment of *Acanthamoeba* infections.

The added value of thioridazine and perhexiline in the treatment of *Acanthamoeba* keratitis should be evaluated with animal testing to determine whether there is a place for these drugs in the standard treatment regimen. Although variation in the efficacy of drugs between different *Acanthamoeba* strains has been described<sup>53</sup>, we expect that inhibitors of fatty acid oxidation show less variance in efficacy, as these drugs affect an essential metabolic pathway. It cannot be ruled out that these compounds are inhibiting cell proliferation through off-target effects, but as they are active at low concentrations, further investigations are warranted.

To conclude, our study provides an overview of the metabolic characteristics of the infrequently studied *Acanthamoeba*, which results in a new treatment target and possible new treatment options for *Acanthamoeba* keratitis and the rare but deadly disease granulomatous amoebic encephalitis.

### **Funding statement**

This work was funded by the Erasmus MC and the Netherlands Centre for One Health. Sponsors were not involved in study design; collection, analysis and interpretation of data; writing of the report or in the decision to submit the article for publication.

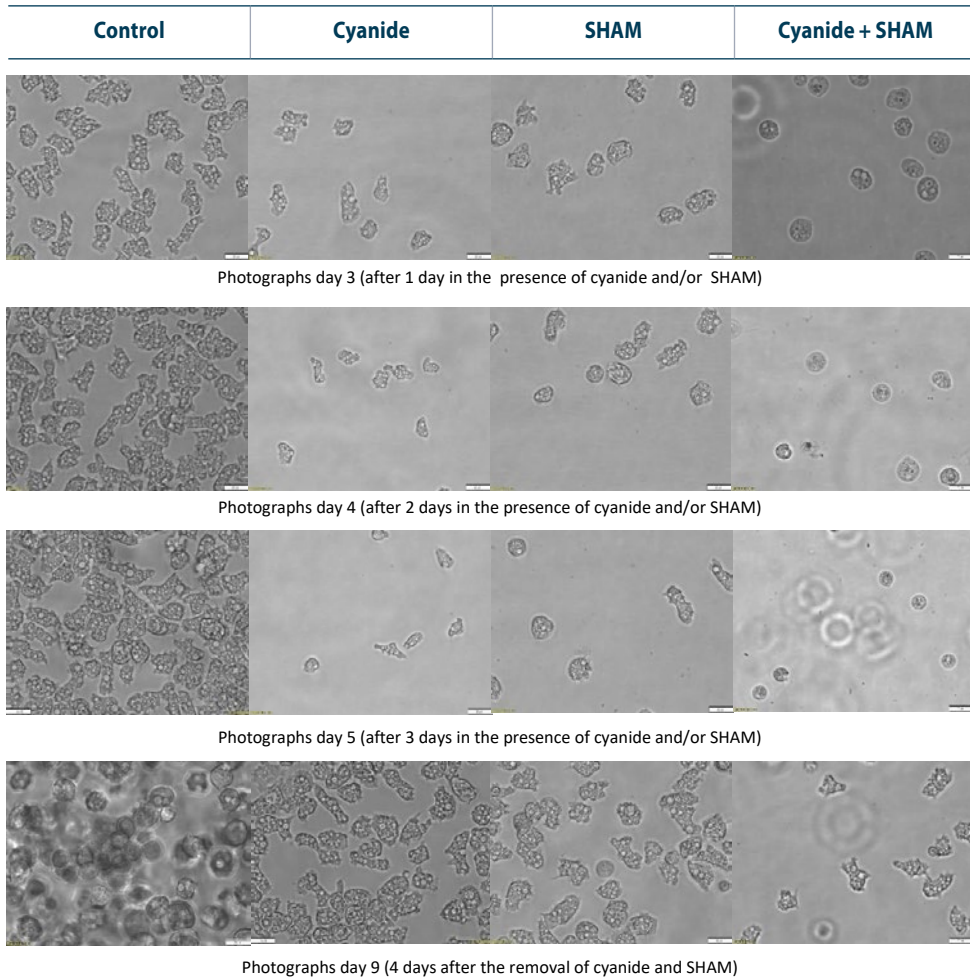
## References

- 1 Cope, J. R., Ali, I. K. & Visvesvara, G. S. in *Hunter's Tropical Medicine and Emerging Infectious Diseases (Tenth Edition)* (eds Edward T. Ryan *et al.*) 814-820 (Elsevier, 2020).
- 2 Sarink, M. J. *et al.* Three encephalitis-causing amoebae and their distinct interactions with the host. *Trends Parasitol* **38**, 230-245 (2022).
- 3 Kalra, S. K., Sharma, P., Shyam, K., Tejan, N. & Ghoshal, U. *Acanthamoeba* and its pathogenic role in granulomatous amebic encephalitis. *Exp Parasitol* **208**, 107788 (2020).
- 4 Akpek, G. *et al.* Granulomatous amebic encephalitis: an under-recognized cause of infectious mortality after hematopoietic stem cell transplantation. *Transpl Infect Dis* **13**, 366-373 (2011).
- 5 Maycock, N. J. & Jayaswal, R. Update on *Acanthamoeba* keratitis: diagnosis, treatment, and outcomes. *Cornea* **35**, 713-720 (2016).
- 6 Bataillie, S., Van Ginderdeuren, R., Van Calster, J., Foets, B. & Delbeke, H. How a devastating case of *Acanthamoeba* sclerokeratitis ended up with serious systemic sequelae. *Case Rep Ophthalmol* **11**, 348-355 (2020).
- 7 Raghavan, A. *et al.* Fulminant *Acanthamoeba* Endophthalmitis After Cataract Surgery-A Case Report. *Cornea* **39**, 1055-1058 (2020).
- 8 Kaufman, A. R. & Tu, E. Y. Advances in the management of *Acanthamoeba* keratitis: A review of the literature and synthesized algorithmic approach. *Ocul Surf* **25**, 26-36 (2022).
- 9 Fidock, D. A., Rosenthal, P. J., Croft, S. L., Brun, R. & Nwaka, S. Antimalarial drug discovery: efficacy models for compound screening. *Nat Rev Drug Discov* **3**, 509-520 (2004).
- 10 Gawryluk, R. M. R., Chisholm, K. A., Pinto, D. M. & Gray, M. W. Composition of the mitochondrial electron transport chain in *Acanthamoeba castellanii*: Structural and evolutionary insights. *Biochim Biophys Acta* **1817**, 2027-2037 (2012).
- 11 Zíková, A., Hampl, V., Paris, Z., Týč, J. & Lukeš, J. Aerobic mitochondria of parasitic protists: Diverse genomes and complex functions. *Mol Biochem Parasitol* **209**, 46-57 (2016).
- 12 Jarmuszkiewicz, W., Sluse, F. E., Hryniewiecka, L. & Sluse-Goffart, C. M. Interactions between the cytochrome pathway and the alternative oxidase in isolated *Acanthamoeba castellanii* mitochondria. *J Bioenerg Biomembr* **34**, 31-40 (2002).
- 13 Antos-Krzeminska, N. & Jarmuszkiewicz, W. External NAD(P)H dehydrogenases in *Acanthamoeba castellanii* mitochondria. *Protist* **165**, 580-593 (2014).
- 14 Antos-Krzeminska, N., Kicinska, A., Nowak, W. & Jarmuszkiewicz, W. *Acanthamoeba castellanii* uncoupling protein: a complete sequence, activity, and role in response to oxidative stress. *Int J Mol Sci* **24**, 12501 (2023).
- 15 Neff, R. J., Neff, R. H. & Taylor, R. E. The nutrition and metabolism of a soil amoeba, *Acanthamoeba* sp. *Physiol Zool* **31**, 73-91 (1958).
- 16 Turner, N. A., Biagini, G. A. & Lloyd, D. Anaerobiosis-induced differentiation of *Acanthamoeba castellanii*. *FEMS Microbiol Lett* **157**, 149-153 (1997).
- 17 Cometa, I., Schatz, S., Trzyna, W. & Rogerson, A. Tolerance of naked amoebae to low oxygen levels with an emphasis on the genus *Acanthamoeba*. *Acta Protozool* **50**, 33 - 40 (2011).
- 18 Carvalho-Kelly, L. F. *et al.* Anaerobic ATP synthesis pathways and inorganic phosphate transport and their possible roles in encystment in *Acanthamoeba castellanii*. *Cell Biol Int* **46**, 1288-1298 (2022).
- 19 Alves, D., Alves, L. M., da Costa, T. L., de Castro, A. M. & Vinaud, M. C. Anaerobic metabolism in T4 *Acanthamoeba* genotype. *Curr Microbiol* **74**, 685-690 (2017).
- 20 Gawryluk, R. M., Chisholm, K. A., Pinto, D. M. & Gray, M. W. Compositional complexity of the mitochondrial proteome of a unicellular eukaryote (*Acanthamoeba castellanii*, supergroup Amoebozoa) rivals that of animals, fungi, and plants. *J Proteomics* **109**, 400-416 (2014).

- 21 Hug, L. A., Stechmann, A. & Roger, A. J. Phylogenetic distributions and histories of proteins involved in anaerobic pyruvate metabolism in eukaryotes. *Mol Biol Evol* **27**, 311-324 (2009).
- 22 Ginger, M. L., Fritz-Laylin, L. K., Fulton, C., Cande, W. Z. & Dawson, S. C. Intermediary metabolism in protists: a sequence-based view of facultative anaerobic metabolism in evolutionarily diverse eukaryotes. *Protist* **161**, 642-671 (2010).
- 23 Leger, M. M., Gawryluk, R. M., Gray, M. W. & Roger, A. J. Evidence for a hydrogenosomal-type anaerobic ATP generation pathway in *Acanthamoeba castellanii*. *PLoS One* **8**, e69532 (2013).
- 24 Clarke, M. *et al.* Genome of *Acanthamoeba castellanii* highlights extensive lateral gene transfer and early evolution of tyrosine kinase signaling. *Genome Biol* **14**, R11 (2013).
- 25 Kanehisa, M., Furumichi, M., Sato, Y., Kawashima, M. & Ishiguro-Watanabe, M. KEGG for taxonomy-based analysis of pathways and genomes. *Nucleic Acids Res* **51**, D587-D592 (2023).
- 26 Bexkens, M. L. *et al.* Lipids are the preferred substrate of the protist *Naegleria gruberi*, relative of a human brain pathogen. *Cell Rep* **25**, 537-543 e533 (2018).
- 27 Neff, R. J., Ray, S. A., Benton, W. F. & Wilborn, M. in *Methods in Cell Biology* Vol. 1 (ed David M. Prescott) 55-83, Academic Press, New York, USA (1964).
- 28 Bexkens, M. L. *et al.* *Schistosoma mansoni* does not and cannot oxidise fatty acids, but these are used for biosynthetic purposes instead. *Int J Parasitol* **49**, 647-656 (2019).
- 29 Bligh, E. G. & Dyer, W. J. A rapid method of total lipid extraction and purification. *Can J Biochem Physiol* **37**, 911-917 (1959).
- 30 Sarink, M. J., Tielens, A. G. M., Verbon, A., Sutak, R. & van Hellemond, J. J. Inhibition of Fatty Acid Oxidation as a New Target To Treat Primary Amoebic Meningoencephalitis. *Antimicrob Agents Chemother* **64**, e00344-20 (2020).
- 31 Chávez-Munguía, B. *et al.* Ultrastructural study of encystation and excystation in *Acanthamoeba castellanii*. *J Eukaryot Microbiol* **52**, 153-158 (2005).
- 32 Bender, D. A. The metabolism of "surplus" amino acids. *Br J Nutr* **108**, S113-S121 (2012).
- 33 Vanlerberghe, G. C. Alternative oxidase: a mitochondrial respiratory pathway to maintain metabolic and signaling homeostasis during abiotic and biotic stress in plants. *Int J Mol Sci* **14**, 6805-6847 (2013).
- 34 Czarna, M. & Jarmuszkiwicz, W. Activation of alternative oxidase and uncoupling protein lowers hydrogen peroxide formation in amoeba *Acanthamoeba castellanii* mitochondria. *FEBS Lett* **579**, 3136-3140 (2005).
- 35 Weisman, R. A. Differentiation in *Acanthamoeba castellanii*. *Annu Rev Microbiol* **30**, 189-219 (1976).
- 36 Siddiqui, R., Dudley, R. & Khan, N. A. *Acanthamoeba* differentiation: a two-faced drama of Dr Jekyll and Mr Hyde. *Parasitology* **139**, 826-834 (2012).
- 37 Schaap, P. & Schilde, C. Encystation: the most prevalent and underinvestigated differentiation pathway of eukaryotes. *Microbiology (Reading)* **164**, 727-739 (2018).
- 38 Müller, M. *et al.* Biochemistry and evolution of anaerobic energy metabolism in eukaryotes. *Microbiol Mol Biol Rev* **76**, 444-495 (2012).
- 39 Mazur, T., Hadaś, E. & Iwanicka, I. The duration of the cyst stage and the viability and virulence of *Acanthamoeba* isolates. *Trop Med Parasitol* **46**, 106-108 (1995).
- 40 Sriram, R., Shoff, M., Booton, G., Fuerst, P. & Visvesvara, G. S. Survival of *Acanthamoeba* cysts after desiccation for more than 20 years. *J Clin Microbiol* **46**, 4045-4048 (2008).
- 41 Alberts, B. *et al.* *Molecular Biology of the Cell (5th ed.)*. W.W. Norton & Company, New York, USA (2008).
- 42 Schmitt, S., Castelvetti, L. C. & Simons, M. Metabolism and functions of lipids in myelin. *Biochim Biophys Acta* **1851**, 999-1005 (2015).
- 43 Butovich, I. A. Meibomian glands, meibum, and meibogenesis. *Exp Eye Res* **163**, 2-16 (2017).

- 44 Kennedy, J. A., Unger, S. A. & Horowitz, J. D. Inhibition of carnitine palmitoyltransferase-1 in rat heart and liver by perhexiline and amiodarone. *Biochem Pharmacol* **52**, 273-280 (1996).
- 45 Weis, B. C., Cowan, A. T., Brown, N., Foster, D. W. & McGarry, J. D. Use of a selective inhibitor of liver carnitine palmitoyltransferase I (CPT I) allows quantification of its contribution to total CPT I activity in rat heart. Evidence that the dominant cardiac CPT I isoform is identical to the skeletal muscle enzyme. *J Biol Chem* **269**, 26443-26448 (1994).
- 46 Shi, R., Zhang, Y., Shi, Y., Shi, S. & Jiang, L. Inhibition of peroxisomal beta-oxidation by thioridazine increases the amount of VLCFAs and Abeta generation in the rat brain. *Neurosci Lett* **528**, 6-10 (2012).
- 47 Van den Branden, C. & Roels, F. Thioridazine: a selective inhibitor of peroxisomal beta-oxidation in vivo. *FEBS Lett* **187**, 331-333 (1985).
- 48 González-Robles, A. *et al.* Ultrastructural, cytochemical and comparative genomic evidence of peroxisomes in three genera of pathogenic free-living amoebae, including the first morphological data for the presence of this organelle in Heteroloboseans. *Genome Biol Evol.* **10**, 1734-1750 (2020).
- 49 Aslostovar, L. *et al.* A phase 1 trial evaluating thioridazine in combination with cytarabine in patients with acute myeloid leukemia. *Blood Adv* **2**, 1935-1945 (2018).
- 50 Svendsen, C. N., Hrbek, C. C., Casendino, M., Nichols, R. D. & Bird, E. D. Concentration and distribution of thioridazine and metabolites in schizophrenic post-mortem brain tissue. *Psychiatry Res* **23**, 1-10 (1988).
- 51 Dhakal, B. *et al.* Perhexiline: Old Drug, New Tricks? A Summary of Its Anti-Cancer Effects. *Molecules* **28** (2023).
- 52 Sallustio, B. C., Westley, I. S. & Morris, R. G. Pharmacokinetics of the antianginal agent perhexiline: relationship between metabolic ratio and steady-state dose. *Br J Clin Pharmacol* **54**, 107-114 (2002).
- 53 Hernandez-Martinez, D. *et al.* Evaluation of the sensitivity to chlorhexidine, voriconazole and itraconazole of T4 genotype *Acanthamoeba* isolated from Mexico. *Exp Parasitol* **197**, 29-35 (2019).

## Supplementary material



**Supplementary Figure S1.** Photographs of *Acanthamoeba castellanii* trophozoites while cultured in the presence of respiratory-chain inhibitors.

The effects of the respiratory-chain inhibitors cyanide and SHAM on the cell growth of *A. castellanii* trophozoites were studied and the results are shown in Figure 2B of the main text. Shown here are photographs taken during those experiments. The white bar is 20  $\mu\text{m}$ .

**Supplementary Table T1:** Fatty acid content of PYG.

Free FA in PYG		Esterified FA in PYG		
	$\mu\text{M}$			$\mu\text{M FA-eq}$
C18:1	2.00	CholEster	18:0	1.10
C16:0	1.95	TAG	54:3	0.43
C18:0	1.42	TAG	52:2	0.39
C18:2	0.71	TAG	52:3	0.19
C16:1	0.51	TAG	54:4	0.18
C15:0	0.45	TAG	50:2	0.18
C14:0	0.44	TAG	54:5	0.16
C17:0	0.14	PC	34:1	0.09
C17:1	0.12	PE	36:1	0.07
C20:1	0.10	SM	24:2	0.04
<b>sum:</b>	<b>7.83</b>		<b>sum:</b>	<b>2.83</b>

The concentration of free and esterified fatty acids in PYG was determined using LC-MS. For the free fatty acids, the ten most abundant fatty acids are shown. For the esterified fatty acids, the ten most abundant lipids containing fatty acids are shown, and per compound the total number of carbon atoms and unsaturations of the acyl chains. For instance, TAG 54:3 denotes a triacylglycerol with a total of 54 carbons and 3 double bonds in the acyl chains, most likely containing 3 oleic acids (C18:1), while PC 34:1 contains one oleic acid (18:1) and one palmitic acid (16:0), or one palmitoleic acid (16:1) and one stearic acid (18:0), or a mixture of both combinations.

Abbreviations: CholEster, cholesterol ester; FA, fatty acids; FA-eq, FA-equivalents; PC, phosphatidylcholine; PE, phosphatidylethanolamine; SM, sphingomyelin; TAG, triacylglycerol

## Supplementary Movies

### ***Supplementary Movie 1 – Combination of movies 2-5 -***

***<https://tinyurl.com/MovieS1Acanth>***

Compilation of four movies made after a one-day incubation of *Acanthamoeba castellanii* trophozoites in four conditions, control (top left), in the presence of cyanide (top right), in the presence of SHAM (bottom left) and in the presence of cyanide plus SHAM (bottom right). This is from the experiment shown in Figure 2B. To enable full-screen inspection of the separate movies, the four original movies are also included (Supplementary Movies 2-5).

### ***Supplementary Movie 2 – Control -***

***<https://tinyurl.com/MovieS2Acanth>***

Movie made after a one-day incubation of *Acanthamoeba castellanii* trophozoites in the absence of inhibitors of the respiratory chain (control incubation) This is from the experiment shown in Figure 2B.

### ***Supplementary Movie 3 – Cyanide -***

***<https://tinyurl.com/MovieS3Acanth>***

Movie made after a one-day incubation of *Acanthamoeba castellanii* trophozoites in the presence of cyanide. This movie is from the experiment shown in Figure 2B.

### ***Supplementary Movie 4 – SHAM -***

***<https://tinyurl.com/MovieS4Acanth>***

Movie made after a one-day incubation of *Acanthamoeba castellanii* trophozoites in the presence of SHAM. This movie is from the experiment shown in Figure 2B.

### ***Supplementary Movie 5 – Cyanide + SHAM -***

***<https://tinyurl.com/MovieS5Acanth>***

Movie made after a one-day incubation of *Acanthamoeba castellanii* trophozoites in the presence of cyanide plus SHAM. This movie is from the experiment shown in Figure 2B.

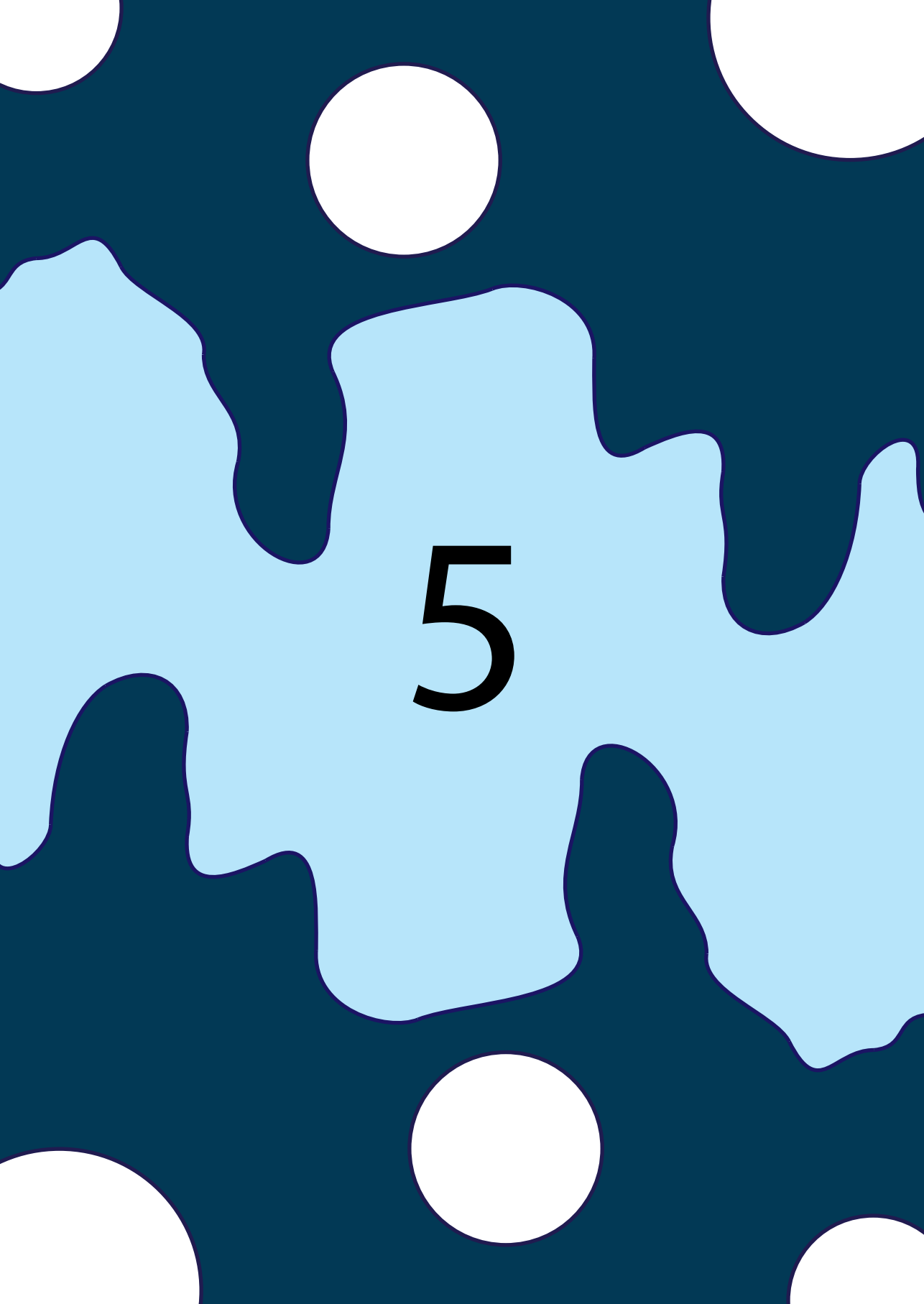
### ***Supplementary Movie 6 – Immediately after opening -***

***<https://tinyurl.com/MovieS6Acanth>***

Movie made after a four-day incubation of *Acanthamoeba castellanii* trophozoites under anaerobic conditions. Directly after ending the anaerobic incubations, the trophozoites could be inspected under the microscope. This movie is from the experiment shown in Figure 2D and Figure 3.

**Supplementary Movie 7 – Four hours after opening -  
<https://tinyurl.com/MovieS7Acanth>**

Movie made after a four-day incubation of *Acanthamoeba castellanii* trophozoites under anaerobic conditions, four hours after the re-introduction of oxygen. This movie is from the experiment shown in Figure 2D and Figure 3.



5

# CHAPTER 5

---

## An international External Quality Assessment Scheme to assess the diagnostic performance of polymerase chain reaction detection of *Acanthamoeba keratitis*

Maarten J. Sarink<sup>1</sup>, Rob Koelewijn<sup>1</sup>, Foekje Stelma<sup>2</sup>, Titia Kortbeek<sup>3</sup>, Lisette van Lieshout<sup>4</sup>, Pieter W. Smit<sup>5</sup>, Aloysius G.M. Tielens<sup>1</sup>, Jaap J. van Hellemond<sup>1</sup>

<sup>1</sup> Department of Medical Microbiology and Infectious Diseases, Erasmus MC University Medical Center, Rotterdam, The Netherlands

<sup>2</sup> Department of Medical Microbiology, Radboudumc Nijmegen, The Netherlands

<sup>3</sup> National Institute of Public Health and the Environment, RIVM, Bilthoven, The Netherlands

<sup>4</sup> Department of Parasitology, Leiden University Medical Centre, Leiden, The Netherlands

<sup>5</sup> Department of Medical Microbiology, Molecular Diagnostics Unit, Maasstad Hospital, Rotterdam, The Netherlands

## Abstract

### Purpose

The purpose of this study was to assess the variation in methods and to determine whether an External Quality Assessment Scheme (EQAS) for polymerase chain reaction (PCR) detection of *Acanthamoeba keratitis* is valuable for the diagnostic process.

### Methods

A multicenter EQAS was introduced, covering 16 diagnostic laboratories. Using *Acanthamoeba castellanii* ATCC strain 30010, 3 sets of samples were prepared, containing different amounts of DNA, cysts, or trophozoites. Samples were masked and sent to the participants with instructions for use and a questionnaire concerning the applied methodologies. Special attention in this questionnaire was given to the used pretreatment methods to assess existing variations in these procedures.

### Results

A large variation in the methodologies and substantial differences in the diagnostic performance were found between participants. In contrast to the DNA samples where all participants had a perfect score, several false negative results were reported for the samples containing cysts or trophozoites. Only 9 participants had an optimal score, whereas one participant reported all samples as negative, one participant reported failures due to inhibition, and the other 5 reported in total 7 false negative results. A clear correlation was noticed between the PCR detection rate and the number of cysts or trophozoites in the sample.

### Conclusions

The results indicate that a pretreatment procedure can be a risky step in PCR-based detections of *Acanthamoeba*, but it improves the sensitivity and reliability, especially of samples containing cysts. Therefore, participation in an EQAS is informative for routine diagnostic laboratories and can assist in improving the laboratory procedures used for the diagnosis of *Acanthamoeba keratitis*.

## Introduction

*Acanthamoeba* is a free-living amoeba that is ubiquitously present around the world in soil and water. It can exist in a trophozoite stage, which is actively moving and feeding, and a cyst stage, which is dormant and stress-resistant. *Acanthamoeba* can cause an infectious keratitis, which leads to blindness if left untreated or is treated with the wrong medication. *Acanthamoeba* keratitis is often seen in contact lens wearers, among which 1 in 21,000 in the Netherlands is affected <sup>1</sup>. In recent years this incidence has been reported to rise <sup>1-3</sup>.

The most important factor that determines the prognosis of *Acanthamoeba* keratitis is an early diagnosis <sup>4</sup>. However, diagnosing *Acanthamoeba* keratitis requires clinical expertise, as symptoms overlap with infectious keratitis caused by other micro-organisms <sup>5</sup>. Many different diagnostic tools are available, all with different characteristics. Direct culture is a laborious and time-consuming diagnostic method, in which the clinical sample is added to a non-nutrient agar plate seeded with Gram-negative bacteria (e.g., *Escherichia coli*), after which *Acanthamoeba* growth must be detected microscopically. Direct visualization of *Acanthamoeba* on the infected eye is also possible using *in vivo* confocal microscopy, but this method requires specialized equipment and personnel <sup>5</sup>. Nucleic acid amplification tests (NAATs), such as PCR, have also been developed to detect *Acanthamoeba* DNA. These NAAT methods have a high sensitivity and can provide rapid results in contrast to the time-consuming culture procedures <sup>6,7</sup>. However, a large diversity of NAATs are in use and so far external quality assessment scheme (EQAS) for these tests are lacking. An EQAS involves the comparison of test results of a laboratory to a source outside of that laboratory, allowing an objective assessment of the diagnostic performance of a laboratory <sup>8</sup>. EQAS have already been used to optimize the detection and evaluation of other infectious diseases using NAATs <sup>9,10</sup>.

Here, we describe the evaluation of the introduction of an EQAS for the detection of *Acanthamoeba* cysts and trophozoites by NAAT. We aimed to assess the variation in methods and to determine whether an EQAS for the detection of *Acanthamoeba* can be of value for the diagnostic process.

## Materials and methods

### Sample preparation

*Acanthamoeba castellanii* ATCC strain 30010 ('Neff') was grown in cell culture flasks at 25°C in PYG medium, which contained proteose peptone, yeast extract, glucose, salt additives (ATCC medium 712), 40 µg/mL gentamicin, 100 units/mL penicillin, and 100 µg/

mL streptomycin, as described before <sup>11</sup>. To prepare samples containing trophozoites, cultures were refreshed with PYG on the day before sampling, to ensure that only trophozoites were obtained. Trophozoites were collected by placing a cell culture flask on ice for 20 minutes and repeatedly tapping to detach trophozoites. To prepare samples with cysts, encystation was induced by replacing the supernatant of a culture of trophozoites growing in logarithmic phase with encystation medium, containing 95 mM NaCl, 5 mM KCl, 8 mM MgSO<sub>4</sub>, 1 mM NaHCO<sub>3</sub>, 0.4 mM CaCl<sub>2</sub> and 20 mM Tris-HCl (pH 9.0), as described before <sup>12</sup>. Cysts were collected by repeatedly tapping and pouring contents out of the cell culture flask. After collection, the trophozoite and the cyst suspensions were washed three times with Tris NaCl (25 mM Tris, 120 mM NaCl, pH 7.4) or encystation medium, respectively. Amoebae were then counted three times using a Bürker cell counter, after which the average count was used to prepare distinct dilutions of the amoebae, cysts in encystation medium and trophozoites in TRIS NaCl. EDTA (5 mM) was added to the trophozoite suspensions to stop trophozoite replication and block DNA degradation. Finally, suspensions of 2000, 200, 20 or 2 amoebae in 200 µL medium were put in screw-cap Eppendorf tubes. Negative controls containing only TRIS NaCl + EDTA or encystation medium were also prepared. Purified *Acanthamoeba* DNA samples were prepared from a dense trophozoite culture, from which DNA was isolated by the MagNA Pure system (Roche, Basel, Switzerland). The isolated DNA was diluted in Tris-HCl (10 mM) + EDTA (0.5 mM) buffer (pH 8.0) supplemented with 10 mg/L Sheared Salmon DNA (Thermo Fisher, Waltham, MA) and 10 mg/L bovine serum albumin (Roche, Basel, Switzerland) to obtain DNA samples with a high, medium or low concentration of *Acanthamoeba* DNA, comparable to the DNA content of the samples with 2000, 200 and 20 amoebae, respectively. A volume of 50 µL of each dilution was added to screw-cap Eppendorf tubes, along with a negative control containing only Tris-HCl + EDTA buffer with supplements.

### Sample validation

The homogeneity of the prepared samples was validated by an expert laboratory by examining 5 randomly chosen replicates. The stability of the samples was tested by 2 expert laboratories by examining the samples directly after preparation, as well as after storage at room temperature for 4 months when the EQAS distribution had been completed, and all results by all participants had been reported.

In this pilot study, 16 laboratories participated in the *Acanthamoeba* External Molecular Quality Assessment Scheme organized by the parasitology section of the Dutch Foundation for Quality Assessment in Medical Laboratories (SKML). All participating laboratories are accredited large hospital microbiological laboratories or national institutes of disease control. The samples were sent in a masked fashion to the participating laboratories, along with instructions for use and a questionnaire (see supplementary material).

## Results

### Validation of the homogeneity and stability of the samples

After preparation, the homogeneity of the samples was verified in an expert laboratory by a five-fold examination using DNA extraction followed by real-time PCR (rtPCR) analysis. The samples containing 20, 200, or 2000 cysts or trophozoites were positive in all these analyses and formed the set of validated samples. For these validated samples the average standard deviation for all separate sample types was less than 1.5 cycles (Supplemental Table S1). Of the samples that according to the dilution series should contain 2 cysts or 2 trophozoites, a positive result was found for only 3 of the 5 cyst samples and 1 of the 5 trophozoite samples. It is possible that due to the intrinsic unreliability of diluting suspensions, some of these samples that were supposed to contain 2 amoebae, contained in fact no amoebae. Another possibility is that the amount of DNA isolated from these samples was below the limit of detection. A combination of both possibilities is conceivable. The samples with 2 amoebae were included for educational purposes in the shipment to the participants, but the reported results of these samples were not used in our evaluation.

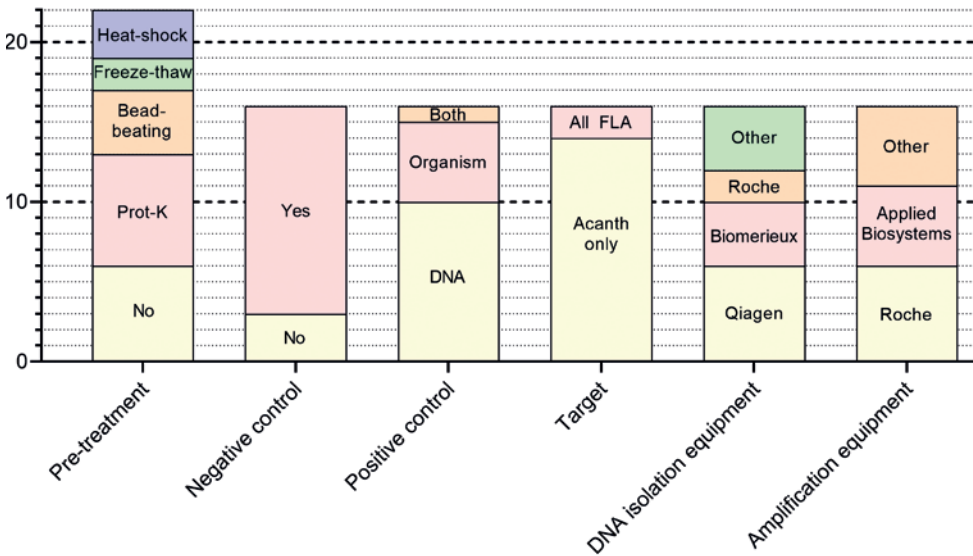


**Figure 1.** Overview of the used methodologies as reported by the 16 participating laboratories.

Several participants used a combination of pre-treatment procedures, which results in a total of reported pre-treatment procedures of over 16. The combinations that were reported were the following: Prot-K + heat-shock: 3 times, Prot-K + freeze-thaw: 2 times, Prot-K + bead-beating: 1 time. "Multiplex" indicates that apart from *A. castellanii*, also the amoebae *Balamuthia mandrillaris* and *Naegleria fowleri* were targeted.

To test the stability of the samples, 2 expert laboratories analyzed them at the time of distribution and retested them circa 4 months later when the distributed samples had been analyzed and reported by all participants. In the period between preparation and retesting, the samples were stored at room temperature, similar to the distributed samples. These examinations revealed an average difference per sample of fewer than 1.5 cycles (Supplemental Table S2) for all sample types (purified DNA, cysts, and trophozoites), demonstrating the stability of all types of samples over the entire study period.

### **Variations in methodology among the participants**

The 16 laboratories that participated in this EQAS did so by reporting results and by completing the online questionnaire (see Appendix), which aimed to provide an overview of the used methodology. Figure 1 shows a summary of the different methods that were used. Before performing DNA extraction by a commercial kit or platform, many participants used a specific pre-treatment to enhance lysis of the amoebae by proteinase K treatment (n= 7/16), bead-beating (n=4/16), heat-shock (n=3/16) or freeze-thawing (n=2/16). Some participants used a combination of these methods, one participant reported pre-treatment as classified and 6 participants did not use any specific treatment before DNA extraction.

The equipment used for DNA extraction originated from several companies, among which Qiagen, Biomerieux, and Roche (Fig. 1). All laboratories used the whole sample volume (200 µL) for DNA extraction. The volume in which the extracted DNA was eluted differed substantially, ranging from 12.5 to 200 µL, with an average of 90.2 µL (median 100 µL). The volume of isolated DNA that was used in the PCR reaction also differed substantially, ranging from 2 to 20 µL (average 6.3 µL, median 5 µL). Laboratories used different equipments for DNA amplification, among which Roche (n=6), Applied Biosystems (n=5) and other (n=5). Four of 16 participants did not include an internal control in their examination protocol, whereas all participants used a positive control, which was a DNA standard (10/16), an *Acanthamoeba* culture (5/16), or both (1/16). Two participants used a multiplex PCR in which also *Balamuthia mandrillaris* and *Naegleria fowleri* were targeted, whereas the other 14 participants used a PCR in which only *Acanthamoeba* spp. was examined.

### **Qualitative results**

All 16 participating laboratories reported qualitative results of DNA amplification tests of samples containing *A. castellanii* DNA, cysts, trophozoites and respective negative controls. All 16 laboratories reported a positive result for all the samples containing purified *A. castellanii* DNA. By contrast, for the samples containing cysts or trophozoites for which DNA had to be isolated first, not all samples were reported to contain amoebae.

The reported results of these samples containing cysts or trophozoites clearly correlated with the number of organisms that were present in the sample (Fig. 2). Ten of the 16 participants reported a positive result for at least 1 of the 2 educational samples, each containing 2 cysts or 2 trophozoites, and 2 of those 10 participants reported positive results for both samples (Supplemental Table S3-A). The sample with 20 cysts or 20 trophozoites was reported as positive by 10 and 12 participants, respectively. Nine of the 10 participants who reported a positive result for the cyst sample, reported a positive result for the trophozoite sample as well. The sample with 200 cysts or 200 trophozoites was reported as positive by 13 and 14 participants, respectively. For the samples containing 20 *Acanthamoeba* cysts or trophozoites, possible aliquoting errors cannot explain the lower detection rate than observed for the samples containing 200 amoebae because the validation by 5-fold analysis by a single laboratory showed only small quantitative differences in these samples.

The incorrect results were not evenly distributed among participants, as one participant reported inhibition for all samples containing amoebae and another participant reported negative results for those samples (Supplemental Table S3-A). Altogether, for the 6 validated amoeba samples, 9 participants reported all correct qualitative results, 3 reported a single false negative result, 2 reported 2 false negative results, and as

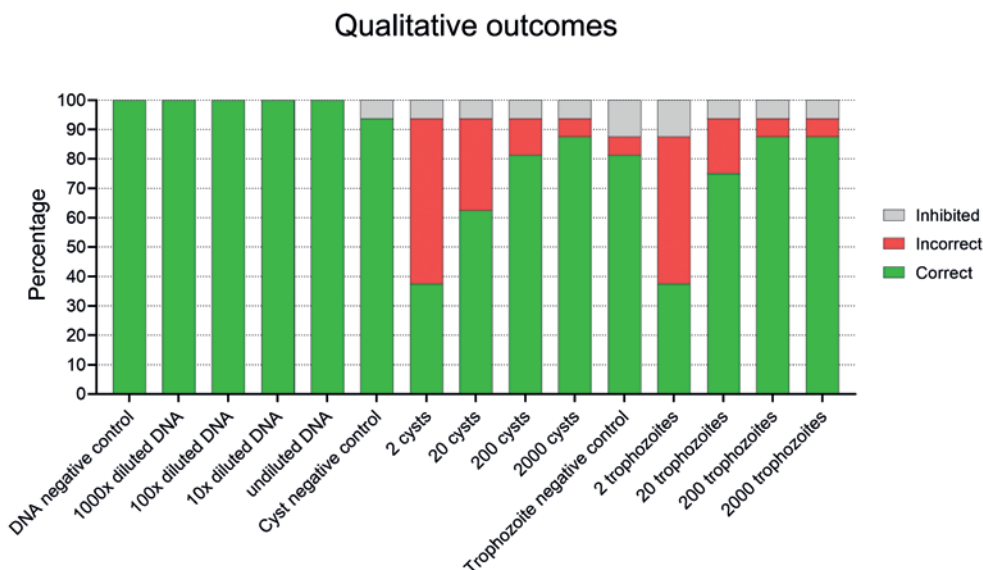


**Figure 2.** Qualitative results of samples containing different numbers of either cysts or trophozoites.

All 16 participants reported for all samples their results and these are all included in the figure.

mentioned earlier, one participant reported 6 false negative results, and another one reported 6 failures of examination due to inhibition of the DNA replication (Supplemental Fig. S1 and Supplemental Table S3-B).

### **Quantitative results**

All participants used an rtPCR method for the DNA amplification and reported their results also in a semiquantitative manner by providing the C<sub>q</sub>-values, which indicate the PCR cycle at which the fluorescent signal of the rtPCR reactions exceeded the threshold for background fluorescence. A high C<sub>q</sub>-value indicates a low quantitative load of amoebae, whereas low C<sub>q</sub>-value indicates a higher quantitative load of amoebae. Supplemental Table S3 contains all reported C<sub>q</sub>-values and the calculations used in our evaluations. Rather large differences between the participants were reported in the C<sub>q</sub>-values of the DNA samples. However, the amplification of the 3 DNA samples resulted for all participants in a regular, stepwise decrease in C<sub>q</sub>-values with increasing DNA content from low through medium to high. This means that although differences exist between the participants in the efficiency of the PCR reaction, within each laboratory the results of the analyses of the three samples with different DNA content are consistent (Supplemental Figure S1A).

The results of the analyses of the validated amoeba samples were not as good as the ones of the DNA samples, although the 2 laboratories that reported inhibition or negative results for all amoeba samples were not included in this further evaluation. As mentioned, 5 of the 14 remaining laboratories reported in total 7 false negative results for the validated amoeba samples (Supplemental Fig. S1 B-C and Supplemental Table S3-B). Furthermore, in sharp contrast to the stepwise decrease in C<sub>q</sub>-values with an increasing amount of DNA that was reported by all laboratories for the set of the 3 different DNA samples, in more than half of the laboratories, the analyses of the sets of 20, 200, and 2000 cysts or trophozoites did not result in this predictable pattern (Supplemental Fig. S1 B-C). Merely 5 laboratories reported such a consistent pattern for both the cyst and the trophozoite samples.

Details of the variation in the results of the participating laboratories were further investigated. The entire analytical procedure for amoeba samples consists of several steps: a pretreatment if applied, the DNA isolation, and the rtPCR method. As a measure of the efficiency of this entire analytical procedure, the average of the reported C<sub>q</sub>-values of the 3 cyst samples plus the 3 trophozoite samples was calculated for each participant. False negative results were assigned a C<sub>q</sub>-value of 39.5, as this was the highest C<sub>q</sub>-value reported by any participant for these amoeba samples. After this calculation, the participants were sorted in ascending order (1→14), based on this combined performance in the 6 samples containing amoebae (Fig. 3A and Supplemental Table S3-C). The average

Cq-values of the sets of DNA, cyst, and trophozoite samples are shown in Figure 3 in panels B, C, and D, respectively (Supplemental Table S3-D). The difference in the average Cq-value between the most efficient analysis (lowest Cq-value) and the least efficient one (highest Cq-value) was smaller for the set of DNA samples (6.3) than for the sets of cyst (9.3) and trophozoite (8.1) samples (Figure 3 B, C, D; Supplemental Table S3-D). In addition, the spreading around the median Cq-value was much higher in the amoeba samples than in the DNA samples. Fifty percent (8/16) of the analyses of the DNA samples were within the range of plus 1 Cq-value to minus 1 Cq-value of the median Cq-value, whereas 14% (2/14) of the cysts analyses and 21% (3/14) of the trophozoite analyses were within that range (Figure 3 and Supplemental Table S3-E).

### Relationship between methodology and reported low or high Cq-values

The participants reported the details of their procedure which enabled the calculation of the percentage of the amount of DNA isolated from the sample that was used in the PCR. As all laboratories used the entire sample (200 µL) for the extraction of DNA, this is also the percentage of the original sample used in the PCR reaction. This ranged from 1.5% to 16.7% with an average of 7.6% (median 8.2%). This percentage of the original sample that was used in the PCR reaction was plotted per participant against the average Cq-value of the 6 amoeba samples (Supplemental Fig. S2). This graph reveals that there was no correlation between the percentage of the original sample used in the PCR reaction and the performance of the analysis of these amoeba samples.

Figure 3 shows for each participant whether a pretreatment was used in the procedure for the amoeba samples and if so, which one(s). Square symbols are used for participants who reported not using any form of pre-treatment, and circles are used for the participants who used some form of pretreatment. Inspection of the results of the analyses of the cyst samples indicates that using some form of pretreatment improves the overall performance of these samples, as 6 of the 7 participants who scored a Cq-value below the median use a pretreatment procedure and had no false negative results (Fig. 3C). Consequently, 5 of the 6 laboratories that did not use a pretreatment procedure reported an average Cq-value above the median value for the set of cyst samples. Furthermore, 3 of those 5 participants with an average Cq-value above the median and not using a pretreatment reported a false negative result for one of these cyst samples (Figure 3C). For the set of trophozoite samples, the difference in performance, whether or not a pre-treatment was part of the analytical procedure, was less extreme. Three of the 7 participants who scored for the set of trophozoite samples, an average Cq-value below the median, did not use any pretreatment (Fig. 3D). Furthermore, for the set of cyst samples, all 5 participants who reported the lowest Cq-values used some form of pretreatment, whereas for the

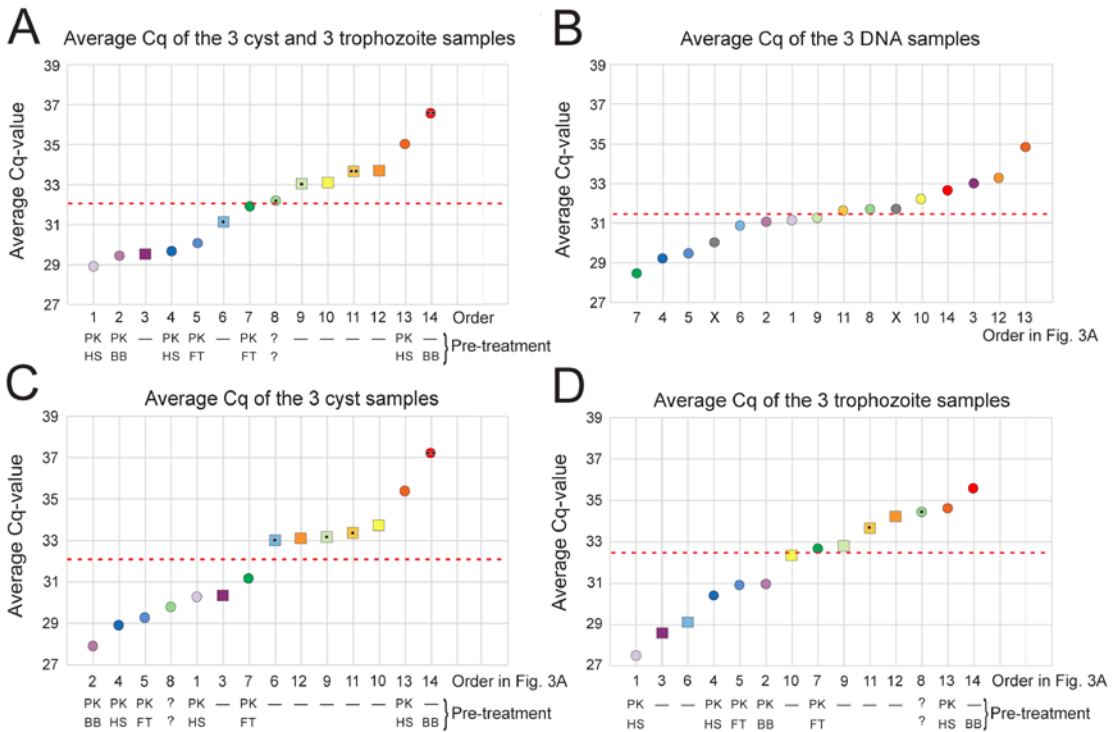


**Figure 3.** Variation in the Cq-values as reported by the participants for the various sample types.

The participants were sorted in ascending order (1→14) based on their average Cq-value of the 3 cyst plus the 3 trophozoite samples (panel A). Square symbols indicate that the participant did not use a pre-treatment in the analysis of the amoeba samples. Circles indicate that the participant used a pre-treatment in the analyses of the amoeba samples and this pre-treatment is presented underneath the graph. In the top line beneath each graph is shown whether proteinase K was used as pre-treatment (PK); in the bottom line beneath each graph is shown whether (also) another pre-treatment was used, BB = bead-beating; HS = Heat-Shock; FT = Freeze-thaw cycle; ? = unknown pre-treatment). Panels B, C and D show in the same way the average Cq-values of the DNA, the cyst and the trophozoite samples, respectively. Each black dot in the circles and squares indicates a false negative result in the samples of that graph. To facilitate a comparison of the results of the participants in the various sample types, underneath graphs B, C and D is the order number shown of that participant in the spectral sorting from violet (1) to red (14) in panel A. For example, the participant with the lowest average Cq-value for the 3 DNA samples (green circle, utmost left in panel B) was sorted as #7 in panel A. The individual indicator color of the circle or square is for each participant the same in the 4 graphs. The median Cq-value is indicated in each graph (A-D) with a dashed red line. For details and calculations see Supplemental Table S3.

trophozoite samples, 2 of the 5 laboratories that reported the lowest Cq-values did not use any pretreatment and even scored the second and third best Cq-value (Fig. 3D).

## Discussion

Early diagnosis of *Acanthamoeba* keratitis is critical, as this leads to more favorable outcomes compared with late diagnosis<sup>4</sup>. Therefore, an easily implemented, reliable, and sensitive diagnostic tool is needed, aspects in which NAAT are potentially superior to all other currently used diagnostic methods. However, the exact procedures that are used for NAAT-based detection of *Acanthamoeba* spp. differ substantially between laboratories. By participating in an EQAS, laboratories can compare results and identify methodologies that might affect their diagnostic performance.

Overall, we found a clear correlation between the number of *Acanthamoeba* cysts or trophozoites in the samples and the detection rate. In the samples containing 20 cysts or trophozoites, the detection rate was considerably lower than in the samples containing 200 cysts or trophozoites (Fig. 2). Although the exact numbers of *Acanthamoeba* cysts and/or trophozoites present in clinical samples are unknown, it is assumed that only a few amoebae are retrieved in cornea scrapings from patients, indicating the importance of successfully detecting low numbers of amoebae.

The ultimate goal for *Acanthamoeba* diagnostics is an excellent qualitative performance, that is, a high detection rate. However, the qualitative performance is related to the quantitative one, and therefore, the quantitative performance also deserves attention. In case of samples with only a few amoebae, laboratories with relatively high Cq-values for the cyst and trophozoite samples run a higher risk of false negative results than laboratories with a more efficient analysis of amoeba samples.

The relative quantitative performances in this EQAS for the sets of DNA, cyst, and trophozoite samples were determined by sorting the participants based on the average of their reported Cq-values for these sets (Fig. 3). This revealed, as could be expected, that the variation in the efficiency to detect amoeba DNA is greater for the cyst and trophozoite samples, which have to be subjected to the entire procedure of pretreatment, DNA extraction, and amplification than for the samples that contain already isolated amoeba DNA and only need DNA amplification by PCR. Comparing the efficiencies (average Cq-values) of the analyses of the sets of samples by the various participants revealed that laboratories that reported low Cq-values for cysts tended to also report low Cq-values for trophozoites (Fig. 3C,D). However, comparing per participant the results for the set of DNA samples with the results for the 2 sets of amoeba samples shows that laboratories with a high efficiency (low Cq-value) for the DNA samples not automatically also scored well (low Cq-value) in the amoeba samples (Fig. 3A,B).

One of the limitations of this EQAS is that no clinical samples were used but that laboratory-grown cultures were distributed. This could have influenced the results, as corneal scrapings contain other components than the culture medium. However, obtaining homogeneous and sufficient volumes of representative clinical specimens (cornea scrapings) is impossible for *Acanthamoeba*. In other words, any EQAS needs to make use of cultured material. Another limitation is that only one *Acanthamoeba* strain was used in this EQAS. However, as all used molecular targets were aimed at conserved regions of the *Acanthamoeba* genome, it is unlikely that using multiple strains will change the results of the participating laboratories.

Although an EQAS is a valuable tool to analyse and compare the relative performance of diagnostic laboratories, an EQAS on the NAAT diagnostics of *Acanthamoeba* is not the most ideal way to decide what the best pre-treatment procedure is for clinical samples. The number of participants and variations in the pre-treatment procedures, and especially the various possible combinations thereof, are usually limited. The conclusive identification of pre-treatment procedures that result in a reliable detection of *Acanthamoeba* in a routine diagnostic setting, awaits further systematic studies. Still, based on our findings some general remarks on the pros and cons of the various pre-treatment procedures can now be made.

The use of any pretreatment in an *Acanthamoeba* NAAT is meant to improve the lysis of the cysts and trophozoites, resulting in the release of the intracellular DNA, which can then be amplified in the subsequent PCR step. The observation that none of the 6 laboratories that use proteinase K in their pretreatment procedure, reported a false negative result for the 6 amoeba samples, indicates that the use of proteinase K is a helpful addition for a reliable procedure (Fig. 3A). It is unknown whether a pretreatment consisting only of proteinase K would lead to similar results, as all 6 of these laboratories used next to proteinase K another method in addition to proteinase K in the pretreatment; heat-shock, bead-beating, or a freeze-thaw cycle.

The use of a pretreatment procedure can pose the risk that the extra handling steps that are involved in the pretreatment procedure result in extra technical or logistic hurdles, leading to inadequate results. In that respect, the addition of proteinase K, the use of a heat-shock or a freeze-thaw cycle seem not too challenging. Bead-beating, in all its variants, a fierce physical homogenization method, seems to be a good choice for pretreatment in *Acanthamoeba* diagnostics, because the cysts are very robust. On the other hand, in contrast to the other 3 methods, any bead-beating variant necessarily involves an extra transfer of the sample and dilution of the usually small samples. The laboratory with the most efficient analysis of the cyst samples used proteinase K and bead-beating (Fig. 3C).

However, the other laboratory that used bead-beating (but without the use of proteinase K) reported 2 false negatives for the 3 samples containing cysts (Fig. 3C). Beat-beating was also used by the 2 laboratories that were not included in the quantitative evaluation, as they reported inhibition or negative results for all amoeba samples.

As mentioned earlier, this EQAS cannot be used and was not meant to identify the ultimate method for the diagnosis of *Acanthamoeba* keratitis. This study was developed to demonstrate that the development of an EQAS for the NAAT-based detection of *Acanthamoeba* cysts and trophozoites benefits clinical laboratories, as they can compare their methods and results with those of others, which can provide suggestions for improvements.

### **Acknowledgements**

The authors express their gratitude to the participants of this EQAS for their willingness to use their data for this study and to Nicolette van der Ham for expert technical assistance.

## References

- 1 Randag, A. C. *et al.* The rising incidence of *Acanthamoeba* keratitis: A 7-year nationwide survey and clinical assessment of risk factors and functional outcomes. *PLoS One* **14**, e0222092 (2019).
- 2 Carnt, N. *et al.* *Acanthamoeba* keratitis: confirmation of the UK outbreak and a prospective case-control study identifying contributing risk factors. *Br J Ophthalmol* **102**, 1621, (2018).
- 3 Roozbahani, M. *et al.* *Acanthamoeba* keratitis: are recent cases more severe? *Cornea* **37**, 1381-1387, (2018).
- 4 List, W. *et al.* Evaluation of *Acanthamoeba* keratitis cases in a tertiary medical care centre over 21 years. *Sci Rep* **11**, 1036 (2021).
- 5 Szentmáry, N. *et al.* *Acanthamoeba* keratitis - Clinical signs, differential diagnosis and treatment. *J Curr Ophthalmol* **31**, 16-23 (2019).
- 6 Maubon, D. *et al.* Development, optimization, and validation of a multiplex real-time PCR assay on the BD MAX platform for routine diagnosis of *Acanthamoeba* keratitis. *J Mol Diagn* **22**, 1400-1407 (2020).
- 7 Hoffman, J. J. *et al.* Comparison of culture, confocal microscopy and PCR in routine hospital use for microbial keratitis diagnosis. *Eye*, (2021).
- 8 WHO. *WHO manual for organizing a national external quality assessment programme for health laboratories and other testing sites*, <<https://apps.who.int/iris/handle/10665/250117>> (2016).
- 9 Cools, P. *et al.* First international external quality assessment scheme of nucleic acid amplification tests for the detection of *Schistosoma* and soil-transmitted helminths, including *Strongyloides*: A pilot study. *PLoS Negl Trop Dis* **14**, e0008231 (2020).
- 10 Selb, R. *et al.* External quality assessment (EQA) of *Neisseria gonorrhoeae* antimicrobial susceptibility testing in primary laboratories in Germany. *BMC Infect Dis* **20**, 514 (2020).
- 11 Sarink, M. J. *et al.* *Acanthamoeba castellanii* interferes with adequate chlorine disinfection of multidrug-resistant *Pseudomonas aeruginosa*. *J Hosp Infect* **106**, 490-494 (2020).
- 12 Sohn, H. J. *et al.* Efficient liquid media for encystation of pathogenic free-living amoebae. *Korean J Parasitol* **55**, 233-238 (2017).

## Supplementary material

### Questionnaire

**Question 1:** Does pre-processing of SKML *Acanthamoeba* samples in your laboratory involve a freeze-thaw cycle prior to DNA extraction?

**Question 2:** Does pre-processing of SKML *Acanthamoeba* samples in your laboratory involve a bead-beating procedure prior to DNA extraction?

**Question 3:** Does your laboratory treat the SKML *Acanthamoeba* samples before DNA extraction with an additional proteolysis treatment besides the lysis of the manufacturers protocol?

**Question 4:** Does your laboratory treat the SKML *Acanthamoeba* samples before DNA extraction with an additional proteolysis treatment besides the lysis of the manufacturers protocol? If so, is this procedure performed at a higher temperature than room temperature?

**Question 5:** Does your laboratory perform any other pre-processing steps prior to DNA extraction from *Acanthamoeba* samples?

**Question 6:** Which equipment/kit used for DNA isolation? In case the DNA isolation is not performed according to the guidelines of the manufacturer, please describe the changes to the protocol.

**Question 7:** What is the volume of the *Acanthamoeba* sample that is used in your laboratory for DNA-extraction?

**Question 8:** What is the elution volume of extracted DNA from *Acanthamoeba* samples in your laboratory?

**Question 9:** What is the volume of extracted DNA that is used in the subsequent PCR reaction in your laboratory?

**Question 10:** Which Nucleic acid amplification test (NAAT) method is used?

**Question 11:** Which equipment is used for DNA amplification?

**Question 12:** From which supplier is the PCR mastermix for DNA amplification obtained?

**Question 13:** Which method is used to detect DNA amplification?

**Question 14:** Does your DNA amplification method include an internal inhibition control to check proper amplification of DNA?

**Question 15:** Does your protocol for DNA amplification methodology include a positive control for each target to check proper amplification of the target?

**Question 16:** Does your DNA amplification method include calibration series of a positive control to report positive results in a quantitative manner?

**Question 17:** Which temperature profile is used for the NAAT method is used?

**Question 18:** Which DNA target is used for DNA amplification of *Acanthamoeba*?

**Question 19:** Which primers and probes are used for DNA amplification of *Acanthamoeba*?

**Question 20:** Is the target designed to also detect presence of other pathogenic free-living amoeba such as *B. mandrillaris* and/or *N. fowleri*?

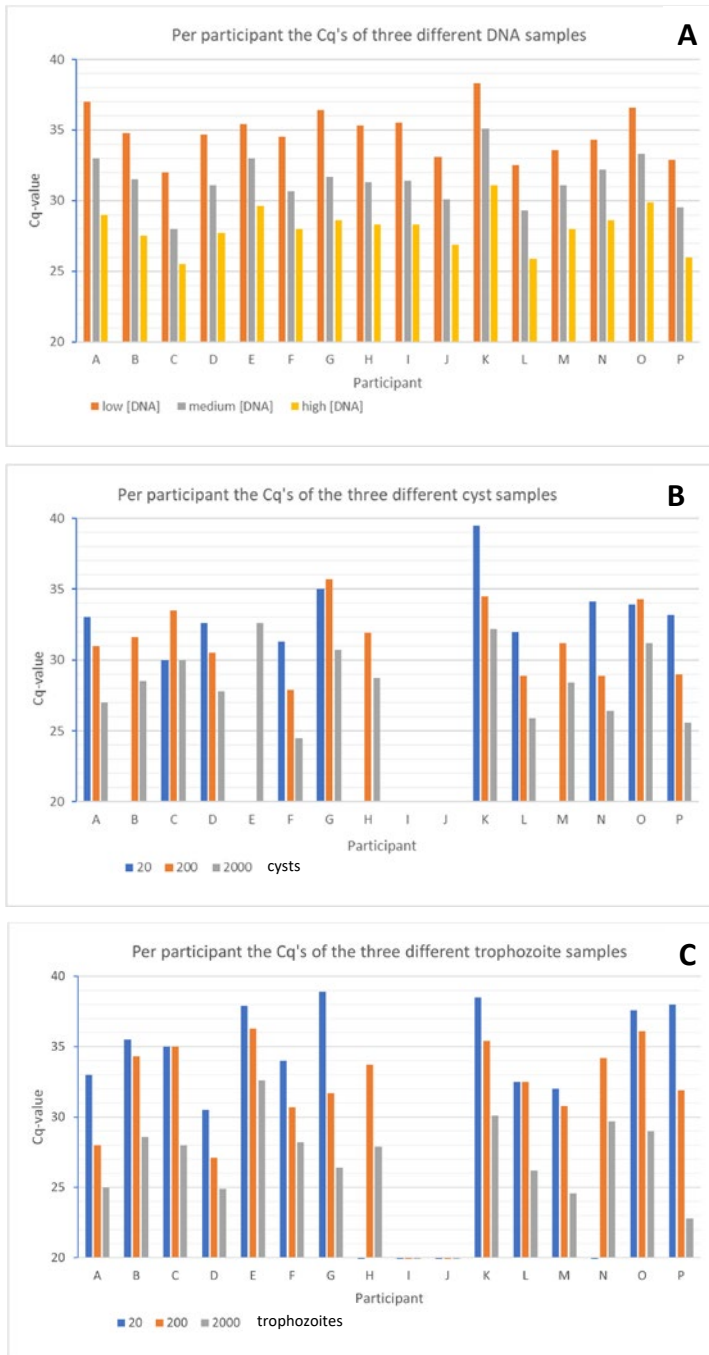


**Figure S1.** The Cq-values reported by the individual participants for the three sets, each with three different samples of DNA (panel A), cysts (panel B) and trophozoites (panel C).

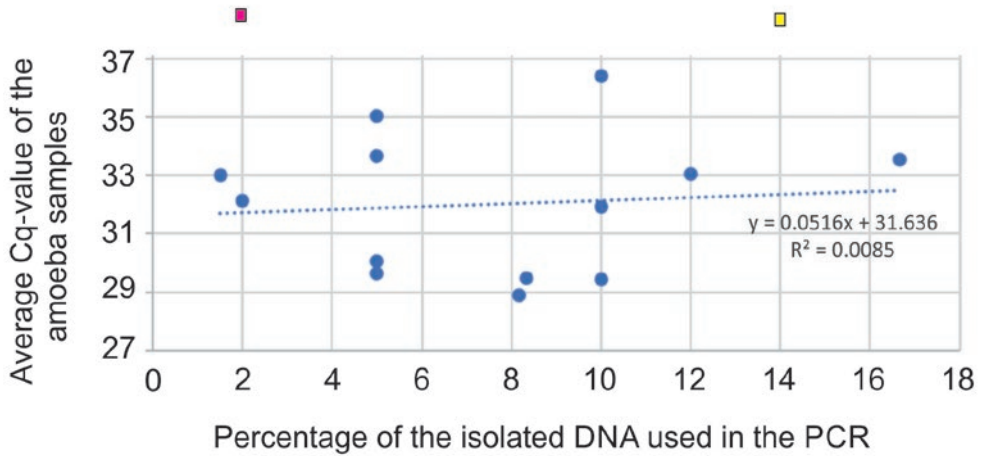


**Figure S2.** The quantitative efficiency of the measurements of the *Acanthamoeba* containing samples in relation to the percentage of the isolated DNA that was used in the PCR reaction, which is also the percentage of the original amoeba samples as all participants used the entire sample for the DNA isolation.

This percentage is plotted against the average of the Cq-values of the 3 trophozoite and 3 cyst samples, as reported by the participants (Figure 3A). Two participants could not be included in this graph as they could not report the Cq-values of the amoeba samples. One of those, using 2% of the isolated DNA, reported negative results for all amoeba samples and is represented in this figure with a magenta square above the graph. The other, using 14% of the isolated DNA, reported inhibition for all amoeba samples and is here represented with a yellow square. For details and calculations see Supplementary Table S3. One participant did not report DNA input volume and as such was excluded.

**Table S1.** Uniformity of the samples was verified by an expert laboratory by a five-fold determination of the Cq-value of the amoeba samples

Sample type	20 cysts	200 cysts	2000 cysts	20 trophozoites	200 trophozoites	2000 trophozoites
Replicate 1	32.2	29.0	26.4	32.4	29.7	25.6
Replicate 2	28.2	27.8	25.0	32.3	29.4	26.7
Replicate 3	28.8	28.8	24.9	32.5	29.1	24.1
Replicate 4	30.6	28.3	25.1	34.0	29.1	26.5
Replicate 5	30.3	28.8	24.6	33.5	29.1	25.4
Average	30.0	28.5	25.2	32.9	29.3	25.7
Standard deviation	1.4	0.4	0.6	0.7	0.2	0.9

**Table S2.** The stability of the samples was examined by two expert laboratories by comparison of the Cq-value at the time of distribution (Cq start) with the Cq-value 4 months later (Cq 4 mo)

Sample	Expert lab 1			Expert lab 2			Average $\Delta^c$
	Cq start	Cq 4 mo	$\Delta^a$	Cq start	Cq 4 mo	$\Delta^a$	of labs 1 and 2
20 cysts	32.6	32.0	0.6	31.3	31.1	0.2	0.40
200 cysts	30.5	30.0	0.5	27.9	28.8	-0.9	-0.20
2000 cysts	27.8	27.4	0.4	24.5	27.2	-2.7	-1.15
20 trophozoites	30.5	30.0	0.5	34.0	33.5	0.5	0.50
200 trophozoites	27.1	26.7	0.4	30.7	30.6	0.1	0.25
2000 trophozoites	24.9	24.4	0.5	28.2	25.8	2.4	1.45
Low [DNA]	34.7	33.4	1.3	34.5	34.7	-0.2	0.55
Medium [DNA]	31.1	30.2	0.9	30.7	31.7	-1.0	-0.05
High [DNA]	27.7	27.5	0.2	28.0	28.2	-0.2	0
							0.19
		Average $\Delta^b$	0.59		Average $\Delta^b$	-0.20	

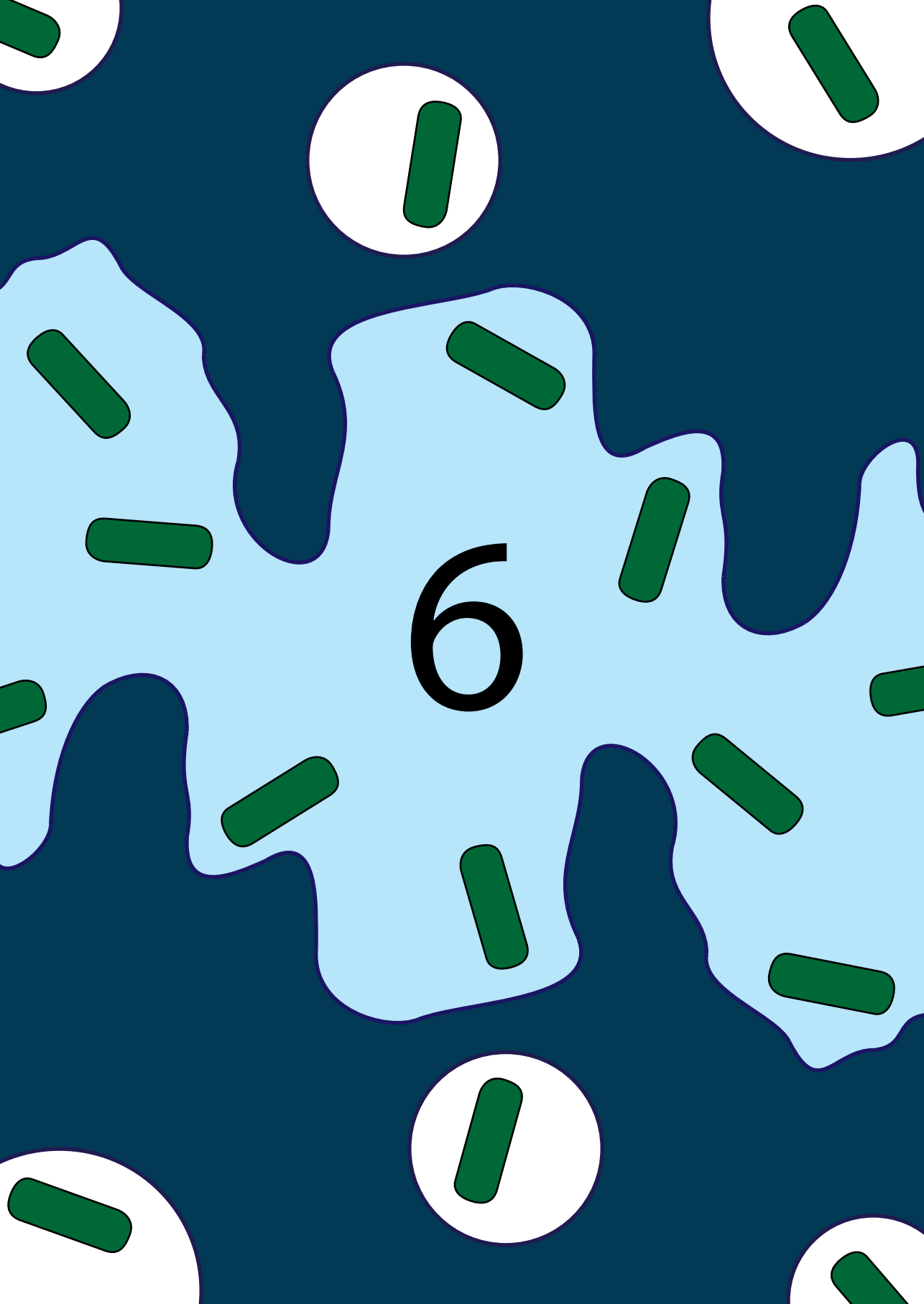
<sup>a</sup> the difference between the Cq-value at the time of distribution and 4 months later ( $\Delta = \text{Cq start} - \text{Cq after 4 months}$ )

<sup>b</sup> the average of the averages per laboratory

<sup>c</sup> the average difference of the two laboratories per sample

**Supplementary Table S3** was omitted from this thesis for practical reasons due to the size of the table. This table can be accessed online at <https://links.lww.com/ICO/B552>





6

# CHAPTER 6

---

*Vermamoeba vermiformis* resides in water-based heater-cooler units and can enhance *Mycobacterium chimaera* survival after chlorine exposure

Maarten J. Sarink<sup>1</sup>, Wiggert A. van Cappellen<sup>2</sup>, Aloysius G.M. Tielens<sup>1</sup>, Anthony van Dijk<sup>3</sup>, Ad J.J.C. Bogers<sup>3</sup>, Jurriaan E.M. de Steenwinkel<sup>1</sup>, Margreet C. Vos<sup>1</sup>, Jülüette A. Severin<sup>1</sup>, Jaap J. van Hellemond<sup>1</sup>

<sup>1</sup> Department of Medical Microbiology and Infectious Diseases, Erasmus MC University Medical Center Rotterdam, The Netherlands

<sup>2</sup> Erasmus Optical Imaging Center and Department of Pathology, Erasmus MC University Medical Center Rotterdam, The Netherlands

<sup>3</sup> Department of Cardiothoracic Surgery, Erasmus MC University Medical Center Rotterdam, The Netherlands

## Summary

### Background

*Mycobacterium chimaera* colonizes water-based heater-cooler units (HCUs), from which it can spread to patients during surgery. *Vermamoeba vermiformis* is a free-living waterborne amoeba, which was consistently present within HCUs.

### Aim

To determine whether these amoebae can be involved in the persistent presence of *M. chimaera*.

### Methods

An in-vitro disinfection model.

### Findings

Increased survival of *M. chimaera* was observed after chlorine exposure in the presence of *V. vermiformis*. Confocal microscopy demonstrated the intracellular presence of *M. chimaera* in *V. vermiformis*.

### Conclusion

In this way, *V. vermiformis* can contribute to the persistent presence of *M. chimaera* in HCUs. Cleaning and disinfection protocols should take this phenomenon into account.

## Introduction

*Mycobacterium chimaera* is a non-tuberculous mycobacterium (NTM) which is ubiquitously found in the aqueous environment <sup>1</sup>. It was first identified in 2004 but was rediscovered as a pathogen in 2013 when Achermann *et al.* described the first cases of *M. chimaera* infections following cardiothoracic surgery <sup>2</sup>. Since then, many more cases have been identified worldwide. A link was found between disseminated disease caused by *M. chimaera* and the use of water-based heater-cooler units (HCUs) during surgery <sup>1,3</sup>. These HCUs, also known as heater-cooler devices (HCDs) consist of a closed circuit with water tanks and use water as a heat-transfer medium to regulate the body temperature of the patient. In these HCUs, *M. chimaera* and other NTM can be present <sup>4</sup>. Due to the presence of fans and the bioaerosol-forming capacity of *M. chimaera*, transmission of this mycobacterium from the HCU to the surgical field can occur, with subsequent infection of the patient. In order to minimize the risk of infection, HCUs have been modified to reduce aerosolization and compliance with the manufacturer's instructions for cleaning, disinfection and maintenance is advised by regulatory authorities. Several disinfectants are recommended by the manufacturers, including peracetic acid and chlorine (in fact hypochlorite). However, NTM colonization of the HCUs can persist even when these measures are strictly followed, which is thought to be due to the formation of biofilms <sup>4,5</sup>. To prevent infections of the patients, the HCUs used in cardiothoracic surgery in our hospital were placed outside the operating theatre, in a dedicated space, although this solution requires extra tubing and renovation of the operating theatre.

*Vermamoeba vermiformis* is a water-borne free-living amoeba, which is ubiquitously present in the environment. Worldwide, *V. vermiformis* has been isolated from natural freshwater reservoirs, tap water, swimming pools and hospital environments. The amoeba itself is of very low pathogenicity, although many interactions have been described between *V. vermiformis* and a wide range of pathogenic bacteria <sup>6</sup>. It is known that *V. vermiformis* can act as a host or transport vehicle for *Legionella pneumophila*, *Pseudomonas aeruginosa* and several NTMs. Furthermore, it has been shown that *V. vermiformis* cysts are resistant to chlorine disinfection <sup>7</sup>. We hypothesized that when *V. vermiformis* colonizes HCUs, *M. chimaera* could be present inside these amoebae, thereby resisting disinfectants.

## Materials & Methods

### Setting and sampling

During this study, our hospital used four 3T HCU systems (LivaNova, London, UK). The water within the compartments was replaced with filter-sterilized water each day after use.

In addition, the units were cleaned once every two weeks with Puristeril340. Sampling of HCU-water occurred at regular intervals (see Supplementary Figure S1). Before sampling, the tubing connecting the HCU to the cardiopulmonary equipment was removed and the exit point was cleaned with ethanol 70% after which the contents of each compartment were collected separately in sterile containers.

## Strains and materials

The presence of *M. chimaera* in the HCU systems was determined by filtering 200 mL of HCU-water through a 0.2 µm filter. Subsequently, this filter was segregated with a gentleMACS dissociator (Milteny Biotec BV, Leiden, The Netherlands), after which the contents were added to a mycobacterial growth indicator tube (MGIT; Becton, Dickinson and Company, Franklin Lakes, NJ, USA) and incubated for six weeks at 35°C in the BD Bactec MGIT 960 automated mycobacterial detection system (Becton, Dickinson and Company, Franklin Lakes, NJ, USA). Once growth was detected, DNA was isolated from the culture by MagNa Pure 96 (Roche, Basel, Switzerland) according to the manufacturers' protocol. NTM identity was determined with the GenoType Mycobacterium CM (Hain Lifescience, Nehren, Germany) test system. If *Mycobacterium intracellulare* identity was demonstrated, high-resolution molecular identification was performed by amplification of the 16S–23S rRNA internal transcribed spacer gene by PCR, after which the sequence of the DNA amplification product was determined by Sanger sequencing (Baseclear, Leiden, The Netherlands).

*M. chimaera* stocks were prepared by addition of 200 µL from an MGIT in which growth was detected by the above-described procedure, to a flask with Middlebrook 7H9 broth medium (Difco Laboratories, Detroit, MI, USA) supplemented with 10% oleic acid-albumin-dextrose-catalase enrichment (OADC; Becton, Dickinson and Company, Franklin Lakes, NJ, USA), 0.5% glycerol (Scharlau Chemie S.A, Sentmenat, Spain) and 0.05% Tween 80 (Sigma Chemical Co., St. Louis, MO, USA). Subsequently, this flask was incubated under shaking conditions at 96 rpm at 37°C until the culture became turbid, after which frozen stocks were prepared by transfer of the flask contents into Eppendorf tubes and stored at -80°C.

The presence of free-living amoebae in the system 3T HCU was determined by filtering 500 mL HCU-water (sampled as described above) through a 0.2-µm filter, after which the filter was divided into four equal parts and placed upside down on non-nutrient (NN) agar plates seeded with *E. coli* ATCC 25922. Plates were sealed and incubated at 25°C, after which amoeba presence was checked by twice-weekly microscopic inspection. Morphologically, only one species of amoeba was identified. The amoeba strain used in the disinfection experiments was obtained by subculturing an agar block on new NN agar plates seeded with *Escherichia coli*, as attempts to culture the amoebae in axenic

conditions were unsuccessful. The identity of the free-living amoebae was determined by DNA isolation from collected material of a fully grown plate with amoebae, after which the 18S rRNA gene was amplified by PCR using the primers Ami6F1, Ami6F2 and Ami9R, as described previously<sup>8</sup>. The sequence of the amplified DNA product was determined as described above. The amount of free-living amoebae in HCU-water was determined according to Moussa *et al.*<sup>9</sup>.

### Antibiotic susceptibility testing

Broth microdilution was performed according to ISO standard 20776-1 using ciprofloxacin, doxycycline, moxifloxacin, rifampicin, ethambutol, amikacin and streptomycin, which were all obtained from Sigma (Sigma-Aldrich, Zwijndrecht, The Netherlands). For *E. coli* ATCC 25922, the microdilution plates were examined after overnight incubation at 37°C. For *M. chimaera*, the microdilution plates were examined after four days of incubation at 37°C with 5% CO<sub>2</sub>.

### Disinfection

We used the in-vitro disinfection protocol with chlorine (hypochlorous acid) as described earlier<sup>10</sup> to investigate whether, in the presence of *V. vermiformis*, *M. chimaera* is protected against disinfectant. This procedure was necessary because the Puristeril340, used for disinfection of HCUs, cannot be neutralized effectively, which is necessary to investigate for the survival of *M. chimaera*. Briefly, *V. vermiformis* trophozoites were collected by adding 1 mL of sterile filtered HCU-water to an NN agar plate seeded with *E. coli* ATCC 25922 and *V. vermiformis*, after which the plate was scraped and liquid was collected. Co-culture experiments were prepared in sterile HCU-water in 24-well plates by addition of 10<sup>7</sup> colony-forming units (cfu) of *M. chimaera* from a frozen stock with or without 10<sup>5</sup> *V. vermiformis* trophozoites in a total volume of 1 mL, corresponding to a multiplicity of infection (MOI) of 100:1. To all wells, ciprofloxacin was added to obtain a 0.5 mg/L concentration in order to kill *E. coli* ATCC 25922 without affecting the growth of *M. chimaera* (see Supplementary Table S1 for antibiotic susceptibility profiles). After four days of incubation at 25°C, the 24-well plates were placed on ice for 20 min, after which the well contents were collected by vigorous pipetting. The contents of the wells with or without *V. vermiformis* were pooled in two separate flasks and then divided over Eppendorf tubes. These tubes were centrifuged at 1000 g for 5 min, and the supernatant was discarded. The pellets were resuspended in 1 mL of 1000 ppm available chlorine by immediately and intermittently vortexing to ensure that dispersed cells were all exposed to the disinfectant. Exposure to chlorine was neutralized after 30 s, 2 min, or 5 min by addition of sodium thiosulfate (Sigma, St Louis, MO, USA) to obtain a final concentration of 4 mg/mL sodium thiosulfate. After washing with PBS, all 1-mL samples were transferred to Eppendorf tubes containing 250-280 mg of glass beads of 1 mm diameter. Subsequently, all tubes were bead-beaten at 30 shakes per second for 16

cycles of 30 s on and 30 s off to lyse *V. vermiformis* and to release intracellular *M. chimaera*. Bead-beating did not have negative effects on *M. chimaera* (results not shown). Ciprofloxacin was added to the samples to obtain a final concentration of 0.25 mg/L, after which serial dilutions of the samples were prepared in PBS with 0.25 mg/L ciprofloxacin to prevent growth of *E. coli* ATCC 25922. A total volume of 800  $\mu$ L (four times 200  $\mu$ L) of undiluted sample was plated on four separate Middlebrook 7H10 (Difco Laboratories, Detroit, MI, USA) agar plates supplemented with 10% OADC (Becton, Dickinson and Company, Sparks, MD, USA), resulting in a limit of detection of 0.1 log cfu/mL. Ten-fold serial dilutions of the same sample were also plated on Middlebrook plates. All plates were incubated for three weeks at 37°C with 5% CO<sub>2</sub>, after which cfu were counted. From each condition with growth after exposure to disinfectant, three colonies were analysed by matrix-assisted laser desorption-ionization time-of-flight mass spectrometry (Maldi Biotyper, Bruker Microflex LT, Bruker, London, UK) to confirm *M. chimaera* identity. These disinfection studies were performed in two independent experiments, each in duplicate wells.

### Confocal microscopy

*V. vermiformis* trophozoites were grown on coverslips in the presence or absence of *M. chimaera* for 4 h in a six-well plate, after which the coverslips were fixed with 4% formaldehyde for 1 h. Subsequently, the coverslips were washed twice with sterile filtered HCU-water before permeabilization for 20 min in 0.1% v/v Triton X-100, which was afterwards washed away twice. Samples were then stained using the BD BBL TB Auramine-Rhodamine T staining (Becton, Dickinson and Company, MD, USA) and subsequent propidium iodide staining (0.33  $\mu$ g/mL in saline-sodium citrate buffer for 5 min) with washing in between with sterile HCU-water. Samples were examined by a Leica SP5 confocal laser scanning microscope (Leica, Mannheim, Germany). Auramine dye was measured with the 458 nm laser line of an argon laser emission BP 470-530. Propidium iodide dye was measured with a 561 nm laser line and a BP 570-640 emission filter. Images were made with an HXP PL APO 63.0 oil immersion lens with a 1.4 numerical aperture. Three-dimensional renderings were made with the Amira software package (Thermo Fisher, Waltham, MA, USA) after deconvolution with the Huygens software (SVI, Hilversum, The Netherlands).

## Results and discussion

In our hospital, the presence of amoebae and *M. chimaera* in the system in the four 3T HCUs was determined at regular intervals over the course of 2 years. The presence of *M. chimaera* over time in the HCUs is shown in Supplementary Figure S1. Amoebae were detected at all nine time points in 18/18 tested samples (100%) and *M. chimaera* was present in 11/102 samples (11%) collected at 13 time points over a period of two years.

These results show that despite regular cleaning and disinfection of the HCUs with Puristeril340 according to the manufacturer's instructions, not only *M. chimaera* and other NTM persistently colonize the HCUs but amoebae do so as well. The concentration of amoebae in HCU-water was determined on two separate occasions from the patient and cardioplegic compartments of an HCU and ranged from 275 to 1204 amoebae per litre. Samples of the content of the HCUs were collected without disturbing any biofilms that might have been present, and therefore, the presence of only planktonic micro-organisms was determined. As most amoebae and *M. chimaera* live in biofilms, the actual presence of amoebae and *M. chimaera* in HCUs is probably substantially higher.

Species determination of the isolated amoebae from the HCUs demonstrated their identity as *V. vermiformis*. Clearly, *M. chimaera* as well as *V. vermiformis* are present in the HCUs. Therefore, an *in-vitro* disinfection model was used to compare the efficacy of chlorine disinfection of *M. chimaera* in the presence and absence of *V. vermiformis*. After four days of incubation with *M. chimaera*, all *V. vermiformis* were encysted (Supplementary Figure S2A and S2B). At this time point, *M. chimaera* survival after chlorine exposure was determined (Figure 1). The survival after chlorine exposure of these encysted *M. chimaera* was significantly higher than the survival in the absence of *V. vermiformis* (Figure 1A). After incubation without *V. vermiformis*, virtually no *M. chimaera* survived 2-min or 5-min exposure to 1000 ppm available chlorine. In the presence of *V. vermiformis*, however, approximately 2 log cfu/mL and 1 log cfu/mL *M. chimaera* were still viable after 2 min and 5 min of chlorine exposure, respectively. This observed difference in sensitivity to chlorine might be explained by two factors. First, it could be due to the baseline difference in the presence of *M. chimaera* after four days of incubation with or without *V. vermiformis*, as *M. chimaera* counts were approximately 2 log cfu/mL in incubations without *V. vermiformis*, and approximately 4 log cfu/mL in the presence of *V. vermiformis*. This indicates that *M. chimaera* survives in nutrient-poor HCU-water better in the presence of *V. vermiformis* than in its absence, thereby resulting in a denser population that is exposed to the effects of chlorine. Second, *V. vermiformis* could also directly protect *M. chimaera* from the effects of chlorine, as it is known that a range of bacterial species can survive within cysts of *V. vermiformis*, among which are mycobacteria<sup>11</sup>. Therefore, we used confocal microscopy to examine the interaction between the *M. chimaera* and *V. vermiformis* strains isolated from the HCU, which revealed *M. chimaera* to be present indeed inside *V. vermiformis* (Figure 1B-E). Surface rendering images can be viewed in Supplementary Videos S1 and S2. Whether *M. chimaera* was located within a vacuole or within the cytoplasm of *V. vermiformis* cannot be determined because this technique does not differentiate between these compartments. However, irrespective of whether *M. chimaera* is present in the vacuole or in the cytoplasm of *V. vermiformis*, *M. chimaera* will be shielded from disinfectants in both situations.

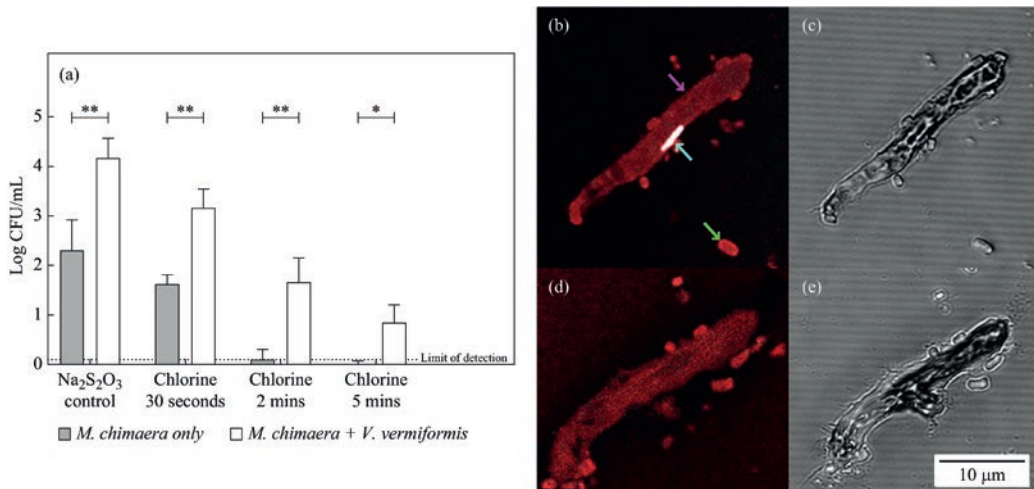


**Figure 1.** Disinfection and interaction between *V. vermiformis* and *M. chimaera*, both isolated from heater-cooler units.

(A) Survival of *M. chimaera* following chlorine disinfection, after 4 days of incubation in the presence or absence of *V. vermiformis*. Significant differences: \*\*:  $P < 0.01$ ; \*:  $P < 0.05$ . The limit of detection is indicated with the dotted line. Bright-field (C and E) and fluorescence (B and D) confocal microscopy images of *V. vermiformis* incubated for four hours with *M. chimaera* (B and C) and without *M. chimaera* (D and E). Samples were permeabilised and stained with propidium iodide, which illuminates *V. vermiformis*, *E. coli* and *M. chimaera* (red), and auramine, which only illuminates *M. chimaera* (white).

The formation of a biofilm is known to interfere with disinfection, also in the case of *M. chimaera* in HCU<sup>s</sup> <sup>4,5,12</sup>. *V. vermiformis* is also an inhabitant of biofilms <sup>13</sup>, and as such the amoebae could add to the problem of disinfection. Figure S2 shows bright-field images of the situation in our *in-vitro* co-culture experiments, which might indicate the formation of biofilm, although research into specific evidence of biofilm formation was not conducted. In our disinfection model, the biofilm that might have been formed during the four days of incubation was deliberately disrupted during sampling to release amoebae and mycobacteria trapped in biofilms and to expose them to the chlorine. Consequently, our experiments demonstrated enhanced survival of *M. chimaera* by *V. vermiformis* after chlorine disinfection in the absence of biofilms.

*M. chimaera* persistence in HCUs, despite regular cleaning and disinfection, remains a problem, and therefore, it is now advised to place water-based HCUs outside the operating room. Our study shows that the presence of amoebae, such as *V. vermiformis*, can contribute to the problem of this persistent presence of *M. chimaera* in HCUs. This could either be through increased survival of *M. chimaera* in HCU water which contains *V. vermiformis* (resulting in higher baseline concentrations and subsequent increased survival after disinfectant exposure), or through protection of *M. chimaera* by *V. vermiformis* cysts, as demonstrated by confocal microscopy. Cleaning and disinfection protocols should take this phenomenon of increased survival of *M. chimaera* caused by the presence of amoebae into account.

### **Acknowledgements**

The authors would like to thank Wim van Vianen and Diana van Netten for technical assistance.

## References

- 1 Riccardi, N. *et al.* *Mycobacterium chimaera* infections: An update. *J Infect Chemother* **26**, 199-205 (2020).
- 2 Achermann, Y. *et al.* Prosthetic valve endocarditis and bloodstream infection due to *Mycobacterium chimaera*. *J Clin Microbiol* **51**, 1769-1773 (2013).
- 3 van Ingen, J. *et al.* Global outbreak of severe *Mycobacterium chimaera* disease after cardiac surgery: a molecular epidemiological study. *Lancet Infect Dis* **17**, 1033-1041 (2017).
- 4 Ditommaso, S., Giacomuzzi, M., Memoli, G. & Zotti, C. M. Failure to eradicate non-tuberculous mycobacteria upon disinfection of heater-cooler units: results of a microbiological investigation in northwestern Italy. *J Hosp Infect* **106**, 585-593 (2020).
- 5 Siddam, A. D. *et al.* Characterization of Biofilm Formation by *Mycobacterium chimaera* on Medical Device Materials. *Front Microbiol* **11**, 586657 (2020).
- 6 Delafont, V., Rodier, M.-H., Maisonneuve, E. & Cateau, E. *Vermamoeba vermiformis*: a Free-Living Amoeba of Interest. *Microbial Ecology* **76**, 991-1001 (2018).
- 7 Fouque, E., Héchard, Y., Hartemann, P., Humeau, P. & Trouilhé, M. C. Sensitivity of *Vermamoeba (Hartmannella) vermiformis* cysts to conventional disinfectants and protease. *J Water Health* **13**, 302-310 (2015).
- 8 Thomas, V., Herrera-Rimann, K., Blanc, D. S. & Greub, G. Biodiversity of amoebae and amoeba-resisting bacteria in a hospital water network. *Appl Environ Microbiol* **72**, 2428-2438 (2006).
- 9 Moussa, M., Marcelino, I., Richard, V., Guerlotté, J. & Talarmin, A. An Optimized Most Probable Number (MPN) Method to Assess the Number of Thermophilic Free-Living Amoebae (FLA) in Water Samples. *Pathogens* **9** (2020).
- 10 Sarink, M. J. *et al.* *Acanthamoeba castellanii* interferes with adequate chlorine disinfection of multidrug-resistant *Pseudomonas aeruginosa*. *J Hosp Infect* **106**, 490-494 (2020).
- 11 Sanchez-Hidalgo, A., Obregón-Henao, A., Wheat, W. H., Jackson, M. & Gonzalez-Juarrero, M. *Mycobacterium bovis* hosted by free-living-amoebae permits their long-term persistence survival outside of host mammalian cells and remain capable of transmitting disease to mice. *Environ Microbiol* **19**, 4010-4021 (2017).
- 12 Falkinham, J. O., 3rd. Disinfection and cleaning of heater-cooler units: suspension- and biofilm-killing. *J Hosp Infect* **105**, 552-557 (2020).
- 13 Kuiper, M. W., Wullings, B. A., Akkermans, A. D., Beumer, R. R. & van der Kooij, D. Intracellular proliferation of *Legionella pneumophila* in *Hartmannella vermiformis* in aquatic biofilms grown on plasticized polyvinyl chloride. *Appl Environ Microbiol* **70**, 6826-6833 (2004).

## Supplementary material

**Table S1.** Broth microdilution susceptibility of the environmental *M. chimaera* isolate and *E. coli* ATCC strain 25922 to various antibiotics.

Antibiotic	MIC (mg/L)	
	<i>M. chimaera</i>	<i>E. coli</i> ATCC 25922
Ciprofloxacin	2	≤0.25
Doxycyclin	8	2
Moxifloxacin	0.5	≤0.25
Rifampicin	≤0.25	4
Ethambutol	16	≥128
Amikacin	16	4
Streptomycin	8	16

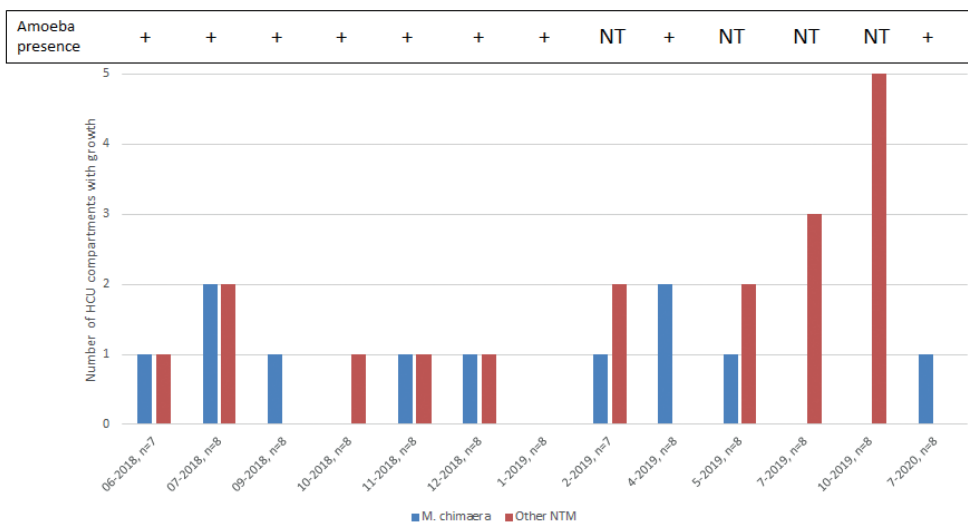


**Figure S1.** Presence of amoebae, *M. chimaera* and other nontuberculous mycobacteria (NTM), in heater-cooler units (HCUs).

NTM measurements included sampling of both compartments of the four HCUs, totalling 8 samples. Abbreviations; + indicates the presence of amoebae in both compartments and NT indicates not tested; n indicates the number of compartments tested for the presence of NTMs; For sampling and detection procedures, see methods section.

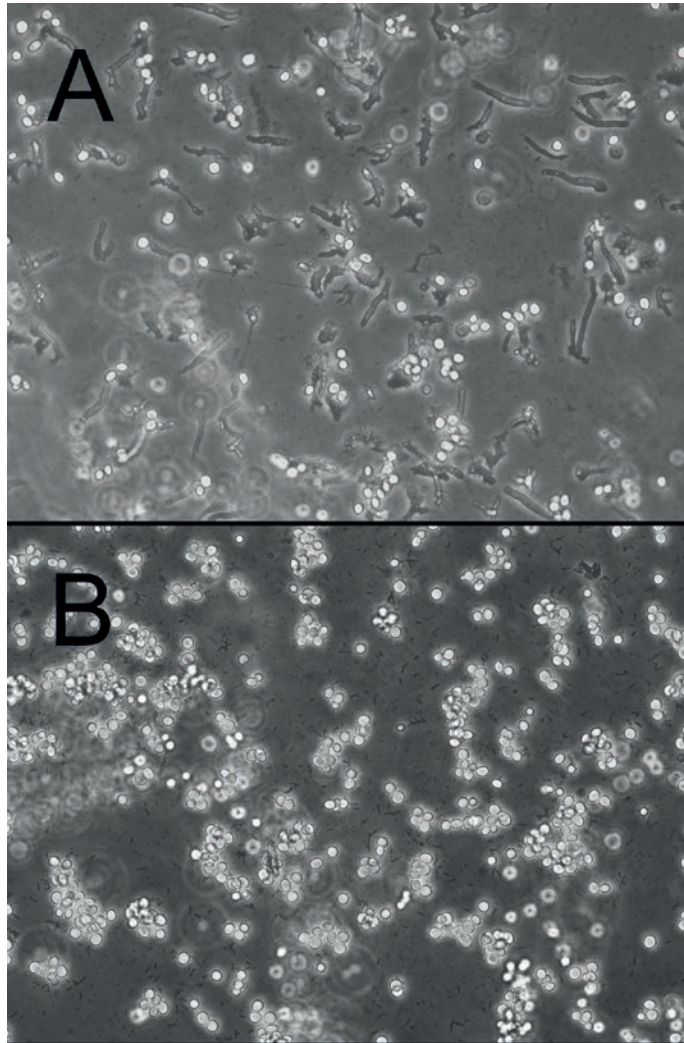
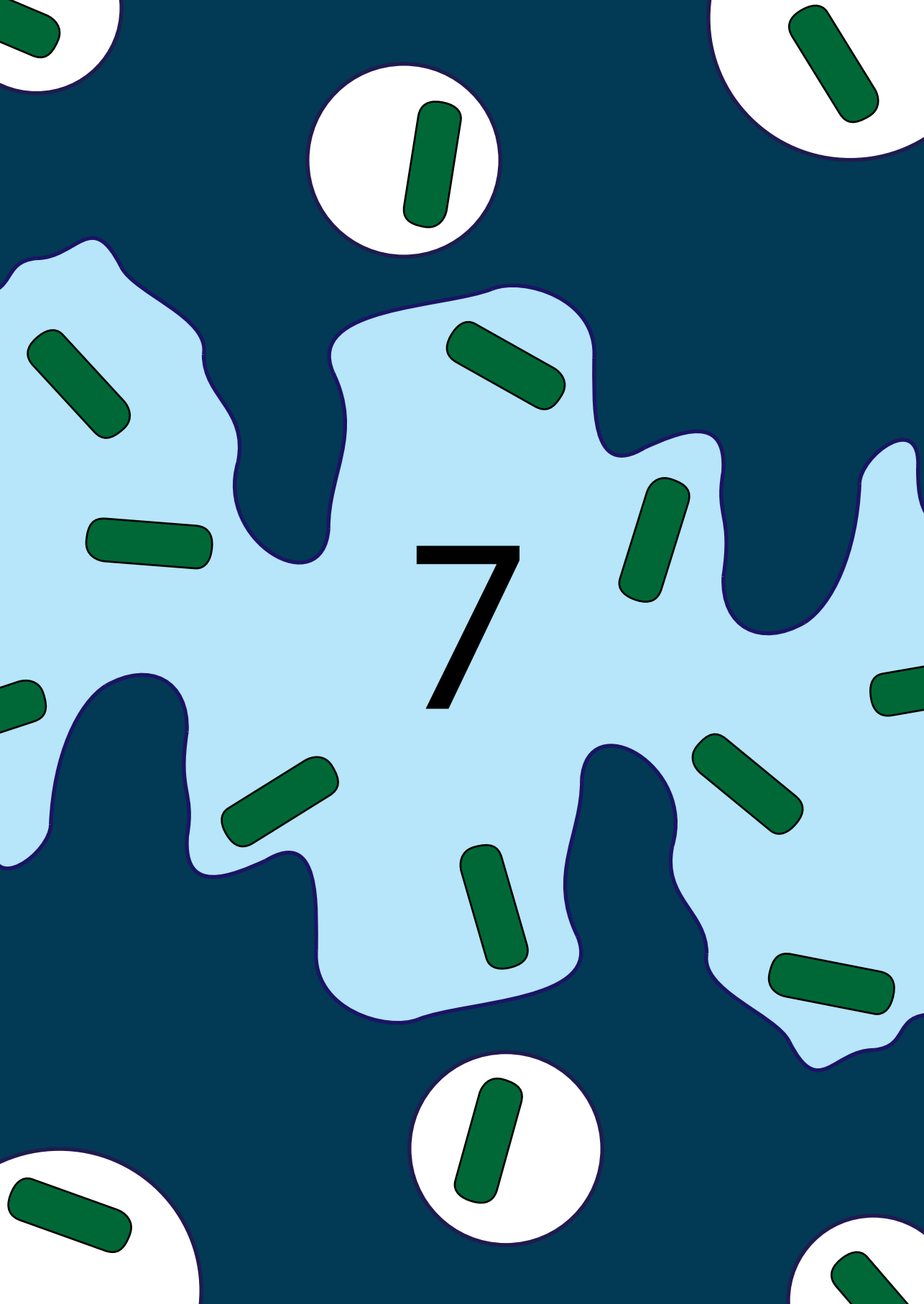


**Figure S2.** Bright-field images of a co-culture with *V. vermiformis* and *M. chimaera*, directly after inoculation (A) and after 4 days of co-incubation (B).

**Supplementary videos S1** and **S2** can be accessed online at <https://doi.org/10.1016/j.jhin.2022.12.011>





7

# CHAPTER 7

---

*Acanthamoeba castellanii* interferes with adequate chlorine disinfection of multidrug-resistant *Pseudomonas aeruginosa*

Maarten J. Sarink<sup>1</sup>, Jannette Pirzadian<sup>1</sup>, Wiggert A. van Cappellen<sup>2</sup>,  
Aloysius G.M. Tielens<sup>1</sup>, Annelies Verbon<sup>1</sup>, Juliëtte Severin<sup>1</sup>, Jaap J. van Hellemond<sup>1</sup>

<sup>1</sup> Department of Medical Microbiology and Infectious Diseases, Erasmus MC University Medical Center, Rotterdam, The Netherlands

<sup>2</sup> Erasmus Optical Imaging Center and Department of Pathology, Erasmus MC University Medical Center, Rotterdam, The Netherlands

## Summary

Verona-Integron-encoded-Metallo- $\beta$ -lactamase-positive *Pseudomonas aeruginosa* (VIM-PA) is a cause of hard-to-treat nosocomial infections, and can colonize hospital water networks alongside *Acanthamoeba*. We developed an *in-vitro* disinfection model to examine whether *Acanthamoeba castellanii* can harbour VIM-PA intracellularly, allowing VIM-PA to evade being killed by currently used hospital disinfectants. We observed that *A. castellanii* presence resulted in significantly increased survival of VIM-PA after exposure to chlorine for 30 s or for 2 min. This undesirable effect was not observed after disinfection by 70% alcohol or 24% acetic acid. Confocal microscopy confirmed the presence of VIM-PA within *A. castellanii* pseudocysts. Our data indicate that *A. castellanii* contributes to persistent VIM-PA colonization of water systems after chlorine treatment.

## Introduction

Multidrug-resistant strains of *Pseudomonas aeruginosa* (PA) are an important cause of nosocomial infections and are involved in hospital outbreaks worldwide <sup>1</sup>. PA infections are associated with increased morbidity and mortality in hospitalized patients <sup>1</sup>. Furthermore, if these bacteria harbour a Verona Integron-encoded Metallo- $\beta$ -lactamase (VIM) gene, treatment options are even more limited, as VIM-producing PA can hydrolyse all classes of  $\beta$ -lactams except monobactam antibiotics, resulting in resistance against the carbapenems, an important class of antibiotics for treatment of PA infections.

PA can be found in moist environments, such as water networks, which are well-known environmental sources of PA outbreaks in hospitals <sup>2</sup>. Transmission within hospitals occurs through unidentified and presumably persistent sources that are most likely in the water distribution systems or wastewater drains <sup>3,4</sup>. Despite extensive infection prevention measures, PA is in many settings still able to spread <sup>3,5</sup>. Like PA, *Acanthamoeba castellanii* is also present in hospital water networks. These protozoa are known to co-occur with PA at the same locations, and PA were shown to be present intracellularly in *Acanthamoeba* spp. isolated from a hospital water system <sup>6,7</sup>. This phenomenon was confirmed *in vitro*, as phagocytosed PA were shown to remain viable during encystation of *Acanthamoeba* trophozoites <sup>8</sup>. *Acanthamoeba* cysts are known to be resistant to several disinfection treatments used in healthcare settings <sup>9</sup>. Therefore, we hypothesized that PA could survive in hospital environments and resist disinfection by being concealed within *A. castellanii*.

## Methods

### Strains and materials

*Acanthamoeba castellanii* ATCC strain 30010 ('Neff') was grown in cell culture flasks at 25°C in PYG medium, which contained proteose peptone, yeast extract, glucose, salt additives (ATCC medium 712), 40  $\mu$ g/mL gentamicin, 100 units/mL penicillin, and 100  $\mu$ g/mL streptomycin. All experiments were started with trophozoites growing in logarithmic phase. The PA strain used in all experiments (VIM-PA-R15111) harboured a VIM gene, was isolated from a sink in our hospital, and had caused an outbreak that was recently described <sup>3</sup>. VIM-PA was grown to stationary phase in tryptic soy broth, after which glycerol stocks were prepared by addition of glycerol to a final concentration of 10% (v/v). Stocks were stored at -20°C until use and bacterial density was determined by plating on blood agar plates (BD Diagnostics, Breda, The Netherlands).

The 1000 ppm chlorine disinfection solution was prepared directly before each experiment by addition of 1.5 L lukewarm tap water to an Ecolab (St Paul, MN, USA) Medicarline tablet, resulting in sodium dichloroisocyanurate as a source of free active chlorine. Ethanol (70%, v/v) was purchased from Fresenius Kabi (Bad Homburg, Germany) and 24% (v/v) acetic acid was prepared by dilution of 96% acetic acid (Merck, Kenilworth, NJ, USA) in distilled water.

### ***In-vitro* disinfection**

*A. castellanii* trophozoites were collected by placing a cell culture flask on ice for 20 min and repeatedly tapping to detach trophozoites. The contents of the cell culture flask were transferred to a 50 mL tube and centrifuged at 1000 g, after which the pellets were washed once with phosphate-buffered saline (PBS). The VIM-PA glycerol stocks were thawed and diluted in PBS. Co-culture experiments were prepared in 24-well plates by addition of  $10^6$  colony-forming units VIM-PA to 1 mL PBS with or without 25,000 *A. castellanii* trophozoites, corresponding to a multiplicity of infection of 1:40. After incubation at 25 °C for 14 days, the 24-well plate was placed on ice for 20 min, after which the well contents were collected into separate tubes by vigorous pipetting. The collected material was centrifuged at 1000 g, after which the supernatant was discarded, and the pellet was treated with 1 mL of various disinfectant solutions. Samples were then immediately and intermittently vortexed to ensure that dispersed cells were exposed to the disinfectant. Exposure to chlorine was neutralized after 30 s, after 2 min, or after 5 min by adding sodium thiosulfate (Sigma, St Louis, MO, USA) to obtain a final concentration of 4 mg/mL, which converts chlorine to chloride, thereby ending chlorine treatment. The effect of ethanol was abolished after 30 s or after 2 min by dilution with 9 mL PBS. After centrifugation, the chlorine- and ethanol-neutralized samples were washed three times with 1 mL PBS. Acetic acid was removed after 30 minutes by washing 3 times with 1 mL PBS. Exposure times were chosen based on infection prevention guidelines on disinfection, manufacturers' instructions, or literature <sup>10,11</sup>. After washing, all samples (with and without *A. castellanii*) were transferred to Eppendorf tubes with 250-280 mg of glass beads with 1 mm diameter and bead-beaten at 30 shakes per second for 16 cycles of 30 s on and 30 s off to lyse *A. castellanii* trophozoites, pseudocysts and cysts, and release intracellular VIM-PA. A total volume of 800  $\mu$ L was plated on four separate blood agar plates, resulting in a limit of detection of 0.1 log<sub>10</sub> cfu/mL. Serial dilutions of the same sample were also plated on blood agar plates. Blood agar plates were incubated overnight at 37°C, after which the numbers of cfu were counted. From each plate with growth after exposure to disinfectants, one colony was analysed by matrix-assisted laser desorption–ionization time-of-flight mass spectrometry (Maldi Biotyper, Bruker Microflex LT, Bruker, London, UK) to confirm PA identity. Experiments were performed in at least two independent experiments, each in duplicate wells.

## Confocal microscopy

Similar to the *in-vitro* disinfection, *A. castellanii* trophozoites were grown in the presence or absence of VIM-PA for 14 days. The well contents were then sampled and centrifuged at 1000 g, after which 800  $\mu$ L of the supernatant was discarded. *P. aeruginosa* antibody 95/159 Alexa Fluor 647 (4  $\mu$ L) (Novus Biologicals, Littleton, CO, USA) was added to the resuspended cell pellet and incubated at room temperature for 30 min, after which the samples were washed three times with 1 mL PBS and fixed in 0.4% formaldehyde (Fresenius Kabi). Samples were examined by a Leica SP5 confocal laser scanning microscope (Leica, Mannheim, Germany). Autofluorescence was measured with the 488nm laser line of an argon laser emission BP500-550. Alexa 647 dye was measured with 633nm laser line and a BP650-720 emission filter. Images were made with an HXP PL APO 63.0 oil immersion lens with a 1.4 numerical aperture. Three-dimensional renderings were made with the Amira software package (Thermo Fisher, Waltham, MA, USA) after deconvolution with the Huygens software (SVI, Hilversum, The Netherlands).

## Statistics

GraphPad Prism 8 (GraphPad Software, San Diego, USA) was used to analyse the results. A one-tailed unequal variances t-test was used to determine statistical significant difference.

## Results and discussion

This study developed an *in-vitro* disinfection model to determine the efficacy of VIM-PA disinfection in the presence or absence of *A. castellanii*. In our model, VIM-PA was incubated in PBS with or without *A. castellanii* trophozoites for 14 days preceding *in-vitro* disinfection in order to allow phagocytosis of the bacteria by *A. castellanii* trophozoites. Survival of VIM-PA after *in-vitro* disinfection with selected disinfectants for several exposure times is shown in Figure 1. Survival of VIM-PA after chlorine exposure was higher in the presence of *A. castellanii* at all examined time-points. The largest significant difference ( $P < 0.001$ ) was observed after 2 min of chlorine exposure, as all VIM-PA incubated without amoebae were killed, whereas 3  $\log_{10}$  CFU/mL of VIM-PA survived chlorine treatment in the presence of *A. castellanii*. After 5 min of chlorine exposure in the absence of *A. castellanii*, a very small amount of VIM-PA survived (on average 43 cfu/mL), which is a 99.99% reduction compared to a 100% reduction after 2 min of chlorine exposure. In the presence of *A. castellanii*, a time-dependent effect was observed, as survival of VIM-PA decreased upon prolonged exposure to chlorine. By contrast with chlorine disinfection, no significant difference in survival was observed between VIM-PA incubated in the presence or absence of *A. castellanii* after exposure to 24% acetic acid or 70% ethanol. Exposure to 24% acetic acid for 30 min resulted in survival of  $< 1 \log_{10}$  cfu/mL VIM-PA irrespective of the presence

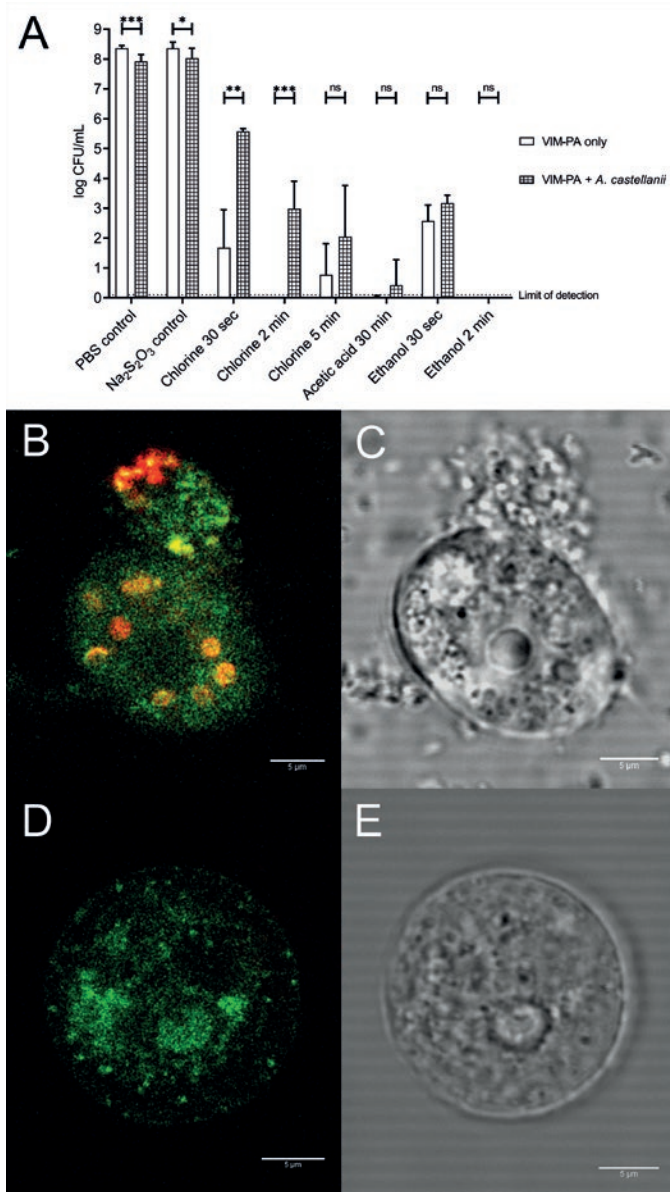


**Figure 1.** Interaction between *A. castellanii* and VIM-PA.

Panel A: Survival of VIM-PA after disinfection with indicated disinfection methods. VIM-PA was incubated with or without *A. castellanii* in PBS for 14 days at 25°C before disinfection with 1000 ppm chlorine, 70% ethanol or 24% acetic acid. Subsequently, samples were bead-beaten and plated on blood agar plates, which were incubated for 24 hours at 37°C before colony forming units (CFU) were counted. Asterisks indicate significant differences. \*\*\*:  $p < 0.001$ ; \*\*:  $p < 0.01$ ; \*:  $p < 0.05$ ; ns: not significant. Panels B-E: Confocal microscopy images of *A. castellanii* pseudocysts after 14 days of culture with VIM-PA (2B and 2C) and without VIM-PA (2D and 2E), stained with *P. aeruginosa*-specific antibody (red). Green colour is autofluorescence of *A. castellanii* and VIM-PA.

of *A. castellanii*. A 30 s exposure to 70% ethanol resulted in the survival of  $\sim 3 \log_{10}$  cfu/mL of VIM-PA in the absence of *A. castellanii*. A small, non-significant increase in survival of VIM-PA was observed in the presence of *A. castellanii*. Exposure to 70% ethanol for 2 min did result in total eradication of VIM-PA in the sample, irrespective of the presence of *A. castellanii*.

The disinfection model was set up to mimic a hospital water system with the possibility of forming a biofilm. A characteristic of our model is that the microbial biofilm was disrupted before disinfection, as micro-organisms were harvested by vigorous pipetting, resulting in dispersed cells being exposed to disinfectant. We hypothesized that VIM-PA was protected against chlorine disinfection after internalization by *A. castellanii* in our co-culture conditions, which was demonstrated by confocal microscopy using *P. aeruginosa*-specific antibody staining (Figure 1B-E). Surface rendering images can be viewed in Supplementary Videos S1 and S2, which clearly demonstrate the intracellular presence of VIM-PA in *A. castellanii*. We studied only the ATCC *Acanthamoeba* “Neff” laboratory strain, although it is known that resistance to disinfection may differ between *Acanthamoeba* strains<sup>9</sup>. However, as it has been shown that environmental strains are more resistant to disinfection than laboratory strains, this could mean that the effects we observed are an underestimation of what actually occurs in the environment<sup>9</sup>.

The 14-day incubation in our experiments resulted in a mixed population of trophozoites, cysts, and pseudocysts. Pseudocyst formation, like cyst formation, is induced by stress, but pseudocysts are morphologically different from cysts<sup>12</sup>. We observed pseudocyst formation immediately after *A. castellanii* trophozoites were treated with chlorine, contrary to treatment with ethanol (70%) or acetic acid (24%) (Supplementary Videos S3-5). We suggest that these pseudocyst and cyst stages of *A. castellanii* are responsible for the observed survival of VIM-PA, as our confocal images show the presence of VIM-PA inside pseudocysts (Figure 1B-E). Previous studies have shown that *Acanthamoeba* cysts can survive chlorine exposure, which means that chlorine does not reach intracellular VIM-PA<sup>9</sup>.

Current literature points to biofilm formation as the main cause of inefficient bacterial disinfection<sup>13</sup>. In addition to biofilm formation, we now propose another mechanism for inefficient disinfection: survival within *A. castellanii*. Intracellular survival of VIM-PA in *A. castellanii* can be considered synergistic to biofilm formation in the ability to decrease disinfectant efficacy, as *A. castellanii* is known to inhabit biofilms as well<sup>14</sup>. Previous studies have shown that PA transmission may occur from the hospital environment to patients, in whom it can cause serious infections<sup>15</sup>. Our findings indicate that *A. castellanii* can play an important role in the persistence of VIM-PA in hospitals and thus could result

in the presence of an environmental source from which VIM-PA transmission to patients can occur.

Other bacteria could take advantage of the protective cover of *acanthamoeba* as well, as it has been shown that many different types of bacteria can survive inside *acanthamoeba*. A clear example is *Legionella pneumophila*, as a recent article showed persistent *L. pneumophila* presence in a water system in which *acanthamoeba* was also present during disinfection with monochloramine <sup>16</sup>. In addition, multiple non-tuberculous mycobacteria have been shown to co-occur with *acanthamoeba* in a hospital water network <sup>17</sup>. Furthermore, *Stenotrophomonas maltophilia* and *Achromobacter xylosoxidans* have been isolated from *Acanthamoeba* spp. <sup>18</sup>. All these pathogenic bacteria may survive chlorine disinfection in hospital water systems inside amoebae as well.

Our results show that *A. castellanii* can decrease the effectiveness of standard chlorine disinfection of VIM-PA, but not of disinfection with 70% ethanol and 24% acetic acid. As ethanol has a limited applicability for the disinfection of wastewater drains, 24% acetic acid for 30 min is a promising option to obtain effective disinfection. Our findings are in concordance with the results of a recent study which showed that 30 min exposure to 24% acetic acid effectively decontaminated sinks with metallo- $\beta$ -lactamase-producing PA, and reinforce the use of 24% acetic acid as an environmental decontamination method in clinical practice <sup>10</sup>.

## Funding

This work was funded by the Erasmus MC, the Netherlands Centre for One Health and Erasmus University Rotterdam (EUR) Fellowship no. 105866. Sponsors were not involved in study design; collection, analysis and interpretation of data; writing of the report or in the decision to submit the article for publication.

## Declaration of interest

Declarations of interest: none.

## References

- 1 Persoon, M. C. *et al.* Mortality related to Verona Integron-encoded Metallo- $\beta$ -lactamase-positive *Pseudomonas aeruginosa*: assessment by a novel clinical tool. *Antimicrob Resist Infect Control* **8**, 107-107 (2019).
- 2 Breathnach, A. S., Cubbon, M. D., Karunaharan, R. N., Pope, C. F. & Planche, T. D. Multidrug-resistant *Pseudomonas aeruginosa* outbreaks in two hospitals: association with contaminated hospital waste-water systems. *J Hosp Infect* **82**, 19-24 (2012).
- 3 Voor In 't Holt, A. F. *et al.* VIM-positive *Pseudomonas aeruginosa* in a large tertiary care hospital: matched case-control studies and a network analysis. *Antimicrob Resist Infect Control* **7**, 32 (2018).
- 4 Walker, J. & Moore, G. *Pseudomonas aeruginosa* in hospital water systems: biofilms, guidelines, and practicalities. *J. Hosp. Infect.* **89**, 324-327 (2015).
- 5 Knoester, M. *et al.* An integrated approach to control a prolonged outbreak of multidrug-resistant *Pseudomonas aeruginosa* in an intensive care unit. *Clin Microbiol Infect* **20**, O207-215 (2014).
- 6 Cateau, E., Delafont, V., Hechard, Y. & Rodier, M. H. Free-living amoebae: what part do they play in healthcare-associated infections? *J Hosp Infect* **87**, 131-140 (2014).
- 7 Michel, R., Burghardt, H. & Bergmann, H. *Acanthamoeba* isolated from a highly contaminated drinking-water system of a hospital exhibited natural infections with *Pseudomonas aeruginosa*. *Zentralbl Hyg Umweltmed* **196**, 532-544 (1995).
- 8 Siddiqui, R., Lakhundi, S. & Khan, N. A. Interactions of *Pseudomonas aeruginosa* and *Corynebacterium* spp. with non-phagocytic brain microvascular endothelial cells and phagocytic *Acanthamoeba castellanii*. *Parasitol Res* **114**, 2349-2356 (2015).
- 9 Coulon, C., Collignon, A., McDonnell, G. & Thomas, V. Resistance of *Acanthamoeba* cysts to disinfection treatments used in health care settings. *J Clin Microbiol* **48**, 2689-2697 (2010).
- 10 Stjärne Aspelund, A. *et al.* Acetic acid as a decontamination method for sink drains in a nosocomial outbreak of metallo- $\beta$ -lactamase-producing *Pseudomonas aeruginosa*. *J Hosp Infect* **94**, 13-20 (2016).
- 11 Dutch Working Party on Infection Prevention. Richtlijn reiniging en desinfectie van ruimten, meubilair en voorwerpen. (2009).
- 12 Kliescikova, J., Kulda, J. & Nohynkova, E. Stress-induced pseudocyst formation--a newly identified mechanism of protection against organic solvents in acanthamoebae of the T4 genotype. *Protist* **162**, 58-69 (2011).
- 13 Behnke, S. & Camper, A. K. Chlorine dioxide disinfection of single and dual species biofilms, detached biofilm and planktonic cells. *Biofouling* **28**, 635-647 (2012).
- 14 Huws, S. A., McBain, A. J. & Gilbert, P. Protozoan grazing and its impact upon population dynamics in biofilm communities. *J Appl Microbiol* **98**, 238-244 (2005).
- 15 Hota, S. *et al.* Outbreak of multidrug-resistant *Pseudomonas aeruginosa* colonization and infection secondary to imperfect intensive care unit room design. *Infect Control Hosp Epidemiol* **30**, 25-33 (2009).
- 16 Casini, B. *et al.* Detection of viable but non-culturable legionella in hospital water network following monochloramine disinfection. *J Hosp Infect* **98**, 46-52 (2018).
- 17 Ovrutsky, A. R. *et al.* Cooccurrence of free-living amoebae and nontuberculous Mycobacteria in hospital water networks, and preferential growth of *Mycobacterium avium* in *Acanthamoeba lenticulata*. *Appl Environ Microbiol* **79**, 3185-3192 (2013).
- 18 Gomes, T. S. *et al.* Presence and interaction of free-living amoebae and amoeba-resisting bacteria in water from drinking water treatment plants. *Sci Total Environ* **719**, 137080 (2020).

## Supplementary material

**Table S1.** Antibiotic susceptibility profile of VIM-positive *P. aeruginosa* strain VIM-PA-R15111.

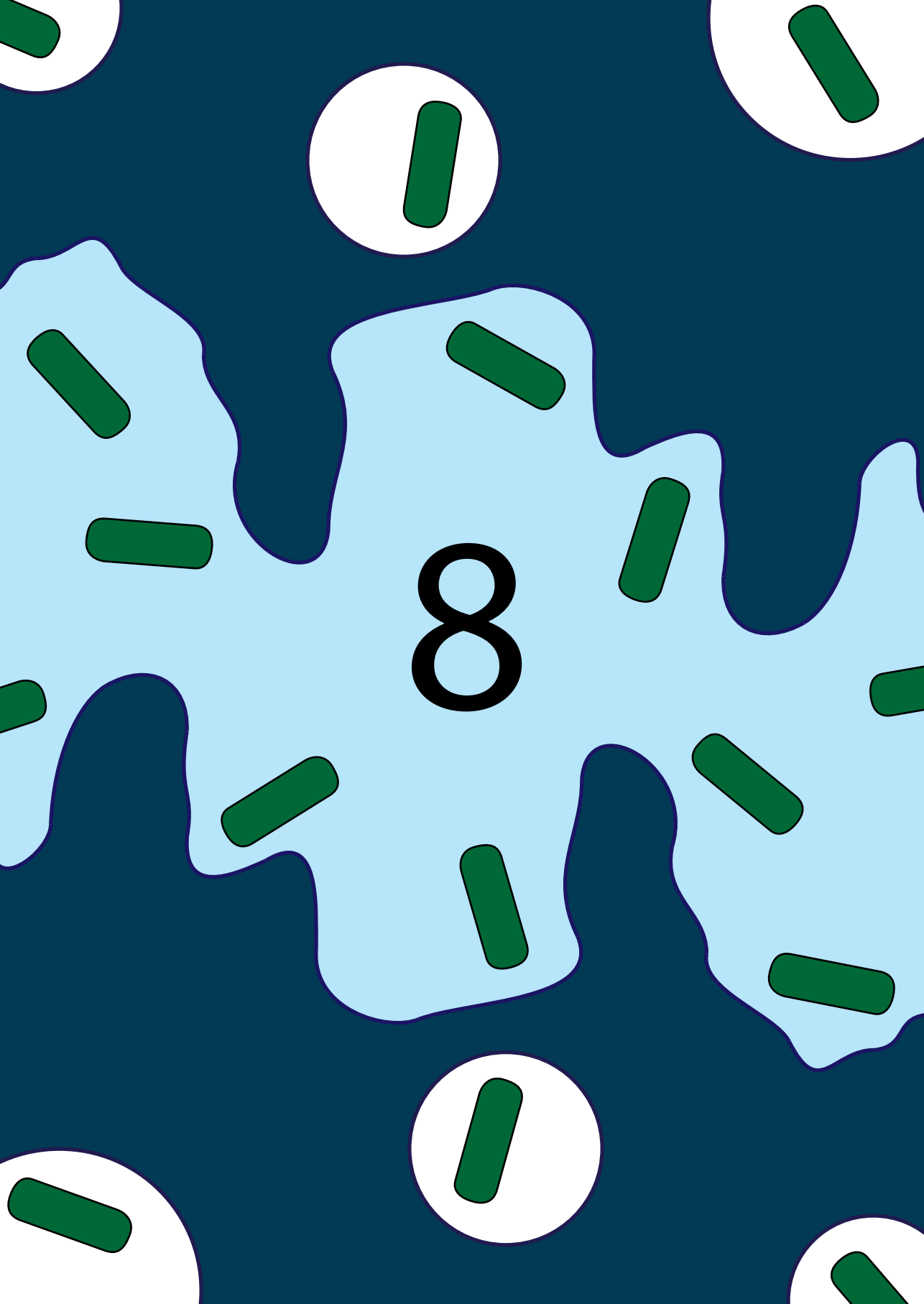
Antibiotic	MIC ( $\mu\text{g/mL}$ )	Susceptibility according to EUCAST
Piptazobactam	> 64	R
Imipenem	> 8	R
Meropenem	1	S
Ceftazidime	16	R
Gentamicin	> 8	R
Tobramycin	> 8	R
Ciprofloxacin	> 2	R
Colistin	$\leq 0.5$	S
Fosfomycin	$\leq 16$	S

Susceptibility profile was determined by the VITEK 2 system (bioMérieux, Marcy l'Etoile, France).

**Supplementary Movies S1-S5** can be accessed online at:

<https://doi.org/10.1016/j.jhin.2020.09.019>





# CHAPTER 8

---

*Acanthamoeba castellanii* can facilitate plasmid transfer between environmental *Pseudomonas* spp.

Maarten J. Sarink<sup>1</sup>, Lara Grassi<sup>1</sup>, Aloysius G.M. Tielens<sup>1</sup>, Annelies Verbon<sup>1,2</sup>,  
Margreet C. Vos<sup>1</sup>, Wil Goessens<sup>1</sup>, Nikolaos Strepis<sup>1</sup>, Corné H.W. Klaassen<sup>1</sup>,  
Jaap J. van Hellemond<sup>1</sup>

<sup>1</sup> Department of Medical Microbiology and Infectious Diseases, Erasmus MC University Medical Center, Rotterdam, The Netherlands

<sup>2</sup> Department of Internal Medicine, University Medical Center Utrecht, Utrecht, The Netherlands

Submitted

## Abstract

The conditions in which antimicrobial resistance (AMR) genes are transferred in natural environments are poorly understood. *Acanthamoeba castellanii* (a cosmopolitan environmental amoeba) feeds on bacteria by phagocytosis, which places the consumed bacteria closely together in a food vacuole (phagosome) of the amoeba. This way, amoebae can facilitate genetic exchanges between intra-amoebal bacteria. We studied this phenomenon in the clinically relevant bacteria *Pseudomonas oleovorans* and *Pseudomonas aeruginosa* (strain 957). The internalisation of both the plasmid donor and acceptor bacteria was shown by confocal microscopy. In seven independent experiments, an on average 12-fold increase in transfer of the  $\text{bla}_{\text{VIM-2}}$  gene between these two *Pseudomonas* strains was observed in the presence of *A. castellanii* compared to its absence. Negligible or no plasmid transfer was observed from *P. oleovorans* to 18 other investigated strains of *P. aeruginosa*. AMR gene transfer via plasmids between *Pseudomonas* species is highly strain-dependent and *A. castellanii* can substantially enhance plasmid transfer. This process of plasmid transfer might also occur between other bacteria and predatory protozoa, such as amoebae that reside in the gut of humans and animals.

## 1. Introduction

Antimicrobial resistance (AMR) has been declared by the World Health Organization to be one of the top 10 global public-health threats facing humanity <sup>1</sup>. Misuse and overuse of antibiotics are the main drivers for selection of bacteria that are resistant to antibiotics. In addition, AMR can spread via horizontal gene transfer (HGT) of AMR genes. The conditions in which AMR genes are transferred in natural environments are poorly understood, although stress, nutrient supply and cell density can affect the HGT rate <sup>2</sup>. Studies in natural aquatic environments revealed that biofilms are so-called hotspots for HGT <sup>2</sup>. Biofilms are composed of a mixture of organisms, containing prokaryotes as well as eukaryotes. *Acanthamoeba* spp. are eukaryotes often present in biofilms. This unicellular protozoa feeds on bacteria by phagocytosis, and in this process places bacteria together in a food vacuole (phagosome). Most bacteria are lysed and degraded, but some can survive or even kill the amoeba <sup>3-5</sup>. One of the bacterial species that can survive predation by *Acanthamoeba* spp. is *Pseudomonas aeruginosa*, which can live and multiply in the food vacuoles of this amoeba <sup>6</sup>. *P. aeruginosa* and *Acanthamoeba* spp. were shown to be present together in floor drains of a general hospital <sup>7</sup>. *P. aeruginosa* can cause opportunistic nosocomial infections in humans that are often hard to treat, due to reduced susceptibility to multiple antibiotics. Resistance to the last-line antibiotic class of carbapenems is especially worrisome, as bloodstream infections with a carbapenem-resistant *P. aeruginosa* (CRPA) result in increased mortality compared to infections with a carbapenem-susceptible counterparts<sup>8</sup>. The Verona-Integron-encoded-Metallo- $\beta$ -lactamase ( $bla_{VIM-2}$ ) resistance gene, which results in CRPA, is not only found in *P. aeruginosa*, but also in non-pathogenic *Pseudomonas* spp., which could act as a reservoir of AMR genes <sup>9</sup>. Amoebae can act as a place that favours genetic exchanges between bacteria <sup>5,10</sup>. In the food vacuoles (phagosomes) of amoebae, different bacteria from the environment will end up together in closed vacuoles, which might enhance the transfer of mobile genetic elements (e.g. plasmids). Hence, amoebal predation could facilitate HGT of AMR genes <sup>5</sup>. This concept is rarely studied with clinically relevant bacteria. Therefore, we examined the transfer rate of a plasmid encoding the  $bla_{VIM-2}$  gene, between two different *Pseudomonas* species (*P. oleovorans* to *P. aeruginosa*) in the presence and absence of *A. castellanii*.

## 2. Methods

### 2.1 Strains

*Acanthamoeba castellanii* ATCC strain 30010 was grown in cell culture flasks at 25°C in PYG medium, which contains proteose peptone, yeast extract and glucose with salt additives

(ATCC medium 712) <sup>11</sup>. This medium was supplemented with 40 µg/mL gentamicin, 100 units/mL penicillin and 100 µg/mL streptomycin. The *Pseudomonas oleovorans* donor strain carrying a plasmid harboring the *bla*<sub>VIM-2</sub> gene was isolated from a hospital sink in the Erasmus MC University Medical Center Rotterdam, the Netherlands. All used *Pseudomonas aeruginosa* acceptor strains were isolated from wet hospital environments in the Erasmus MC, except for *P. aeruginosa* ATCC strain 27853, which was obtained from the American Type Culture Collection (Manassas, Virginia, USA). Bacteria were grown on Trypticase Soy Agar (TSA) II with 5% Sheep Blood (BD Biosciences, Franklin Lakes, New Jersey, USA).

## 2.2 Fluorescent labelling and confocal imaging

The intracellular location of both *Pseudomonas* species after phagocytosis by *Acanthamoeba* was examined by fluorescent labelling and confocal microscopy. *P. oleovorans* was fluorescently stained using 1 mg/mL Fluorescein isothiocyanate isomer I (FITC) (Sigma-Aldrich, USA) and *P. aeruginosa* strain 957 was separately stained using 1 mg/mL Lectin PNA, Alexa Fluor 647 Conjugate (Invitrogen, USA) suspended in DMSO (MERCK KGaA, Germany). Staining of both *Pseudomonas* species was performed by incubation of the bacteria with the dye in PBS with 5% glycerol (Sharlau, Spain) and 2 mM MgCl<sub>2</sub> (Sigma-Aldrich, USA) for 1 hour, while gently swirling, at room temperature. Subsequently, the excess dye was removed by washing with PBS 5 and 3 times, respectively. *A. castellanii* were then incubated in PBS for 1 hour at 25°C with both stained *Pseudomonas* species in the ratio of 1:1:1. After incubation the samples were fixated for 30 minutes on ice in 8% formaldehyde (MERCK KGaA, Germany) before imaging. Confocal images were taken using the Leica SP5 confocal laser scanning microscope (Leica, Germany), deconvoluted with the Huygens software (SVI, Hilversum, The Netherlands) and reconstructed using Fiji37.

## 2.3 Gene transfer experiments

To harvest *A. castellanii* trophozoites, cell culture flasks were placed on ice for 20 minutes, after which the nutrient-rich medium was removed by two subsequent washing steps with 1% PYG in PBS (v/v). *P. oleovorans* and *P. aeruginosa* strains were grown overnight on TSA, after which an 0.5 optical density (OD) at 600 nm suspension was prepared in 1% PYG in PBS. A predetermined quantity containing  $1 \times 10^7$  *P. oleovorans* and  $1 \times 10^7$  of one of the *P. aeruginosa* strains were added to each well of a 24-well plate with or without  $2 \times 10^5$  *A. castellanii* in 1% PYG in PBS in a total volume of 1 mL. The applied *in vitro* co-culture conditions (1% PYG in PBS without shaking) were a mimic of the low nutrient situation in the hospital water system. After incubation for 24 hours at 25°C the 24-well plate was placed on ice for 20 minutes. Next, the content of each well was collected by vigorous pipetting and transferred into tubes containing 250-280 mg of 1 mm diameter glass beads. To release viable intracellular bacteria from the amoeba, bead-beating was

performed 16 times for 30 seconds on and 30 seconds off. This bead-beating procedure did not affect the viability of the *Pseudomonas* spp. (Figure S1). After bead-beating, serial dilutions were plated on TSA as well as on Mueller Hinton (MH) II agar plates containing 4 mg/L meropenem, 2 mg/L tobramycin and 25 mg/L 1,10-phenanthroline. Resistance genes encoding for meropenem and tobramycin-resistance are plasmid encoded and therefore meropenem and tobramycin were applied as selective agents. To select for *P. aeruginosa*, 1,10-phenanthroline was used, as described in <sup>12</sup>. TSA plates were incubated for 24 hours at 37°C, after which colonies of *P. oleovorans* and *P. aeruginosa* could be quantified, as colonies of both species could be differentiated by their different morphology on TSA agar plates. MH plates with selective compounds were incubated for 48 hours at 37°C. Plasmid transfer rate was determined by dividing the CFU on selective plates by the total number of CFU (donor + acceptor, expressed in 10<sup>8</sup>) present at the end of the incubation. All experiments were performed in duplicate or more where indicated.

## 2.4 Real-time PCR, MALDI-TOF and conventional PCR

In each gene-transfer experiment for each condition, three colonies were examined by both real-time PCR and Matrix-assisted laser desorption/ionization with time-of-flight mass spectrometry (MALDI-TOF-MS) (Bruker, Billerica, Massachusetts, USA) to confirm the presence of the *bla*<sub>VIM-2</sub> gene and the *P. aeruginosa* identity, respectively. Real-time PCR was performed in a LightCycler 96-well plate (Roche, Basel, Switzerland) by mixing a small aliquot of a colony with 10 µL of LightCycler 480 Probes Master (Roche), 5 µL of *bla*<sub>VIM</sub>-PCR probe mix (Table S2) and 5 µL of PCR-grade water <sup>13</sup>. Samples were run in a LightCycler 480II instrument (Roche) with pre-denaturation at 95°C for 5 minutes; amplification of 50 cycles between 95°C for 5 seconds and 60°C for 30 seconds and final cooling at 40°C for 1 minute.

Conventional PCR was used to examine the integrity of the *bla*<sub>VIM-2</sub> containing plasmid after incorporation of the *bla*<sub>VIM-2</sub> gene in the recipient *P. aeruginosa*-957 strain. Primers were designed for six regions in the original plasmid in *P. oleovorans*, located 20-30 kb from each other (Table S2). All primers were used at a concentration of 0.5 µM. In a 96-well plate (Roche), 5 µL of extracted DNA was mixed with 1.25 µL of forward primer, 1.25 µL of reverse primer, 12.5 µL of PCR Faststart PCR Master Mix (Roche) and 5 µL of PCR-grade water. Samples were run in a Biometra TAdvanced PCR thermocycler instrument (Labgene Scientific SA, Châtel-St-Denis, Switzerland) with the following conditions: pre-denaturation at 95°C for 10 minutes; 30 cycles of denaturation at 95°C for 30 seconds, annealing at 55°C for 30 seconds, and extension at 72°C for 1 minute; followed by final extension for 10 minutes at 72°C and cooling to 4°C. The DNA amplicons were separated by electrophoresis on a 2% agarose gel (Sphaero Q, Gorinchem, The Netherlands, and Thermo Scientific, Waltham Massachusetts, USA) and visualized by staining with SYBR® Safe DNA Gel Stain (Invitrogen, Carlsbad, California, USA).

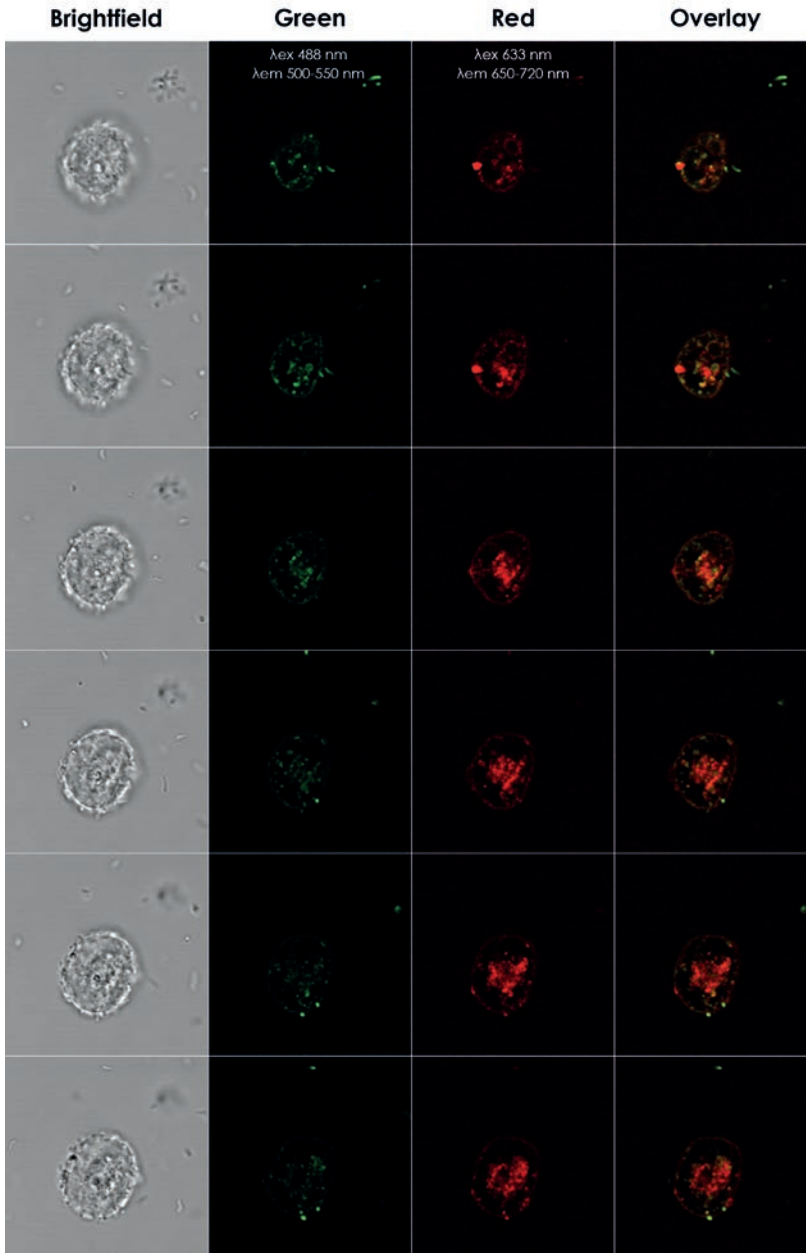


**Figure 1.** Images taken by confocal microscopy of co-cultures with *A. castellanii*, *P. oleovorans* and *P. aeruginosa-957*.

Shown are z-stacks (sections of 1  $\mu$ m) of bright field and fluorescent images at indicated wavelengths. *A. castellanii* was incubated together with *P. oleovorans* (stained by FITC – shown in green) and *P. aeruginosa-957* (stained with Lectin PNA bound to Alexa 647 – shown in red) in PBS for one hour, after which samples were fixated and examined by confocal microscopy. The scale bar is 10  $\mu$ m.

## 3. Results

### 3.1 Ingestion of *Pseudomonas* by *A. castellanii*

The uptake by *A. castellanii* of both *P. aeruginosa*-957 and *P. oleovorans* after 90 minutes of co-incubation was shown by confocal microscopy, as the distinctly fluorescent-stained *Pseudomonas* species were both observed inside *A. castellanii* (Figure 1). This result confirms our previous study which showed the intracellular presence of *P. aeruginosa* in *A. castellanii*<sup>3</sup>. Subsequently, the growth dynamics of both *Pseudomonas* species were examined in the presence and absence of *A. castellanii* in a low-nutrient medium. This demonstrated that of both *Pseudomonas* species the total number increased in the absence of *A. castellanii* (Figure 2A). In the presence of *A. castellanii*, the number of *P. oleovorans* dropped substantially whereas the number of *P. aeruginosa*-957 increased. It is known that bacterial evolution resulted in bacteria resistant to destruction by free-living amoebae<sup>4-6</sup>. This could explain why *A. castellanii* trophozoites did not digest the *P. aeruginosa*-957 strain

### 3.2 Determination of the transfer efficiency

The transfer efficiency of the  $bla_{VIM-2}$  gene from *P. oleovorans* to the *P. aeruginosa*-957 strain was examined by co-culturing these two *Pseudomonas* species together for 24 hours in the presence or absence of *A. castellanii*, followed by examination of the number of bacteria on selective as well as non-selective agar plates. Real-time PCR and MALDI-TOF analysis were performed to confirm the presence of the  $bla_{VIM-2}$  gene and *P. aeruginosa* identity of the obtained colonies on the selective agar plates, respectively. In total, this experiment was performed seven times. It demonstrated an on average 12-fold (range 1 to 47) higher plasmid transfer rate in the presence of *A. castellanii* compared to its absence (Figure 2B). The plasmid-transfer rate per 10<sup>8</sup> bacteria ranged from 2000 to 224,625 in the absence of *A. castellanii* and from 11,530 to 1,990,196 in the presence of *A. castellanii*. The presence of the entire plasmid (size: 158 kbp) with the  $bla_{VIM-2}$  gene in colonies growing on the selective plates was confirmed by additional conventional PCR analysis (Figure S2-S3).

## 4. Discussion

This study started with an experiment where the plasmid-transfer efficiency was tested twice with in total 19 *P. aeruginosa* strains: ATCC strain 27853 plus 18 strains isolated from wet hospital environments, including strain 957 described above. The experiment showed that the  $bla_{VIM-2}$  gene could be transferred from *P. oleovorans* to *P. aeruginosa* in the above-mentioned strain 957, and in only three other *P. aeruginosa* strains, but in these three strains the plasmid transfer rate was negligible compared to the rate with

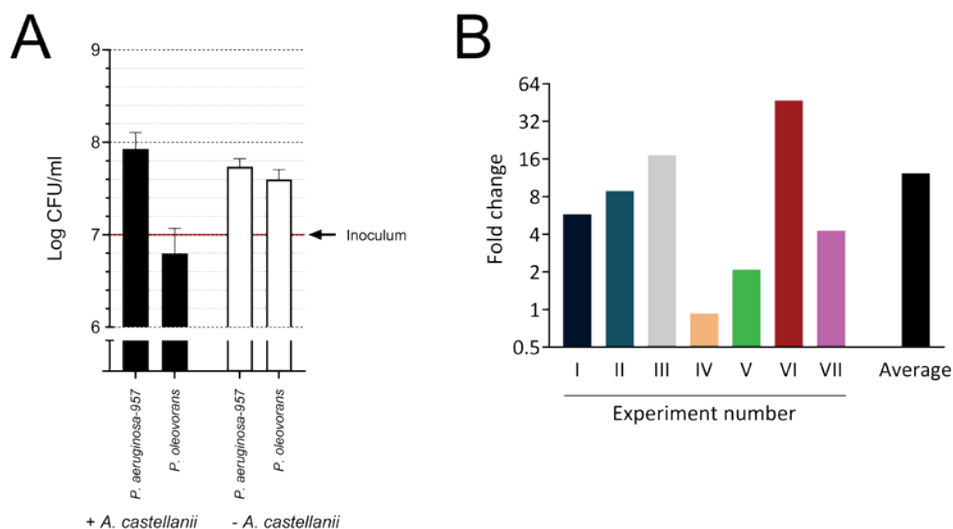


**Figure 2.** Transfer rate of the plasmid encoded  $bla_{VIM-2}$  gene from *P. oleovorans* to *P. aeruginosa-957* in the presence or absence of *A. castellanii*.

Panel A shows the number of colony-forming units (CFU) on tryptic soy agar of *P. oleovorans* and *P. aeruginosa-957* after 24 hours of incubation in a low-nutrient medium (1% PYG in PBS (v/v)) in the presence (+ *A. castellanii*) or absence (- *A. castellanii*) of *A. castellanii*.  $1 \times 10^7$  *P. oleovorans* and  $1 \times 10^7$  *P. aeruginosa-957* (indicated with a red line) were added at the start of the incubation, with or without  $2 \times 10^5$  *A. castellanii*. Panel B shows the difference in fold change in the recipients /  $10^8$  CFU formed by *P. oleovorans* and *P. aeruginosa-957* in the presence of *A. castellanii* compared to its absence. Culture conditions were used as described for panel A. After 24 hours of co-culture, the contents were added to tryptic soy agar to determine CFU counts as well as to selective plates containing 4 mg/L meropenem, 2 mg/L tobramycin and 25 mg/L 1,10-phenanthroline to determine the number of recipients.

*P. aeruginosa-957* (Table S1). Furthermore, the transfer rate in these three strains was not substantially increased in the presence of *A. castellanii*. These experiments showed that AMR gene transfer between *Pseudomonas* species is highly strain-dependent. This indicates that there are specific strain properties that determine the rate of acquisition, which could be due to the plasmid incompatibility groups of the examined strains<sup>14</sup>, although many other factors could be of influence<sup>15</sup>. The mechanisms behind increased transfer in the presence of *A. castellanii* and why this is also strain-dependent are currently unresolved.

The presence of a large variety of AMR genes in *Acanthamoeba* spp present in wastewater has been reported, which suggests that the bacteria inside amoebae may significantly contribute to the transmission of these genes in the surrounding environments<sup>16</sup>. Since the investigated *Pseudomonas* strains in this study were isolated from wet hospital environments, our observation is clinically relevant because transfer of AMR genes

between bacteria can occur in hospital-water systems after which resistant bacteria can spread within the hospital and to the community <sup>17</sup>. The enhanced AMR transfer by *A. castellanii* could also apply to other predatory protozoa, such as amoebae that reside in the gut of humans and animals. The gastrointestinal tract plays an important role in the transfer of plasmids and can host many different protozoa <sup>18</sup>. In this way, protozoa could also have a big impact on AMR transfer among bacteria in the gastrointestinal tract environment of humans.

### **Acknowledgements**

Sven van Dun and Willem-Jan de Leeuw are thanked for excellent technical assistance with gene-transfer experiments. Gert van Cappellen is thanked for excellent technical assistance with the confocal microscope.

## References

- 1 World Health Organization. *Antimicrobial resistance fact sheet*, <<https://www.who.int/news-room/fact-sheets/detail/antimicrobial-resistance>> (2022).
- 2 Michaelis, C. & Grohmann, E. Horizontal Gene Transfer of Antibiotic Resistance Genes in Biofilms. *Antibiotics (Basel)* **12** (2023).
- 3 Sarink, M. J. *et al.* *Acanthamoeba castellanii* interferes with adequate chlorine disinfection of multidrug-resistant *Pseudomonas aeruginosa*. *J Hosp Infect* **106**, 490-494 (2020).
- 4 Greub, G. & Raoult, D. Microorganisms resistant to free-living amoebae. *Clin Microbiol Rev* **17**, 413-433 (2004).
- 5 Moliner, C., Fournier, P. E. & Raoult, D. Genome analysis of microorganisms living in amoebae reveals a melting pot of evolution. *FEMS Microbiol Rev* **34**, 281-294 (2010).
- 6 Michel, R., Burghardt, H. & Bergmann, H. *Acanthamoeba*, naturally intracellularly infected with *Pseudomonas aeruginosa*, after their isolation from a microbiologically contaminated drinking water system in a hospital. *Zentralbl Hyg Umweltmed* **196**, 532-544 (1995).
- 7 Mooney, R. *et al.* *Acanthamoeba* as a protective reservoir for *Pseudomonas aeruginosa* in a clinical environment. *J Hosp Infect* (2024).
- 8 Persoon, M. C. *et al.* Mortality related to Verona Integron-encoded Metallo- $\beta$ -lactamase-positive *Pseudomonas aeruginosa*: assessment by a novel clinical tool. *Antimicrobial resistance and infection control* **8**, 107-107 (2019).
- 9 Brovedan, M. A. *et al.* *Pseudomonas putida* group species as reservoirs of mobilizable Tn402-like class 1 integrons carrying bla(VIM-2) metallo- $\beta$ -lactamase genes. *Infect Genet Evol* **96**, 105131 (2021).
- 10 Bertelli, C. & Greub, G. Lateral gene exchanges shape the genomes of amoeba-resisting microorganisms. *Front Cell Infect Microbiol* **2**, 110 (2012).
- 11 American Type Culture Collection. *ATCC Medium: 712 PYG w/ Additives*, <<https://www.atcc.org/-/media/product-assets/documents/microbial-media-formulations/7/1/2/atcc-medium-712.pdf>>
- 12 Keeven, J. K. & DeCicco, B. T. Selective medium for *Pseudomonas aeruginosa* that uses 1,10-phenanthroline as the selective agent. *Appl Environ Microbiol* **55**, 3231-3233 (1989).
- 13 Pirzadian, J. *et al.* Novel use of culturomics to identify the microbiota in hospital sink drains with and without persistent VIM-positive *Pseudomonas aeruginosa*. *Sci Rep* **10**, 17052 (2020).
- 14 Bethke, J. H. *et al.* Environmental and genetic determinants of plasmid mobility in pathogenic *Escherichia coli*. *Sci Adv* **6**, eaax3173 (2020).
- 15 Fraikin, N., Couturier, A. & Lesterlin, C. The winding journey of conjugative plasmids toward a novel host cell. *Curr Opin Microbiol* **78**, 102449 (2024).
- 16 Conco-Biyela, T. *et al.* Metagenomics insights into microbiome and antibiotic resistance genes from free living amoeba in chlorinated wastewater effluents. *Int J Hyg Environ Health* **258**, 114345 (2024).
- 17 Kehl, K. *et al.* Dissemination of carbapenem resistant bacteria from hospital wastewater into the environment. *Sci Total Environ* **806**, 151339 (2022).
- 18 León-Sampedro, R. *et al.* Pervasive transmission of a carbapenem resistance plasmid in the gut microbiota of hospitalized patients. *Nat Microbiol* **6**, 606-616 (2021).

## Supplementary material

**Table S1.** Efficiency of transfer of a plasmid encoding *bla*<sub>VIM-2</sub> from *P. oleovorans* to different *P. aeruginosa* strains.

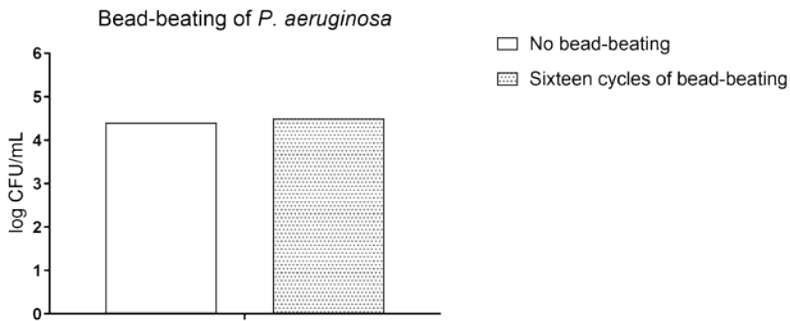
Acceptor strain	Recipients/10 <sup>8</sup> bacteria			
	1st experiment		2nd experiment	
	with <i>A. castellanii</i>	without <i>A. castellanii</i>	with <i>A. castellanii</i>	without <i>A. castellanii</i>
<i>P. aeruginosa</i> 559	0	0	0	0
<i>P. aeruginosa</i> 620	0	0	0	0
<i>P. aeruginosa</i> 623	1	0	16	10
<i>P. aeruginosa</i> 630	0	0	0	0
<i>P. aeruginosa</i> 631	28	19	12	14
<i>P. aeruginosa</i> 772	0	0	0	0
<i>P. aeruginosa</i> 781	0	0	0	0
<i>P. aeruginosa</i> 957	11530	2000	1990196	224625
<i>P. aeruginosa</i> 959	0	0	0	0
<i>P. aeruginosa</i> 960	0	0	0	0
<i>P. aeruginosa</i> 1201	0	0	0	0
<i>P. aeruginosa</i> 1203	0	0	0	0
<i>P. aeruginosa</i> 1212	0	0	0	0
<i>P. aeruginosa</i> 1383	2	0	2	2
<i>P. aeruginosa</i> 1432	0	0	0	0
<i>P. aeruginosa</i> 1437	0	0	0	0
<i>P. aeruginosa</i> 1463	0	0	0	0
<i>P. aeruginosa</i> 1479	0	0	0	0
<i>P. aeruginosa</i> ATCC 27853	0	0	0	0

Shown are the number of recipients per 10<sup>8</sup> colony forming units (CFU) in two separate experiments. *P. oleovorans* and the listed *P. aeruginosa* strains were incubated together in the presence or absence of *A. castellanii* for 24 hours in 1% PYG in PBS (v/v), after which the contents were added to tryptic soy agar to determine CFU counts as well as to selective plates containing 4 mg/L meropenem, 2 mg/L tobramycin and 25 mg/L 1,10-phenanthroline to determine the number of recipients.

**Table S2.** Primer sequences of target genes.

Target gene	Primer	Sequence
<i>bla</i> <sub>VIM</sub>	Forward	GCAAATTGGACTTCCYGTA
	Reverse 1	GACGGTGATGCGTACGTTG
	Reverse 2	CCCTAAGGGCATCAACTCC
dotG	Forward	GGCATCTTCAATCACGGTTT
	Reverse	GGGGCTGGTTATTGGTTTTT
pdeF	Forward	GTGCTGTCTCGCATTACGAA
	Reverse	CTCTATCGTCAGACCGACA
chpB	Forward	CCATTCCTATCACCGAGCAC
	Reverse	GCAGGGCTTCATCTATGGTC
<i>bla</i> <sub>VIM-2</sub>	Forward	GCAAATTGGACTTCCTGTAA
	Reverse	CGCTCGATGAGAGTCCTTCT
mobA	Forward	GTCTCCATCGCCTTCACCT
	Reverse	GCACACATCCTGTTACCAC
pilP	Forward	TAATCCCGGAGGAATACCG
	Reverse	CCAAGCAGGAAGAAGAGCTG

Shown are forward and reverse primer sequences of listed target genes.

**Figure S1.** Effect of sixteen cycles of bead-beating on *P. aeruginosa* colony-forming unit (CFU) count.

A suspension of *P. aeruginosa* was subjected to sixteen cycles (30 seconds on and 30 seconds off) of bead-beating with 1 mm glass beads using a Qiagen TissueLyser II. Before and after bead-beating, a sample was added to TSA to determine CFU counts. This experiment was performed once.

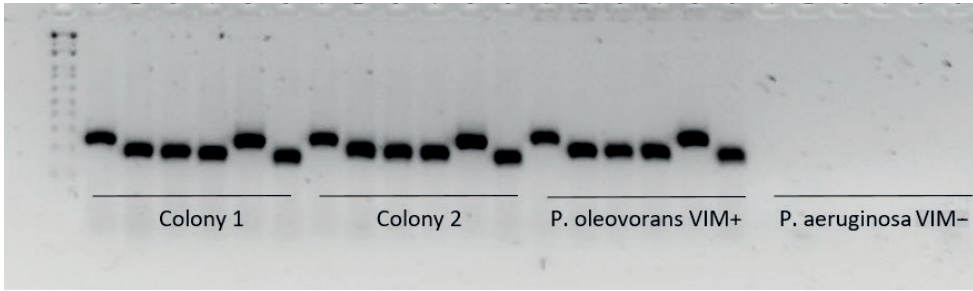


**Figure S2.** Conventional PCR analysis to examine the intactness of the *bla*<sub>VIM-2</sub>-containing plasmid in recipients.

*P. oleovorans* and *P. aeruginosa* were incubated in presence or absence of *A. castellanii* for 24 hours, after which the cells were added to selective plates. A total of 56 colonies present on the selective plates were tested for the presence of the entire plasmid. Shown are the results of two colonies and the positive (*P. oleovorans*) and negative (*P. aeruginosa*) controls. The other 54 colonies showed the same positive result (not shown). The target genes (present on the *bla*<sub>VIM-2</sub>-containing plasmid, see Figure S2) are indicated above the respective lanes. 1: *dotG*; 2: *pdeF*; 3: *chpB*; 4: *bla*; 5: *mobA*; 6: *pilP*.

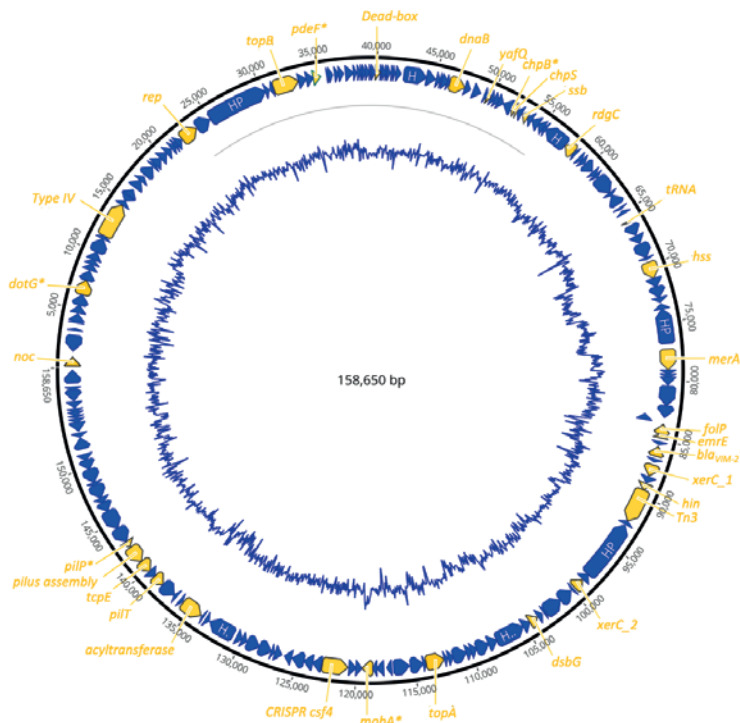


**Figure S3.** Plasmid map of the *bla*<sub>VIM-2</sub> containing plasmid from *P. oleovorans*. The plasmid sequence is visualised in Geneious Prime (geneious, Auckland, New Zealand). Genes with functions of interest are indicated in yellow. Non-annotated genes (hypothetical proteins) are indicated in blue. The target genes used to determine the presence of the entire plasmid are indicated with an asterisk.



# CHAPTER 9

---

Summarising discussion and  
perspectives

## Amoebae and evolution

Amoebae and bacteria have coexisted for millions of years and have developed complex interactions with each other. These interactions cover the whole range of symbiosis, varying from commensalism where no harm is done to the host, and mutualism where both organisms benefit, to parasitism, where one organism benefits at the expense of the host <sup>1</sup>. Most bacteria are simply eaten by amoebae, but some bacteria arose that can resist this predation and even kill the amoeba instead <sup>2</sup>. Others can survive inside the amoeba, and the amoeba can then protect them from harmful external conditions <sup>3</sup>. These interactions have shaped amoebae and bacteria into the creatures they now are. As a secondary effect, the interactions between amoebae and bacteria impact the relationship of these organisms with humans today.

Amoebae exist in many shapes and sizes and are present in various clades of the phylogenetic tree. As such, amoebae can be classified in many different ways. For the purposes of this thesis, a distinction is made in the way of living and pathogenic capabilities (Table 1).

**Table 1.** Classification of amoebae based on lifestyle and pathogenicity.

	<b>Free-living</b>	<b>Dependent on host</b>
Non-pathogenic	<b>Free-living organism</b> <i>Naegleria gruberi</i> <i>Vermamoeba vermiformis</i>	<b>Commensal</b> <i>Entamoeba dispar</i>
Pathogenic	<b>Facultative parasite</b> <i>Naegleria fowleri</i> <i>Acanthamoeba</i> spp. <i>Balamuthia mandrillaris</i>	<b>Obligate parasite</b> <i>Entamoeba histolytica</i>

Infection of a human by a pathogenic free-living amoeba (FLA) can be detrimental to the human host, as described in chapter 2. Most other parasites take maximum advantage of their human host by causing long-term infections that allow for the generation of large numbers of offspring <sup>4,5</sup>. FLA did not develop such a relationship with humans, and this independence of human hosts is reflected in the severity of the diseases that they can cause. A brain infection by *Naegleria fowleri* usually results in death within one week after symptom onset <sup>6,7</sup>. An eye infection by *Acanthamoeba* spp. might develop slowly, but is very hard to eradicate and can lead to blindness if left untreated for too long <sup>8</sup>. Brain infections by *Acanthamoeba* spp. or *Balamuthia mandrillaris* result in death in over 90% of cases, and even if the so far most optimal therapy is given, over 75% of patients still die <sup>9,10</sup>.

On the other hand, the co-evolution of bacteria with amoebae has provided bacteria with a so-called “training ground” for interactions with the human immune system<sup>11</sup>. For instance, amoebae bear many similarities with macrophages (phagocytosis and lysosomal degradation), and mechanisms to survive phagocytosis by amoebae overlap with mechanisms to survive phagocytosis by macrophages. Examples include *Legionella* spp., *Mycobacterium* spp., and *Chlamydia* spp.<sup>11</sup>. Indirectly, by protecting bacteria within cysts an amoeba can ensure the survival of bacteria in conditions in which these bacteria would normally perish. This leads to a more widespread presence of these bacteria and subsequently an increased risk of infection for humans.

The enigmatic destructive nature of pathogenic FLA described in chapter 2, warrants investigation into all of their aspects, as a better understanding of the amoeba host interaction is required to improve the until now poor efficacy of treatment.

## Energy metabolism of FLA

### Substrate preferences

*Naegleria* spp. live in freshwater all around the world. They are mostly found in organic-material containing habitats such as lakes, groundwater, sewage systems and geothermal waters<sup>12</sup>. Within these habitats, *Naegleria* spp. can be found in biofilms, where they feed on bacteria. The energy metabolism of *Naegleria gruberi*, a non-pathogenic relative of *Naegleria fowleri*, was found to be different from most other parasites, as it prefers lipids over glucose as a food source<sup>13</sup>. This remarkable discovery could in hindsight be explained by the fact that bacteria, the natural food source of *N. gruberi*, have a relatively high lipid content compared to carbohydrates, such as glucose. Furthermore, *Naegleria* spp. can live in biofilms, which contain a lot of extracellular matrix, and a wide range of lipids<sup>14</sup>. To determine whether this nutrient preference is restricted to a phylogenetic subgroup or is related to the lifestyle of the protozoa, we extended our research to an evolutionary unrelated amoeba that possesses a similar lifestyle: *Acanthamoeba* spp. This amoeba is located in a different phylogenetic supergroup compared to *N. gruberi*, but (similar to *N. gruberi*) feeds on bacteria. Therefore, we hypothesized that *Acanthamoeba* spp. share metabolic properties with *N. gruberi*.

We found that *A. castellanii* has a branched electron-transport chain with two terminal oxidases that both have the capacity to support oxygen respiration. We showed that *A. castellanii* trophozoites can instantaneously alter the use of the two separate branches and can redirect the flow of electrons from one branch to the other. The inhibition of the alternative oxidase (AOX) resulted in halted growth of *A. castellanii* trophozoites. The

most likely explanation for this finding is that the AOX has a crucial role in protecting against oxidative stress. Upon removal of the AOX inhibitor, growth was again observed, indicating that this process is reversible. A similar result was found when complex III was inhibited with potassium cyanide, which resulted in halted growth that was reversible upon removal of the inhibitor. Although genomic and proteome analyses indicated that this amoeba has anaerobic capacity<sup>15-17</sup>, we revealed that *A. castellanii* trophozoites need oxygen for normal functioning. The amoebae take on a rounded form in anaerobic conditions and halt movement and growth, but quickly return to their trophozoite shape and recommence migration and growth when oxygen is again available, similar to the results observed in the experiments with electron-transport chain inhibitors. Experiments with radioactively labelled substrates revealed a remarkably similar nutrient preference of *A. castellanii* compared to *N. gruberi*. Lipids were catabolized by *A. castellanii* at high rates compared to glucose, resulting in a 45-fold larger amount of ATP produced as a result of the oxidation of lipids compared to the oxidation of glucose. Finally, we observed that the presence of lipids stimulated the growth of *A. castellanii*, underlining the importance of lipids in the metabolism of *A. castellanii*.

## **Diagnosis and treatment of infections caused by free-living amoebae**

### **Diagnostic methods**

The road towards a diagnosis of an infection with a pathogenic FLA is challenging, as an infection by these organisms is not routinely suspected. Only when the usual causes of infection (bacterial, viral, fungal) are excluded and the usual treatments do not have an effect, pathogenic FLA are considered as a cause of infection. This results in significant doctor's delay which has a major impact on the outcome. Another challenge is to obtain quick and accurate results after an appropriate sample is acquired. Amoebae can be detected in patient samples in three ways: using microscopy, culturing or molecular diagnostics. Microscopy is routinely available, but recognizing an amoeba within cerebrospinal fluid requires expertise that is not always available. Culturing amoebae is laborious and time-consuming, which is not ideal in a situation of a brain infection where time is of the essence. Molecular techniques, on the other hand, have enormous potential to produce quick and highly sensitive results. Metagenomic next-generation sequencing (mNGS) has also been described to be of diagnostic value<sup>18-20</sup>. This latter method is unbiased and therefore does not require prior knowledge of potential pathogens. In this way, mNGS can detect pathogenic FLA even if these organisms are not suspected as a cause of infection.

For *Acanthamoeba* keratitis, the before-mentioned aspects of obtaining a diagnosis are also true <sup>21</sup>. Ophthalmologists need to be aware of the possibility of *Acanthamoeba* as the cause of the infection, and once *Acanthamoeba* keratitis is suspected, the presence of *Acanthamoeba* can be determined using multiple diagnostic tools. The advantages and limitations of the most common methods are shown in table 2.

**Table 2.** Overview of options to diagnose *Acanthamoeba* keratitis.

Method	Material	Advantages	Limitations
Culture	Corneal scrapings	Low material costs	Laborious and time-consuming
Direct confocal microscopy	The cornea is directly visualized	Quick	Requires expensive specialized equipment and highly trained personnel
Nucleic-acid amplification tests (NAAT)	Corneal scrapings	High sensitivity, relatively quick, can be easily implemented	High costs, no standardization

While each diagnostic method has its own advantages and limitations, NAAT-based tests are generally considered to be the most sensitive and easiest to implement. However, there is no standardization in methodology, and for that reason, a large diversity of NAATs is expected to be in use. Therefore, we conducted a survey on methodology in combination with an external quality assessment scheme (EQAS) for the detection of *Acanthamoeba* trophozoites and cysts. We found that a large variation in methodologies was used, especially concerning the pre-treatment methods that were applied before DNA was extracted. The diagnostic performance also varied substantially, with seven of sixteen participants reporting false negative results. Direct correlation of performance with pre-treatment methods proved difficult, but some interesting findings included that five out of the six laboratories that did not use a pre-treatment procedure reported an average C<sub>q</sub>-value above the median value for the set of cysts samples. Furthermore, again for the cyst samples, all five participants that reported the lowest C<sub>q</sub> values used some form of pre-treatment. Two of the laboratories that used bead-beating reported inhibited or false negative results of all samples. These findings indicate that the use of any pre-treatment should be carefully considered in NAAT-based detection of *Acanthamoeba*. On the one hand, it can improve the sensitivity, especially when samples contain cysts. On the other hand, the extra handling steps can be a source of error and can result in false negative results. However, the EQAS cannot directly be used to identify the best NAAT-based method to detect *Acanthamoeba*, but it is informative for routine diagnostic laboratories to assist in the evaluation of the performance of their NAAT-based detection of *Acanthamoeba* in clinical practice. We have compared different pre-treatment methods

in our laboratory, which led to adjustments in the methodology and an improvement in the detection of *Acanthamoeba*.

## Novel drug targets

Developing new drugs for infections can be done using roughly two different strategies. On one side, there is high-throughput screening (HTS), while on the other side, there is a target-based approach. In the case of HTS a large library of random compounds is tested against a pathogen, in the hope of finding some that have an inhibitory effect on growth. This strategy involves a lot of repetitive labour, and thus automated systems and robotics can be of use. A target-based approach focuses on the identification of a pathogen-specific process that can be inhibited and thus this strategy involves more fundamental research. Besides learning more about the processes going on inside a pathogen, this strategy can identify a new class of drugs that could be active against a pathogen.

### *Naegleria spp.*

New drugs for the treatment of Primary Amoebic Meningoencephalitis (PAM) are urgently needed. The current treatment regimen includes amphotericin B and miltefosine, which have been developed for the treatment of fungal and parasitic infections, respectively. Repurposing drugs is the most promising way to obtain new drugs for the treatment of PAM, as there is no financial incentive for pharmaceutical companies to develop new drugs for such a rare and fulminant disease. We applied the target-based strategy in our search for new drugs against PAM. We discovered that the nutritional preference of *N. gruberi* is unusual, as the amoebae preferred fatty acids over glucose. This unique feature can be utilized to identify new treatment options. Human cells do not rely on lipid oxidation to the same extent as *N. gruberi*, making this an interesting therapeutic target. There are multiple existing drugs that inhibit fatty acid metabolism, either by design or as a secondary effect. An overview of these drugs with their respective properties and inhibitory effects on *N. fowleri* and *A. castellanii* is shown in Table 3. We found that several of these drugs inhibited the growth of *N. gruberi* as well as *N. fowleri*. Furthermore, synergy was found between a number of fatty acid oxidation inhibitors when combined with miltefosine. The most promising findings were that thioridazine and perhexiline were effective in very low concentrations *in vitro*. The pharmacokinetic properties of thioridazine indicate that growth inhibitory concentrations can be achieved in humans and therefore this drug could be a last resort option in patients with PAM. As the mortality of patients with PAM is very high, clinicians are probably more likely to administer drugs of which only *in vitro* data are available, than for infections with low mortality. However, *in vivo* studies should also be performed to substantiate our claims.

**Table 3.** Overview of characteristics of known inhibitors of fatty acid oxidation and their inhibitory effect on *N. fowleri* and *A. castellanii*.

Drug	Developed for the treatment of	Main target	Secondary effect	IC <sub>50</sub> - <i>N. fowleri</i> (μM)	IC <sub>50</sub> - <i>A. castellanii</i> (μM)
Thioridazine	Schizophrenia and psychosis	Dopamine receptors	Inhibition of peroxisomal β-oxidation	5-10	2-4
Perhexiline	Angina pectoris	Carnitine palmitoyltransferase-1	None	5-20	1-2
Valproic acid	Epilepsy	Unclear, possibly sodium channels and histone deacetylases	Inhibition of mitochondrial β-oxidation	*	*
Etomoxir	Type 2 diabetes and heart failure	Carnitine palmitoyltransferase-1	None	100-150	40-80
Orlistat	Obesity	Lipase	None	*	*

An asterisk (\*) indicates no inhibitory effect.

### *Acanthamoeba* spp.

There is insufficient knowledge on how to manage infections caused by *Acanthamoeba*, particularly when it comes to treating *Acanthamoeba* Granulomatous Amoebic Encephalitis (GAE)<sup>10</sup>. A limited number of drugs are known to be effective *in vitro*, and even fewer drugs have shown activity *in vivo*, underscoring the urgent need for new treatment options. Similar to *Naegleria* spp., the preference for fatty acids as a nutrient source for energy metabolism could be utilized to discover potential new treatment options for infections with *Acanthamoeba* spp. We therefore exposed *A. castellanii* to the same drugs that were effective against *N. gruberi* and *N. fowleri*. The findings were similar to those in both *Naegleria* spp., with thioridazine and perhexiline strongly inhibiting growth in concentrations attainable in serum and brain tissue. Preliminary data (not shown) indicate that the *in vitro* efficacy of known antifungal and antibacterial drugs that are often used to treat GAE is highly variable. We found that some often-used drugs for GAE showed negligible effects on *A. castellanii* growth *in vitro*, such as trimethoprim-sulfamethoxazole, rifampicin, fluconazole and sulfadiazine. Potent *in vitro* effects were seen of voriconazole, which inhibited growth in low concentrations. Voriconazole is currently not part of the recommended regimen for the treatment of *Acanthamoeba* GAE, and as such these preliminary results are worthwhile to investigate further.

## Consequences of interactions between FLA and bacteria

### FLA as a shelter for bacteria

Most commonly, *Acanthamoeba* is found in soil, dust, and fresh or salt water sources. However, *Acanthamoeba* can also be found in swimming pools <sup>22</sup>, cooling towers <sup>23</sup>, drinking water distribution systems <sup>24</sup> and hospital sewage systems <sup>25,26</sup>. In all places there is continuous interaction between amoebae and bacteria, resulting in relationships varying from predation to symbiosis. One of the bacteria they regularly encounter is *Pseudomonas aeruginosa*, a pathogen that can cause life-threatening infections, mostly in immunocompromised patients <sup>27</sup>. *P. aeruginosa* has been described to survive inside *Acanthamoeba* cysts <sup>28</sup>. This *Acanthamoeba* life stage is resistant to drought, chemical stress, temperature stress and disinfection treatments <sup>29</sup>. We have shown that *P. aeruginosa*, whilst inside *A. castellanii*, can survive chlorine exposure, a disinfectant that is routinely used to disinfect hospital surroundings.

This research was extended to the non-pathogenic FLA *Vermamoeba vermiformis*. *V. vermiformis* is known to act as a host or transport vehicle for several bacteria, among which mycobacteria <sup>25,30,31</sup>. The significance of *V. vermiformis* could be substantial because of its widespread presence in fresh surface water <sup>32</sup>, recreational waters <sup>33</sup> and engineered water systems all around the world <sup>34</sup>. We found that *V. vermiformis* was also present in the water inside heater-cooler units (HCU), which are used during cardiothoracic surgery. The compartments with water inside of an HCU were previously found to be the source of *Mycobacterium chimaera* <sup>35</sup>. *M. chimaera* can cause a disseminated infection when it directly enters the body. This can occur during cardiothoracic surgery when the bacterium is aerosolized and displaced from the HCU to the operating area <sup>36</sup>. Despite the implementation of different disinfection strategies, *M. chimaera* can persist within the HCU <sup>37</sup>. We hypothesized that *V. vermiformis* could play a role in the persistence of *M. chimaera* inside the water compartments of HCU. We found in our *in vitro* study that the presence of *V. vermiformis* increased the survival of *M. chimaera* after chlorine exposure <sup>38</sup>. In this way, *V. vermiformis* acts as a facilitator for *M. chimaera*, either via direct protection through its sturdy cyst shell or via enabling increased replication of *M. chimaera*. Both these mechanisms could also work in parallel.

As HCU are routinely cleaned with chlorine, *V. vermiformis* cysts and intracellular *M. chimaera* could persist after cleaning, albeit in low concentrations. *V. vermiformis* could then transform back into trophozoites, which prompts *M. chimaera* to start replicating

inside *V. vermiformis* and eventually escape into the extracellular environment, from which it could then infect patients. Before the next cleaning, the amoebal and bacterial burden within the HCU would be high. In this situation, *M. chimaera* could be inside *V. vermiformis* cysts, resulting in the survival of both organisms after another round of cleaning and disinfection, creating a new chance for *M. chimaera* to infect patients. A possible solution to this problem would be to use a disinfectant that is cysticidal or to place the HCU outside the operating theatre. In the Erasmus MC, no new cases occurred after placement of the HCU outside the operating theatre.

### FLA as a facilitator of plasmid transfer among bacteria

While inside *Acanthamoeba* spp., bacteria are exposed to a range of hydrolytic enzymes which are meant to break down the bacterium. However, some bacteria can survive inside *Acanthamoeba* spp.<sup>39,40</sup>. The mechanisms by which this occurs are not fully understood. For some bacterial species such as *Legionella* spp. the inhibition of phagosome-lysosome fusion has been described to be of importance<sup>41</sup>, but for others such as *Vibrio cholerae*, a toxin-related process is involved in survival<sup>2</sup>. Phagocytosis results in stress for the bacterium, which has been shown for *Escherichia coli* and *V. cholerae*, as both organisms activate the SOS-response upon interaction with *A. castellanii*<sup>42,43</sup>. Furthermore, bacteria are placed together in close proximity in a vacuole and as such, bacteria might be more prone to exchange genetic material. This has also been supported by other studies, which have dubbed amoebae as a “melting pot” in which genetic material can be exchanged between different bacteria<sup>44-46</sup>. Antimicrobial resistance genes (ARG) are examples of clinically important genetic material that can be exchanged, resulting in a bacterium becoming resistant to a certain antibiotic. We set out to determine whether *A. castellanii* was able to promote the transfer of a plasmid containing an ARG between different *Pseudomonas* spp. We therefore set up an *in vitro* experiment in which different environmental *Pseudomonas aeruginosa* strains were placed together with an environmental *P. oleovorans*, in the presence and absence of *A. castellanii*. The *P. oleovorans* carried a plasmid that contained a Verona-Integron-encoded-Metallo- $\beta$ -lactamase ( $bla_{VIM-2}$ ), which results in resistance to carbapenem antibiotics. We found that the  $bla_{VIM-2}$  gene was, compared to all the other used strains, efficiently transferred to one specific acceptor strain (957). Furthermore, the transfer rate was greatly increased in the presence of *A. castellanii* compared to its absence. We also performed confocal imaging, which revealed the presence of both donor (*P. oleovorans*) and acceptor (*P. aeruginosa*-957) species inside *A. castellanii*. As all three organisms can be isolated from hospital water systems, this *in vitro* situation could reflect the real-world situation. However, the extent to which this contributes to the spread of ARG in the hospital environment should be further investigated.

## Concluding remarks and future perspectives

The four most important findings of our research are (i) the importance of oxygen for normal functioning of FLA, (ii) the preference for lipids as a food source, resulting in new possible treatment options for infections with pathogenic FLA, (iii) the protection of *P. aeruginosa* and *M. chimaera* by cysts of FLA against disinfection with chlorine, and (iv) the facilitation by *A. castellanii* of plasmid transfer between *P. oleovorans* and *P. aeruginosa*.

We have shown that metabolic experiments using labelled substrates are essential to determine the metabolic properties of microorganisms. Modelling based on genomic information can provide interesting hypotheses, but always needs to be validated using experimental metabolic studies. Many genes could still be present in micro-organisms as remnants of a distant past, where the gene was once active, but now no longer is. We have made an effort to connect fundamental research to clinical application, with the identification of a drug target and possible new treatment options. Our research can be extended in multiple ways. First, lipid oxidation inhibitors need to be investigated in an *in vivo* model of PAM and GAE. Furthermore, the development of new drugs to inhibit fatty acid oxidation is an active research field in cardiology<sup>47</sup>. Any new drugs that are developed should be evaluated for their inhibitory effect on the growth of *N. fowleri* and *Acanthamoeba* spp. It might be tempting to make changes to the structure of the already identified fatty acid oxidation inhibitors to enhance their activity. However, it will not be possible to ever bring these new compounds to market for treatment of PAM or GAE, due to the rarity and fatality of these diseases. Therefore, future endeavours should focus on the repurposing of existing and approved drugs. Lastly, the importance of fatty acid oxidation as a means of generating ATP is not yet studied in other pathogenic protozoa. As such, metabolic studies and the evaluation of fatty acid oxidation inhibitors should be extended to other pathogenic protozoa.

We have described the metabolism of actively growing *A. castellanii* trophozoites, but the metabolism of cysts and pseudocysts is still unknown. Pseudocysts are proposed to be a separate life stage from cysts (but this is debated), which develop rapidly in response to acute environmental changes<sup>48</sup>. Cysts and pseudocysts can survive for long periods in nutrient-poor conditions and likely halt their metabolism during this period. However, studies regarding the metabolic activity of cysts and pseudocysts are lacking. Regarding respiration, we have preliminary data that pseudocysts consume approximately 11% of the oxygen that actively growing trophozoites consume. The oxygen consumption of cysts was too low to measure using our experimental methods (Clark-type electrode). Further studies regarding the (halted) metabolism and respiration of pseudocysts and cysts are needed.

In the field of diagnosis and treatment of *Acanthamoeba* keratitis, our research could be extended as well. We have shown that many different pre-treatment methods are used in clinical practice. However, it remains unknown which method is most effective at detecting *Acanthamoeba* trophozoites and cysts. We have unpublished data that show that a freeze-thaw cycle results in excellent detection of *Acanthamoeba* cysts, without the extra handling steps that are involved in a physical disruption method like bead-beating. We have updated and validated our pre-treatment method for clinical samples which now includes a freeze-thaw cycle. Future directions in the treatment of *Acanthamoeba* keratitis could include fatty acid oxidation inhibitors. The toxic effects of these compounds on the eye are unknown and should be investigated, as high concentrations of the different drugs can possibly be achieved. Furthermore, a novel method of delivering miltefosine has been studied *in vivo*, by using a contact lens impregnated with the drug<sup>49</sup>. This revolutionary method deserves attention and might be used for other drugs as well.

Interactions between different micro-organisms is a neglected area of research. For practical reasons, usually monocultures are used in research. However, in nature, this situation is virtually absent, because a plethora of different micro-organisms is normally present. Interactions between micro-organisms are also significant in patients. An interesting example is the presence of bacteria inside *Acanthamoeba* recovered from patients with *Acanthamoeba* keratitis. These bacteria are believed to exacerbate damage to the corneal epithelium<sup>39,50</sup>. We were able to reveal some very interesting relationships between FLA and bacteria, such as the protection of bacteria by FLA cysts. This principle could extend to other bacteria as well, as other pathogens such as *Legionella pneumophila* and multiple nontuberculous mycobacteria have been shown to co-occur with *Acanthamoeba* spp. in a hospital water network<sup>26,51</sup>. To circumvent the problem of bacteria surviving inside FLA cysts, not only the bactericidal activity of disinfectants should be assessed, but the cysticidal activity should also be evaluated. We showed in chapter 7 that acetic acid was effective in killing *P. aeruginosa*, even in the presence of *Acanthamoeba castellanii*, which makes this disinfectant a promising option for disinfection of the hospital surroundings.

We observed the increased transfer of a large plasmid containing an ARG between *P. oleovorans* and a specific strain of *P. aeruginosa* in the presence of *A. castellanii*. Several remarkable aspects of this finding deserve further attention. Eighteen other *P. aeruginosa* strains did not acquire the plasmid, or only at negligible rates. This could be due to plasmid incompatibility groups<sup>52</sup>, but many other factors could play a role, such as the presence of secretion systems or the capacity to form a biofilm<sup>53</sup>. More research is needed to elucidate the mechanisms behind our findings. Furthermore, the plasmid transfer was greatly increased in the presence of *A. castellanii*, the reasons of which are yet unexplained.

Internalization of both the plasmid donor and acceptor bacteria, and also the resulting stressful conditions may be involved. A possible mechanism could be the activation of the SOS-response, which has been described in *E. coli* and *V. cholerae* after predation by *A. castellanii*<sup>42,43</sup>. However, many other mechanisms could be responsible, such as upregulation of the plasmid copy number by the donor or reduced activity of the foreign DNA detection systems by the acceptor<sup>54</sup>, which warrants further research. Our findings can be extended to many different amoebae and many different bacteria and therefore much more is still to be discovered. A promising example is the interaction between gut amoeba and bacteria living in the gastrointestinal tract. Furthermore, the interaction between FLA and other environmental bacteria that cause hospital-acquired infections, such as *Acinetobacter baumannii*, can be promising. Lastly, environmental studies in the hospital can be useful to determine the extent to which these interactions are happening.

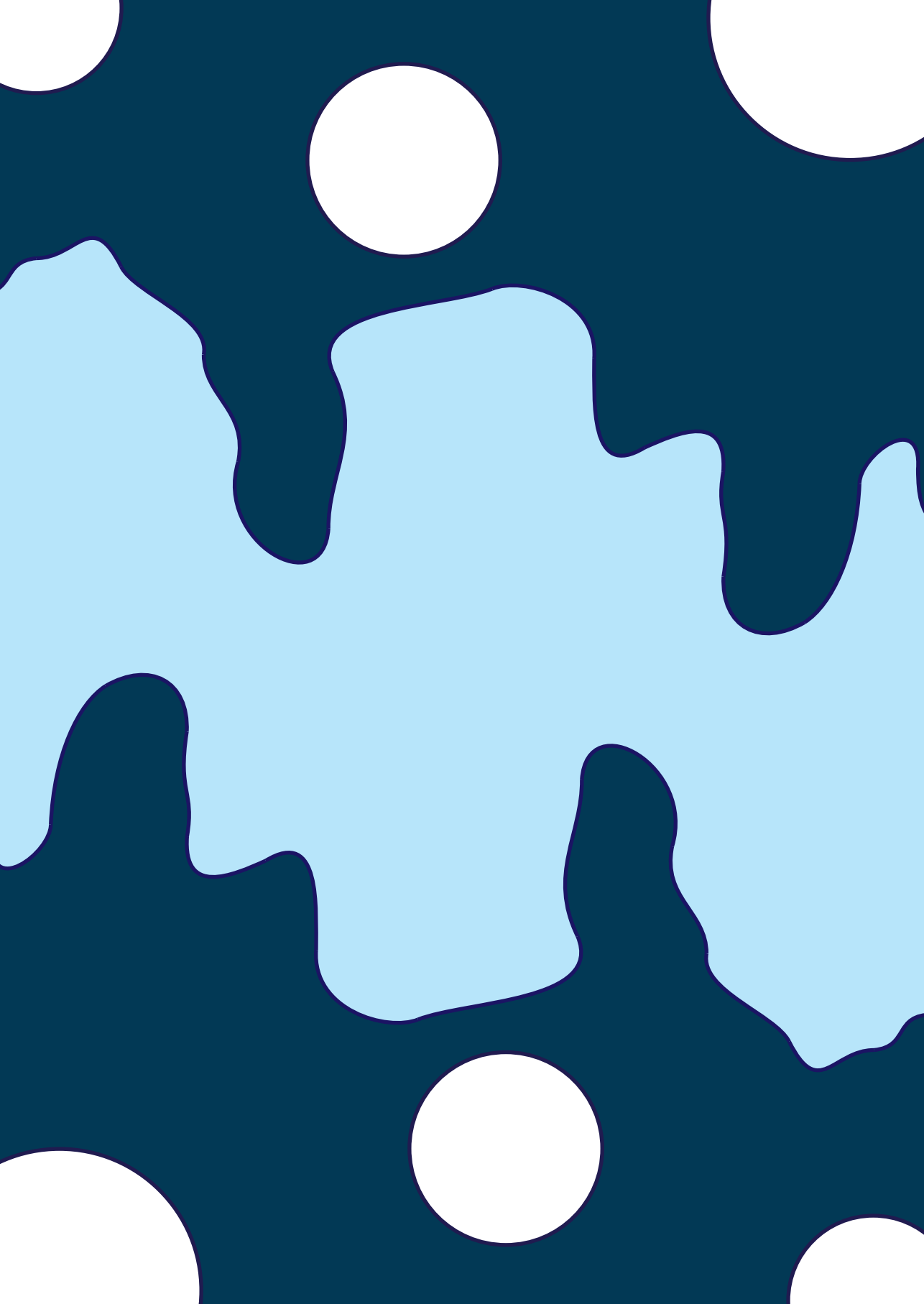
We have shown that FLA can be positioned at various locations on the pitch when it comes to infection. They can defend other microorganisms by protecting them from harmful substances when these bacteria are inside cysts. They can also assist other microorganisms by facilitating the exchange of genetic material. On the other hand, some FLA can attack and be perpetrators of infection themselves. An infection by an FLA oftentimes results in death and treatment is difficult. For these deadly infections, we discovered new treatment targets and possible drugs, which need further clinical validation before they can be applied.

## References

- 1 Shi, Y. *et al.* The Ecology and Evolution of Amoeba-Bacterium Interactions. *Appl Environ Microbiol* **87** e01866-20 (2021).
- 2 Van der Henst, C. *et al.* Molecular insights into *Vibrio cholerae*'s intra-amoebal host-pathogen interactions. *Nat Commun* **9**, 3460 (2018).
- 3 Lambrecht, E. *et al.* Protozoan Cysts Act as a Survival Niche and Protective Shelter for Foodborne Pathogenic Bacteria. *Appl Environ Microbiol* **81**, 5604-5612 (2015).
- 4 Lima, T. S. & Lodoen, M. B. Mechanisms of Human Innate Immune Evasion by *Toxoplasma gondii*. *Front Cell Infect Microbiol* **9**, 103 (2019).
- 5 Lindblade, K. A., Steinhart, L., Samuels, A., Kachur, S. P. & Slutsker, L. The silent threat: asymptomatic parasitemia and malaria transmission. *Expert Rev Anti Infect Ther* **11**, 623-639 (2013).
- 6 Maciver, S. K., Piñero, J. E. & Lorenzo-Morales, J. Is *Naegleria fowleri* an emerging parasite? *Trends Parasitol* **36**, 19-28 (2020).
- 7 Hall, A. D., Kumar, J. E., Golba, C. E., Luckett, K. M. & Bryant, W. K. Primary amebic meningoencephalitis: a review of *Naegleria fowleri* and analysis of successfully treated cases. *Parasitol Res* **123**, 84 (2024).
- 8 Szentmáry, N. *et al.* *Acanthamoeba* keratitis - Clinical signs, differential diagnosis and treatment. *J Curr Ophthalmol* **31**, 16-23 (2019).
- 9 Król-Turmińska, K. & Olender, A. Human infections caused by free-living amoebae. *Ann Agric Environ Med* **24**, 254-260 (2017).
- 10 Spottiswoode, N. *et al.* Challenges and advances in the medical treatment of granulomatous amebic encephalitis. *Ther Adv Infect Dis* **11**, 20499361241228340 (2024).
- 11 Molmeret, M., Horn, M., Wagner, M., Santic, M. & Abu Kwaik, Y. Amoebae as Training Grounds for Intracellular Bacterial Pathogens. *Appl Environ Microbiol* **71**, 20-28 (2005).
- 12 De Jonckheere, J. F. Origin and evolution of the worldwide distributed pathogenic amoeboflagellate *Naegleria fowleri*. *Infect Genet Evol* **11**, 1520-1528 (2011).
- 13 Bexkens, M. L. *et al.* Lipids are the preferred substrate of the protist *Naegleria gruberi*, relative of a human brain pathogen. *Cell Rep* **25**, 537-543 e533 (2018).
- 14 Karygianni, L., Ren, Z., Koo, H. & Thurnheer, T. Biofilm Matrixome: Extracellular Components in Structured Microbial Communities. *Trends Microbiol* **28**, 668-681 (2020).
- 15 Clarke, M. *et al.* Genome of *Acanthamoeba castellanii* highlights extensive lateral gene transfer and early evolution of tyrosine kinase signaling. *Genome Biol* **14**, R11 (2013).
- 16 Ginger, M. L., Fritz-Laylin, L. K., Fulton, C., Cande, W. Z. & Dawson, S. C. Intermediary metabolism in protists: a sequence-based view of facultative anaerobic metabolism in evolutionarily diverse eukaryotes. *Protist* **161**, 642-671 (2010).
- 17 Leger, M. M., Gawryluk, R. M., Gray, M. W. & Roger, A. J. Evidence for a hydrogenosomal-type anaerobic ATP generation pathway in *Acanthamoeba castellanii*. *PLoS One* **8**, e69532 (2013).
- 18 Huang, S. *et al.* A pediatric case of primary amoebic meningoencephalitis due to *Naegleria fowleri* diagnosed by next-generation sequencing of cerebrospinal fluid and blood samples. *BMC Infect Dis* **21**, 1251 (2021).
- 19 Che, X., He, Z., Tung, T. H., Xia, H. & Lu, Z. Diagnosis of primary amoebic meningoencephalitis by metagenomic next-generation sequencing: A case report. *Open Life Sci* **18**, 20220579 (2023).
- 20 Hirakata, S. *et al.* The application of shotgun metagenomics to the diagnosis of granulomatous amoebic encephalitis due to *Balamuthia mandrillaris*: a case report. *BMC Neurol* **21**, 392 (2021).
- 21 List, W. *et al.* Evaluation of *Acanthamoeba* keratitis cases in a tertiary medical care centre over 21 years. *Sci Rep* **11**, 1036 (2021).

- 22 Chaúque, B. J. M., Dos Santos, D. L., Anvari, D. & Rott, M. B. Prevalence of free-living amoebae in swimming pools and recreational waters, a systematic review and meta-analysis. *Parasitol Res* **121**, 3033-3050 (2022).
- 23 Soares, S. S., Souza, T. K., Berté, F. K., Cantarelli, V. V. & Rott, M. B. Occurrence of Infected Free-Living Amoebae in Cooling Towers of Southern Brazil. *Current Microbiology* **74**, 1461-1468 (2017).
- 24 Javanmard, E. *et al.* Molecular identification of waterborne free living amoebae (*Acanthamoeba*, *Naegleria* and *Vermamoeba*) isolated from municipal drinking water and environmental sources, Semnan province, north half of Iran. *Exp Parasitol* **183**, 240-244 (2017).
- 25 Nisar, M. A. *et al.* Molecular screening and characterization of *Legionella pneumophila* associated free-living amoebae in domestic and hospital water systems. *Water Res* **226**, 119238 (2022).
- 26 Ovrutsky, A. R. *et al.* Cooccurrence of free-living amoebae and nontuberculous Mycobacteria in hospital water networks, and preferential growth of *Mycobacterium avium* in *Acanthamoeba lenticulata*. *Appl Environ Microbiol* **79**, 3185-3192 (2013).
- 27 Pezzani, M. D. *et al.* Frequency of bloodstream infections caused by six key antibiotic-resistant pathogens for prioritization of research and discovery of new therapies in Europe: a systematic review. *Clin Microbiol Infect* **30**, S4-S13 (2023).
- 28 Siddiqui, R., Lakhundi, S. & Khan, N. A. Interactions of *Pseudomonas aeruginosa* and *Corynebacterium* spp. with non-phagocytic brain microvascular endothelial cells and phagocytic *Acanthamoeba castellanii*. *Parasitol Res* **114**, 2349-2356 (2015).
- 29 Coulon, C., Collignon, A., McDonnell, G. & Thomas, V. Resistance of *Acanthamoeba* cysts to disinfection treatments used in health care settings. *J Clin Microbiol* **48**, 2689-2697 (2010).
- 30 Petitjean, M. *et al.* The rise and the fall of a *Pseudomonas aeruginosa* endemic lineage in a hospital. *Microb Genom* **7**, 000629 (2021).
- 31 Delafont, V., Rodier, M.-H., Maisonneuve, E. & Cateau, E. *Vermamoeba vermiformis*: a Free-Living Amoeba of Interest. *Microb Ecol* **76**, 991-1001 (2018).
- 32 Kuiper, M. W. *et al.* Quantitative detection of the free-living amoeba *Hartmannella vermiformis* in surface water by using real-time PCR. *Appl Environ Microbiol* **72**, 5750-5756 (2006).
- 33 Nazar, M. *et al.* Molecular identification of *Hartmannella vermiformis* and *Vannella persistens* from man-made recreational water environments, Tehran, Iran. *Parasitol Res* **111**, 835-839 (2012).
- 34 Valster, R. M., Wullings, B. A., Bakker, G., Smidt, H. & van der Kooij, D. Free-living protozoa in two unchlorinated drinking water supplies, identified by phylogenetic analysis of 18S rRNA gene sequences. *Appl Environ Microbiol* **75**, 4736-4746 (2009).
- 35 van Ingen, J. *et al.* Global outbreak of severe *Mycobacterium chimaera* disease after cardiac surgery: a molecular epidemiological study. *Lancet Infect Dis* **17**, 1033-1041 (2017).
- 36 Riccardi, N. *et al.* *Mycobacterium chimaera* infections: An update. *J Infect Chemother* **26**, 199-205 (2020).
- 37 Ditommaso, S., Giacomuzzi, M., Memoli, G. & Zotti, C. M. Failure to eradicate non-tuberculous mycobacteria upon disinfection of heater-cooler units: results of a microbiological investigation in northwestern Italy. *J Hosp Infect* **106**, 585-593 (2020).
- 38 Sarink, M. J. *et al.* *Vermamoeba vermiformis* resides in water-based heater-cooler units and can enhance *Mycobacterium chimaera* survival after chlorine exposure. *J Hosp Infect* **132**, 73-77 (2022).
- 39 Rayamajhee, B. *et al.* The role of naturally acquired intracellular *Pseudomonas aeruginosa* in the development of *Acanthamoeba* keratitis in an animal model. *PLoS Negl Trop Dis* **18**, e0011878 (2024).
- 40 Rayamajhee, B. *et al.* *Acanthamoeba*, an environmental phagocyte enhancing survival and transmission of human pathogens. *Trends Parasitol* **38**, 975-990 (2022).
- 41 Guimaraes, A. J., Gomes, K. X., Cortines, J. R., Peralta, J. M. & Peralta, R. H. *Acanthamoeba* spp. as a universal host for pathogenic microorganisms: One bridge from environment to host virulence. *Microbiol Res* **193**, 30-38 (2016).

- 42 Carruthers, M. D., Bellaire, B. H. & Minion, F. C. Exploring the response of *Escherichia coli* O157:H7 EDL933 within *Acanthamoeba castellanii* by genome-wide transcriptional profiling. *FEMS Microbiol Lett* **312**, 15-23 (2010).
- 43 Rahman, M. H. *et al.* Protozoal food vacuoles enhance transformation in *Vibrio cholerae* through SOS-regulated DNA integration. *The ISME Journal* **16**, 1993-2001 (2022).
- 44 Moliner, C., Fournier, P. E. & Raoult, D. Genome analysis of microorganisms living in amoebae reveals a melting pot of evolution. *FEMS Microbiol Rev* **34**, 281-294 (2010).
- 45 Bertelli, C. & Greub, G. Lateral gene exchanges shape the genomes of amoeba-resisting microorganisms. *Front Cell Infect Microbiol* **2**, 110 (2012).
- 46 Price, C. T. D. *et al.* Amoebae as training grounds for microbial pathogens. *mBio*, e0082724 (2024).
- 47 Wen, J. & Chen, C. From Energy Metabolic Change to Precision Therapy: a Holistic View of Energy Metabolism in Heart Failure. *J Cardiovasc Transl Res* **17**, 56-70 (2023).
- 48 Kliescikova, J., Kulda, J. & Nohynkova, E. Stress-induced pseudocyst formation--a newly identified mechanism of protection against organic solvents in acanthamoebae of the T4 genotype. *Protist* **162**, 58-69 (2011).
- 49 Chen, L. *et al.* Topical Sustained Delivery of Miltefosine Via Drug-Eluting Contact Lenses to Treat *Acanthamoeba* Keratitis. *Pharmaceutics* **14**, 2750 (2022).
- 50 Rayamajhee, B. *et al.* Assessment of genotypes, endosymbionts and clinical characteristics of *Acanthamoeba* recovered from ocular infection. *BMC Infect Dis* **22**, 757 (2022).
- 51 Casini, B. *et al.* Detection of viable but non-culturable legionella in hospital water network following monochloramine disinfection. *J Hosp Infect* **98**, 46-52 (2018).
- 52 Bethke, J. H. *et al.* Environmental and genetic determinants of plasmid mobility in pathogenic *Escherichia coli*. *Sci Adv* **6**, eaax3173 (2020).
- 53 Michaelis, C. & Grohmann, E. Horizontal Gene Transfer of Antibiotic Resistance Genes in Biofilms. *Antibiotics (Basel)* **12**, 328 (2023).
- 54 Virolle, C., Goldlust, K., Djermoun, S., Bigot, S. & Lesterlin, C. Plasmid Transfer by Conjugation in Gram-Negative Bacteria: From the Cellular to the Community Level. *Genes (Basel)* **11**, 1239 (2020).



# APPENDICES

---

Nederlandstalige samenvatting  
Dank(kruis)woord  
Curriculum vitae  
PhD portfolio  
List of publications

## Nederlandstalige samenvatting

### Amoeben en evolutie

Amoeben bestaan er in veel verschillende soorten en maten. Zo kunnen de amoeben uit het genus “*Chaos*” wel 5 millimeter (500 micrometer) groot zijn, maar er zijn ook amoeben zoals “*Nuclearia*” die zo’n 10 tot 30 micrometer groot zijn. Deze verschillen zijn het gevolg van miljoenen jaren van evolutionaire druk, waarbij willekeurige mutaties leiden tot een voordeel of nadeel in overleving. Zoals er verschillende groottes van amoeben bestaan, zijn er ook grote verschillen in hoeverre amoeben gevaarlijk zijn voor de mens. Het overgrote gedeelte van de amoeben kan geen infectie veroorzaken bij mensen. Echter zijn er een paar die dit wel kunnen, we noemen deze amoeben dan “pathogeen”. Voorbeelden van pathogene amoeben zijn “*Entamoeba histolytica*” en “*Naegleria fowleri*”. Een ander onderscheid binnen amoeben kan gemaakt worden in de mate van afhankelijkheid van de mens. Een klassieke parasiet heeft een gastheer nodig om te kunnen blijven leven en om nakomelingen te produceren. Dit staat in contrast met een organisme dat geen gastheer nodig heeft en dus “vrij-levend” is. In tabel 1 is een overzicht te zien van amoeben, ingedeeld op basis van pathogeniciteit en afhankelijkheid van de mens.

**Tabel 1.** Indeling van amoeben in mate van afhankelijkheid van de mens en pathogeniciteit

	Vrij-levend	Afhankelijk van de mens
Apathogeen	<b>Vrij-levend organisme</b> <i>Naegleria gruberi</i> <i>Vermamoeba vermiformis</i>	<b>Commensaal</b> <i>Entamoeba dispar</i>
Pathogeen	<b>Facultatieve parasiet</b> <i>Naegleria fowleri</i> <i>Acanthamoeba</i> spp. <i>Balamuthia mandrillaris</i>	<b>Obligate parasiet</b> <i>Entamoeba histolytica</i>

Dit proefschrift bevat onderzoek naar vrij-levende amoeben, waarbij de pathogene varianten extra onder de loep zijn genomen. Deze amoeben kunnen ernstige infecties bij mensen veroorzaken, zoals herseninfecties door *Naegleria fowleri*, of ooginfecties door *Acanthamoeba* spp. Hiernaast is er in dit proefschrift aandacht besteed aan de interacties tussen amoeben en bacteriën.

### Pathogene vrij-levende amoeben

Er zijn drie soorten pathogene vrij-levende amoeben omschreven: *Naegleria fowleri*, *Acanthamoeba* spp. en *Balamuthia mandrillaris*. Alle drie deze soorten kunnen een infectie van de hersenen veroorzaken, en *Acanthamoeba* spp. kan ook een infectie van het oog veroorzaken.

***Naegleria fowleri***

Deze amoëbe kan voorkomen in warm zoet water, zoals ondiepe meren, warmwater bronnen en onvoldoende gechloreerde zwembaden. Als deze amoëbe in de neus terecht komt kan deze via de neuszenuw naar de hersenen gaan, waarna een ernstige infectie volgt welke vrijwel altijd leidt tot de dood. Er zijn op dit moment weinig behandelopties.

***Acanthamoeba spp.***

Er zijn veel verschillende soorten *Acanthamoeba*, daarom is er hier geen “achternaam” omschreven. De meeste *Acanthamoeba* spp. geven eenzelfde soort infectie, namelijk een ooginfectie van het hoornvlies (cornea). Dit komt met name voor bij mensen die contactlenzen dragen. Het duurt vaak lang voordat de juiste diagnose is gesteld en de behandeling is intensief. Ook komt het regelmatig voor dat de behandeling mislukt en er opnieuw een infectie plaatsvindt. Hiernaast kan *Acanthamoeba* spp. bij mensen met een ernstig verzwakt immuunsysteem een herseninfectie veroorzaken. Ook dit ziektebeeld is erg moeilijk te behandelen en leidt vaak tot de dood.

***Balamuthia mandrillaris***

Deze amoëbe is voor het eerst ontdekt in een mandril (vandaar de naam), waarbij het een herseninfectie gaf. Ook bij mensen kan deze amoëbe een infectie van de hersenen veroorzaken en ook hier zijn de behandelopties beperkt en is een infectie vaak dodelijk.

**Het metabolisme van vrij-levende amoeben**

Aangezien een infectie van de hersenen met één van de drie eerder genoemde amoeben in veel gevallen leidt tot de dood, zijn er nieuwe behandelopties nodig. Een medicament heeft vaak een specifiek proces waarop deze ingrijpt, zoals de opbouw van de celwand of het maken van DNA. In het geval van vrij-levende amoeben is het metabolisme (de voedingsstoffen die de amoëbe gebruikt) een interessant doelwit van nieuwe medicatie. Onderzoek naar *Naegleria gruberi* (het niet-pathogene zusje van *Naegleria fowleri*) heeft namelijk aangetoond dat deze amoëbe lipiden boven glucose verkiest als bron van energie. Er kan gebruik gemaakt worden van deze unieke eigenschap door het remmen van dit proces. In ons onderzoek hebben we aangetoond dat remmers van de vetzuuroxidatie leidt tot sterke remming van de groei van *Naegleria gruberi* en *Naegleria fowleri*. Daarnaast hebben we laten zien dat *Acanthamoeba castellanii* eenzelfde voorkeur heeft voor vetzuren boven glucose. Ook hier waren remmers van de vetzuuroxidatie effectief in het remmen van de groei. Mogelijk kunnen deze middelen dus in de toekomst ingezet worden voor de behandeling van infecties met *Naegleria fowleri* of *Acanthamoeba castellanii*. Tot slot hebben we in ons onderzoek naar het metabolisme laten zien dat *Acanthamoeba castellanii* zuurstof nodig heeft om normaal te functioneren. In een

anaerobe omgeving stoppen de trofozoieten met bewegen en krijgen ze een ronde vorm. Als er weer zuurstof bij de amoeben komt, veranderen ze weer in trofozoieten en bewegen ze weer verder alsof er niets is gebeurd.

## Diagnostiek bij infecties door pathogene vrij-levende amoeben

Het duurt vaak lang voordat een infectie met een vrij-levende amoebe wordt vastgesteld, omdat de arts niet snel aan deze verwekker denkt. Vaak wordt dit pas overwogen wanneer andere oorzaken zijn uitgesloten en standaardbehandelingen niet effectief zijn, wat leidt tot vertraging en slechtere uitkomsten. Zodra een infectie met een vrij-levende amoebe vermoed wordt, is het zaak om deze zo snel en accuraat mogelijk aan te tonen. Amoeben kunnen worden gedetecteerd via microscopie, kweek of met moleculaire technieken. Microscopie vereist expertise en kweken is tijdrovend. Moleculaire technieken bieden snelle en gevoelige resultaten, maar wij hebben in ons onderzoek aangetoond dat er grote verschillen zijn in de methoden die laboratoria gebruiken. Met een kwaliteitsrondzending kunnen laboratoria beoordelen of de diagnostiek die zij uitvoeren van voldoende kwaliteit is. Hiernaast kunnen ze processen in de diagnostiek identificeren waar verbetering mogelijk is.

## Interacties tussen vrij-levende amoeben en bacteriën

Amoeben hebben sinds hun ontstaan al interacties met bacteriën, welke variëren van commensalisme (beide organismen hebben een voordeel) tot parasitisme (één van de twee maakt gebruik van de ander). De meeste amoeben voeden zich met bacteriën door deze op te slokken middels fagocytose, maar er zijn bacteriën die dit proces kunnen weerstaan. Zo kunnen bacteriën in amoeben overleven en kunnen ze profiteren van bescherming van hun celwand. Hiernaast zijn er zelfs bacteriën die amoeben kunnen doden. Wij hebben in ons onderzoek de interactie bestudeerd tussen verschillende amoeben en verschillende bacteriën, welke staan omschreven in tabel 2. Ook de belangrijkste conclusies kunnen in deze tabel teruggevonden worden.

**Tabel 2.** In dit proefschrift onderzochte amoeben en bacteriën en de conclusies van dit onderzoek

Amoebe	Bacterie	Conclusie
<i>Vermamoeba vermiformis</i>	<i>Mycobacterium chimaera</i>	<i>M. chimaera</i> kan in <i>V. vermiformis</i> overleven en kan hierdoor blootstelling aan chloor weerstaan
<i>Acanthamoeba castellanii</i>	<i>Pseudomonas aeruginosa</i>	<i>P. aeruginosa</i> kan in <i>A. castellanii</i> overleven en kan hierdoor blootstelling aan chloor weerstaan
<i>Acanthamoeba castellanii</i>	<i>Pseudomonas aeruginosa</i> en <i>Pseudomonas oleovorans</i>	Zowel <i>P. aeruginosa</i> als <i>P. oleovorans</i> kan in <i>A. castellanii</i> aanwezig zijn. Een plasmide met hierop een resistentie-gen wordt in aanwezigheid van <i>A. castellanii</i> efficiënt overgedragen.

## Conclusie

Vrij-levende amoeben kunnen verschillende rollen spelen. Enerzijds kunnen ze andere pathogene micro-organismen beschermen en de uitwisseling van genetisch materiaal tussen deze micro-organismen bevorderen. Anderzijds kunnen ze ook zelf een infectie veroorzaken, welke dodelijk kan zijn. Ons onderzoek heeft nieuwe behandelopties voor deze infecties geïdentificeerd, maar verder onderzoek is nodig voordat deze kunnen worden toegepast in de klinische praktijk.

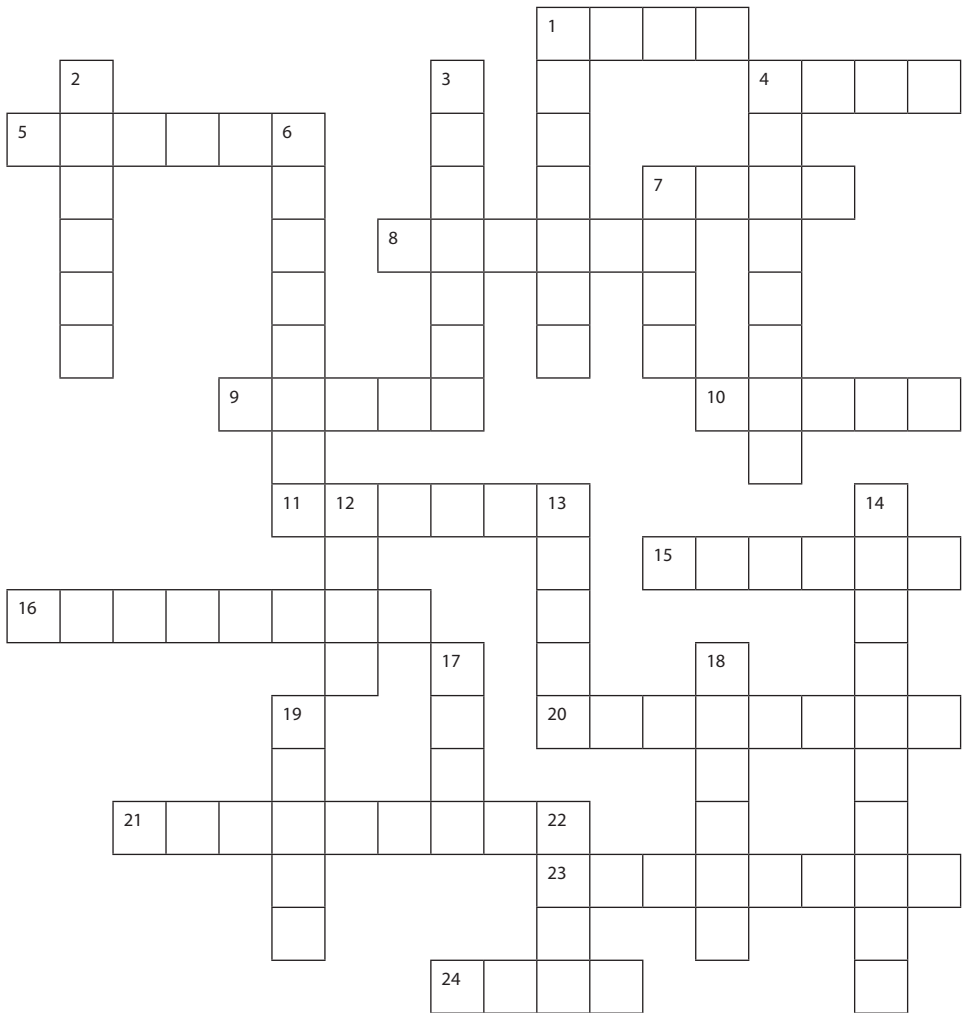
## Dank(kruis)woord

Abiding by family-tradition, my thank-you chapter is unconventional, as it is a crossword puzzle of all the first names of people that helped me in my PhD these past years! Of course you can never summarize someone in a few words, so you of course mean much more than just these descriptions ☺. Furthermore, there are probably people that I forgot which are not in the puzzle, so feel free to add some cubes and fill in your name, let me know your description!

The solution will be accessible online after my defense via:

<https://photos.app.goo.gl/gv6uFmdo5GGMbwx19>

Horizontally		Vertically	
1	Extremely passionate Italian sunshine-bringer	1	Gedreven opleidings- en onderwijs-bazin
4	Ongeëvenaarde optimist en meester van het compromis	2	Boulderboy
5	Slightly melodramatic cat lover, enthusiast of fine products	3	Elegante multi-hobbyiste met parasitologische passie
7	Marathonkoning en altijd vriendelijke allesweter op het lab	4	Charismatische (op)leider
8	Gezellige Brabantse superslecht-lijst luisteraar	6	Master of Linux, bringer of data science
9	Immer positieve mede-AIOS met aanstekelijke lach	7	Vrolijke feminist, had goede discussies met 19 verticaal
10	Onmisbaar in de keuken en ver daarbuiten	12	Science fanatic and good-natured Aussie
11	Intussen inheemse TB-onderzoeker en MMB-AIOS	13	Enthousiaste en open sociale studente
15	Doppio-kenner en de eerste klimmer, tevens eed van Hippocrates-breker	14	Ongekend minutieuze heavy metal-liefhebber
16	Would not crawl under the table upon 10-0 loss ;)	17	De allerliefste, allerbeste en allerbelangrijkste, ik hou van jou ∞
20	Grenzeloze verbandenlegger en indrukwekkende duizendpoot	18	Mede Joost fan en chaotische festivalvaller
21	Groep van wijzen met zeer indrukwekkende achtergronden	19	Tafelvoetbaltopper, had goede discussies met 7 verticaal
23	Grandioze woordmagiër en nog steeds gepassioneerde labrat	22	Bizzey-loving cosmopolitan
24	Doortastende doorzetter, zowel in het lab als bij de voetbal(tafel)		



## **Curriculum vitae**

Maarten Just Sarink was born on March 16th of 1992 in Gouda, The Netherlands. He attended the Goudse scholengemeenschap Leo Vroman where he successfully completed his secondary education (VWO) in 2010. In that same year he started his medical studies at the Erasmus MC in Rotterdam, where he obtained his bachelor's degree in 2014. During his master's clinical internships he came in contact with a medical microbiologist, who sparked his interest in infectious diseases. He then decided to do an internship at the department of Medical Microbiology and Infectious Diseases at the Erasmus MC in the tuberculosis research group of dr. Jurriaan de Steenwinkel. During this internship he studied dormancy in tuberculosis involving the 18b strain and the effects of known and new anti-tuberculosis drugs on this strain. Following this internship he obtained his medical degree in 2017. In that same year he started his Ph.D. on free-living amoebae under the supervision of prof. dr. Lodewijk Tielens and prof. dr. Jaap van Hellemond, which resulted in this thesis. In 2021 he started as a resident in Medical Microbiology (dr. Lonneke Bode and dr. Jurriaan de Steenwinkel) during which he finished writing this thesis. Maarten is married to Rosalie Sarink-Werlich and together they have two sons: Mads (2022) and Jip (2025).

## PhD Portfolio

PhD candidate: Maarten Sarink  
 Institute: Erasmus MC  
 Department: Medical Microbiology and Infectious Diseases  
 Promotors: Prof. Dr. A.G.M. Tielens, Prof. Dr. A. Verbon, Prof. Dr. J.J. van Hellemond

### Awards

EMBO workshop: Molecular advances and parasite strategies in host infection – Best poster	2018
EMBO Short-term Fellowship grant	2019

### Multi-day conferences

Science Days of Department of Internal Medicine of Erasmus MC – Antwerp	2018
EMBO workshop: Molecular advances and parasite strategies in host infection – Les Embiez	2018 (poster)
British Society for Parasitology Spring Meeting – Manchester	2019 (speaker)
ECCMID – Lisbon	2022 (online, poster)
ECCMID – Barcelona	2024 (poster + flash session)

### Scientific meetings

Netherlands Society for Parasitology – spring meeting	2017
	2018 (speaker)
	2021
Netherlands Society for Parasitology – fall meeting	2017
	2018
	2019
	2021
Netherlands Society for Parasitology – Clinical parasitology meeting	2017 (speaker)
	2019
	2021
	2022 (speaker)

Netherlands Centre for One Health meetings	2017 (3x) 2018 (2x) 2019 (poster)
ACE Migratory Health & Neglected Tropical Diseases meetings	2017 2018 (2x) 2019 (2x organiser)
Departmental Science Day	2017 (speaker) 2019 (poster)
KNVM / DMT meeting: Microbial Typing: Current Research	2018
NVAMM symposium	2018 2019 2020
AAV Science Day	2018

### **Courses**

Genomics in Molecular Medicine – Erasmus Summer Programme	2017
Genome-wide Association Studies – Erasmus Summer Programme	2017
Basic Course on “R” – Molmed Course	2017
Microscopic Image Analysis: From Theory to Practice – Molmed Course	2018
Workshop on Photoshop and Illustrator CS6 – Molmed Course	2018
Follow-up Workshop on Photoshop and Illustrator CS6 – Molmed Course	2018
Bioconductor Workshop – Molmed Course	2018
Masterclass: Advances in Genomics Research – Erasmus Summer Programme	2018
Erasmus MC Summer Lectures – Erasmus Summer Programme	2018
Biomedical Research Techniques – MolMed course	2018
Scientific Integrity Course – Erasmus MC	2019
“Fenotypische interpretatie van de antimicrobiële gevoeligheidsbepaling” – Molmed Course	2019
Laboratory Diagnosis of Human Parasitic Infections	2020

## Teaching

Teaching of medical students	2017
	2018
	2019
	2020
	2021
Supervision of Master students	
- Anna Mykytyn	2018
- Willem Jan de Leeuw	2019
- Nadia van der Meijs	2019
- Sven van Dun	2019 – 2020
- Dorenda Schoorl	2020 – 2021
- Lara Grassi	2020 – 2021
Supervision of Bachelor students	
- Shi You Fu	2017
- Aïsha Jedidi	2023
- Sarbani Bag	2024

## List of publications

### Publications in this thesis

**Sarink MJ**, Tielens AGM, Verbon A, Sutak R, van Hellemond JJ. Inhibition of Fatty Acid Oxidation as a New Target To Treat Primary Amoebic Meningoencephalitis. *Antimicrobial Agents and Chemotherapy*. Jul 2020. PMID: 32513800.

**Sarink MJ**, Pirzadian J, van Cappellen WA, Tielens AGM, Verbon A, Severin JA, van Hellemond JJ. *Acanthamoeba castellanii* interferes with adequate chlorine disinfection of multidrug-resistant *Pseudomonas aeruginosa*. *Journal of Hospital Infection*. Nov 2020. PMID: 32976863.

**Sarink MJ**, van der Meijs NL, Denzer K, Koenderman L, Tielens AGM, van Hellemond JJ. Three encephalitis-causing amoebae and their distinct interactions with the host. *Trends in Parasitology*. Mar 2022. PMID: 34758928.

**Sarink MJ**, van Cappellen WA, Tielens AGM, van Dijk A, Bogers AJJC, de Steenwinkel JEM, Vos MC, Severin JA, van Hellemond JJ. *Vermamoeba vermiformis* resides in water-based heater-cooler units and can enhance *Mycobacterium chimaera* survival after chlorine exposure. *Journal of Hospital Infection*. Feb 2023. PMID: 36572347.

**Sarink MJ**, Koelewijn R, Stelma F, Kortbeek T, van Lieshout L, Smit PW, Tielens AGM, van Hellemond JJ. An International External Quality Assessment Scheme to Assess the Diagnostic Performance of Polymerase Chain Reaction Detection of *Acanthamoeba* Keratitis. *Cornea*. Aug 2023. PMID: 37155347.

**Sarink MJ**, Mykytyn A, Jedidi A, Houweling M, Brouwers J, Ruijter G, Verbon A, van Hellemond JJ, Tielens AGM. *Acanthamoeba castellanii* trophozoites need oxygen for normal functioning and lipids are their preferred substrate, offering new possibilities for treatment. *International Journal for Parasitology*. Jan 2025. PMID 39490506

**Sarink MJ**, Grassi L, Tielens AGM, Verbon A, Vos MC, Goessens W, Strepis N, Klaassen CHW, van Hellemond JJ. *Acanthamoeba castellanii* can facilitate plasmid transfer between environmental *Pseudomonas* spp. Submitted for publication

## Other peer-reviewed publications

**Sarink MJ**, Koelewijn R, Slingerland BCGC, Tielens AGM, van Genderen PJJ, van Hellemond JJ. Performance of the commercially available SERION ELISA classic *Echinococcus* IgG test for the detection of cystic echinococcosis in clinical practice. *Journal of Helminthology*. Sep 2019. PMID: 29950187.

Bexkens ML, Zimorski V, **Sarink MJ**, Wienk H, Brouwers JF, De Jonckheere JF, Martin WF, Opperdoes FR, van Hellemond JJ, Tielens AGM. Lipids Are the Preferred Substrate of the Protist *Naegleria gruberi*, Relative of a Human Brain Pathogen. *Cell Reports*. Oct 2018. PMID: 30332635.

**Sarink MJ**, van Genderen PJJ, Tielens AGM, van Hellemond JJ. Ruptured *Echinococcus granulosus* cysts in migrants: Is excessive antigen release causing false negative serology? *Travel Medicine and Infectious Disease*. May-Jun 2020. PMID: 31051264.

Pieterman ED, **Sarink MJ**, Sala C, Cole ST, de Steenwinkel JEM, Bax HI. Advanced Quantification Methods To Improve the 18b Dormancy Model for Assessing the Activity of Tuberculosis Drugs In Vitro. *Antimicrobial Agents and Chemotherapy*. Jun 2020. PMID: 32340993.

Akbar N, Kaman WE, **Sarink MJ**, Nazmi K, Bikker FJ, Khan NA, Siddiqui R. Novel Antiamoebic Tyrocidine-Derived Peptide against Brain-Eating Amoebae. *ACS Omega*. Aug 2022. PMID: 36033708.

**Sarink MJ**, Bakker IL, Anas AA, Yusuf E. A study on the performance of ChatGPT in infectious diseases clinical consultation. *Clinical Microbiology and Infection*. Aug 2023. PMID: 37207982.

**Sarink MJ**, Bode LGM, Croughs P, de Steenwinkel JEM, Verkaik NJ, van Westreenen M, Vogel M, Yusuf E. Less Is More: When to Repeat Antimicrobial Susceptibility Testing. *Journal of Clinical Microbiology*. Aug 2023; PMID: 37436180.

**Sarink MJ**, Bras W, Te Lintel Hekkert F, Voor In 't Holt AF, Severin JA. Swimming pool policies for carriers of highly-resistant micro-organisms receiving rehabilitation care in the Netherlands. *Journal of Hospital Infection*. Nov 2023; PMID: 37722564.

Timmer CA, Igloi Z, **Sarink MJ**, GeurtsvanKessel C, van Nood E. Dengue vaccination: when and for whom? *Nederlands Tijdschrift voor Geneeskunde*. Nov 2024. PMID 39606865.

